IMMUNOSUPPRESIVE PROPERTIES OF PEPTIDYL-FLUOROMETHYL KETONES AND THE ROLE OF OXIDATIVE STRESS IN T CELL ACTIVATION AND PROLIFERATION

Thesis submitted for the degree of Doctor of Philosophy at
Monash University

by

Tanuja Rajah
School of Science

August 2015

CONTENTS

IMMUNOSUPPRESIVE PROPERTIES OF PEPTIDYL-FLUOROMETHYL KETONES AND THE ROLE OF OXIDATIVE STRESS IN T CELL ACTIVATION AND PROLIFERATION

Tanuja Rajah

It is well established that caspases are involved in T cell activation and proliferation. Many of the early studies relied on peptidyl-fluoromethylketone (FMK) caspase inhibitors, such as z-VAD-FMK. Recently, z-VAD-FMK and z-IETD-FMK were shown to block T cell proliferation without inhibiting caspase activation. These results suggest that the inhibition of T cell proliferation by these peptidyl-FMK caspase inhibitors is independent of their caspase inhibition properties. In contrast, z-FA-FMK, commonly used as a negative control peptide for the FMK-containing caspase inhibitors, blocked T cell proliferation as well as inhibiting caspase processing. In the present study, several analogues of z-FA-FMK were examined to determine whether peptidyl-FMKs block mitogen-induced T cell activation and proliferation through the inhibition of specific targets or due to non-specific effects of the FMK group. The results showed that only z-FA-FMK blocks T cell proliferation whereas z-FA-diazomethylketone (DMK) has little effect while z-FA-chloromethylketone (CMK) was toxic and killed all the cells. This suggests that the FMK moiety may play an important role in blocking T cell activation and proliferation. Interestingly, replacing the alanine in z-FA-FMK with phenylalanine, z-FF-FMK, blocked T cell proliferation to a higher degree than z-FA-FMK. Similar to z-FA-FMK, z-FF-FMK inhibited T cell blast formation, CD25 and CD69 expression and cell cycle entry while inhibiting caspase processing in activated T cells. When peptidyl-methyl ketones were tested on Jurkat T cells, it was found that only z-FA-FMK and z-FF-MK blocked T cell proliferation. Next the mechanism of z-FA-FMK-, z-FF-FMK- and z-VAD-FMK-induced block of proliferation in primary and Jurkat T cells was examined. Several studies have shown that the cellular redox state plays an important role in T cell activation and proliferation. Thus, the effect of these three compounds on intracellular glutathione (GSH) levels and reactive oxygen species (ROS) generation was explored. The data showed that intracellular GSH was depleted while ROS generation was increased following treatment with the peptidyl-FMK inhibitors in primary and Jurkat T cells. The addition of the low molecular weight thiols GSH, N-acetylcysteine (NAC) and L-cysteine, readily reversed the inhibition of T cell proliferation induced by these peptidyl-FMK inhibitors, whereas D-cysteine, which cannot be metabolised to GSH had no effect. Furthermore, GSH, NAC and L-cysteine fully restored the caspase-8 and caspase-3 processing in anti-CD3-activated primary T cells treated with z-FA-FMK and z-FF-FMK. In conclusion, the results suggest that the immunosuppressive effect of z-FA-FMK, z-FF-FMK and z-VAD-FMK is likely due to the induction of oxidative stress and GSH depletion in T cells.

DECLARATION

Except where due reference has been made in the text and to the best of my knowledge, this thesis contains no materials previously published or extracted in whole or in part and presented by me for the award of any other degree or diploma to any University.

……..
Tanuja Rajah
7th August 2015

Accepted by,

……...
Prof Chow Sek Chuen
Monash University
7th August 2015

ACKNOWLEDGEMENTS

First and foremost I would like to thank my supervisor, Prof Sek Chuen for his guidance and leadership during my PhD studies. Secondly, to my lab mates and now close friends, Kiat Yee, Wai Leong and Eveline, for their helpful suggestions and assistance over the years. I shall miss our daily breakfasts and conversations.

I would like to thank the lab staff of Sime Darby Medical Centre, in particular Ramli and Ruku, for their readiness to extract blood from my donors, and to the donors themselves, without whom these studies would not have been possible.

A huge thank you to my family who encourage me every step of the way. My amazing parents, Shoba and Vincent deserve much credit for guiding me through life and teaching me that I can achieve anything I set my mind to. Papa, thanks to you I was able spend three wonderful years in Melbourne. I shall always look back fondly on those days and cherish them greatly. Mama, you have been a constant source of support and reassurance and for that I'm grateful. Also thanks to my beautiful sister, Tashna, for putting up with my bouts of insanity. To my amazing grandparents, Kamala and Jeyaraj, this thesis is dedicated to the both of you. Your faith in me motivates me to always do better. I am sure that I'm the luckiest granddaughter in the world.

Finally, I am indebted to my husband, Jonathan, who has shown me unconditional love. Your ability to remain upbeat even during the challenges of my doctoral years provided me with much needed perspective. I am truly thankful for having you in my life.

PUBLICATIONS

The following refer to the manuscript in appendix 1 and 2, respectively.

RAJAH, T. & CHOW, S. C. 2014. The inhibition of human T cell proliferation by the caspase inhibitor z-VAD-FMK is mediated through oxidative stress. *Toxicol Appl Pharmacol,* 278(2)**,** 100-6.

RAJAH, T. & CHOW, S. C. 2015. Suppression of human T cell proliferation mediated by the cathepsin B inhibitor, z-FA-FMK is due to oxidative stress. *PLoS ONE,* 10(4).

CHAPTER ONE

Introduction

1.1 The immune system

The immune system is absolutely indispensable as it protects the human body against infection by bacteria, viruses, parasites and foreign bodies as well as tumour development. It can be divided into two parts: the innate immune system, which reacts immediately towards an infection but is non-specific, and the adaptive immune system, which is specific for the pathogen or tumour.

1.1.1 Innate immune system

The innate immune system is our body's first line of defence against invading pathogens and lacks immunologic memory. It consists of physical barriers, secretory molecules and cellular components of the immune system such as neutrophils, monocytes and macrophages. Epithelial surfaces, which separate the internal and external environments, form a physical barrier that is impermeable to most infectious agents. Continuous shedding of the outermost skin layer as well as the secretion of mucus, antimicrobial peptides and cytokines assist in the removal of bacteria and other infectious agents (Gallo et al., 2002, Elias, 2007). These physical barriers are effective in preventing the invasion of pathogens. However, when there is damage to tissues and the pathogen successfully breaches these barriers, it is quickly engulfed by phagocytic cells, such as macrophages and neutrophils, which are recruited to the site of infection. To discriminate pathogens from host cells, macrophages posses receptors for carbohydrates that are not normally exposed on "self" molecules, such as mannose (Fraser et al, 1998). In addition, macrophages and neutrophils distinguish pathogens by having receptors for antibodies and complement which ultimately serves to enhance phagocytosis (Aderem and Underhill, 1999). The release of pro-inflammatory cytokines such tumor necrosis factor-α (TNF-α) and interleukin-1β (IL-1 β) from

macrophages enhances the migration of further immune cells to the site of infection (Parkin and Cohen, 2001). The innate immunity also frequently involves plasma proteins which exist as inactive zymogens and undergo proteolytic activation in response to pathogens (Sakamoto et al., 1998). These proteins are collectively known as the complement system and function to enhance the innate immune system. For example, a proteolytic cleavage fragment of the complement component C3, the C3b molecule, is deposited on the surface of pathogens. This improves the phagocytosis of the pathogen as phagocytic cells have receptors for C3b (Law, 1988). In addition, certain complement fragments cause the release of inflammatory mediators from mast cells and act as a neutrophil chemoattractant (Hartmann et al., 1997) while some complement proteins contribute to the direct killing of pathogens (Frank and Fries, 1991). Besides its role in innate immunity, the complement system also contributes to the initiation of the adaptive immune response, which is activated if the innate immune system fails to halt the invasion by the pathogen (Medzhitov and Janeway, 1997, Sakamoto et al., 1998).

1.1.2 Adaptive immune system

The adaptive immune system can be broadly classified into two types of responses: the humoral response and the cell-mediated response which are carried out by difference classes of lymphocytes, namely B lymphocytes (B cells) and T lymphocytes (T cells), respectively. A characteristic of the adaptive immune response is the use of antigen-specific receptors on lymphocytes to target invading pathogens or tumour cells. To start with, the antigen is presented and recognised by the T cells, leading to T cell activation and proliferation and subsequent differentiation to a sufficient number of effector cells to destroy the pathogen. Once the pathogen is eliminated, the majority of the expanded activated T cells undergo apoptosis to restore

homeostasis. However, the surviving T cells remain as long-lived memory cells and are able to react more quickly on subsequent exposure of the pathogen (Sallusto et al., 1999, Delves and Roitt, 2000a, Delves and Roitt, 2000b).

B cells recognise antigen from extracellular pathogen due to a unique cell surface receptor called the B cell receptor (BCR) (Corcos et al., 2001). Once activated, B cells proliferate and differentiate into plasma cells which secrete antibodies of the same specificity as the BCR into the blood (Reales et al., 2005). The antibodies bind the pathogens thereby inactivating them by blocking their ability to bind to receptors on host cells. Antibody binding also labels the pathogens for phagocytosis. In cell-mediated immune responses, T cells recognise antigen which is presented on the surface of a host cell (Parkin and Cohen, 2001). Recognition of antigen by the T cell receptor (TCR) leads to T cell activation and differentiation into effector T cells.

1.1.3 The T cell-mediated immune response

Effector T cells can be subdivided into helper T cells and cytotoxic T cells. Helper T cells express the CD4 molecule and secrete cytokines that stimulate B cells to proliferate and mature into antibody secreting cells. The other major subset, cytotoxic or killer T cells express the CD8 molecule and directly kill virally infected cells or tumour cells.

1.1.3.1 Antigen recognition by T cells

Naïve T cells continuously move from one lymphoid tissue to another via blood or lymph until they encounter an antigen presenting cell (APC) bearing its antigen or an infected cell, in the case of $CD8^+$ cytotoxic T cells. APCs include dendritic cells (the interdigitating dendrintic cells

of lymph nodes, veiled cells in the blood, and Langerhan's cells in the skin), B cells and macrophages (Parkin and Cohen, 2001). Of these cells, the dendritic cells are especially important in activating primary naïve T cells (Figure 1.1).

To ensure that only damaging antigens elicit an immune response, T cell activation requires that the antigen is presented to the T cell within the peptide binding groove of the major histocompatability complex (MHC) protein. Following uptake of the pathogen into the cell, proteolysis of the pathogen proteins occurs to generate antigenic peptides and peptide-MHC complex is then expressed on the cell surface (Villadangos and Ploegh, 2000, Gromme and Neefjes, 2002). Antigen loading onto MHC can occur in two ways. First, the antigen may be produced endogenously within the cells, processed through intracellular processing pathways and complexed with MHC class I. Otherwise, APCs might take up exogenous antigen by endocytosis, processed via a different pathway and re-expressed with MHC class II molecules. $CD4^+$ T cells recognise antigens presented by MHC class II molecules whereas $CD8^+$ T cells recognise antigens presented by MHC class I molecules.

Contact between the T cell and APC or infected cell is maintained by several adhesion molecules. One such adhesion molecule is the lymphocyte function associated antigen-1 (LFA-1) which is found on the T cell surface and binds to its ligand, intercellular adhesion molecule-1 (ICAM-1) on the APC (Lollo et al., 1993, Labadia et al., 1998) . Recognition of the antigen by the TCR initiates the T cell to secrete either cytokines to stimulate the cell (if it is a T helper cell) or factors to induce cell death (if it is a T cytotoxic cell).

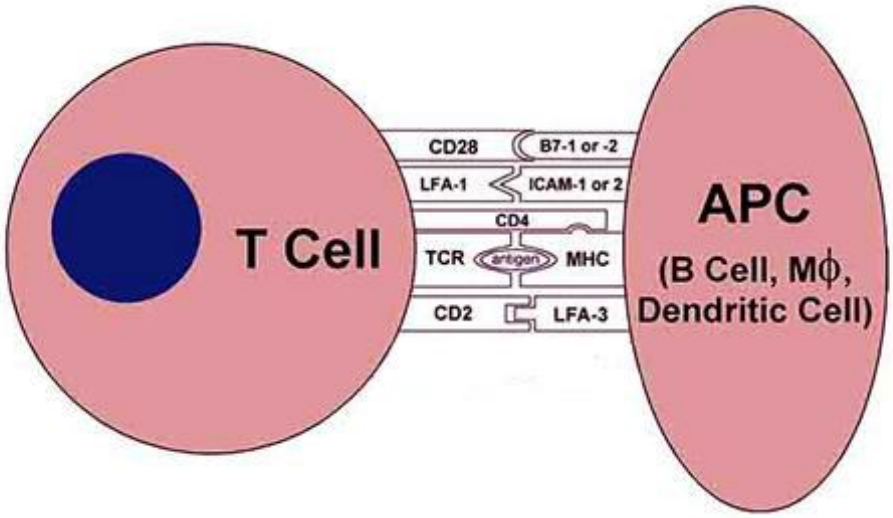

Figure 1.1 T cell interaction with APC

The peptide antigen (red circle) is presented to the T cell in conjunction with the MHC molecule. Once contact is made by the binding of LFA-1 (lymphocyte function associated antigen-1) on the T cell to ICAM-1 (intercellular adhesion molecule-1) on the APC, the TCR (T cell receptor) binds to the MHC-antigen complex (adapted from Laroux, 2004).

1.1.3.2 Role of co-stimulation

T cells require two signals to become fully activated. The first signal is provided by the antigen-MHC complex on the membrane of the APC to the TCR. A second co-stimulatory signal is provided by the interaction between co-stimulatory molecules expressed by the APC and the T cell (Figure 1.2). The principal co-stimulatory molecule that is expressed on the T cell surface is CD28 (Alegre et al., 2001, Collins et al., 2002) which interacts with B7.1 (CD80) and B7.2 (CD86) on the membrane of the APC. Signalling through CD28 synergises with the TCR-mediated signals, thus lowering the threshold for T cell activation. By binding to the ligands B7.1 and B7.2, CD28 inhibits the molecule CTLA-4, found on the surface of T cells and which also can bind to B7.1 and B7.2, from inhibiting T cell proliferation. In the absence of a co-

stimulatory signal, T cells activated by the antigen alone become anergic (unreactive) or die via apoptosis as a safeguard against inappropriate T cell activation (Schwartz, 1990).

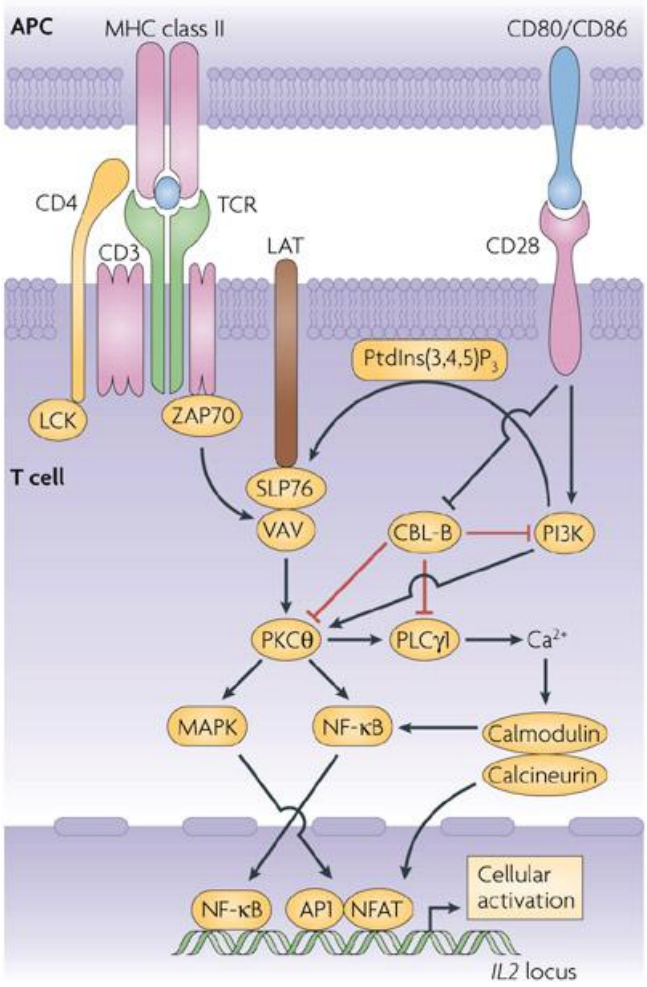

Figure 1.2 Major signaling pathways in T cell activation

Signals delivered by the engagement of the TCR (signal 1) and co-stimulatory molecules such as CD28 (signal 2) induce different signalling pathways that result in the activation of multiple transcription factors. Ligation of the TCR by peptide–MHC complexes triggers the recruitment of signalling molecules, such as phospholipase Cγ1 (PLCγ1), which induces the Ca^{2+} influx, nuclear factor of activated T cells (NFAT) and protein kinase Cθ (PKCθ), which regulate the nuclear factor-κB (NFκB) and activator protein 1 (AP1) pathways, respectively. These pathways control nuclear transcriptional and gene activation. In the nucleus, NFAT cooperates with AP1 and other transcription factors to induce a programme of gene expression that leads to interleukin-2 (IL-2) production (adapted from Miller et al., 2007).

1.1.3.3 Secretion and response to interleukin-2

The cytokine interleukin-2 (IL-2) is a potent T cell growth factor and is critical for clonal expansion. IL-2 is synthesised and secreted following T cell recognition of antigens (Hentsch et al., 1992) and is tightly regulated at the mRNA level by signals from the TCR and CD28 (Powell et al., 1998). IL-2 binds to and signals through a receptor complex consisting of three distinct subunits, namely IL-2Rα (CD25), IL-2Rβ (CD122) and IL-2Rγ (CD132) (Nelson and Willerford, 1998). Together, the three subunits form the functional IL-2 receptor (IL-2R) on the T cell surface (Gaffen, 2001). The IL-2/IL-2R interaction stimulates the expansion, differentiation and survival of antigen-specific helper T cells and cytotoxic T cells (Stern and Smith, 1986, Malek et al., 2002). The cytokine IL-2 acts in an autocrine and paracrine manner to drive T cell proliferation in response to antigen activating nuclear factor κB (NFκB) which ultimately drives cell cycle progression.

1.2 Apoptosis

The number of cells in an organism is tightly regulated throughout life by controlling the rate of cell division as well as the rate of cell death. The ability of cells to commit suicide is a fundamental property of all multicellular organisms (Lockshin and Zakeri, 2001). The phrase *programmed cell death* was introduced in relation to insect tissue development in 1964, suggesting that cell death during development occurs via a sequence of controlled steps and ultimately leads to defined self-destruction (Lockshin and Williams, 1964). In 1972, the term apoptosis was coined by Kerr and his colleagues in order to describe the morphological processes leading to controlled cell death. The word *apoptosis* is of Greek origin, meaning "falling off", as leaves fall off trees during autumn, and serves to remind us that controlled cell death is an essential process in every living being. This highly organized method of cell death begins from the moment an organism is created from a single cell and continues into adulthood. In this manner, death becomes an intricate part of life.

During development, cells are produced in great excess and usually undergo programmed cell death. At times it seems wasteful for so many cells to die, especially as the vast majority of them are healthy at the time of their demise. However, it is this removal of surplus or redundant cells which contributes to the maintenance and sculpturing of multicellular biological systems (Raff, 1998, Meier et al., 2000). For example, during embryonic development, digits appear as spade like structures and only separate into fingers and toes because cells in the interdigital mesenchymal tissue undergo apoptosis. In the developing vertebrate nervous system, more than half of the nerve cells produced normally die soon after they are formed (Hutchins and Barger, 1998). Structures that once served a function but are no longer needed, such as a tadpole's tail

during metamorphosis, are also eliminated by apoptosis (Helbing et al., 2007). Throughout the life of an adult, most of the developing lymphocytes, including those that are harmful or self-reactive, are eliminated by cell death. This cycle of production and elimination serves to ensure that a ready supply of functional and efficient cells are maintained while keeping the lymphocyte numbers relatively constant (Rathmell and Thompson, 2002).

The importance of apoptosis is emphasized by the many diseases associated with either increased or inhibited apoptosis. Diseases caused by excessive cell death include certain neurodegenerative disorders such as Parkinson's disease and Alzheimer's disease, ischemic injury due to cardiovascular occlusion and specific viral illnesses (Thompson, 1995). On the other hand, insufficient apoptosis can lead to autoimmune disorders such as systemic lupus erythematosus, viral latency and most notably, cancer (Henderson et al., 1991, Thompson, 1995).

A number of hallmark morphological features are characteristic of apoptotic cell death. Some of the earliest recognizable morphologic changes are compaction and segregation of chromatin into crescentic caps that become marginated against the nuclear envelope, reduction in nuclear size and condensation of the cytoplasm (Arends et al., 1990). Dilation of the endoplasmic reticulum is also observed, but the mitochondria remain morphologically normal during the early phase. Later, progression of condensation leads to budding and separation of both the nucleus and cytoplasm into discrete, membrane-bound apoptotic bodies. Externalisation of phosphatidylserine marks apoptotic cells for phagocytosis and so, these apoptotic bodies are quickly phagocytosed by neighbouring cells and macrophages without activating an immune response (Wyllie et al., 1980, Fadok et al., 1992, Kerr et al., 1994) . In contrast, cells undergoing

necrosis display an early swelling of organelles which finally disintegrate after rupture of the cell membrane (Majno and Joris, 1995).

1.2.1 Caspases

Many of the processes involved in apoptotic cell death are mediated by a family of cysteine proteases that cleave substrates with aspartic acid residues, known as caspases (Yuan et al., 1993, Nicholson and Thornberry, 1997). Currently, 14 mammalian caspases have been identified (Figure 1.3) with all, except for caspases -11, caspase-12 and caspase-13 being expressed in humans (Yan and Shi, 2005). Caspases were first discovered through work in the nematode *C. elegans*, where the deletion or mutation of CED-3 gene resulted in the abolition of programmed cell death that would normally occur (Yuan et al., 1993). Later, the CED-3 gene was demonstrated to be related to the human IL-1β-converting enzyme, now renamed caspase-1 (Cerretti et al., 1992, Thornberry et al., 1992). Overexpression of IL-1β-converting enzyme was also shown to be sufficient to induce apoptosis in mammalian cells (Miura et al., 1993).

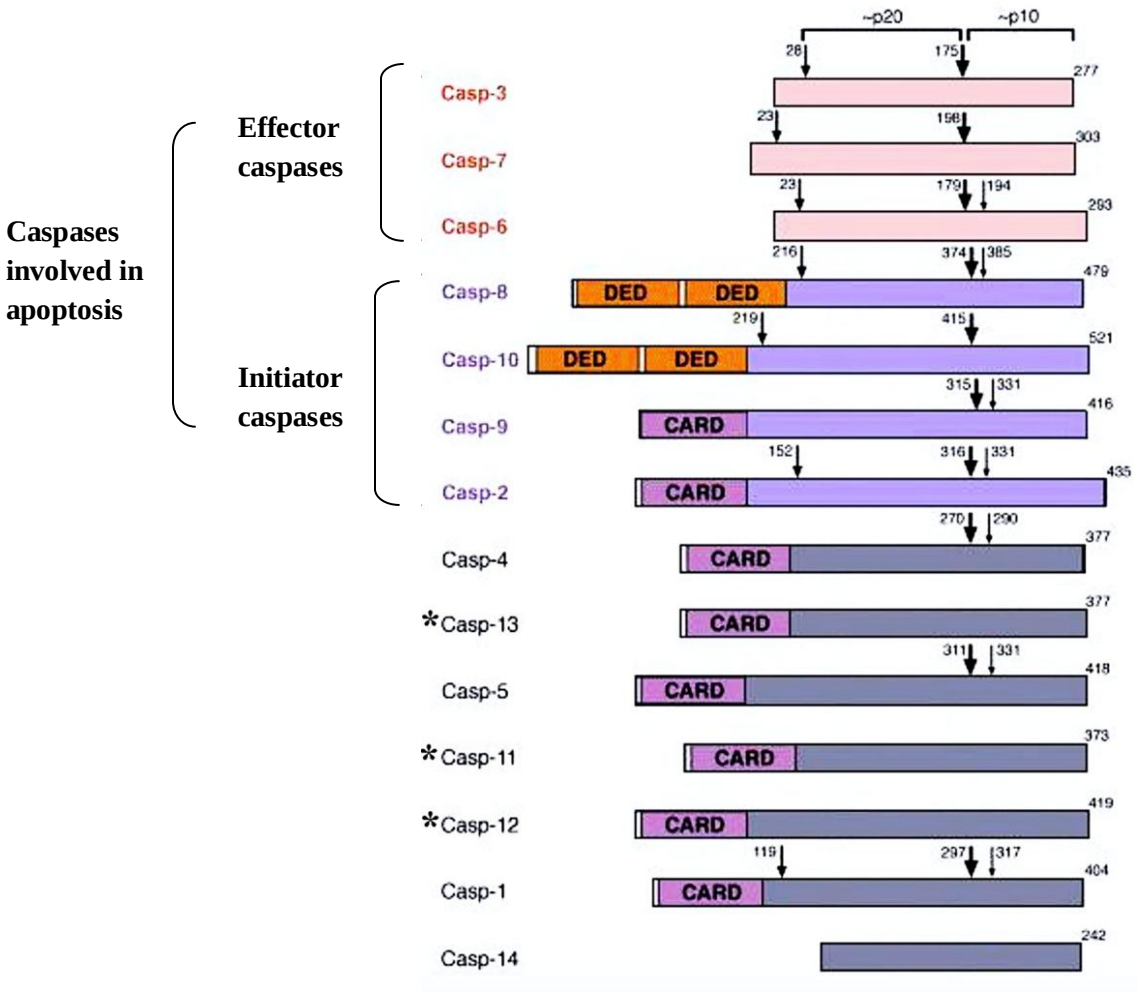

Figure 1.3 Members of the caspase family

The effector caspases (-3, -6 and -7) are highlighted pink and contain short prodomains. The initiator caspases (-2, -8, -9 & -10) are highlighted blue. They possess long prodomains which contain either tandem death-effector domains (DED) (orange) or caspase-recruitment domain (CARD) (purple). The large arrows indicate the first cleavage site during proteolytic activation which separates the large (p20) and small (p10) subunits. Subsequent cleavage sites are indicated by the medium and small arrows. *caspases that are not expressed in humans (adapted from Shi, 2002b).

Based on the homology and function of each caspase, the family of caspases has been categorized into three subfamilies; the apoptosis initiator caspase-2, caspase-8, caspase -9 and caspase-10; the apoptosis effector caspase-3, caspase-6 and caspase-7; and the inflammatory mediator caspase-1, caspase-4, caspase-5, caspase-11, caspase-12, caspase-13, and caspase-14 (Zimmermann et al., 2001). Each member of the caspase family exists as an inactive zymogen or pro-enzyme (~30-50 kDa) with three domains; an N-terminal prodomain, a large (~20 kDa) and C-terminal small (~10 kDa) subunit. Initiator caspases contain a long N-terminal prodomain of more than 90 amino acids that contain sequence motifs which allows them to interact with adaptor molecules. For example, caspase-2 and caspase-9 contain a caspase-recruitment domain (CARD) while caspase-8 and caspase-10 contain two death effector domains (DED) (Danial and Korsmeyer, 2004). On the other hand, effector caspases have a shorter prodomain of ~ 20-30 amino acids (Yan and Shi, 2005). Dimerization and/or proteolytic cleavage of initiator caspases, immediately following an aspartic acid residue, separates the large and small subunits and removes the N-terminal prodomain, all required for caspase activation (Thornberry and Lazebnik, 1998). The initiator caspases generally works upstream of the effector caspases. Once activated, initiator caspases propagate the apoptotic signal by cleaving effector caspases. The effector caspases then cleave essential proteins in the cell, for example DNA repair enzymes such as poly (ADP-ribose)polymerase which leads to the cleavage of chromatin (Margolin et al., 1997) and proteins supporting the nuclear membrane which causes dismantling of the nucleus (Nicholson and Thornberry, 1997). However, caspase activation does not always result in apoptosis. In recent years, it has also been implicated in other central biological processes such as inflammation, T cell proliferation and differentiation (Kennedy et al., 1999, Zeuner et al.,

1999, Fadeel et al., 2000). Two main pathways are known to activate caspases; the intrinsic pathway and the extrinsic pathway (Figure 1.4).

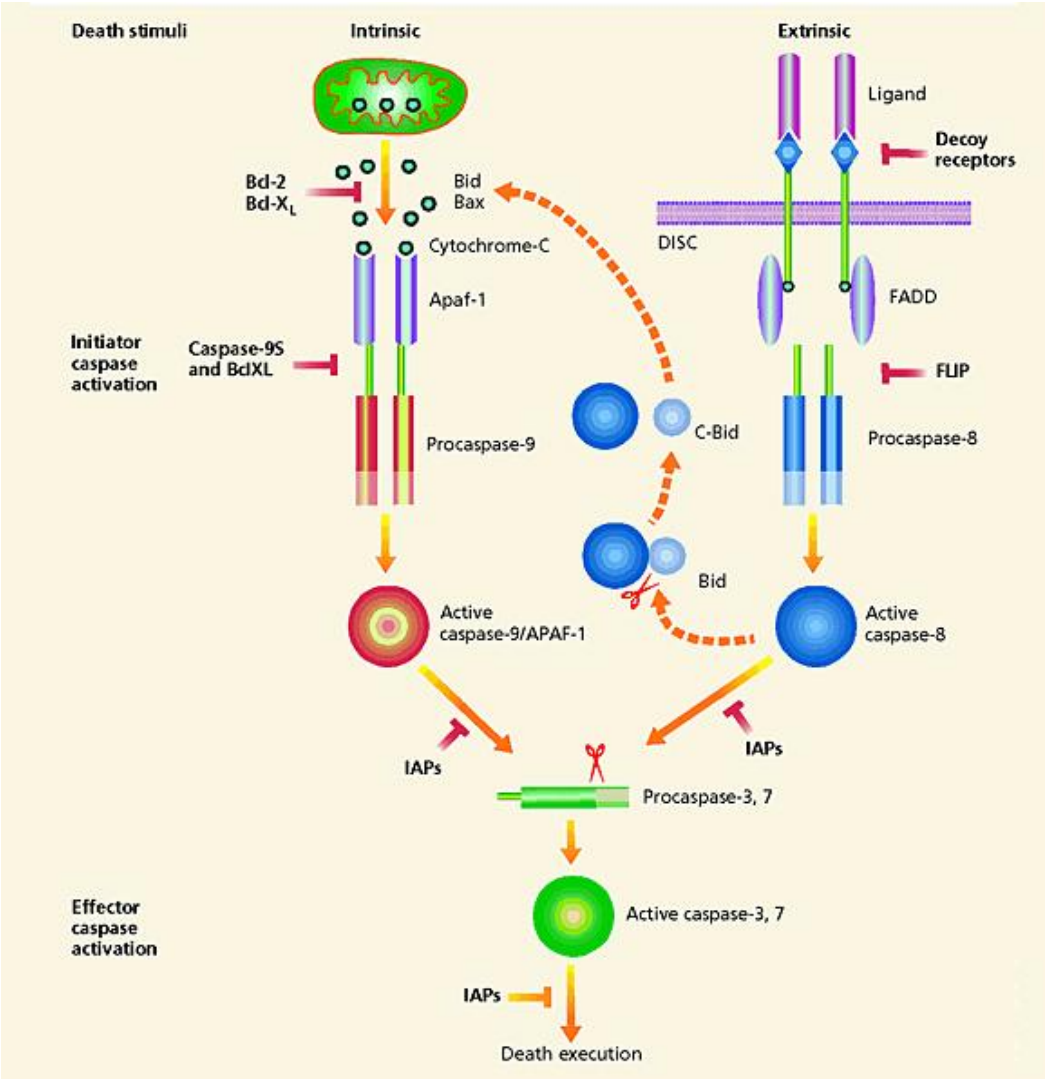

Figure 1.4 The intrinsic and extrinsic apoptotic pathways

Apoptosis can be induced by both intracellular stress and receptor-mediated signaling. Both intrinsic and extrinsic pathways lead to activation of caspases in a stepwise fashion. Activation of caspase-9 and -8, the two apical caspases of the two pathways, requires their recruitment to respective complexes known as apoptosome and DISC through interactions with their corresponding adapter proteins Apaf-1 and FADD. Once these apical caspases become activated, they in turn proteolytically activate downstream caspases, such as caspase-3 and -7, which are executioners of cell death (Zheng and Flavell, 2000).

1.2.2 Intrinsic pathway

The intrinsic pathway is activated by intracellular stimuli such as stress, cytotoxic drugs, DNA damage and nutrient starvation (Boatright and Salvesen, 2003). The mitochondrion plays a key role in mediating this pathway and serves as an amplification mechanism for the receptor mediated or extrinsic pathway. Disruption of the outer mitochondrial membrane (OMM) leads to the release of apoptogenic proteins, such as cytochrome c, from the mitochondrial inter-membrane space into the cytosol. Once in the cytosol, cytochrome c binds to the apoptotic protease-activating factor-1 (Apaf-1) and causes a conformational change which results in the activation of Apaf-1 (Li et al., 1997, Danial and Korsmeyer, 2004, Schafer and Kornbluth, 2006). Subsequently, cytochrome c/Apaf-1 interacts with the caspase recruitment domains (CARD) of individual pro-caspase-9 molecules to form an apoptosome complex (Zou et al., 1999, Schafer and Kornbluth, 2006). Pro-caspase-9 molecules are now in close proximity and are able to dimerize. This triggers the activation of pro-caspase-9, which then activates other effector caspases, such as caspase-3 to propagate apoptosis. Second mitochondrial-derived activator of caspase/direct inhibitor of apoptosis-binding protein with low pI (Smac/DIABLO) are proteins that normally reside in the mitochondria. However, following disruption of the OMM, these proteins are released into the cytosol, along with cytochrome c (Salvesen and Duckett, 2002). While cytochrome c mediates apoptosis through the formation of the apoptosome, Smac/DIABLO promotes caspase activation by inhibiting the family of endogenous caspase inhibitors, inhibitor of apoptosis protein (IAP) (Zimmermann et al., 2001, Yan and Shi, 2005).

Members of the B-cell lymphoma-2 (Bcl-2) family have long been recognized as regulators of the mitochondrial pathway (Breckenridge and Xue, 2004). To date, more than 24 members of the

Bcl-2 family have been identified (Yan and Shi, 2005) with all members containing at least one of four unique Bcl-2 homology domains (BH1-BH4) (Chen et al., 2005). According to their structure and function, Bcl-2 proteins are divided into anti-apoptotic and pro-apoptotic categories (Figure 1.5). Anti-apoptotic proteins, such as Bcl-2, Bcl-w and Bcl-X_L, possess four BH domains while pro-apoptotic proteins contain either three BH domains (BH1-BH3), for example Bax, Bak and Bok, or only one (BH3-only), such as Bid and Bad (Chen et al., 2005). Anti-apoptotic members inhibit mitochondrial pore formation through direct binding to Bax/Bak via the formation of heterodimers, thereby counteracting the latter's effect on the mitochondria (Cheng et al., 2001, Cory and Adams, 2002). On the other hand, pro-apoptotic members containing three BH domains promote the disruption of the OMM via the formation of pores in the membrane. This allows for the release of apoptotic factors such as cytochrome c and Smac/DIABLO (Cory and Adams, 2002, Yan and Shi, 2005). BH3-only members mainly inhibit anti-apoptotic proteins by binding to them and thus allowing the activation of Bax/Bak to trigger mitochondrial permeabilization (Zimmermann et al., 2001). Therefore, the fate of a cell is determined by the level of pro-and anti-apoptotic proteins.

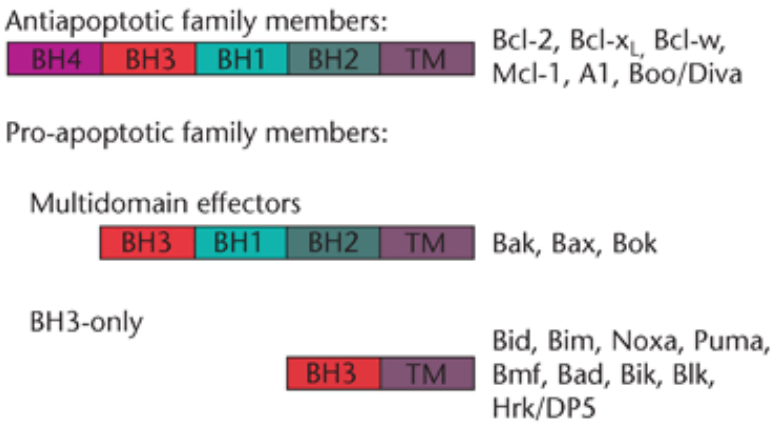

Figure 1.5 The Bcl-2 family members

Bcl-2 proteins can be subdivided into two categories according to their Bcl-2 homology domain (BH): anti-apoptotic members, which contain all four BH domains and pro-apoptotic members, which possess either three BH domains or only the third BH domain (BH3-only) (adapted from Parsons and Green, 2010).

1.2.3 Extrinsic pathway

The extrinsic pathway is activated due to death-receptor ligation, such as the binding of the Fas ligand (FasL) and tumor necrosis factor-α (TNF-α) to their related cell surface receptor (Hengartner, 2000). These receptors possess a death domain (DD) in their intracellular region which interacts with adaptor proteins such as the Fas-associated death domain (FADD) and tumor necrosis factor-associated death domain (TRADD) (Danial and Korsmeyer, 2004). In addition to the c-terminal DD, these adaptor proteins also contain tandem DEDs at the amino-terminus (Carrington et al., 2006) which binds to an analogous domain within pro-caspase-8. Upon recruitment, pro-caspase-8 oligomerization leads to the production of active caspase-8 through self-cleavage. This completes the formation of the death-inducing signaling complex (DISC) (Boatright and Salvesen, 2003). Caspase-10 also possesses DEDs and is recruited to the DISC but does not propagate the apoptotic signal in the absence of caspase-8 (Sprick et al.,

2002). Activation of caspase-8 cleaves caspase-3 into separate large and small subunits (Stennicke et al., 1998). Subsequent removal of the prodomain of caspase-3 from the large subunit is mediated by autoprocessing (Han et al., 1997). Activated caspase-3 propagates the caspase cascade by activating other effector caspases, such as caspase-2 and caspase-6 (Slee et al., 1999). This caspase activity results in the direct cleavage of several essential cellular proteins, including DNA fragmentation factor-40 (DFF40) and DNA repair enzymes like poly(ADP-ribose)polymerase (PARP), which lead to the cleavage of chromatin (Margolin et al., 1997) and proteins supporting the nuclear membrane causing the dismantling of the nucleus (Nicholson and Thornberry, 1997). These actions ultimately result in destruction of the cell.

According to Scaffidi and colleagues (1998), the extrinsic pathway requires the activation of the intrinsic pathway for an amplification mechanism. Two types of apoptotic signaling pathways stem from death receptors: Type 1 and Type II. In Type I, the production of caspase-8 is sufficient to activate caspase-3, leading to direct apoptosis. In Type II, the production of caspase-8 is limited and thus, requires apoptotic signals to be amplified through the mitochondria (Scaffidi et al., 1998). Here, the Bcl-2 family plays an important role in the crosstalk between extrinsic and intrinsic pathways. Activated caspase-8 cleaves the BH3 domain in the pro-apoptotic Bcl-2 protein, Bid, to release a fragment called truncated Bid (tBid). tBid then interacts with Bax and Bak to form a pore in the mitochondrial membrane, leading to the release of pro-apoptotic factors, such as cytochrome c, and ultimately, to the formation of the apoptosome along with Apaf-1 and caspase-9 (as occurs in the intrinsic pathway) (Yin, 2006).

1.2.4 Synthetic caspase inhibitors

Caspases have been implicated in various pathologies caused by either excessive or insufficient apoptosis. For instance, cancers arise when cells do not undergo apoptosis due to defects in the apoptotic pathway while neurodegenerative diseases such as Alzheimer's disease and Parkinson's disease arise as a result of excessive apoptosis (Nicholson, 1996). Therefore, it was necessary to elucidate the role of caspases in apoptosis in the hope of finding potential therapies which may be able to halt or delay disease progression. The use of specific synthetic caspase inhibitors has proven essential in the study of caspases during apoptotic cell death (Garcia-Calvo et al., 1998, Ekert et al., 1999, Yagi et al., 2001, Caserta et al., 2003). These caspase inhibitors contain a peptide sequence based on the target cleavage sequence of the substrate and thus act as competitive inhibitors by mimicking the substrate. The family of caspases recognises a sequence of four amino acids in the substrates, designated P4-P3-P2-P1 and cleave substrates after an Asp residue at P1 (Yuan et al., 1993, Shi, 2002a). All the peptide based caspase inhibitors used to date consist of a peptide sequence culminating in an Asp residue, whereas the requirements for amino acid residues at the other positions varies with members of the caspase family (Garcia-Calvo et al., 1998). By exploiting the differences in their substrate specificities, more specific inhibitors can be developed for the caspases (Thornberry et al., 1997, Garcia-Calvo et al., 1998). For example, benzyloxycarbonyl-Val-Ala-Asp-fluoromethylketone (z-VAD-FMK) is a broad spectrum caspase inhibitor (Figure 1.6) while benzyloxycarbonyl-Leu-Glu-His-Asp-fluoromethylketone (z-LEHD-FMK) specifically inhibits caspase-9 (Thornberry et al., 1997, Garcia-Calvo et al., 1998). Conjugated to the C-terminal of the peptide sequence in the caspase inhibitor is an electrophilic carboxy-terminal group such as a ketone or aldehyde. The nature of this carboxy-terminal group determines whether the caspase inhibitor is reversible of irreversible.

Aldehydes and ketones bind reversibly to the enzyme target site while halomethylketones, such as fluoromethylketone (FMK) and chloromethylketone (CMK), form an irreversible covalent bond with the S-H group of the cysteine residue in the caspase active site (Garcia-Calvo et al., 1998, Caserta et al., 2003). Finally, to enhance the permeability of the inhibitor, a benzyloxycarbonyl (z) or an acetyl (Ac) group attached to the amino-terminal of the peptide sequence will increase the hydrophobicity of the compound (Van Noorden, 2001).

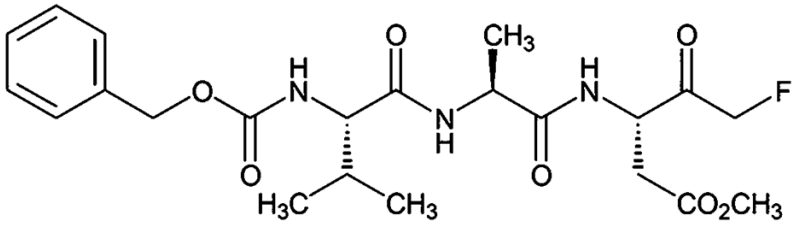

P3 P2 P1

benzyloxycarbonyl-Val-Ala-Asp-fluoromethylketone

Prevents the degradation of amino acids by proteases in the cell	Affinity group for the enzyme active site	Leaving group

Figure 1.6 Structure of a caspase inhibitor

The structure of z-VAD-FMK is given as an example of a caspase inhibitor. Caspase inhibitors comprise of a benzyloxycarbonyl (z) or an acetyl (Ac) group attached to the amino-terminal of the peptide sequence, amino acids ending with an Asp residue and an electrophilic leaving group at the C-terminal of the peptide sequence.

1.3 The role of caspases in T cell activation and proliferation

Inconsistent with their pivotal role in apoptosis, the involvement of caspases in T cell proliferation is now firmly established (Alam et al., 1999, Kennedy et al., 1999, Boissonnas et al., 2002, Chun et al., 2002, Mack and Hacker, 2002, Falk et al., 2004). Evidence for the dual role of caspases in apoptosis and cell proliferation was first described in a study which showed the processing of caspase-3 into its active subunits in proliferating non-apoptotic T cells (Miossec et al., 1997). Several studies later demonstrated the processing of other caspases, such as caspase-6, caspase-7 and caspase-8 following T cell activation (Alam et al., 1999, Kennedy et al., 1999, Bidere et al., 2002, Sturm et al., 2002). Subsequently, the essential role for caspase-8 in the proliferation of T cells was confirmed with caspase-8 mutations in humans and mice (Chun et al., 2002, Salmena et al., 2003). Patients bearing a homozygous caspase-8 mutation displayed diminished proliferation of T, B and natural killer (NK) cells as well as defects in lymphocyte apoptosis and homeostasis (Chun et al., 2002). Those patients exhibited reduced mitogen-induced T cell proliferation, IL-2 secretion and up-regulation of the α-subunit of the IL-2 receptor (CD25) (Chun et al., 2002). Similarly, murine T cells in which the caspase-8 mutation was restricted to the T cell lineage were also unable to proliferate following mitogen-induced activation. In addition, T cells from this murine model showed a reduced in vivo immune response to a viral infection (Salmena et al., 2003). However, in contrast to the humans with caspase-8 mutations (Chun et al., 2002), T cells derived from the caspase-8-deficient murine model were observed to produce IL-2 and to up-regulate CD25 normally in response to activation stimuli in vitro (Salmena et al., 2003).

In support of these findings, peptidyl-FMK caspase inhibitors such z-VAD-FMK, benzyloxycarbonyl-Ile-Glu-Thr-Asp-fluoromethylketone (z-IETD-FMK) and z-LEHD-FMK are shown to inhibit T cell activation and proliferation (Alam et al., 1999, Kennedy et al., 1999). These inhibitors block IL-2 secretion (Kennedy et al., 1999, Falk et al., 2004), up-regulation of CD25 and proper cell cycle-associated proteins (Falk et al., 2004).

1.3.1 Involvement of non-specific effects of the FMK group

Although peptidyl-FMK inhibitors were used as tools to study T cell activation and proliferation in many of the early studies, evidence now shows that these inhibitors may have non-specific effects (Siegel, 2006). For instance the most widely used broad spectrum caspase inhibitor, z-VAD-FMK, has been shown to inhibit other enzymes besides the caspases. These include the lysosomal cysteine protease, cathepsin B (Schotte et al., 1999), peptide:N-glycanase (PNGase) (Misaghi et al., 2006) and picornaviral 2A proteinases (Deszcz et al., 2004). Similarly, the caspase-8 inhibitor, z-IETD-FMK, also inhibited picornaviral 2A proteinases (Deszcz et al., 2004).

In addition, z-VAD-FMK was shown to block T cell proliferation in some studies (Alam et al., 1999, Kennedy et al., 1999, Lawrence and Chow, 2012), but had no effect on T cell proliferation in another (Zapata et al., 1998). Similarly, the caspase-8 inhibitor, z-IETD-FMK, blocked T cell proliferation (Alam et al., 1999, Kennedy et al., 1999, Boissonnas et al., 2002, Lawrence and Chow, 2012) but had no effect in one study (Mack and Hacker, 2002). Likewise, the caspase-3-selective inhibitor, benzyloxycarbonyl-Asp-Glu-Val-Asp-fluoromethylketone (z-DEVD-FMK),

which blocked T cell proliferation (Alam et al., 1999) was found to be less effective in other studies (Kennedy et al., 1999, Boissonnas et al., 2002, Mack and Hacker, 2002).

In agreement with previous data depicting the non-specific effects of peptidyl-FMK inhibitors, z-FA-FMK, a cathepsin B inhibitor which is commonly used as a negative control for the peptidyl-FMK caspase inhibitors (Sarin et al., 1996), was shown to block T cell activation and proliferation (Lawrence et al., 2006). Similar to other caspase inhibitors, z-FA-FMK inhibited blast transformation, IL-2 secretion, CD25 up-regulation and NFκB nuclear translocation (Lawrence et al., 2006).

1.4 Glutathione

The tripeptide L- γ glutamyl-L-cysteinyl-glycine or glutathione is the principal non-protein thiol component of the antioxidant defence system (Pastore et al., 2003). Found in high concentrations in virtually all cells, total glutathione can be free or bound to proteins and functions to protect cellular constituents from the damaging effects of reactive oxygen species (ROS). These ROS are formed during normal physiologic reactions, such as aerobic metabolism, but more dramatically during pathologic reactions by activated neutrophils during the inflammatory responses (Valko et al., 2007). ROS include hydroxyl radicals, superoxide anion, hydrogen peroxide and nitric oxide (Mates et al., 1999).

1.4.1 Structure and functions of glutathione

Glutathione can exist in both the thiol-reduced (GSH) and disulfide-oxidised (GSSG) forms (Kaplowitz et al., 1985) however in the absence of oxidative stress, 90 – 95 % of glutathione exists in its reduced form (Meister and Anderson, 1983, Ginn-Pease and Whisler, 1996). However, in response to stress, it is rapidly consumed by a reaction that results in the generation of GSSG. The structure of GSH is unique due to the peptide bond which links glutamate and cysteine through the γ- carboxyl group of glutamate rather than the conventional α-carboxyl group. The only enzyme that can hydrolyze this unusual bond is γ-glutamyltranspeptidase (GGT), which is only present on the external surfaces of certain cell types (Meister and Anderson, 1983). As a result of this bond, GSH is resistant to intracelluar degradation and is only metabolized extracellularly by cells that express GGT. This allows for GSH to be broken down and its constituent amino acids taken up by cells and converted back to GSH by the enzyme

glutathione reductase. Consequently, the redox status within a cell depends on the relative amounts of reduced and oxidised forms of glutathione.

Glutathione has several functions, mainly exerted when it is present in the reduced form, such as antitoxic and antioxidant effects, regulation of cell cycle progression and apoptosis, storage of cysteine (Suthanthiran et al., 1990, Ballatori et al., 2009, Forman et al., 2009, Lu, 2009, Pallardó et al., 2009).

1.4.2 The γ-glutamyl cycle

GSH is synthesised in the cytoplasm from glutamate, cysteine and glycine by two consecutive reactions by the enzymes γ-glutamylcysteine synthethase and GSH synthase (Figure 1.7). This cycle allows GSH to serve as a continuous source of cysteine which is extremely important as cysteine is very unstable and rapidly auto-oxidises to cystine extracellularly which in turn can generate potentially toxic ROS (Meister, 1988).

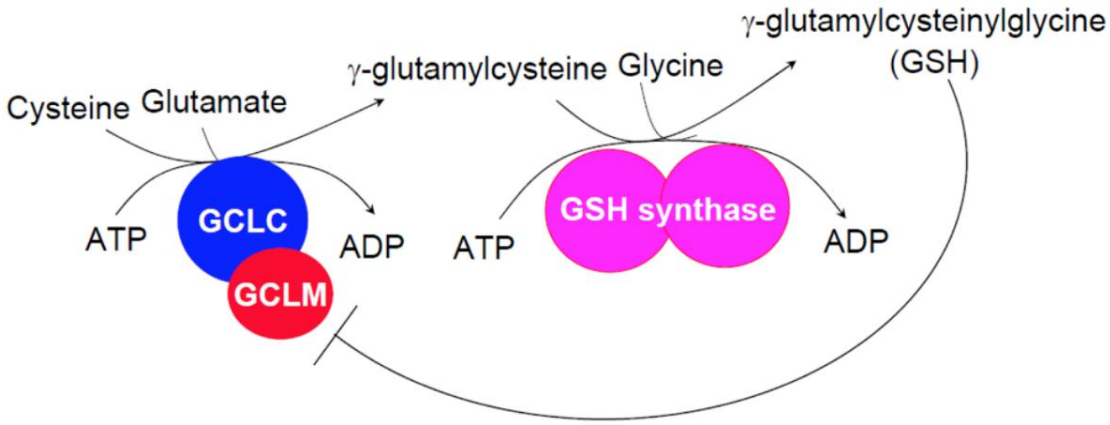

Figure 1.7 GSH synthesis

Synthesis of GSH occurs via a two-step ATP-requiring enzymatic process. The first step is catalyzed by glutamate-cysteine ligase (GCL), which is composed of catalytic and modifier subunits (GCLC and GCLM). This step conjugates cysteine with glutamate, generating γ-glutamylcysteine. The second step is catalyzed by GSH synthase, which adds glycine to γ-glutamylcysteine to form GSH. GSH exerts a negative feedback inhibition on γ-glutamylcysteine synthethase (adapted from Lu, 2013).

1.4.3 The role of glutathione in apoptosis

As described in section 1.2, apoptosis plays a fundamental role during normal physiological processes such as developmental organ remodelling (Kerr et al., 1972, Gerschenson and Rotello, 1992) as well as during removal of self-reactive lymphocyte clones (McCarthy et al., 1992). Although the exact role of GSH depletion in apoptosis is not yet fully defined, accumulating evidence suggests that GSH depletion is an early hallmark in the progression of apoptosis in response to a variety of stimuli (Franco et al., 2007, Circu and Aw, 2008) and regulates both extrinsic and intrinsic apoptotic signalling pathways at distinct check-points. For example, a reduction in GSH content in vitro has been shown to be necessary for the formation of the apoptosome in Jurkat T cells (Sato et al., 2004). In addition, it has been proposed that the released cytochrome c from the mitochondria needs to become oxidised for its pro-apoptotic activation which would require cytosolic GSH levels to be depleted (Coppola and Ghibelli, 2000, Brown and Borutaite, 2008). Furthermore, overexpression of the anti-apoptotic Bcl-2 (Ellerby et al., 1996) and Bcl-xl (Bojes et al., 1997) both lead to increased levels of GSH thereby blocking mitochondrial-induced cell death. Likewise, overexpression of γ-glutamylcysteine synthethase has been found to protect against apoptosis induced by stimuli which activate both the intrinsic and extrinsic pathways (Botta et al., 2004, Fan et al., 2005). On the other hand, knock-out of γ-glutamylcysteine synthethase induces time-dependent apoptosis in various cell types (Diaz-Hernandez et al., 2005). This is further supported by γ-GCS knock-out studies in mice which lead to massive apoptotic cell death and eventual death (Dalton et al., 2004). These observations suggest that apoptosis is regulated by the redox state within the cell and that GSH is the major determinant of the intracellular redox potential.

1.4.4 The role of glutathione in T cell activation and proliferation

Although initially described as a potent reducing agent and major antioxidant within cells, it is now widely accepted that GSH also plays an important role in the initiation and progression of T cell activation (Fischman et al., 1981, Zmuda and Friedenson, 1983, Hamilos and Wedner, 1985, Fidelus et al., 1987, Hamilos et al., 1989). Early studies using diamide (Chaplin and Wedner, 1978) and 2-cyclohexene-1-one (Hamilos and Wedner, 1985, Hamilos et al., 1991) which decrease GSH levels by oxidising GSH and reacting with GSH to form conjugates, respectively, indicated that GSH may be involved lectin-activated T cell proliferation. Subsequently, it was shown that human T cells depleted of GSH using L-buthionine-(*S*, *R*)-sulfoximine (BSO), a specific inhibitor of GSH synthesis, were unable to proliferate in response to mitogenic lectins (Friesen et al., 2004) while exogenous GSH reversed the BSO-induced block on T cell proliferation (Suthanthiran et al., 1990). On the other hand, L-buthionine-(*R*)-sulfoximine, which does not inactivate γ-glutamylcysteine synthethase, did not affect proliferation (Suthanthiran et al., 1990). Furthermore, enhancing intracellular GSH concentrations increases T cell proliferation (Zmuda and Friedenson, 1983, Fidelus et al., 1987) by increasing IL-2 production in vitro (Chen et al., 1994) which is absolutely essential for T cell proliferation. In support of this data, it has been reported that GSH regulates activation-dependent DNA synthesis in human T cells stimulated via their CD2 and CD3 antigens. This study demonstrates that GSH can directly modulate proliferation of highly purified T cells which suggests that GSH is essential for steps close to or at DNA synthesis (Suthanthiran et al., 1990).

However, one study demonstrated that GSH alone is not required for T cell proliferation but rather is only rate limiting in the absence of other low molecular weight thiols, namely N-acetylcysteine (NAC), 2-mercaptoethanol (2-ME) and L-cysteine (Hadzic et al., 2005). NAC

functions as a precursor for GSH synthesis as intracellular deacetylation of NAC provides cysteine for GSH synthesis, the lack of which can be rate limiting (Yim et al., 1994). Additionally, NAC functions as a potent thiol antioxidant due to its ability to scavenge ROS (Sandstrom et al., 1994). On the other hand, 2-ME and L-cysteine enhance GSH synthesis by increasing the supply of intracellular cysteine. This is especially important as T cells are unable to take up cystine and convert it to cysteine (Angelini et al., 2002). Thus, it is likely that T cell proliferation and IL-2 production are mediated by small molecular weight thiols which include GSH (Hadzic et al., 2005).

1.5 Aims

It is now well established that caspase activity is involved during T cell activation and proliferation. Although some light has been shed on the molecular mechanism of caspase activation and regulation during T cell activation, many questions remain unresolved. Previous work has shown that the peptidyl-FMK caspase inhibitors, such as z-VAD-FMK, z-IETD-FMK and z-DEVD-FMK, block T cell activation and proliferation but do not inhibit caspase processing. In contrast, z-FA-FMK, which is commonly used as a negative control for peptidyl-FMK caspase inhibitors, was shown to inhibit T cell activation and proliferation as well as block caspase-3 and caspase-8 processing in activated T cells. Since the peptidyl-FMK caspase inhibitors blocked T cell proliferation, but had little effect on caspase processing in activated T cells, it is likely that a non-caspase protease is involved in caspase processing in activated T cells. The main objective of the work presented in this study is to investigate whether peptidyl-FMK inhibitors block mitogen-induced T cell activation and proliferation through the inhibition of specific targets, in particular caspases, or due to non-specific effects of the FMK group. To this end, several analogues of z-FA-FMK will be examined for their immunosuppressive properties on T cell activation and proliferation using both primary T cells and Jurkat, a human leukemic cell line. Based on studies depicting the importance of GSH in T cell activation and proliferation, the role of GSH will also be investigated. This study will provide a better understanding on the regulation of T cell activation and proliferation via the caspases. These findings may offer a number of targets for therapeutic intervention in selectively blocking T cell activation for immunosuppressive therapy.

CHAPTER TWO

Materials & Methods

2.1 MATERIALS

2.1.1 Reagents

Material	Supplier
Ammonium sulphate	Sigma, USA
Annexin V-FITC	Becton Dickinson, UK
Anti-caspase 2	Santa Cruz, USA
Anti-caspase 3	Santa Cruz, USA
Anti-caspase 6	Santa Cruz, USA
Anti-caspase 8	Santa Cruz, USA
Anti-caspase 9	Santa Cruz, USA
Anti-CD25-FITC	BD Pharmingen, UK
Anti-CD3 (OKT3) antibody	Purified from OKT3 hybridoma supernatant using Hi-Trap Protein G Column
Anti-CD69-PE	BD Pharmingen, UK
Anti-PARP	Alexis Biochemicals, UK
Anti-β-actin	Sigma, USA
Avidin-HRP	Sigma, USA
b-FA-FMK	MP Biomedicals, UK
b-VAD-FMK	MP Biomedicals, UK
Bradford reagent	Bio-Rad, USA
BrdU	Roche, Switzerland
Bromophenol blue	Sigma, USA
BSA	Merck, Germany
BSO	Sigma, USA
CFSE	Molecular Probes, UK
D-cysteine	Sigma, USA
DHE	Sigma, USA
DMSO	Sigma, USA
DTT	Sigma, USA
ECL detection reagents	Amersham, UK
EtOH	J. Kollin, UK

Fetal Calf Serum	Hyclone, UK
Glutamine	Sigma, USA
Glycerol	Sigma, USA
Glycine	Sigma, UK
GSH	Sigma, USA
HEPES	Sigma, USA
Hi-Trap Protein G Column	GE Healthcare, UK
Hoechst	Molecular Probes, UK
HRP-conjugated rabbit anti-goat	Dako, UK
HRP-conjugated goat anti-mouse	Dako, UK
HRP-conjugated goat anti-rabbit	Dako, UK
Hybond C nitrocellulose membrane	Amersham, UK
Hyperfilm	Amersham, UK
IL-2	Pharmacy Department, Leicester Royal Infirmary, UK
L-cysteine	Sigma, USA
Lymphoprep^{TM}	Axis Shield, Norway
MCB	Sigma, USA
MeOH	R & M Chemicals, UK
NAC	Sigma, USA
NEM	Sigma, USA
OKT3 hybridoma	American Type Tissue Culture, Rockville, USA
Paraformaldehyde	Sigma, USA
PBS	Sigma, USA
Penicillin/Streptomycin	Gibco, USA
PMSF	Sigma, USA
Ponceau-S solution	Sigma, USA
Propidium Iodide	Sigma, USA
RNase A	Sigma, USA
RPMI	Gibco BRL, UK
SDS	Biorad, USA
STS	Sigma, USA

Tris base	Sigma, USA
Triton-X	Sigma, USA
Tween-20	Sigma, USA
Vacutainers®	Becton Dickinson, UK
z-FA-CMK	MP Biomedicals, UK
z-FA-DMK	MP Biomedicals, UK
z-FA-FMK	Bachem, Switzerland
z-FF-FMK	Merck, USA
z-VAD-FMK	Bachem, Switzerland
z-VRPR-FMK	Bachem, Switzerland
z-YVAD-FMK	Bachem, Switzerland

2.2 Tissue culture techniques

2.2.1 Blood collection and preparation of peripheral blood mononuclear cells (PBMCs)

Peripheral venous blood samples were obtained from healthy volunteers, with appropriate ethical clearance and volunteer consent. The blood was drawn into heparin-coated Vacutainers® and used within 3 h. To prepare PBMCs, the blood samples were diluted 1:1 with warmed complete RPMI 1640 medium supplemented with 10 % (v/v) fetal calf serum (FCS), 2 mM L-glutamine, penicillin (100 units/ml) and streptomycin (100 μg/ml). PBMCs were isolated from the diluted blood using density gradient centrifugation (Ulmer et al, 1984). In brief, diluted blood (20 ml) was carefully layered onto 20 ml Lymphoprep™ in 50 ml tubes and centrifuged at 930 x g for 20 min at 25°C. The mononuclear cells were then removed from the interface between the Lymphoprep™ and the blood plasma. The PBMCs were washed twice with PBS at 300 x g for 10 min at 25°C and re-suspended in complete medium and kept at 37°C and 5 % CO_2 until used. The viability of PBMCs was assessed using trypan blue exclusion assay and routinely found to be > 95 %.

2.2.2 Activation of T cells

To activate T cells, PBMCs were treated with antibodies to the CD3 moiety of the CD3-T Cell Receptor (TCR) complex which directly activates the signaling pathway emanating from the TCR. Anti-CD3 was coated onto wells in tissue culture plates for 2 h at 37°C in PBS. Unbound anti-CD3 was removed and the wells were rinsed with fresh PBS prior to adding the PBMCs. Where indicated, peptidyl-methyl ketones were added prior to the addition of cells. For experiments involving antioxidants, PBMCs were treated with peptidyl-methyl ketones and

antioxidants simultaneously. DMSO was used as a carrier solvent for the peptidyl-methyl ketones and the maximum concentration added to the cells was less than 0.2 %.

2.2.3 Generation of cycling T cells

To generate cycling T cells, PBMCs were treated with anti-CD3 (5μg/ml) for 24 h before being subjected to density gradient centrifugation to remove any dead cells. The purified activated T cells were then re-seeded at a density of 5 x 10^5 cells/ml in complete medium supplemented with human recombinant 25 U/ml IL-2 (rIL-2). The cells were re-seeded in fresh complete medium supplemented with rIL-2 every 3 days and maintained in culture for 7 days before used in experiments involving peptidyl-methyl ketones.

2.2.4 Jurkat T cells

The human leukemic T cell line, Jurkat E6.1 clone, Jurkat A3 clone (wild type) and caspase-$8^{-/-}$ Jurkat T cells, a gift from Dr. J. Blenis (Harvard Medical School, Boston, USA). The cells were maintained in the logarithmic growth phase via passage every 2 – 3 days and re-seeding at a density of 5 x 10^5 cells/ml in complete RPMI 1640 medium and cultured in a humidified atmosphere at 37°C and 5 % CO_2. The caspase-$8^{-/-}$ Jurkat T cells were confirmed to be deficient in caspase-8 via Western blotting (data not shown).

2.2.5 Jurkat T cell treatments

Jurkat T cells (2.5 x 10^5 cells/ml) were treated with varying concentrations of peptidyl-methyl ketones in a final volume of 200 μl in 96-well plates. The cells were assayed at 24 h intervals

over 3 days. For experiments involving antioxidants, Jurkat T cells were treated with peptidyl-methyl ketones in the presence or absence of antioxidants where indicated.

2.3 Cell Biology Techniques

2.3.1 Bromodeoxyuridine (BrdU) incorporation proliferation assay

Primary T cell proliferation was determined by the incorporation of BrdU, an analog of the DNA precursor thymidine, into the total DNA of proliferating cells. In brief, PBMCs (1 x 10^6 cells/ml) were seeded in duplicate into wells of a 96-well plate at a final volume of 100 µl. The cells were stimulated with plate bound anti-CD3, in the presence or absence of peptidyl-methyl ketones as outlined in Section 2.2.2. At 24 h intervals, 10 µM BrdU was added to each well and incubated for 3 h in a humidified atmosphere at 37°C with 5 % CO_2 in air. At the end of the culture period, the cells in the plate were centrifuged at 2000 rpm for 10 min and the supernatant discarded. The cells were washed with PBS and after centrifugation, the supernatants were carefully removed. The cells in the plates were left to dry at 60°C for 1 h before fixing with 200 µl ethanol (70 %) in HCl (final concentration 0.5 M) for 30 min at -20°C. Following fixation, the nuclear DNA in the cells was partially digested with nuclease for 30 min at 37°C. After washing three times with PBS supplemented with 10 % FCS, a peroxidase-labeled antibody to BrdU was added to the fixed cells and incubated for 1 h. After three rounds of washing with PBS (10 % FCS), a peroxidase substrate was added to catalyse the cleavage of the substrate to yield a colored reaction product. The absorbance of the samples was determined using a microplate reader with a wavelength of 405 nm and a reference wavelength of 495 nm. The colour intensity is directly correlated to the level of BrdU incorporated into cellular DNA.

2.3.2 Monitoring cell division using carboxyfluorescein diacetate succinimidyl ester (CFSE) labeling

CFSE is a cell membrane-permeable fluorescein-based dye commonly used to track the successive generations of proliferating cells (Lyons and Parish, 1994). In addition to fluorescein, CFSE contains two acetate groups and a succinimidyl ester group. Upon entry into cells, the esterases within the cells will remove the acetate groups resulting in a membrane-impermeable dye which binds irreversibly to intracellular proteins via the interaction between the succinimidyl ester group and free amines on proteins. Due to this covalent coupling reaction, CFSE can be retained within cells for extremely long periods of time. By monitoring the cellular fluorescence intensity, which is reduced by half and distributed evenly between daughter cells during cell division, successive cell divisions can be identified. In brief, PBMCs (5×10^7 cells/ml) were incubated with 5 μM CFSE in PBS for 10 min at 37°C in the dark. The cells were then washed twice in complete medium to remove unbound CFSE. The CFSE-labeled PBMCs (1×10^6 cells/ml) were stimulated with plate bound anti-CD3, in the presence or absence of peptidyl-methyl ketones. Following treatments, cell samples were taken at 24 h intervals, re-suspended in 1 ml PBS before analysed using flow cytometry. For all flow cytometry procedures, including those described in subsequent sections, the samples were gated to include small resting T cells and large activated T cells (T cell blasts). For CFSE analysis, an excitation wavelength of 488 nm was used (detected in the FL-1 channel). Unstained cells were used to calibrate the machine prior to each experiment.

2.3.3 Determination of cell viability using propidium iodide (PI)

PI is a DNA-binding dye that is impermeable to live cells but in dead cells where the cell membrane integrity is lost, PI accumulates in the cells and binds to the nuclear DNA. In brief, treated cells (1 x 10^6) were washed in ice-cold PBS before re-suspending in 1 ml ice-cold PBS. PI solution (25 µl of 20 µg/ml) was added to the cell suspension, mixed and the uptake of PI was immediately assessed by flow cytometry with an excitation wavelength of 595nm (FL-3 channel). Prior to each experiment, the machine was calibrated using unstained cells.

2.3.4 Cell cycle analysis

Treated cells (1 x 10^6) were washed with PBS and re-suspended in 200 µl ice-cold PBS. Cold 70 % EtOH (1.2 ml) was added drop-wise to the cell suspension while vortexing to ensure the cells were fully dispersed. The cells were then fixed at 4°C overnight. The fixed cells were washed twice in PBS to ensure all traces of ethanol were removed to avoid the inhibition of RNase A. The cells were then re-suspended in 1 ml of PBS containing PI (50 µg/ml) and RNase A (100 µg/ml) and incubated for 30 min at 37°C. Following incubation, the cells were washed and re-suspended in 500 µl PBS prior to analysis using flow cytometry.

2.3.5 Immunofluorescence of cell surface molecules using flow cytometry

Treated cells (1 x 10^6) were washed in ice-cold PBS and re-suspended in 50 µl staining buffer (PBS containing 2 % BSA). Fluorochrome-conjugated antibody (anti-CD25-FITC or anti-CD69-PE) in a final dilution of 1:50 was added to the cells. The cells were incubated on ice for 30 min, washed twice in staining buffer before being analysed using flow cytometry. Excitation wavelengths of 488 nm (FL-1 channel) (anti-CD25-FITC) and 532 nm (FL-2 channel) (anti-

CD69-PE) were used. The machine was calibrated using unstained cells prior to each experiment.

2.3.6 Detection of externalised phosphatidylserine (PS) during apoptosis using FITC-conjugated Annexin V

One of the earliest events that occur during apoptosis is the loss of the plasma membrane asymmetry. In apoptotic cells, PS is translocated from the inner to the outer leaflet of the plasma membrane, thereby exposing PS to the external cellular environment (Kagan et al., 2003). Because annexin V protein has a high affinity for PS and readily binds to exposed PS in the presence of calcium, annexin V-FITC staining is commonly used to identify apoptotic cells at an early stage of apoptosis. Counter-staining with PI enables the discrimination between early and late apoptotic/necrotic cells. In brief, treated cells (1×10^6) were washed in PBS and re-suspended in 1 ml annexin-V binding buffer (PBS + 1 mM $CaCl_2$). The cell suspension (100 µl) was incubated with 1.5 µl each of FITC-labelled annexin V and PI at room temperature in the dark for 15 min. A further 400 µl of binding buffer was added to the cells prior to analysis using flow cytometry. Excitation wavelengths of 488 nm (FL-1 channel) (annexin-V-FITC) and 595 nm (FL-3 channel) (PI) were used. The machine settings were adjusted using samples stained only with either annexin-V-FITC or PI to compensate for any overlap in the two detection channels prior to each experiment.

2.3.7 Detection of nuclear morphological changes during apoptosis using Hoechst 33342 nuclear DNA dye

The Hoechst dye has been widely used to detect the nuclear morphological changes in apoptotic cells (Oberhammer et al., 1993). This is a DNA-binding dye and fluoresces blue following UV excitation. In contrast to normal cells, the nuclei of apoptotic cells have highly condensed chromatin and thus fluoresce brightly compared to healthy cells. The condensed chromatin causes the nuclei to appear small and can also take the form spherical beads or crescents around the periphery of the nucleus. In this study, nuclear morphological changes of apoptotic cells were examined by staining with Hoechst 33342. In brief, treated cells (1×10^6) were washed with cold PBS and the cell pellet re-suspended in 50 µl of 4 % paraformaldehyde (PFA) which was added drop-wise whilst vortexing to prevent cell clumping. After incubation at room temperature for 30 min, 50 µl Hoechst 33342 solution (8 µg/ml) was added to the cell suspension and left overnight at 4°C in the dark. The cells were then centrifuged at 5000 rpm for 10 min and the supernatants removed before re-suspended in 10 µl PBS/glycerol (50:50, v/v). An aliquot of 5 µl of the cell suspension was placed onto a glass slide, mounted with a cover slip and viewed under fluorescence microscopy. A minimum of 300 cells was scored for each sample. Slides were stored for later viewing by sealing the cover slips with nail varnish and storing in the dark at 4°C.

2.3.8 Detection of glutathione (GSH) using monochlorobimane (MCB)

A commonly used method to determine GSH in cells is via the use of MCB, a cell permeable probe that reacts with intracellular GSH to form a highly fluorescent blue adduct. Cells (1×10^6 cells/ml) in a final volume of 100 µl in wells of a 96-well plate were stimulated with plate bound anti-CD3, in the presence or absence of peptidyl-methyl ketones and antioxidants. After

treatment, the cells were centrifuged down at 3500 rpm for 10 min and washed with 100 µl PBS. The supernatants were carefully removed before adding 100 µl of MCB (100 µM) in PBS for 30 min at 37°C in the dark. The fluorescence intensity of the samples in 96-well plates was determined on a fluoro-microplate reader with excitation and emission wavelengths of 390 and 460 nm, respectively. The fluorescent intensity is directly correlated to the level of GSH in each sample. A control containing media alone plus MCB was used as a blank and subtracted from the sample absorbances.

The ability of GSH to react directly with the peptidyl-methyl ketones was examined by a modified MCB assay adapted from the method used by Debiton and colleagues (2003). In brief, the peptidyl-methyl ketones (final concentration 100 µM) and GSH (final concentration 100 µM) were mixed together in 90 µl PBS, pH 7.4 in 96-well plates. The plates were incubated for 2 h at 37°C before addition of 10 µl MCB (final concentration 5 mM) and incubated for a further 30 min at 37°C. Fluorescence at 390/460 nm was measured and the results expressed as a percentage of control after subtraction of blank values.

2.3.9 Detection of ROS in cells using dihydroethidium (DHE)

DHE is a cell permeable dye which fluoresces red upon reaction with superoxide anions and is used extensively to monitor ROS production in cells (Owusu-Ansah et al., 2008). To measure the production of ROS, treated cells (1×10^6) were washed and the cell pellet re-suspended in 1 ml of pre-warmed serum-free RPMI with 2 µl of DHE solution (5 mM). The cells were incubated in the dark for 30 min at 37°C, washed with ice-cold PBS before re-suspending in 1 ml of PBS prior to analysis using flow cytometry. The fluorescent 2-hydroxyethidium was assessed with an

excitation wavelength of 532 nm (FL-2 channel) and the flow cytometer was calibrated using unstained cells prior to each experiment.

2.3.10 Statistical analysis

The data were analysed using standard error of means (SEM) as calculated by the software GraphPad Prism 5. Comparisons of the differences between untreated and treated groups were conducted using one-way ANOVA followed by Dunnett's post test.

2.4 Biochemical techniques

2.4.1 SDS-PAGE and Western blotting

2.4.1.1 Recipes for buffers and gels

Buffers	**Recipe**
Stacking gel buffer	0.5 M Tris, pH 6.8, 0.4 % SDS
Running buffer	25 mM Tris, 192 mM glycine, 0.1 % SDS
Transfer buffer	25 mM Tris, 192 mM glycine, 20 % MeOH
TBS	20 mM Tris, 137 mM NaCl, pH 7.6
TBS-T	TBS, 0.1 % Tween-20
Lysis buffer	0.1 M NaCl, 0.01 M Tris HCl (pH 7.6), 0.001 M EDTA, 1 % Triton-X, 1 mM PMSF (added fresh prior to use)
Loading buffer (4x)	8 % SDS, 40 % glycerol, 200 mM Tris HCl (pH 6.8), 0.08 % bromophenol blue, 200 mM DTT (added fresh prior to use)
Membrane stripping buffer	62.5 mM Tris, pH 6.8, 2 % SDS, 100 mM DTT (added fresh prior to use)

Material	**5 % Stacking gel** (3 ml)
dH_2O (ml)	2.25
Stacking gel buffer (µl)	375
40 % polyacrylamide (µl)	375
TEMED (µl)	3.2
APS (0.1 mg/ml) (µl)	24

Material	**13 % Resolving gel** (8 ml)
1.5 M Tris, pH 8.8 (ml)	2
40 % polyacrylamide (ml)	2.6
dH_2O (ml)	3.36
20 % SDS (µl)	40
TEMED (µl)	6
APS (0.1 mg/ml) (µl)	60

2.4.1.2 Preparation of resolving and stacking gels

The Biorad Miniprotean SDS-PAGE apparatus was used for all protein electrophoresis experiments. The large (10.2 x 8.3 cm) spacer plates (with attached 1.5 mm spacers) and small (10.2 x 7.3 cm) glass plates were thoroughly washed with dH_2O and air-dried. The plates were arranged properly in the casting chamber and held together using plastic clamps, making sure that the bottom edge of both plates were flush against the rubber gasket and secured into the casting frame by engaging the spring loaded lever. Once the casting chamber was set up, it was checked for leakage by adding 2 ml of dH_2O. If there was no leakage, the dH_2O was poured off and any traces removed using filter paper.

A 13 % resolving gel was used for all caspases. The resolving gel mixture was carefully pipetted into the space between the plates up to a level 1 cm from below the level of the comb teeth, once inserted. dH_2O (2 ml) was carefully pipetted onto the resolving gel immediately after casting in order to obtain an even top layer. After the resolving gel polymerized (1 h later), the dH_2O was drained and all traces removed using a filter paper. Then, a freshly prepared stacking gel solution was carefully layered on top of the resolving gel to about 0.5 cm from the top of the short glass, and a clean 10-well 1.5 mm comb inserted into the space between the plates, making sure the

comb ridge was aligned with the top of the short plate. After the gel had polymerized (1 h later), the comb was gently removed and the plates were removed from the casting stand and placed into the electrode assembly inside the tank. Once secured in the electrode assembly, the wells were rinsed using running buffer and the tank filled with running buffer.

2.4.1.3 Protein determination using Bradford dye reagent

Treated cells (1 x 10^6) were washed in ice-cold PBS and re-suspended in lysis buffer (10 µl for primary T cells or 25 µl for Jurkat cells). The cells were lysed by three rounds of freezing and thawing in liquid nitrogen. The protein concentration of the whole cell lysates was determined using the Bradford assay. In brief, 2 µl of cell lysates were diluted 18 µl of dH_2O and 5 µl of this diluted cell lysates were loaded in triplicate into wells of a flat bottom 96-well plate. A standard curve of BSA ranging from 125 – 1000 µg/ml (linear range) was run alongside the samples. For the generation of the standard curve, BSA stock (2 mg/ml) diluted in various concentrations with dH_20 and 5 µl of each BSA standard was added to the wells of the same 96-well plate Bradford dye reagent (250 µl) was added to each well and the solution mixed thoroughly. After a 30 min incubation period at room temperature, in the dark, the absorbance of the samples and the standards in the 96-well plate was determined at 595 nm using an ELISA plate reader. The cell extract protein concentrations were calculated using the standard curve generated.

2.4.1.4 Sample preparation

Cell lysate with equivalent of 20 µg protein were transferred to eppendorf tubes and diluted with lysis buffer to the volume of 15 µl. To the cell lysates was added 5 µl loading buffer (4x), mixed and the samples were then boiled for 10 min, cooled down and placed on ice till further use.

2.4.1.5 SDS-PAGE

After all the protein samples were loaded onto the wells, the gel was run at 120 V until the dye front reaches the bottom of the resolving gel.

2.4.1.6 Western blotting

A piece of nitrocellulose membrane was cut to size (7 x 10 cm) and saturated with dH_2O. Along with two pieces of filter paper and two fiber pads per gel, the membrane was then equilibrated in transfer buffer for at least 30 min. Following protein separation, the gel was removed from the tank and the stacking gel carefully removed. The resolving gel was allowed to equilibrate for 30 min in transfer buffer prior to transfer onto the nitrocellulose membrane using wet transfer. The gel holder cassette was prepared as follows:

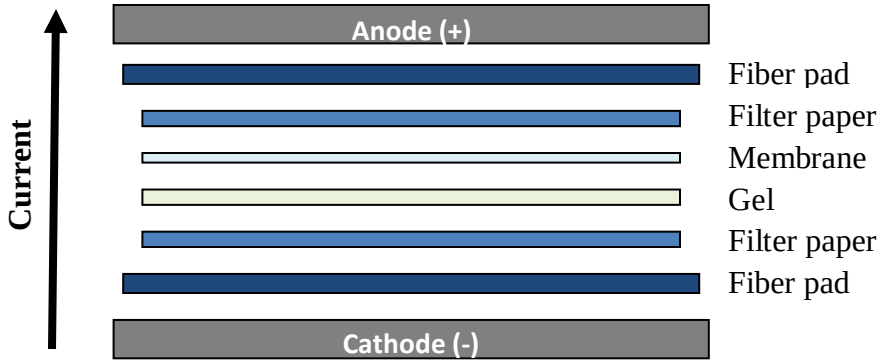

The proteins were transferred at 100 V for 1 h. Following the transfer, the membrane was removed and incubated with Ponceau-S solution for 1 min. The Ponceau-S solution was then washed off with dH_2O to assess whether the proteins had transferred evenly and also to note any loading errors or bubbles which may have occurred during the transfer of proteins onto the membrane. The Ponceau-S stain was then washed off with TBS-T and the membrane blocked

with freshly prepared TBS-T + 5 % non-fat dried milk for 1 h at room temperature with gentle agitation.

2.4.1.7 Immunodetection

After blocking, the membrane was washed twice with TBS-T for 5 min and then incubated with the primary antibody (Table 2.1) overnight at 4ºC. After overnight incubation, the antibody was removed and the membrane taken through one complete wash procedure (see below).

Washing Procedure:

1. TBS-T + 5 % non-fat dried milk (15 min)
2. TBS-T + 5 % non-fat dried milk (2 x 5 min)
3. TBS-T (15 min)
4. TBS-T (2 x 5 min)
5. TBS (10 min)

The membrane was then incubated with the appropriate HRP-conjugated secondary antibody (1:2000) (Table 2.2) in TBS-T for 1 h at room temperature under gentle shaking. Next, the membrane was taken through the complete washing procedure before being overlaid with 4 ml of the ECL reagent for 1 min at room temperature. The ECL reagent was drained off as much as possible by allowing the membrane to touch a piece of folded tissue paper. The membrane was sealed in between sheets of cling film, transferred on to a photographic cassette and exposed onto a sheet of x-ray film in the dark prior to developing. For re-probing for another protein, the membrane was stripped with 10 ml of membrane stripping buffer (see section 2.4.1.1) for 30 min

at 60ºC, blocked for 1 h at room temperature with TBS-T + 5 % non-fat dried milk and re-probed with another primary antibody.

Primary antibody	**Host species**	**Dilution (in TBS-T)**
Caspase 2	Rabbit	1:10000
Caspase 3	Rabbit	1:2000
Caspase 6	Rabbit	1:1000
Caspase 8	Goat	1:1500
Caspase 9	Rabbit	1:2000
β-actin	Mouse	1:5000

Table 2.1 Primary antibodies used for the immunodetection of transferred proteins

Secondary antibody	**Host species**	**Dilution (in TBS-T)**
Anti-goat	Rabbit	1:2000
Anti-mouse	Goat	1:2000
Anti-rabbit	Goat	1:2000

Table 2.2 Secondary antibodies used for the immunodetection of transferred proteins

CHAPTER THREE

Structure activity relationship of peptidyl-methyl ketone-induced immunosuppression and the activation of caspases during T cell activation and proliferation

3.1 Introduction

Peptidyl-fluoromethyl ketones (FMKs) were first designed to reduce the nonspecific alkylation properties of peptidyl-chloromethyl ketones (CMKs) (Rauber et al., 1986). However, once synthesized, peptidyl-FMKs were found to be highly reactive and selective irreversible inhibitors for serine and cysteine proteases (Powers et al., 2002). One of the first peptidyl-FMK inhibitors, benzyloxycarbonyl-Phe-Ala-fluoromethyl ketone (z-FA-FMK) with amino acids phenylalanine and alanine in the P2 and P1 positions respectively, was found to be a potent inactivator of human cathepsin B (Rasnick, 1985, Ahmed et al., 1992). Once bound to the active site, the FMK group alkylates the cysteine residue in the active site and forms a covalent bond, which irreversibly blocks the proteolytic activity of cathepsin B. However, besides blocking cathepsin B, accumulating evidence now suggests that z-FA-FMK may have non-specific effects. For instance, z-FA-FMK was found to inhibit LPS-induced cytokine production in macrophages by blocking the transactivation potential of NFκB (Schotte et al., 2001). In addition, z-FA-FMK at non-toxic concentrations blocks both mitogen and IL-2-mediated primary human T cell proliferation and inhibits blast transformation, IL-2 secretion, CD25 up-regulation and NFκB nuclear transformation (Lawrence et al., 2006). Although commonly used as a negative control for peptidyl-FMK caspase inhibitors, z-FA-FMK (Sarin et al., 1996, McColl et al., 1998) inhibited the processing of caspase-8 and caspase-3 in proliferating T cells but had no effect on the activation of these caspases during Fas-induced apoptosis (Lawrence et al., 2006). These findings suggest that the activation of caspases during T cell activation and proliferation is regulated differently from FasL-induced cell death.

There are also several discrepancies concerning which caspases become activated during T cell activation and proliferation. For example, in one study, T cell activation was shown to trigger the selective processing and activation of downstream caspases (caspase-3, caspase-6 and caspase-7) but not caspase-1, caspase-2 or caspase-4 (Alam et al., 1999). Caspase-8 processing has also been reported following T cell stimulation (Kennedy et al., 1999, Lawrence et al., 2006, Paulsen et al., 2008). However, other studies demonstrate that caspase-8 (Bidere et al., 2002), caspase-3 (Kennedy et al., 1999) and caspase-6 (Paulsen et al., 2008) are not processed in activated T cells. Variability between the experimental conditions used in each study, for example, the employment of different mitogens to activate T cells, coupled with the different concentrations of these mitogens, may account for some of the discrepancies between these reports.

In this chapter, the structure activity relationship of z-FA-FMK immunosuppressive effect and the activation of caspases during primary T cell activation and proliferation were examined.

3.2 Results

In this study, the proliferation of primary human T cells was induced by OKT3, an anti-CD3 monoclonal antibody which crosslink with the TCR-CD3 complex in the presence of monocytes or macrophages present in PBMCs. This mimics antigen-induced T cell proliferation and activates the signaling pathway leading to clonal expansion of T cells. Once activated, T cell proliferation was determined by the incorporation of BrdU into newly synthesized DNA strands of actively proliferating cells.

3.2.1 Anti-CD3-induced T cell proliferation

Initial studies were carried out to determine the optimal concentration of anti-CD3 required to activate primary T cells. Various concentrations of anti-CD3 (2.5, 5 and 7.5 μg/ml) were coated onto wells of a 96-well plate and T cell activation and proliferation was examined over a period of 24, 48 and 72 h. As shown in Figure 3.1, anti-CD3-induced a dose-dependent increase in T cell proliferation which reaches a maximum with 5 μg/ml anti-CD3 after 72 h. The decrease in T cell proliferation at higher concentrations of anti-CD3 (7.5 μg/ml) may be due to cell death as a result of over-stimulation. Based on these results, a concentration of 5 μg/ml anti-CD3 was used to induce T cell proliferation for 72 h in all subsequent experiments.

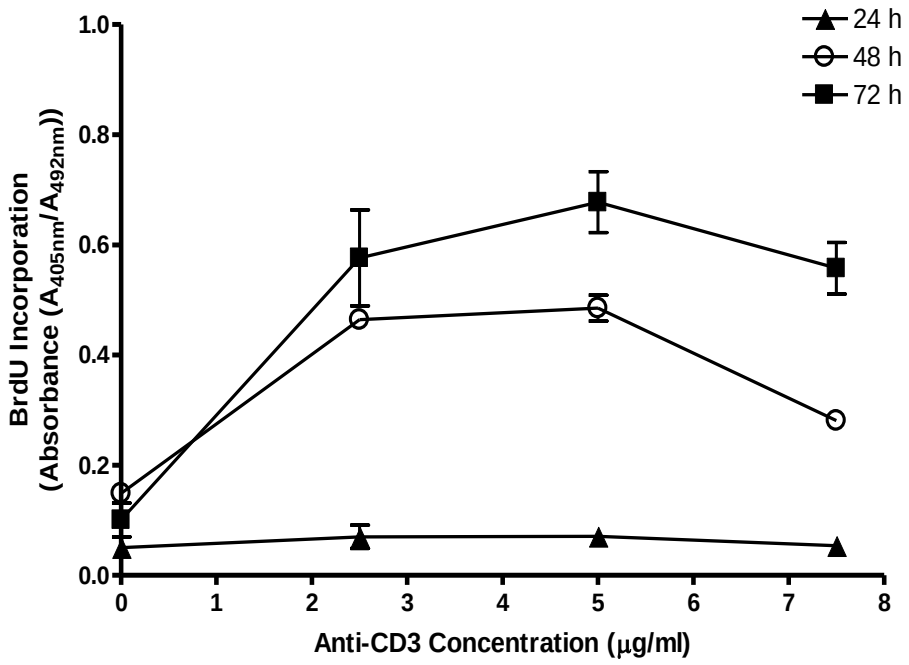

Figure 3.1 BrdU incorporation in stimulated T cells

PBMCs (1 x 10^6/ml) were seeded in duplicate into 96-well plates precoated with various concentrations of anti-CD3 for 24, 48 and 72 h. BrdU incorporation was assessed at each time point as outlined in the Materials and Methods. Results are the mean ± SEM of three independent experiments.

3.2.2 Effect of z-FA-FMK and its analogues on primary T cell proliferation

Previous studies have shown that the cathepsin B inhibitor, z-FA-FMK, effectively inhibited T cell activation and proliferation (Lawrence et al., 2006). In order to further understand the molecular mechanism of z-FA-FMK induced immunosuppression, structure activity studies were carried out using analogues of z-FA-FMK. To this end, the role of the FMK group in suppressing T cell proliferation was first examined using two analogues, z-FA-CMK and z-FA-DMK. As shown in Figure 3.2A, z-FA-FMK inhibited anti-CD3-induced T cell proliferation in a dose-dependent manner, as previously reported (Lawrence et al., 2006). When the FMK group was replaced with the DMK group, z-FA-DMK up to 100 μM had no inhibitory effect on T cell proliferation induced by anti-CD3. In sharp contrast, when the FMK group was replaced with the CMK group, z-FA-CMK completely abolished the anti-CD3-induced BrdU incorporation into primary T cells. The complete inhibition of T cell proliferation in the presence of 25 μM z-FA-CMK suggests that this peptide exerted a toxic effect.

Since only z-FA-FMK blocked T cell activation and proliferation, the result suggests that the FMK moiety plays an important role in the immunosuppressive properties of this peptidyl-methyl ketone observed in human T cells. To further characterise whether the FMK moiety per se in z-FA-FMK is responsible for inhibiting human T cell proliferation, two other FMK-containing methyl ketone peptides, z-YVAD-FMK, a caspase-1 inhibitor and z-VRPR-FMK, a MALT1 inhibitor, were examined. As illustrated in Figure 3.2B, both z-YVAD-FMK and z-VRPR-FMK had little effect on anti-CD3-induced T cell proliferation. This suggests that the FMK group per se is not immunosuppressive and that the suppression of T cell proliferation

induced by z-FA-FMK is likely to involve the combination of the FMK moiety and other parts of the molecule.

All the peptidyl-methyl ketone inhibitors examined so far possess a benzyloxycarbonyl group at the N-terminal. This group functions to protect the peptide against degradation of amino acids by proteases in the cell (Theodoridis, 2000, Isidro-Llobet et al., 2009). To determine whether the benzyloxycarbonyl group plays a role in blocking T cell activation and proliferation, the effect of having a biotin at the N-terminal instead of a benzyloxycarbonyl group was examined. As shown in Figure 3.3A, biotin-FA-FMK (up to 100 µM) was unable to block T cell proliferation after 72 h. To assess whether biotin-FA-FMK enters the cells, streptavidin-conjugated FITC (green fluorescence) was used to label biotin-FA-FMK treated cells prior to UV microscopy examination. As illustrated in Figure 3.3B, no staining was observed in resting control PBMCs, whereas following treatment with biotin-FA-FMK the cells were stained green, thus confirming that this methyl ketone is cell-permeable. This suggests that the benzyloxycarbonyl group at the N-terminal may be necessary for the immunosuppressive effects of z-FA-FMK.

Taken together, the results strongly indicate some degree of specificity in z-FA-FMK-mediated immunosuppression. Since z-FA-FMK has a phenylalanine in the P2 position and alanine in the P1 position, the effect of replacing alanine in P1 with phenylalanine was examined. To this end, the cathepsin L inhibitor, z-FF-FMK, was examined (Urbich et al., 2005, Baumgartner et al., 2007). As shown in Figure 3.4, z-FF-FMK which has phenylalanine in the P1 and P2 position was found to be even more potent in blocking T cell proliferation, with an IC_{50} of 20 µM compared to 50 µM with z-FA-FMK.

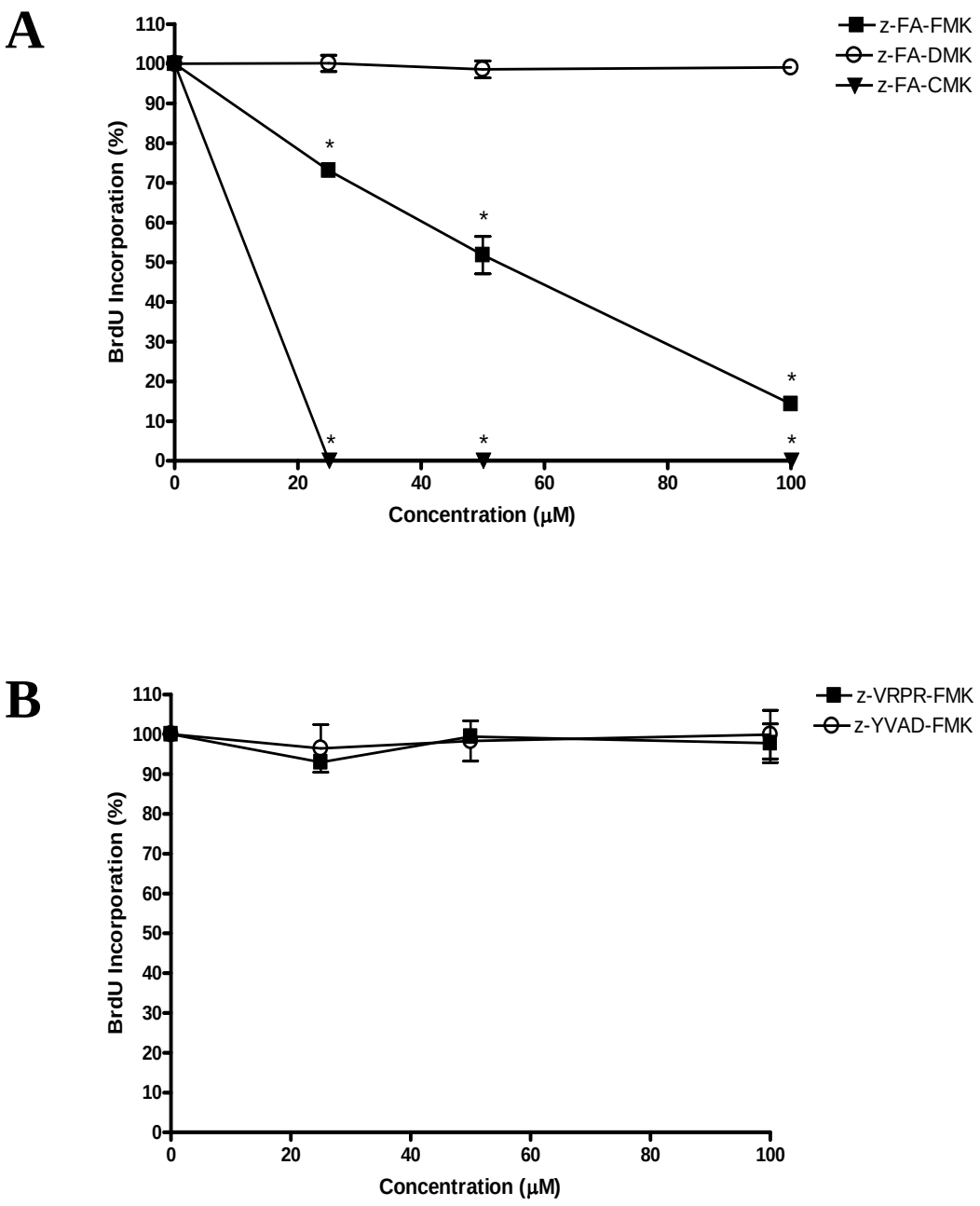

Figure 3.2 Effect of peptidyl-methyl ketones in PBMCs

PBMCs (1 x 10^6/ml) were seeded in duplicate into 96-well plates precoated with anti-CD3 (5 µg/ml) in the presence of (A) z-FA-FMK analogues or (B) various FMK groups at concentrations where indicated. BrdU incorporation was assessed after 72 h as described in the Materials and Methods. Results are the mean ± SEM of at least three independent experiments. *, Significantly decreased ($p < 0.05$) from control.

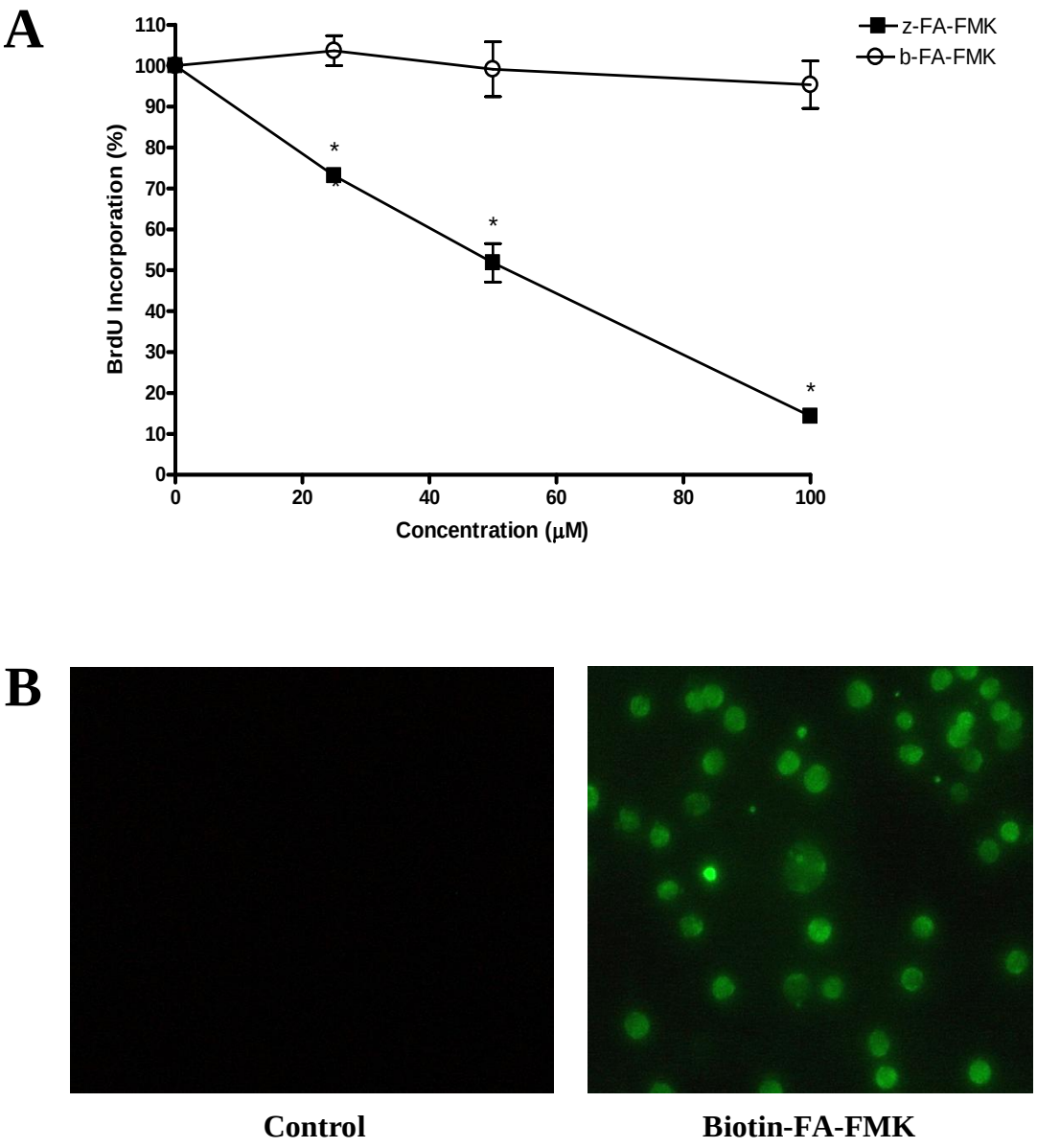

Figure 3.3 Effect of the benzyloxycarbonyl group in PBMCs

PBMCs (1 x 10^6/ml) seeded in duplicate into 96-well plates were precoated with anti-CD3 (5 μg/ml) and in the presence z-FA-FMK or biotin-FA-FMK at concentrations where indicated. (A) BrdU incorporation was assessed after 72 h as described in the Materials and Methods. Results are the mean ± SEM of at least three independent experiments. (B) Control and biotin-FA-FMK-treated PBMCs (1 x 10^6/ml) were stained with streptavidin-conjugated FITC and visualised at using UV microscopy (20x magnification). The results are representative of two separate experiments. *, Significantly decreased ($p < 0.05$) from control.

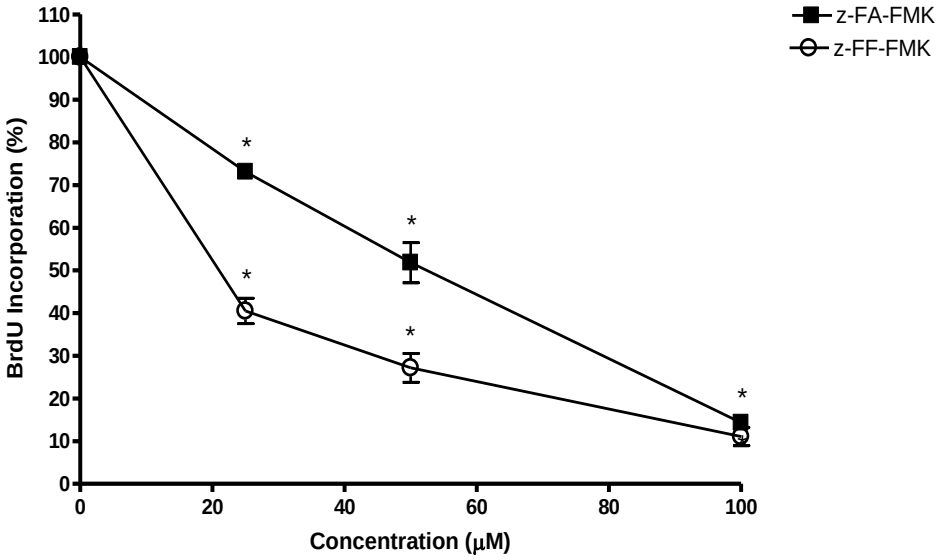

Figure 3.4 Effect of peptidyl-FMK inhibitors with different amino acids in PBMCs

PBMCs (1 x 10^6/ml) were seeded in duplicate into 96-well plates precoated with anti-CD3 (5 μg/ml) in the presence of z-FA-FMK or z-F-FMK at concentrations where indicated. BrdU incorporation was assessed after 72 h as described in the Materials and Methods. Results are the mean ± SEM of at least three independent experiments. *, Significantly decreased ($p < 0.05$) from control.

3.2.3 Toxicity of the peptidyl-methyl ketones in primary T cells

Since z-FA-CMK, z-FA-FMK and z-FF-FMK block T cell proliferation, it was necessary to determine whether the reduction in BrdU incorporation is due to cytotoxic effect. To this end, the toxicity of these inhibitors was examined in PBMCs. As shown in Figure 3.5A, z-FA-FMK did not induce any significant increase in PI uptake compared to control cells ($p > 0.05$). Although in the presence of z-FF-FMK, the PI uptake was slightly increased compared to untreated cells, the results were not significant ($p > 0.05$). In sharp contrast, all the cells took up PI when treated with z-FA-CMK indicating that this peptide was toxic and explains the complete inhibition of T cell proliferation measured by the BrdU incorporation assay (Figure 3.2A). Therefore, these results suggest that the inhibition of T cell proliferation mediated by z-FA-FMK and z-FF-FMK is not due to toxicity. To determine whether T cells become susceptible to peptidyl-methyl ketone-mediated toxicity following stimulation with anti-CD3, the effect of these peptides on the uptake of PI in activated T cells was examined. PBMCs were first activated with anti-CD3 for 24 h before layering onto lymphoprep to remove any dead cells. After centrifugation, the live activated T cells were cultured in the presence of human rIL-2 (25 U/ml) prior to the treatment with various concentrations of peptidyl-methyl ketones. As shown in Figure 3.5B, there was no significant increase in PI uptake in activated T cells incubated with z-FA-FMK and z-FF-FMK compared to untreated cells. These results suggest these peptidyl-FMK inhibitors are not toxic to activated T cells. Similar to resting T cells, activated T cells were equally sensitive to z-FA-CMK as nearly all the cells took up PI after treatment with this methyl ketone peptide (Figure 3.5B). Collectively, these results suggest that the inhibition of T cell proliferation mediated by z-FA-FMK and z-FF-FMK is not due to direct toxicity of these compounds.

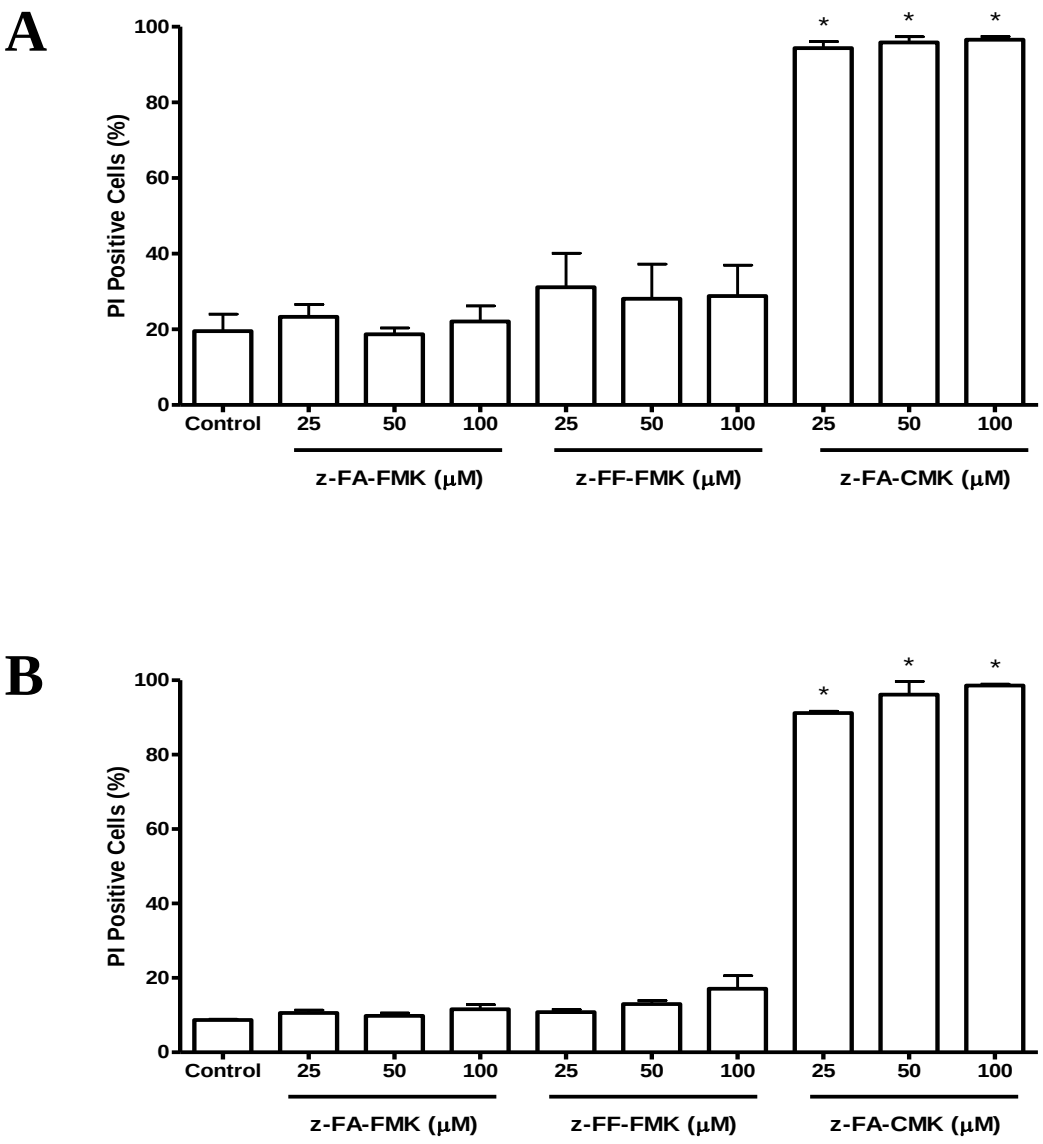

Figure 3.5 Toxicity of peptidyl-methyl ketones in primary T cells

(A) Resting PBMCs (1 x 10^6/ml) were incubated in 24-well plates with various concentrations of z-FA-FMK, z-FF-FMK or z-FA-CMK for 24 h. (B) Activated T cells (1 x 10^6/ml) were seeded in 24-well plates in the presence of rIL-2 (25 U/ml) and treated with z-FA-FMK, z-FF-FMK or z-FA-CMK for 72 h. At the indicated time points, dead cells were identified as PI positive using flow cytometry as described in Materials and Methods. Results are the means ±SEM of three independent experiments. *, Significantly increased ($p < 0.05$) from control.

3.2.4 Effect of z-FA-FMK and z-FF-FMK on mitogen-induced primary T cell division using CFSE labeling

Since z-FF-FMK was more potent in blocking T cell proliferation compared to z-FA-FMK, its effect on T cell activation and proliferation was further characterized. In order to confirm the BrdU incorporation data (Figure 3.4), another approach was used which involves the labeling of cells with the CFSE dye (Parish, 1999). Due to covalent coupling between CFSE succinimidyl group and intracellular molecules, the dye is not transferred to adjacent cells but partitioned equally among daughter cells during cell division. This allows for the analysis of each successive division by the halving of cellular CFSE fluorescence intensity using flow cytometry (Lyons and Parish, 1994). As illustrated in Figure 3.6, cellular CFSE fluorescence intensity remained high in resting T cells after 72 h, indicating that the cells were quiescent. In contrast, T cells that were activated with anti-CD3 for 72 h were actively dividing, indicated by the decrease in cellular CFSE fluorescence intensity. As expected z-FA-FMK (50 and 100 μM) treatments prevented the decrease in cellular CFSE fluorescence intensity compared to control (Lawrence et al., 2006). Similarly, z-FF-FMK treatments also blocked the reduction in cellular CFSE fluorescence intensity, further corroborating the inhibition of T cell proliferation mediated by z-FF-FMK seen earlier (Figure 3.4). The results also demonstrated that z-FF-FMK was more potent compared to z-FA-FMK, blocking of CFSE dilution in the treated cells with concentration as low as 25 μM (Figure 3.6).

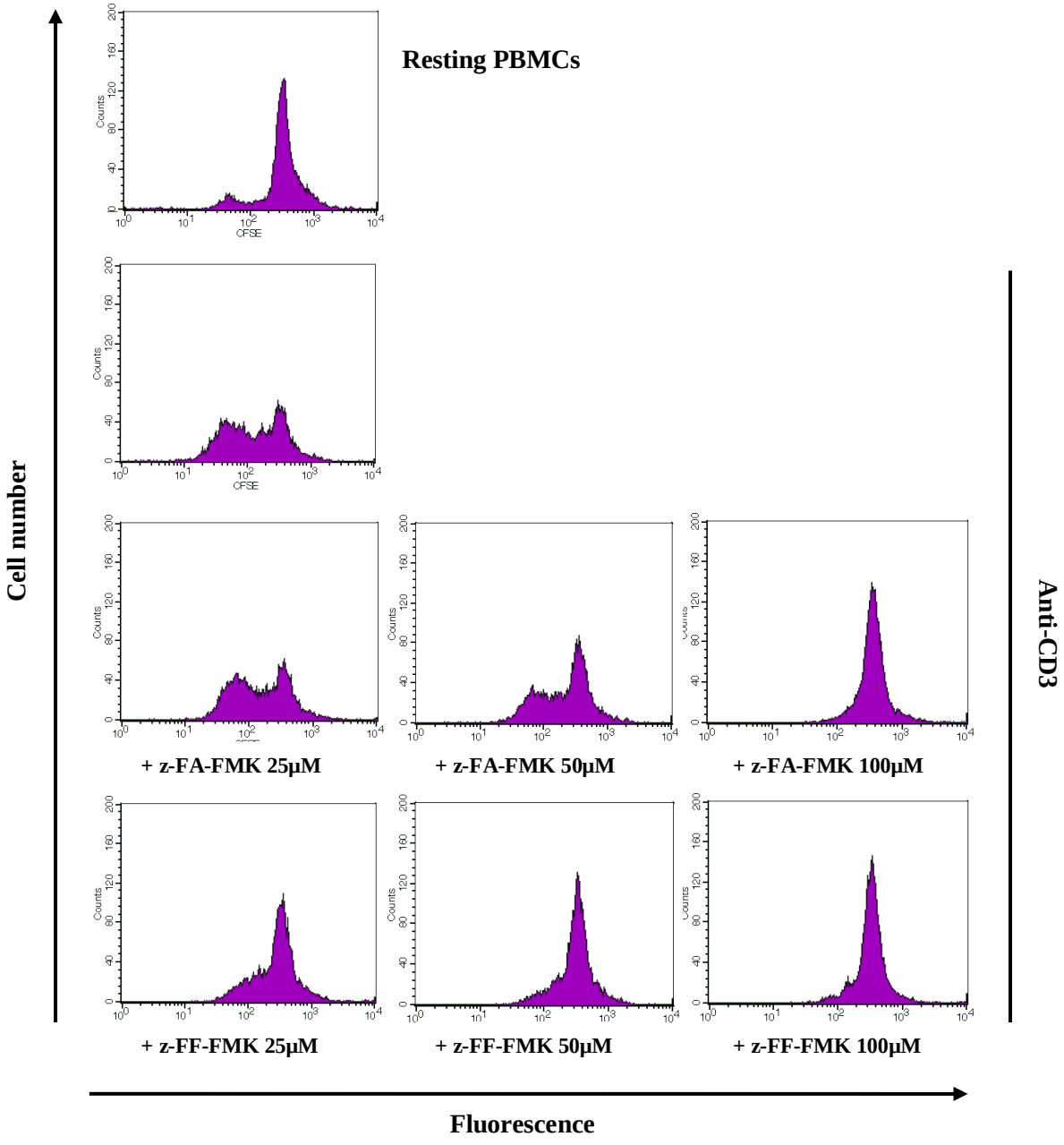

Figure 3.6 Inhibition of anti-CD3-induced cell division by z-FA-FMK and z-FF-FMK

PBMCs (1 x 10^6/ml) were stained with CFSE (5 µM) prior to stimulation with anti-CD3 (5 µg/ml) in the presence or absence of various concentrations of z-FA-FMK or z-FF-FMK. After 72 h, cell division was analysed using flow cytometry as described in Materials and Methods. Unstained cells (both resting and stimulated) were consistently $<10^1$ FL-1. The results are one representative from three independent experiments.

3.2.5 Effect of z-FA-FMK and z-FF-FMK on primary T cell blast formation

Upon T cell activation, resting T cells are transformed into T cell blasts which are recognized by their increased size. To determine whether T cell blast formation is blocked by z-FF-FMK, T cells were stimulated with anti-CD3 antibodies for 72 h and blast formation examined using flow cytometry. As illustrated in Figure 3.7, the percentage of blasts in resting control T cells increased from 11.1 % (control) to 58.8 % following T cell activation. In the presence z-FA-FMK (25 – 100 μM), there was a dose-dependent decrease in T cell blast formation as previously reported (Lawrence et al., 2006). At higher concentrations of z-FA-FMK (50 and 100 μM), the number of T cell blasts dropped to 29.1 % and 15.1 %, respectively. With z-FF-FMK, the inhibition of T cell blasts formation was more pronounced, reducing to 20.7 % at 25 μM. At higher concentrations (50 and 100 μM), the formation of T cell blast was further reduced to 13.1 % and 12.0 %, respectively. These results suggest that the z-FF-FMK inhibits the transformation of resting cells into T cell blasts following mitogen stimulation. Collectively, these results are in good agreement with the BrdU incorporation and cell division results with CFSE (Figure 3.2, Figure 3.4 and Figure 3.5).

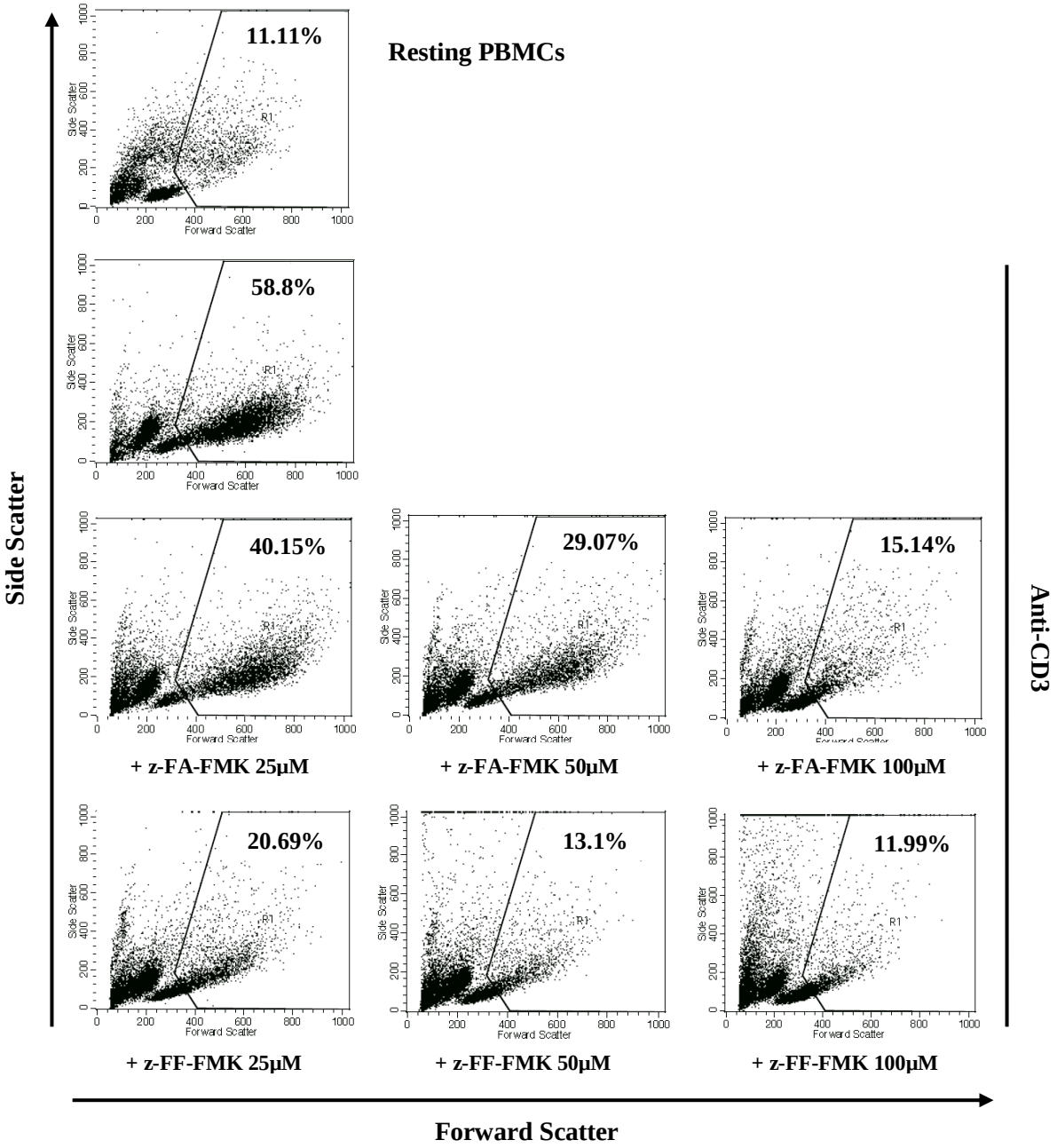

Figure 3.7 Inhibition of T cell blasts formation by peptidyl-FMK inhibitors

PBMCs (1 x 10^6/ml) were activated with anti-CD3 (5 µg/ml) in the presence or absence of various concentrations of z-FA-FMK or z-FF-FMK. After 72 h, transformation of resting T cells into lymphoblasts was determined using flow cytometry as described in Materials and Methods. The results are one representative of three independent experiments. Percentage of T cell blasts with solvent control is 57.5 %.

3.2.6 Effect of z-FA-FMK and z-FF-FMK on CD25 and CD69 up-regulation

In resting T cells, the IL-2 receptor (CD25) is not expressed on the cell surface. However, following T cell activation, IL-2 is synthesised and secreted, and the α-subunit of the IL-2 receptor is up-regulated. Once secreted, IL-2 activates T cells in an autocrine and paracrine fashion and drives T cell proliferation (Nelson, 2004). Therefore, the up-regulation of CD25 is often used as an early marker for T cell activation. As shown in Figure 3.8, the percentage of cells which expressed CD25 increased from 3.6 % in resting T cells to 60.1 % following anti-CD3 stimulation for 72 h. In the presence of z-FA-FMK, CD25 expression was reduced dose-dependently to 46.1 %, 32.5 % and 13.0 % at 25, 50 and 100 μM, respectively, which is very much in line with previous studies (Lawrence et al., 2006). As expected, z-FF-FMK, being more potent in blocking T cell proliferation, reduced the percentage of cells expressing CD25 to 19.96 % at 25 μM. Higher concentrations of z-FF-FMK (50 and 100 μM) did not significantly reduce the expression of CD25 further ($p > 0.05$) compared to 25 μM z-FF-FMK. These findings suggest that these peptidyl-FMK inhibitors may in part inhibit T proliferation through the inhibition of CD25 expression, hence reducing the signals required to drive T cell proliferation mediated by IL-2.

Another early T cell activation marker, CD69, was also examined in the presence of the peptidyl-FMK. As shown in Figure 3.9, CD69 expression increased from 2.87 % in resting T cells to 51.2 % in activated T cells after 72 h. At 25 μM, z-FA-FMK had little effect on CD69 expression whereas at higher concentrations (50 and 100 μM), the expression of CD69 was markedly reduced to 35.7 % and 22.4 %, respectively. Similar to CD25 inhibition (Figure 3.8), z-FF-FMK at 25 μM markedly reduced CD69 expression to 26 % while increasing z-FF-FMK

concentrations (50 and 100 μM) did not significantly reduce CD69 expression any further. The inhibition of CD69 up-regulation in the presence of z-FA-FMK and z-FF-FMK is similar to the effect observed with CD25 expression, suggesting that these peptidyl-FMK inhibitors block the signaling pathways leading to both CD25 and CD69 up-regulation.

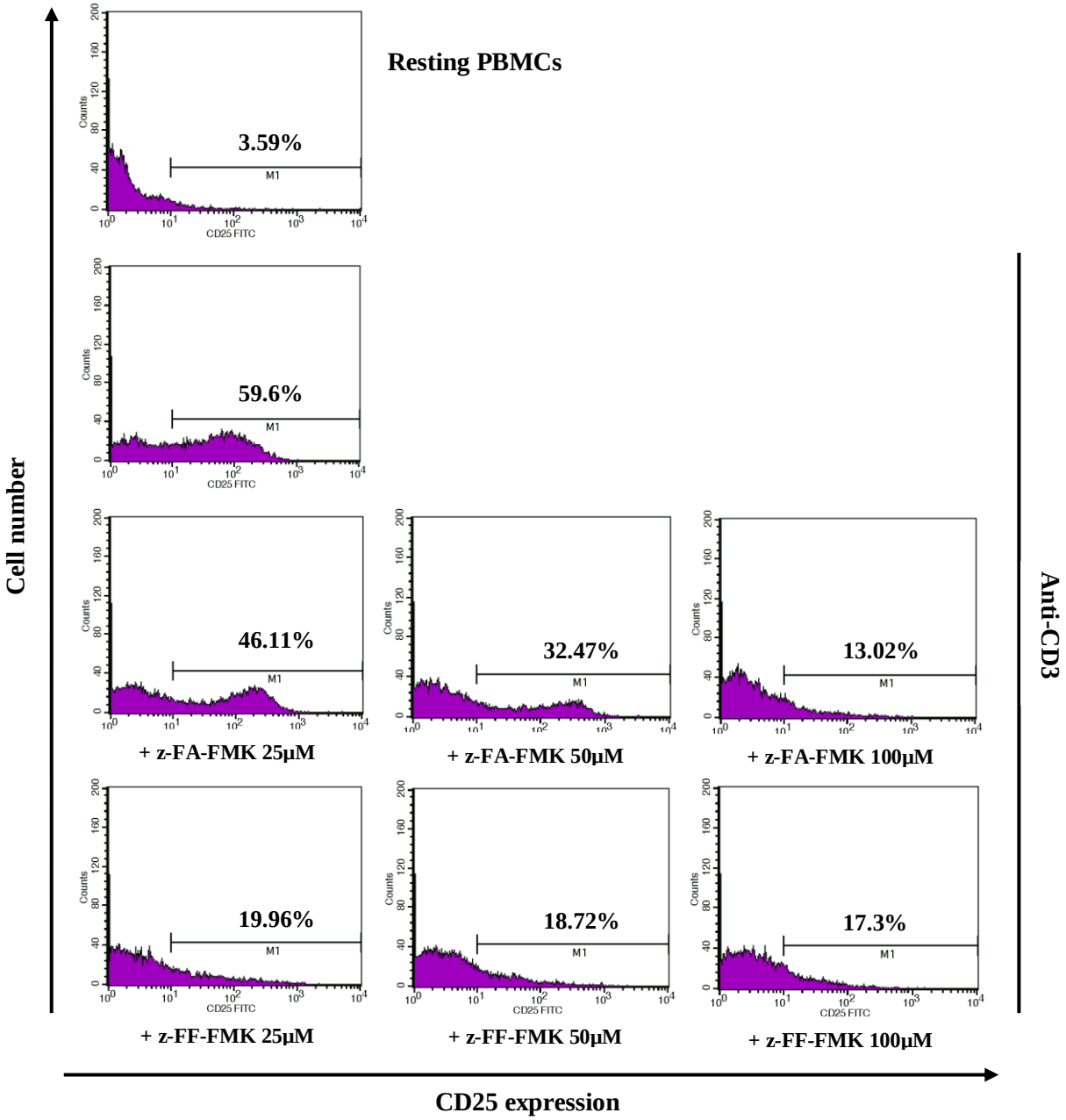

Figure 3.8 Inhibition of CD25 up-regulation by z-FA-FMK and z-FF-FMK

PBMCs (1 x 10^6/ml) were activated with anti-CD3 (5 µg/ml) in the presence or absence of various concentrations of z-FA-FMK or z-FF-FMK. After 72 h, the cells were stained with FITC-conjugated anti-CD25 and analysed using flow cytometry as described in Materials and Methods. The percentage of cells stained positive for CD25 is presented. The results are one representative of three independent experiments.

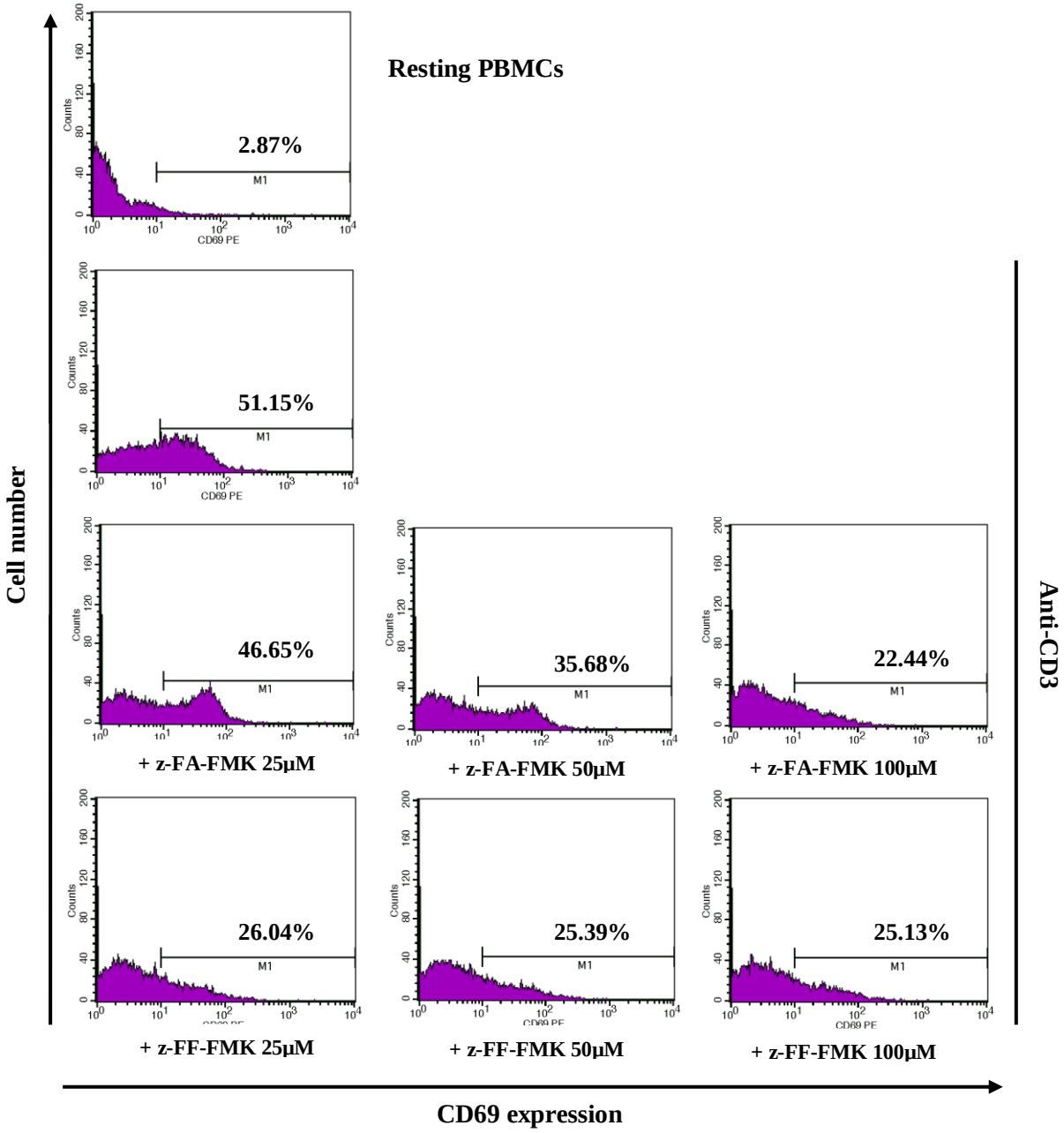

Figure 3.9 Inhibition of CD69 up-regulation by z-FA-FMK and z-FF-FMK

PBMCs (1 x 10^6/ml) were activated with anti-CD3 (5 µg/ml) in the presence or absence of various concentrations of z-FA-FMK or z-FF-FMK. After 72 h, the cells were stained with PE-conjugated anti-CD69 and analysed using flow cytometry as described in Materials and Methods. The percentage of cells stained positive for CD69 is presented. The results are one representative of three independent experiments.

3.2.7 Effect of z-FA-FMK and z-FF-FMK on IL-2 driven T cell proliferation

Since z-FA-FMK and z-FF-FMK inhibited the up-regulation of the IL-2 receptor, CD25 (Figure 3.8), the effect of these peptidyl-FMK inhibitors on IL-2 signaling downstream of CD25 expression was determined. To this end, the effect of these inhibitors on IL-2 driven T cell proliferation was examined. PBMCs were activated with anti-CD3 (5 μg/ml) for 24 h and the T cell blasts isolated using density gradient centrifugation to remove the dead cells. The activated T cells were seeded in fresh medium supplemented with human rIL-2 (25 U/ml) every 3 days. After 7 days, the cells were re-seeded in the presence or absence of various peptidyl-FMK inhibitors in the presence of rIL-2. BrdU incorporation into DNA was determined after a further 72 h of cell culture. As illustrated in Figure 3.10, z-FA-FMK inhibited IL-2-driven T cell proliferation in a dose-dependent manner with an IC_{50} of 50μM. Similar to z-FA-FMK, z-FF-FMK also blocked IL-2 driven T cell proliferation in a dose-dependent manner, but was more potent with an IC_{50} of 25μM.

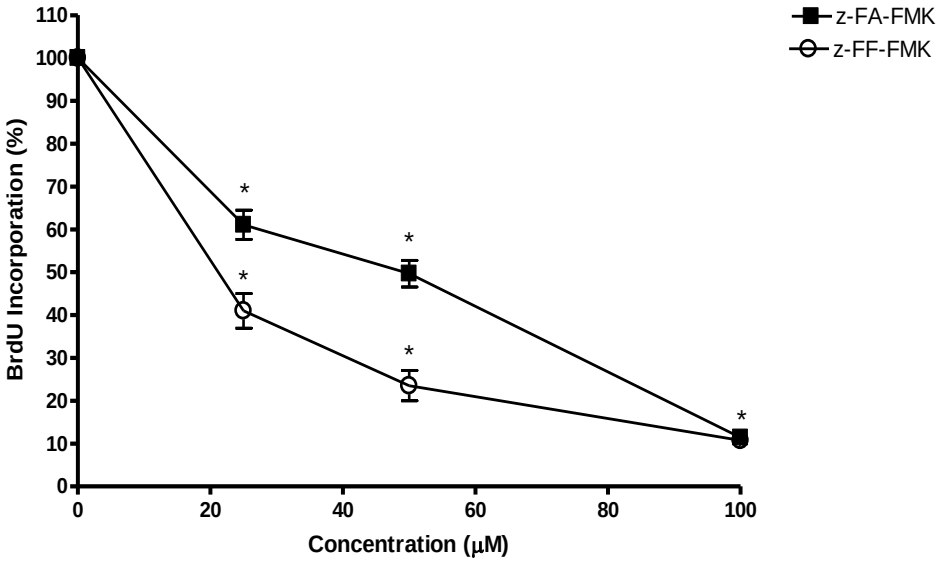

Figure 3.10 Effect of z-FA-FMK and z-FF-FMK on IL-2 driven cycling T cells

Cycling T cells (1 x 10^6/ml) were generated and seeded in duplicate in 96-well plates in the presence of rIL-2 (25 U/ml) and various concentrations of z-FA-FMK or z-FF-FMK. BrdU incorporation was assessed after 72 h by measuring absorbance on a plate reader as described in Materials and Methods. Results are the mean ± SEM of three independent experiments. *, Significantly decreased ($p < 0.05$) from control.

3.2.8 Effect of z-FA-FMK and z-FF-FMK on cell cycle progression in primary T cells

As demonstrated in Figure 3.8 and 3.9, z-FA-FMK and z-FF-FMK block the signaling pathways leading to CD25 and CD69 up-regulation. This finding may explain, in part, the inhibitory effect of the peptidyl-FMKs on T cell proliferation. However, it is also possible that these peptidyl-FMK inhibitors may have an effect on cell cycle progression. To investigate this, PBMCs were activated in the presence of z-FA-FMK or z-FF-FMK and cell cycle progression was determined after 72 h. As shown in Figure 3.11, resting T cells remained in the G_1 phase (91.2 %), whereas after anti-CD3-stimulation, the cells entered the cell cycle as shown by the reduction in the number of cells in the G0/G1 phase (65.3 %) and distribution of the cells in the S/G2/M phases (31.9 %). As reported previously (Lawrence et al., 2006), z-FA-FMK at 25 and 50 μM had little effect on cell cycle progression, whereas in the presence of 100 μM, more cells accumulated in the G_1 phase suggesting that the cell cycle is blocked. In the presence of z-FF-FMK, cell cycle progression was blocked by almost 20 % at 25 μM and higher concentrations (50 and 100 μM) lead to more cells accumulating in the G_1 phase. These results are very much in line with earlier results indicating that z-FF-FMK is more efficient in blocking T cell proliferation compared to z-FA-FMK.

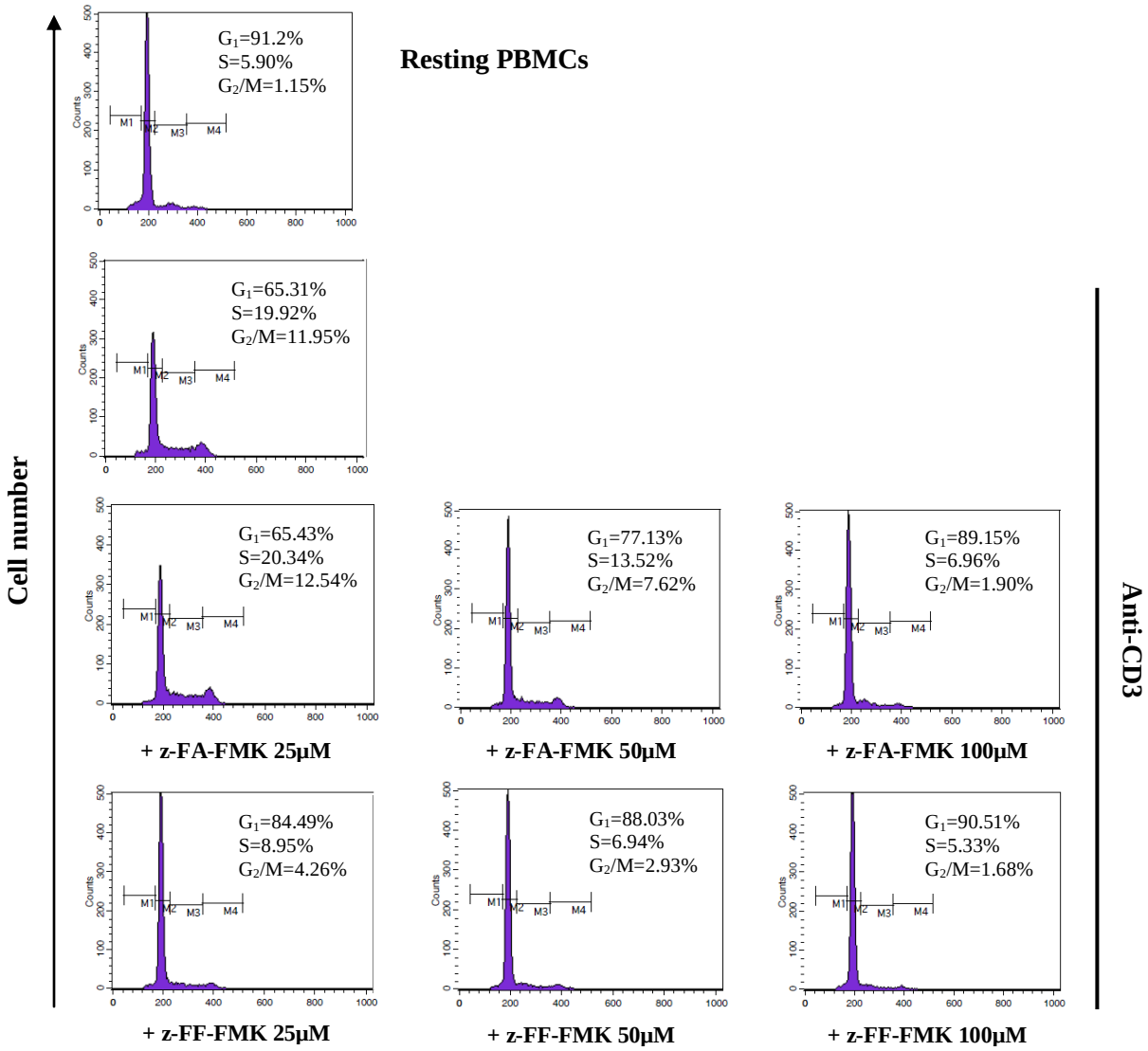

Figure 3.11 Effect of peptidyl-FMK inhibitors on primary T cell cycle

PBMCs (1 x 10^6/ml) were stimulated with anti-CD3 (5 µg/ml) in the presence or absence of various concentrations of z-FA-FMK or z-FF-FMK. After 72 h, the DNA content was analysed after staining with PI. Solvent control G_1 = 66.37 %, S = 18.21 %, G_2/M = 14.37 %. The results are one representative of three independent experiments.

3.2.9 Caspase processing in the absence of apoptosis in activated primary T cells

Previous studies have shown that both caspase-8 and caspase-3 were activated during T cell activation and proliferation (Lawrence et al., 2006). To determine whether other caspases were activated during T cell activation and proliferation, PBMCs were stimulated with anti-CD3 for 24, 48 and 72 h. At each time point, viable activated T cells were isolated using gradient density centrifugation, which remove dead cells such as non-activated PBMCs. Cell lysates from the activated cells were probed for the processing of initiator caspase-8, -2 and -9, as well as the effector caspase-3 and -6 using Western Blot analysis. As a positive control, PBMCs were treated with STS (1 µM) for 2 h to induce apoptosis. As shown in Figure 3.12, none of the caspases examined were activated in resting T cells. However, following anti-CD3-stimulation there was an increase in the processing of caspase-8 as shown by the increase in the p43/p42 intermediate subunits after 48 h which increased further after 72 h. Interestingly, nearly all caspase-2 was processed after 48 h to the p12 active subunit following anti-CD3 stimulation and no further increase in the p12 subunit was observed at 72 h. Caspase-9, the initiator caspase that cleaves caspase-3, was processed to its p35 subunit after stimulation with anti-CD3 for 48 h and was further processed by 72 h. The processing of caspase-3 to its active subunits proceeds via sequential proteolytic steps. The first step involves the removal of the small subunit (p12) from the 32kDa pro-caspase to generate the p20 subunit. Then the prodomain is removed from the p20, which via a p19 intermediate, generates the p17 large subunit (Han et al., 1997). In the activated T cells, most of the pro-caspase-3 was processed 48 h following stimulation with anti-CD3 (Figure 3.12). Western blot analysis also revealed that some pro-caspase-6 was processed in activated T cells from as early as 24 h after anti-CD3 stimulation as seen by the decreased in the

pro-caspase-6 band. As illustrated in Figure 3.12, all the caspases examined were cleaved following apoptosis induced by STS.

As caspase processing is synonymous with apoptosis, several assays were employed to ensure that the activated T cells lack apoptotic characteristics. Firstly, the externalisation of PS, an early marker for apoptotic cells was examined using FITC-labelled annexin V which is frequently used to tag apoptotic cells (Koopman et al., 1994). Simultaneous staining with PI distinguishes apoptotic cells from necrotic cells. As illustrated in Figure 3.13A, similar to control cells, activated T cells did not bind to annexin V or take up PI, suggesting that activated T cells are not apoptotic. As a positive control, STS-treated Jurkat T cells showed a marked increase in annexin V binding indicating that STS-treated cells are apoptotic (Figure 3.13B). Another hallmark of apoptosis is the loss of mitochondrial membrane potential (MMP), which can be detected using the dye, TMRE (Jayaraman, 2005). TMRE is a positively charged molecule that accumulates in the mitochondrial matrix of healthy cells and emits high fluorescence intensity. The loss of this fluorescence intensity seen in apoptotic cells is due to the collapse of the mitochondrial membrane potential which no longer permits the accumulation of TMRE. As shown in Figure 3.13C, activated T cells did not exhibit any loss in the mitochondrial membrane potential, which supports the annexin V binding results demonstrating that activated T cells were not apoptotic. In contrast, STS-treated Jurkat T cells resulted in a loss of mitochondrial membrane potential as observed by the decreased fluorescence intensity (Figure 3.13D). Another characteristic feature of apoptotic cells is the nuclear morphological changes from a normal to condensed or fragmented nuclei in apoptotic cells. To examine this, control and anti-CD3-stimulated T cells were stained with the DNA-binding dye, Hoechst 33342. As shown in Figure 3.13E, activated T

cells have similar morphology as resting cells, suggesting that the activated T cells were not apoptotic. As a positive control, STS-treated T cells exhibited condensed and fragmented nuclei which are characteristic of apoptotic cells.

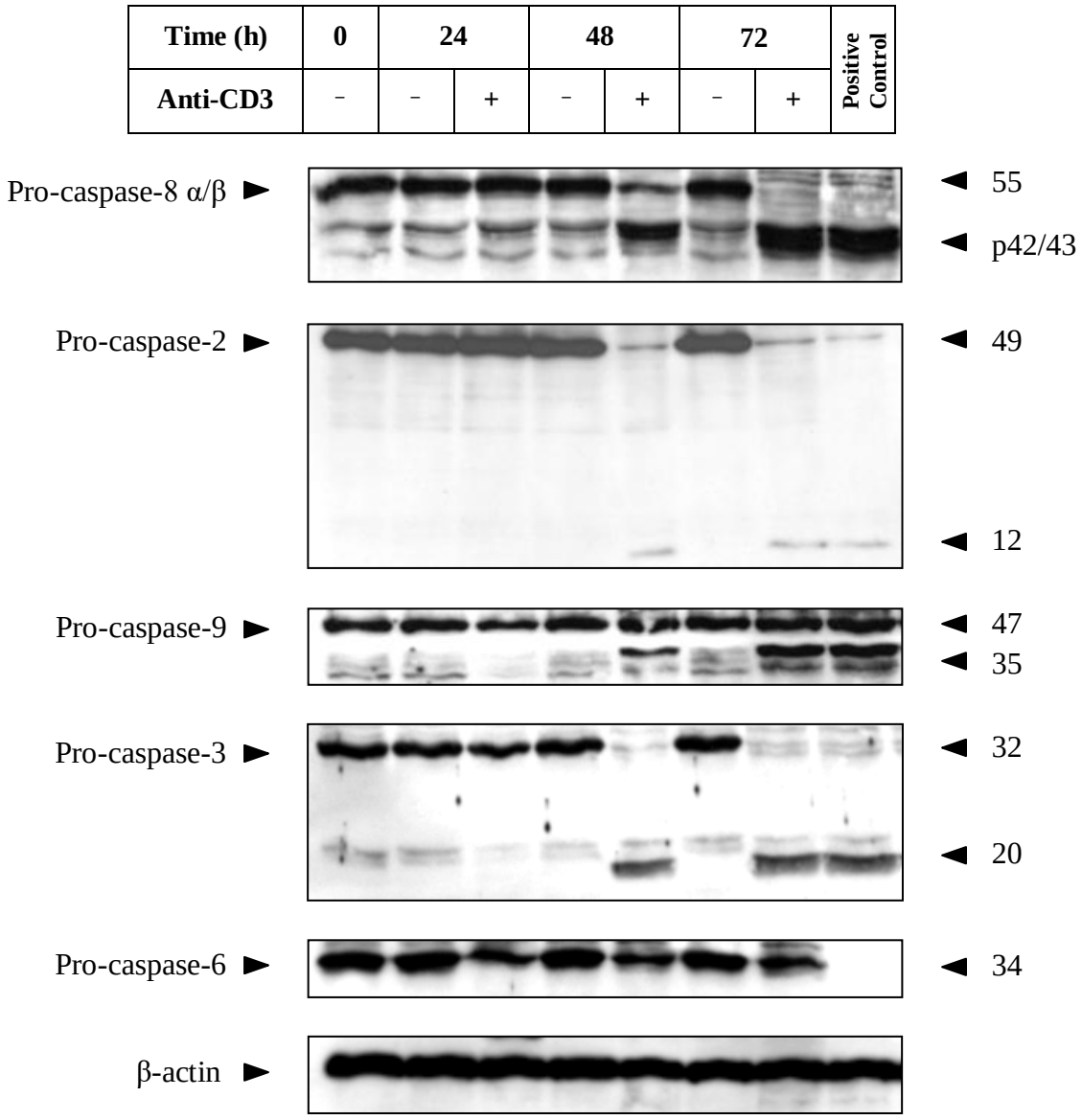

Figure 3.12 Time course profiling of caspases in activated T cells

PBMCs (1 x 10^6/ml) were activated with anti-CD3 (5 µg/ml) for 24, 48 and 72 h. At each time point, the cells were subjected to gradient density centrifugation to obtain pure, activated T cells. Whole cell lysates (20 µg protein) from the activated T cells were resolved using 13 % SDS-PAGE, transferred to nitrocellulose membrane and probed for caspases. STS-treated T cells were used as a positive control. The results are one representative of three independent experiments.

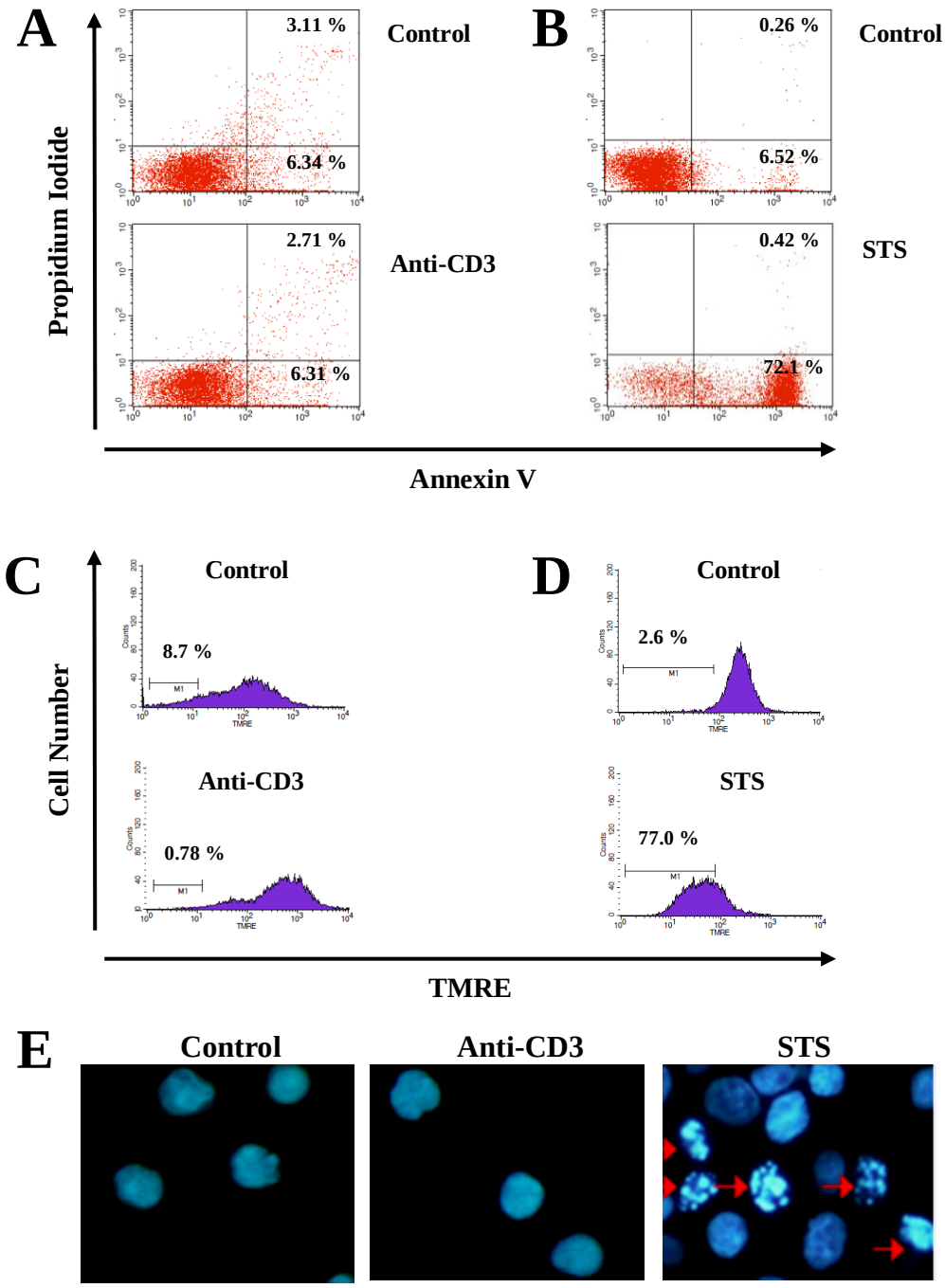

Figure 3.13 Activated T cells show no apoptotic characteristics

PBMCs were stimulated with anti-CD3 for 72 h. The cells were then assayed for apoptotic features as outlined in Materials and Methods. **(A)** Annexin V staining and PI uptake. **(C)** Detection of MMP using TMRE staining. **(E)** Nuclear morphology stained with Hoechst 33342. Arrow indicates an apoptotic nucleus in PBMCs treated with STS. In **(B)** & **(D)** STS-treated Jurkat T cells were used for the positive control. The results are one representative of three independent experiments.

3.2.10 Effect of z-FA-FMK and z-FF-FMK on the activation of caspases in activated primary T cells

Previous studies have shown that z-FA-FMK inhibits T cell activation and proliferation as well as blocking the activation of caspase-8 and caspase-3 (Lawrence et al., 2006). The effect of z-FA-FMK and z-FF-FMK on the activation of caspases besides caspase-8 and caspase-3 was examined. As shown in Figure 3.14A, z-FA-FMK induced a dose-dependent inhibition of caspase-8 processing in T cells following anti-CD3-activation for 72 h. At 25 μM z-FA-FMK, only a small effect on the processing of caspase-8 was observed. This reduction of the p43/42 subunits of caspase-8 became more apparent in the presence of 50 μM z-FA-FMK while at 100 μM, the generation of these subunits was nearly completely inhibited. For caspase-2, treatment with 25 μM z-FA-FMK slightly reduced the processing of caspase-2 to the p12 subunit while higher concentrations (50 and 100 μM) completely blocked the generation of this subunit. Interestingly, the decrease in pro-caspase-6 was completely restored with only 25 μM z-FA-FMK. As for caspase-3, both the loss of the pro-caspase-3 band and the appearance of the p18 subunit were inhibited by 25 μM z-FA-FMK. Higher concentrations (50 and 100 μM) of z-FA-FMK completely abolished the processing of caspase-3. The processing of caspase-9 to its p35 subunit was partially blocked by the presence of 25 and 50 μM z-FA-FMK while the appearance of the p35 subunit was completely inhibited by 100 μM z-FA-FMK. In sharp contrast, z-FF-FMK at 25 μM completely blocked the activation and processing of all the caspases examined (Figure 3.14B). These results are in keeping with previous data (Figure 3.2B) which show that z-FF-FMK is more potent than z-FA-FMK in blocking T cell activation and proliferation.

A

Anti-CD3	–	+	+	+	+
Concentration of z-FA-FMK (μM)	–	–	25	50	100

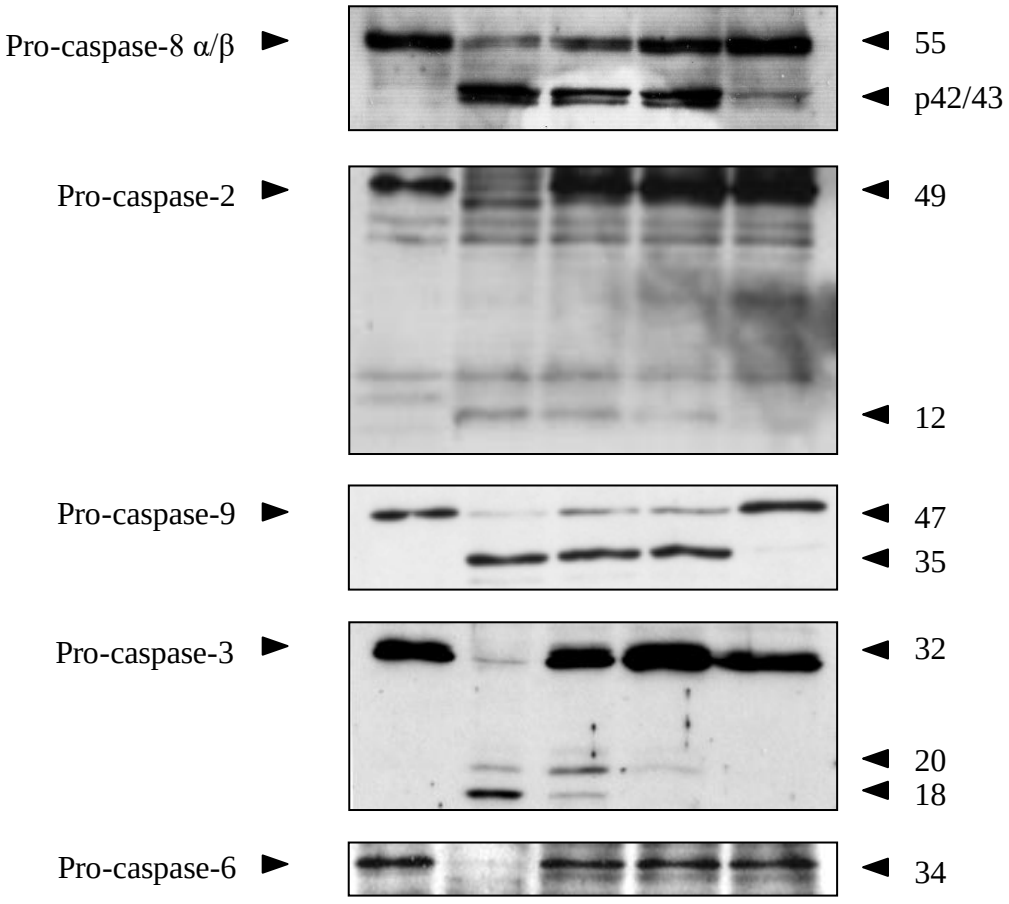

B

Anti-CD3	–	+	+	+	+
Concentration of z-FF-FMK (μM)	–	–	25	50	100

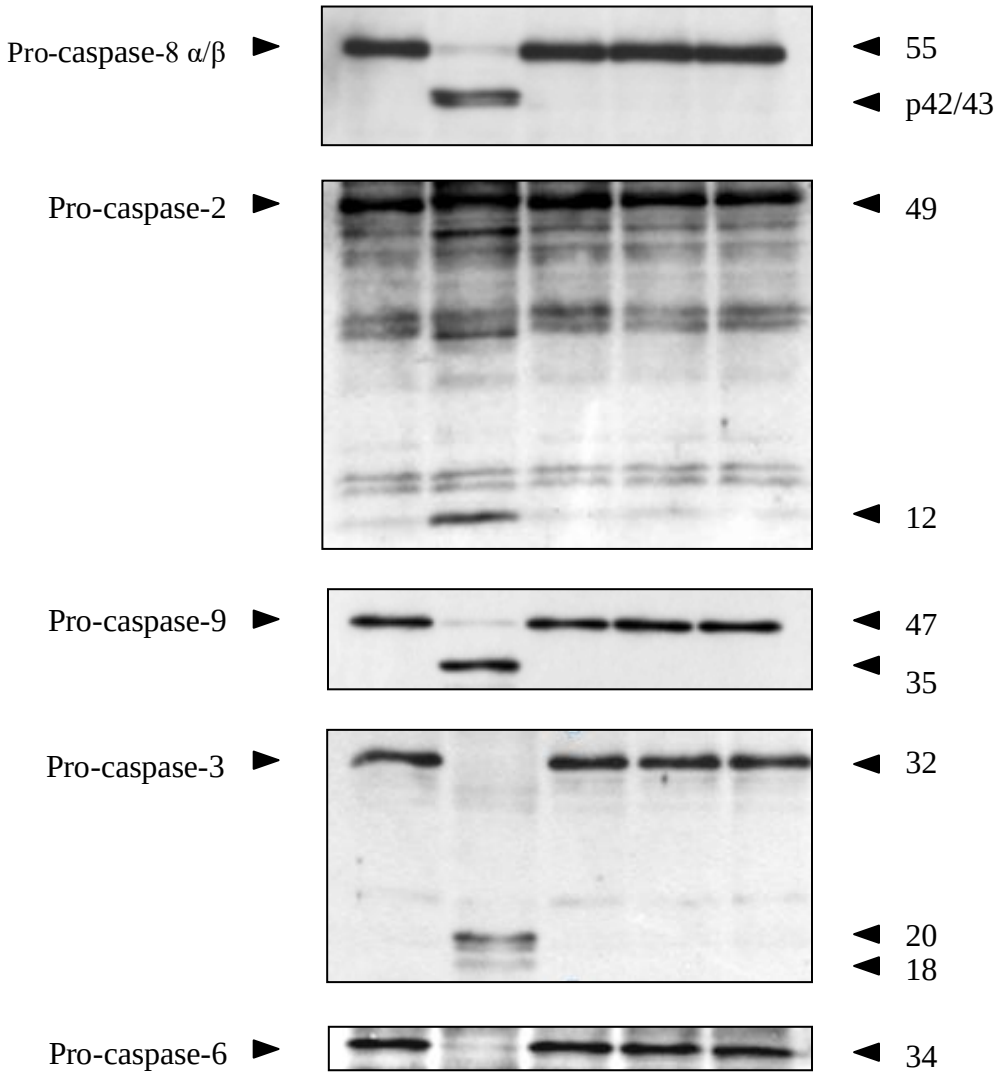

Figure 3.14 Effect of peptidyl-FMK inhibitors on caspase processing in activated T cells

T cells (1 x 10^6/ml) were activated with anti-CD3 (5 μg/ml) in the absence or presence of (A) z-FA-FMK or (B) z-FF-FMK. After 72 h, the cells were subjected to gradient density centrifugation to obtain pure, activated T cells. Whole cell lysates (20 μg protein) were resolved using 13 % SDS-PAGE, transferred to nitrocellulose membrane and probed for caspases. The results are one representative of three independent experiments.

3.3 Discussion

The cathepsin B inhibitor, z-FA-FMK which is commonly used as a negative control for caspase inhibitors (Sarin et al., 1996, McColl et al., 1998) was shown to block mitogen and IL-2-mediated primary T cell activation and proliferation (Lawrence et al., 2006). This finding suggests that a non-caspase protease may be involved in caspase processing in activated T cells. In order to further understand the molecular mechanism that underlies the immunosuppression mediated by z-FA-FMK, structure activity studies were carried out.

In agreement with earlier work (Lawrence et al., 2006), z-FA-FMK inhibited activation-induced T cell proliferation in a dose-dependent manner. However, z-FA-DMK had no effect on primary T cell proliferation while z-FA-CMK, an analogue of z-FA-FMK, having a chlorine atom instead of a fluorine atom in the methyl ketone moiety was toxic and readily induced cell death in T cells. This toxicity is unique to z-FA-CMK since both z-FA-FMK and z-FA-DMK were not toxic. Indeed, it is well documented that peptidyl-methyl ketones with a chlorine atom are more reactive and can result in nonspecific alkylation of proteins which may contribute to their toxicity (Rasnick, 1985, Rauber et al., 1986, Angliker et al., 1987, Otto and Schirmeister, 1997). Besides alkylation of proteins, the CMK group may induce toxicity by reacting with thiol-containing constituents, such as GSH, which are abundant in cells and play a pivotal role in the antioxidant defense system of a cell (Rossman et al., 1974). Since only z-FA-FMK blocked T cell activation and proliferation, the results suggest that the FMK moiety may be responsible for the inhibition of T cell activation and proliferation. Therefore, the effect of two other FMK-containing methyl ketone peptides, z-YVAD-FMK, a caspase-1 inhibitor, and z-VRPR-FMK, a MALT1 inhibitor, was examined. However, both z-YVAD-FMK and z-VRPR-FMK did not

block T cell proliferation which indicates that the FMK group per se is not immunosuppressive. The benzyloxycarbonyl group at the N-terminal also played an important role in the suppression of T cell proliferation mediated by z-FA-FMK since replacing it with biotin (biotin-FA-FMK) completely blocked its immunosuppressive effects. Taken together, the data suggests that the suppression of T cell proliferation induced by z-FA-FMK is likely to involve the combination of the FMK moiety, the peptide part of z-FA-FMK and the benzyloxycarbonyl group at the N-terminal. Further characterization of the role of alanine on the P1 position revealed that replacing it with phenylalanine results in z-FF-FMK being more potent in blocking anti-CD3-induced T cell proliferation compared to z-FA-FMK. Similar to z-FA-FMK, z-FF-FMK which is a cathepsin B and cathepsin L inhibitor (Powers et al., 2002, Urbich et al., 2005, Baumgartner et al., 2007) inhibited blast transformation, CD25 and CD69 expression, IL-2 signaling and cell cycle progression. The finding that z-FF-FMK also blocks primary T cell activation and proliferation further compounds the notion that the inhibition of T cell proliferation may not be due solely to the inhibition of caspases, as previously thought (Alam et al., 1999, Kennedy et al., 1999, Boissonnas et al., 2002, Mack and Hacker, 2002, Falk et al., 2004, Song et al., 2004, Misra et al., 2005). The fact that z-FF-FMK and z-FA-FMK are both cathepsin B inhibitors (Powers et al., 2002) suggests that cathepsin B may have a role in T cell activation and proliferation. However, z-FA-DMK had no effect on T cell activation and proliferation despite it being a cathepsin B inhibitor (Powers et al., 2002). Furthermore, cathepsin B null mice have no phenotype (Deussing et al., 1998), which indicates that cathepsin B is not required for T cell activation. Taken together, this suggests that the immunosuppressive effects of z-FA-FMK and z-FF-FMK are not due to the inhibition of cathepsin B.

The inhibitory effect of peptidyl-FMK caspase inhibitors on T cell activation suggests that caspases play a role in T cell activation and proliferation (Alam et al., 1999, Kennedy et al., 1999). These findings are supported by the observation of lymphocyte activation defects in caspase-8-deficient humans (Chun et al., 2002) and murine T cells (Salmena et al., 2003). How proliferating T cells are able to survive in the presence of the pro-apoptotic activity of caspases is still unclear. The lack of processing of caspase substrates, including PARP (Alam et al., 1999, Lawrence et al., 2006), in proliferating T cells suggest that the activity of effector caspases might be blocked through interaction with endogenous inhibitors like the inhibitor-of-apoptosis proteins (IAP) (Callus and Vaux, 2007, Paulsen et al., 2008). Indeed, one study showed that during human T cell proliferation, the caspase inhibitor X-linked inhibitor-of-apoptosis proteins (XIAP) interacts with cleaved caspase-3 and caspase-7 thereby blocking their full activation, substrate cleavage and cell death (Paulsen et al., 2008). However, interaction with XIAP still resulted in the incomplete processing of caspase-3 to its p20 subunit, in activated T cells, which is adequate for the cleavage of PARP (Stennicke et al., 1998). Another possible mechanism that keeps activated caspases from cleaving substrates that inevitably triggers apoptosis is through limited subcellular compartmentalisation of active effector caspase (Lamkanfi et al., 2007, Koenig et al., 2008, Paulsen et al., 2008). The exact mechanism for the prevention of apoptosis, despite the presence of processed caspases remains to be determined.

In resting T cells, the caspases examined exist as zymogens while each caspase was processed in a time-dependent manner following anti-CD3-activation. Despite z-FA-FMK often being used as a negative control for peptidyl-FMK caspase inhibitors, both caspase-8 and caspase-3 processing is completely blocked in anti-CD3-activated T cells treated with z-FA-FMK (Lawrence et al., 2006). A previous study has shown that z-VAD-FMK and z-IETD-FMK, which readily

suppresses human T cell activation and proliferation, are unable to block the caspase cleavage in proliferating T cells (Lawrence and Chow, 2012). Taken together, these findings suggest that the inhibition of caspase processing is independent of caspase inhibition properties per se. The results from the present study have shown that z-FA-FMK and z-FF-FMK treatment block initiator caspases (caspase-2, caspase-8 and caspase-9) and effector caspases (caspase-3 and caspase-6). In agreement with the findings that z-FF-FMK is a more potent inhibitor of T cell activation and proliferation, as a lower concentration of z-FF-FMK was sufficient to completely block the activation and processing of the caspases in activated T cells. On the other hand, z-FA-FMK treatment blocked caspases in a dose-dependent manner, which is in line with earlier work (Lawrence et al., 2006).

In summary, the structure-activity relationship results presented here suggest that the immunosuppressive properties of z-FA-FMK requires not only the FMK group but also the presence of specific amino acids in the P1 and P2 position as well as the benzyloxycarbonyl group at the N-terminal. The cathepsin L inhibitor, z-FF-FMK, was also identified as a more potent inhibitor of T cell activation and proliferation compared to z-FA-FMK. In addition, the finding that z-FA-FMK and z-FF-FMK readily blocks the processing of caspases in proliferating T cells but do not inhibit caspases per se suggests that the inhibition of caspase processing is unlikely to be the means by which they exert their inhibitory effect on T cell activation.

CHAPTER FOUR

The role of oxidative stress in z-FA-FMK- and z-FF-FMK-induced inhibition of T cell activation and proliferation

4.1 Introduction

In the previous chapter, the structure activity relationship of z-FA-FMK analogues in blocking T cell proliferation as well as inhibiting the processing of caspases was investigated. The results illustrated that the immunosuppressive properties of z-FA-FMK requires not only the FMK group but also the presence of benzyloxycarbonyl group at the N-terminal. When alanine in the P1 position was replaced with phenylalanine, z-FF-FMK was shown to be more potent in blocking anti-CD3-induced T cell proliferation. Similar to z-FA-FMK, z-FF-FMK inhibited blast transformation, CD25 and CD69 up-regulation as well as blocking the proteolytic activation of caspases in non-apoptotic, activated T cells.

A number of studies have reported that some peptidyl-methyl ketones are reactive to GSH (Rossman et al., 1974, Angliker et al., 1987, Powers et al., 2002). In *E. coli*, the papain and synthetic trypsin inhibitor, tosyl-L-lysine-CMK (TLCK) was shown to react with intracellular GSH to inhibit macromolecular synthesis. Addition of GSH was also able to reverse the inhibition of apoptosis caused by TLCK (Rossman et al., 1974). Although peptidyl CMKs are 500 times more reactive to GSH than peptidyl FMKs (Angliker et al., 1987), it is quite possible that peptidyl-FMKs may deplete intracellular GSH at a slower rate.

Numerous studies have now shown that GSH plays an important role in T cell proliferation (Zmuda and Friedenson, 1983, Hamilos and Wedner, 1985, Markovic et al., 2007). For example, GSH depletion via chemicals such as by MSO (Ronzio et al., 1969), DEM (Hidaka et al., 1990, Weber et al., 1990) and BSO (Griffith et al., 1979, Vaziri et al., 2000, Reliene and Schiestl, 2006) has been reported to block T cell proliferation (Fidelus et al., 1987, Gmunder et al., 1990,

Suthanthiran et al., 1990, Gmunder and Droge, 1991). In addition, PBMCs cultured with BSO were unable to enter the S phase of the cell cycle (Messina and Lawrence, 1989). However, when exogenous GSH was added to BSO-treated PBMCs, this block on cell cycle was reversed (Suthanthiran et al., 1990). Increasing intracellular GSH levels using 2-ME was also reported to enhance T cell proliferation mediated by IL-2 as well as anti-CD3-stimulated $CD3^+$ T lymphocytes (Zmuda and Friedenson, 1983, Messina and Lawrence, 1989). These data strengthen the evidence suggesting that cellular redox regulation is a critical step in T cell proliferative responses and suggest a direct relationship between GSH availability and T cell proliferation (Hamilos et al., 1989, Walsh et al., 1995). Therefore, in this chapter, the involvement of oxidative stress in z-FA-FMK and z-FF-FMK immunosuppressive effects was investigated.

4.2 Results

4.2.1 Effect of z-FA-FMK and z-FF-FMK on intracellular GSH and ROS levels in primary T cells

Since reduced levels of intracellular GSH has been linked to diminished T cell proliferation (Hamilos et al., 1989, Walsh et al., 1995), the intracellular GSH levels in activated primary T cells in the presence of z-FA-FMK and z-FF-FMK was examined. To ensure that the level of GSH presented is based on a decrease in intracellular GSH and not reduced cell numbers due to inhibition of cell proliferation compared to control, the GSH levels were normalised to 1 x 10^4 cells per treatment. As illustrated in Figure 4.1, z-FA-FMK and z-FF-FMK at varying concentrations (25 – 100 μM) had little effect on the intracellular GSH levels in activated primary T cells after 6 h compared to control cells. However, after 24 h, both peptidyl-FMK inhibitors induced a significant dose-dependent decrease in intracellular GSH in the treated cells ($p < 0.05$).

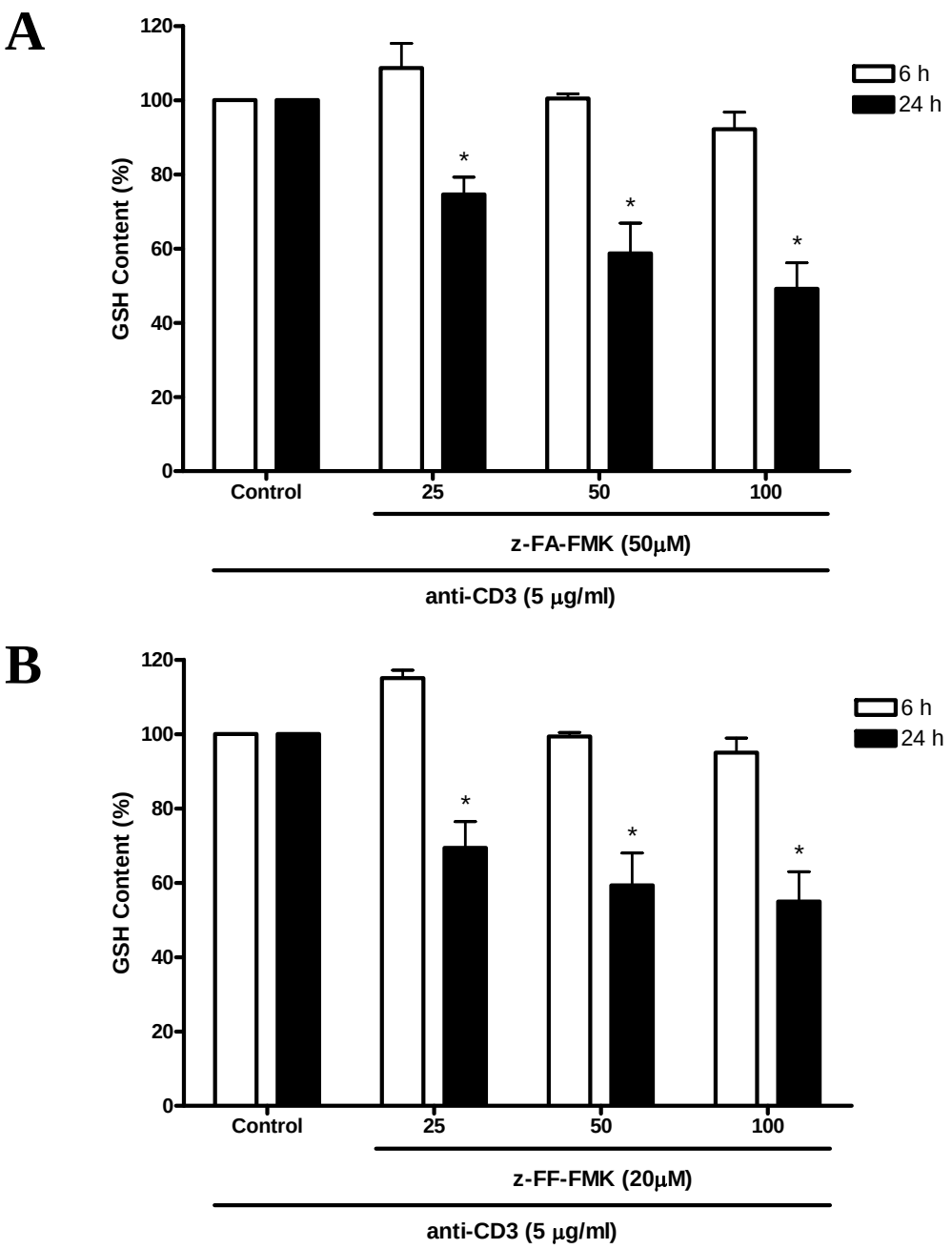

Figure 4.1 Effect of z-FA-FMK and z-FF-FMK on intracellular GSH levels in activated primary T cells

PBMCs (1 x 10^6/ml) were stimulated with anti-CD3 (5 μg/ml) in the presence of various concentrations of (A) z-FA-FMK or (B) z-FF-FMK. The intracellular GSH level was measured after 6 and 24 h using the fluorescent dye MCB and analysed using a spectrophotometer as outlined in the Materials and Methods. Results are the means ± SEM of three independent experiments. *, Significantly decreased ($p < 0.05$) from control.

Since both z-FA-FMK and z-FF-FMK are capable of depleting GSH in anti-CD3-activated T cells, the effect of these peptidyl-FMK inhibitors on ROS generation in these cells was assessed using DHE dye which selectively detects intracellular superoxide anion ($O_2^{\bullet -}$) production (Bindokas et al., 1996, D'Agostino et al., 2007, Owusu-Ansah et al., 2008). As shown in Figure 4.2A, z-FA-FMK at 25 μM had little effect on ROS levels in anti-CD3-activated T cells after 6 h. However, at higher concentrations (50 and 100 μM) z-FA-FMK, ROS production in activated T cells was significantly increased compared to control ($p < 0.05$). After 24 h, ROS generation in anti-CD3-activated T cells was increased significantly in a dose-dependent manner at all z-FA-FMK concentrations examined ($p < 0.05$). Similar to z-FA-FMK, the addition of z-FF-FMK resulted in a significant dose-dependent increase in ROS generation (Figure 4.2B) from as early as 6 h following treatments ($p < 0.05$). Taken together, these results suggest that both z-FA-FMK and z-FF-FMK are able to deplete GSH and induced ROS generation.

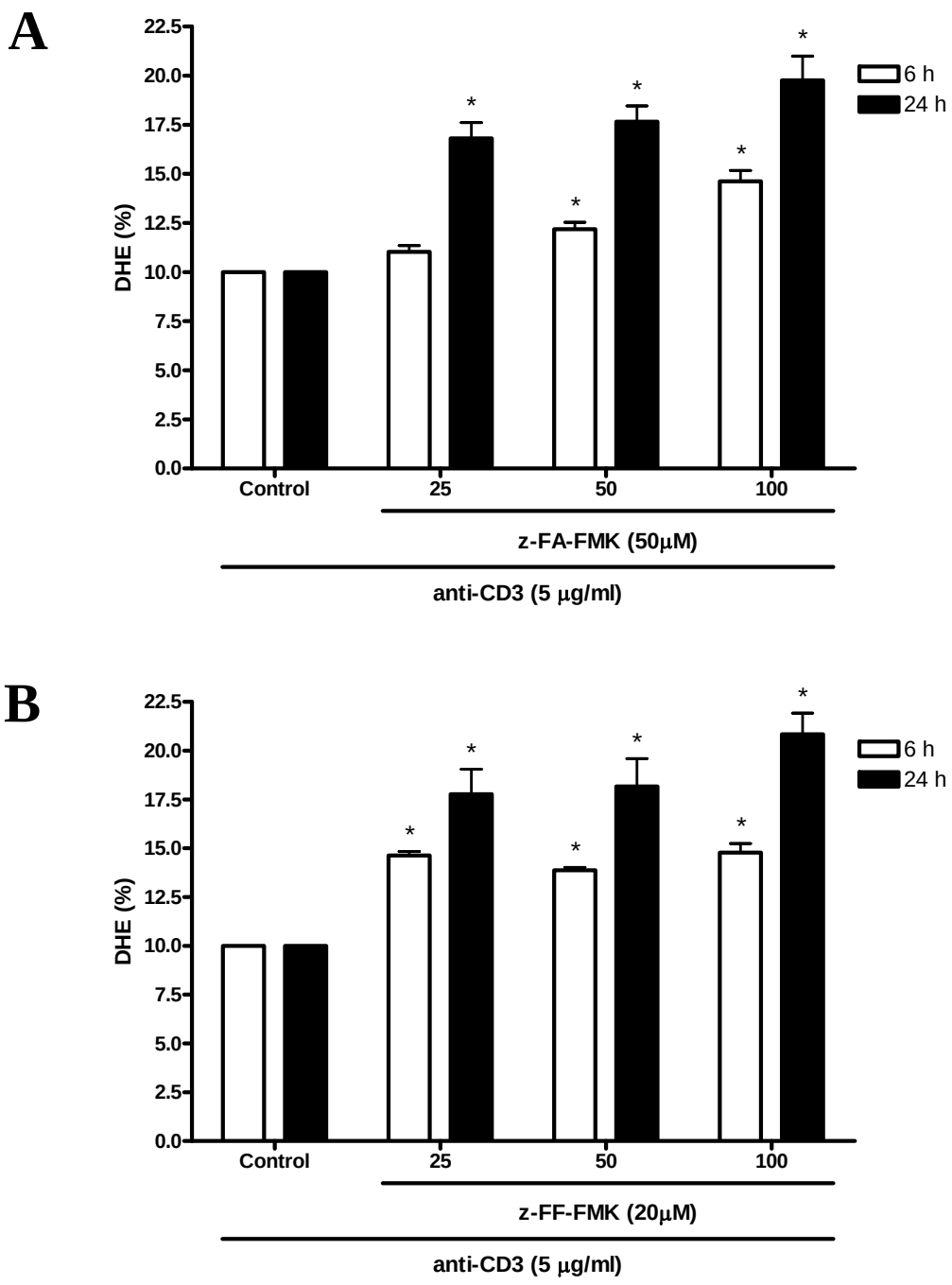

Figure 4.2 Effect of z-FA-FMK and z-FF-FMK on ROS levels in activated primary T cells

PBMCs (1 x 10^6/ml) were stimulated with anti-CD3 (5 μg/ml) in the presence of various concentrations of (A) z-FA-FMK or (B) z-FF-FMK. ROS were measured after 6 and 24 h using the DHE probe and analysed using flow cytometry as described in the Materials and Methods. Results are the means ± SEM of three independent experiments. *, Significantly increased ($p < 0.05$) from control.

4.2.2 Effect of GSH and NAC on the suppression of primary T cell activation and proliferation mediated by z-FA-FMK and z-FF-FMK

The results obtained so far suggest that z-FA-FMK and z-FF-FMK may have blocked T cell activation and proliferation through the depletion of intracellular GSH, which in turn increases ROS levels in the cells. Since previous studies suggest that GSH plays an important role in T cell proliferation (Messina and Lawrence, 1989, Yim et al., 1994, Roozendaal et al., 2002), the effect of exogenously added GSH on z-FA-FMK or z-FF-FMK mediated immunosuppression was examined. To this end, anti-CD3-activated T cells were treated with the peptidyl-FMK inhibitors, at their respective IC_{50}, in the presence of GSH (1.25 – 5 mM) for 72 h. As shown in Figure 4.3A, GSH dose-dependently restored the inhibition of anti-CD3-induced T cell proliferation mediated by z-FA-FMK. GSH at 2.5 mM and above induced a significant increase in T cell proliferation compared to treatment with z-FA-FMK alone and T cell proliferation was completely restored at 5 mM GSH ($p < 0.05$). Similar to z-FA-FMK, GSH also significantly reversed the inhibition of anti-CD3-induced T cell proliferation mediated by z-FF-FMK in a dose-dependent manner (Figure 4.3B) ($p < 0.05$). Collectively, these results suggest that the inhibition of anti-CD3-induced T cell proliferation mediated by these peptidyl-FMK inhibitors is via oxidative stress through the depletion of intracellular GSH.

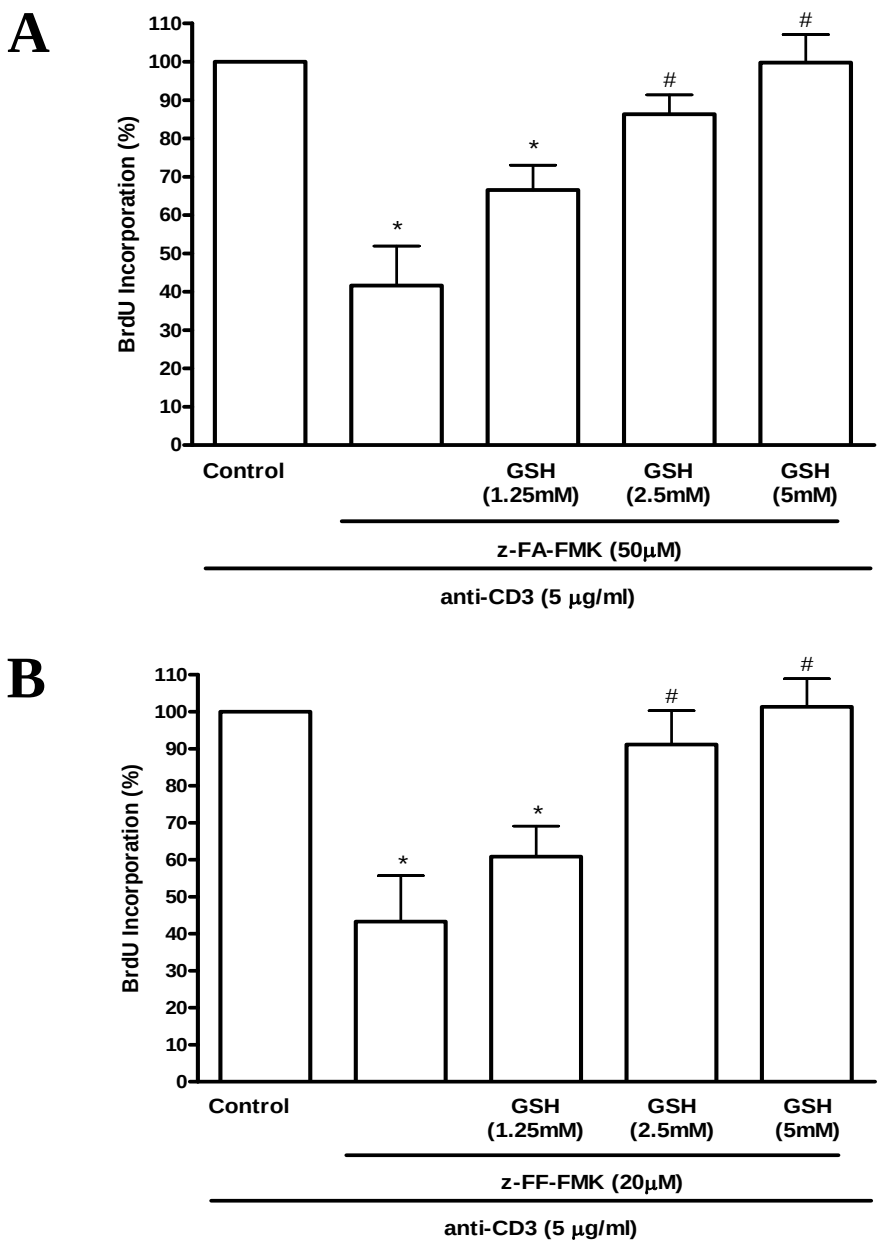

Figure 4.3 Effect of increasing dose of GSH on z-FA-FMK- and z-FF-FMK-induced inhibition of T cell proliferation

PBMCs (1 x 10^6/ml) were stimulated with anti-CD3 (5 μg/ml) together with (A) 50 μM z-FA-FMK or (B) 20 μM z-FF-FMK in the presence of increasing concentrations of GSH. BrdU incorporation was assessed after 72 h by measuring absorbance on a plate reader as outlined in the Materials and Methods. Results are the means ± SEM of at least three independent experiments. *, Significantly decreased ($p < 0.05$) from control; $^{\#}$, Significantly increased ($p < 0.05$) from the respective peptidyl-FMK treatment alone.

As shown in Figure 4.3, the low molecular weight thiol GSH readily restored the inhibition of anti-CD3-stimulated T cell proliferation mediated by z-FA-FMK and z-FF-FMK to control levels. Therefore, it was interesting to determine if another low molecular weight thiol could also reverse the immunosuppressive effects of these peptidyl-FMK inhibitors. To this end, the thiol NAC, known to be a precursor of GSH synthesis (Arranz et al., 2008, Berk et al., 2008, Lavoie et al., 2008) and ROS scavenger (Sandstrom et al., 1994) was examined. As shown in Figure 4.4A, NAC significantly blocked the inhibition of anti-CD3-induced T cell proliferation mediated by z-FA-FMK in a dose-dependent manner (1.25 – 5 mM) ($p < 0.05$). Similarly, as illustrated in Figure 4.4B, NAC dose-dependently (1.25 – 5 mM) blocked z-FF-FMK-induced inhibition of T cell proliferation. A concentration of 1.25 mM NAC and above significantly restored the inhibition of T cell proliferation mediated by z-FF-FMK ($p < 0.05$). Since NAC reversed the inhibition of T cell proliferation mediated by z-FA-FMK and z-FF-FMK, the results further suggest that GSH depletion and oxidative stress play an important role in the immunosuppressive effects of these peptidyl-FMK inhibitors. Based on these results, a concentration of 5 mM low molecular weight thiols was chosen for subsequent experiments.

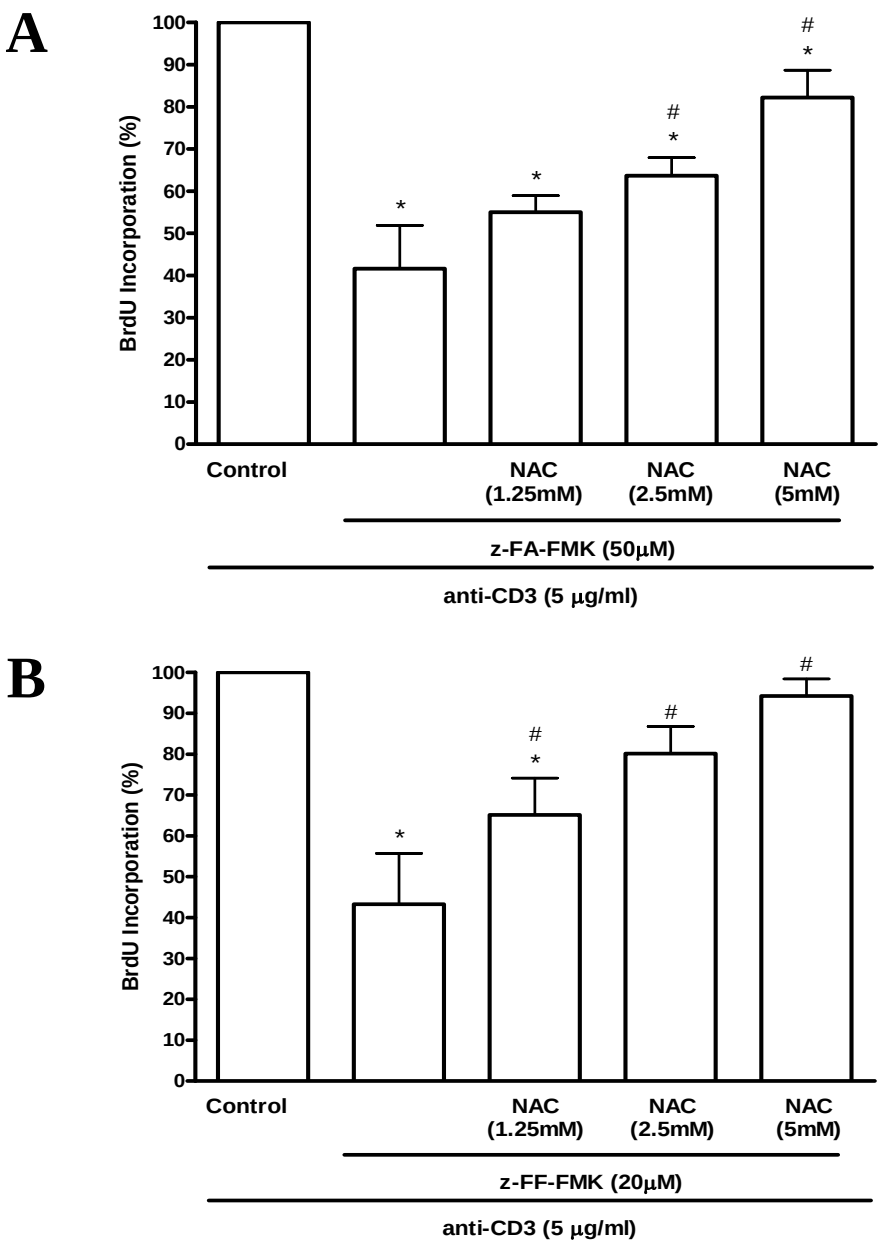

Figure 4.4 Effect of NAC on z-FA-FMK- and z-FF-FMK-induced inhibition of T cell proliferation

PBMCs (1 x 10^6/ml) were co-stimulated with anti-CD3 (5 µg/ml) and with (A) 50 µM z-FA-FMK or (B) 20 µM z-FF-FMK in the presence of increasing concentrations of NAC. BrdU incorporation was assessed after 72 h by measuring absorbance on a plate reader as outlined in the Materials and Methods. Results are the means ± SEM of at least three independent experiments. *, Significantly decreased ($p < 0.05$) from control; #, Significantly increased ($p < 0.05$) from the respective peptidyl-FMK treatment alone.

4.2.3 Effect of various low molecular weight thiols on the suppression of primary T cell activation and proliferation mediated by z-FA-FMK and z-FF-FMK

The findings that NAC was able to restore the immunosuppressive effect mediated by z-FA-FMK and z-FF-FMK suggest that GSH synthesis may be blocked. It is well known that intracellular deacetylation of NAC increases levels of L-cysteine which is required for GSH synthesis (Monick et al., 2003, Hadzic et al., 2005). Therefore, the effect of L-cysteine on the inhibition of T cells proliferation induced by the peptidyl-FMK inhibitors was examined alongside D-cysteine, which cannot be metabolized to GSH. As shown in Figure 4.5, L-cysteine (5 mM) significantly reversed ($p < 0.05$) the inhibition of T cell proliferation induced by z-FA-FMK and z-FF-FMK. However, D-cysteine (5 mM) which has the same reductive power as NAC but cannot be utilized for GSH synthesis (Jones et al, 1995) was unable to restore T cell proliferation blocked by z-FA-FMK and z-FF-FMK. These results suggest that NAC and L-cysteine reversed the immunosuppressive effects of the peptidyl-FMK inhibitors by replenishing intracellular GSH, hence restoring the oxidative state of the cell. As a positive control, BSO (0.5 mM) which selectively inhibits γ-glutamylcysteine synthetase (Griffith et al., 1979) significantly blocked ($p < 0.05$) anti-CD3-activated T cell proliferation. Because GSH is synthetized from glutamate, cysteine and glycine by two consecutive reactions by the enzymes γ-glutamylcysteine synthethase and GSH synthase, the inhibition of γ-glutamylcysteine synthetase effectively blocks the generation of GSH. These data strongly suggest that the immunosuppressive effect induced by z-FA-FMK and z-FF-FMK is due to oxidative stress via the depletion of GSH.

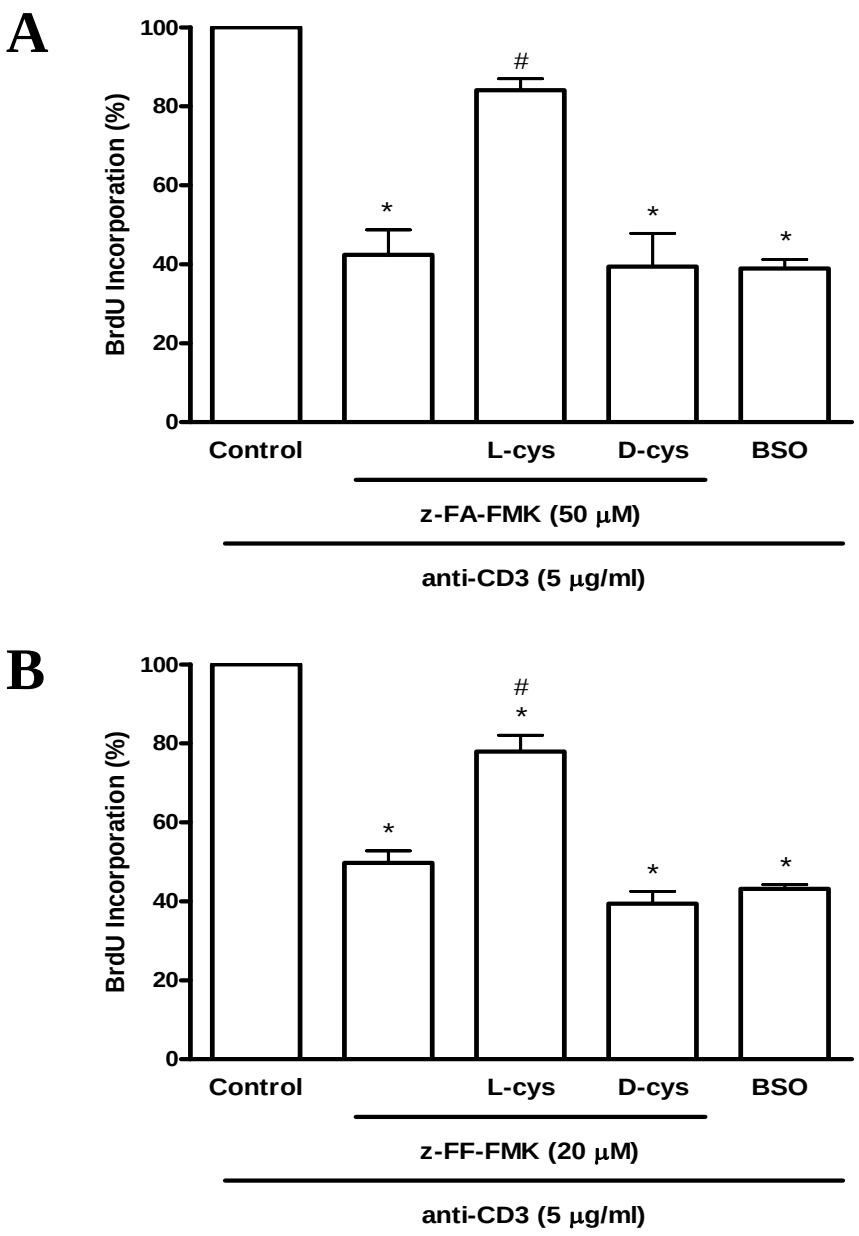

Figure 4.5 Effect of low molecular weight thiols on the inhibition of T cell proliferation induced by z-FA-FMK- and z-FF-FMK

PBMCs (1 x 10^6/ml) stimulated with anti-CD3 (5 µg/ml) were treated with (A) 50 µM z-FA-FMK or (B) 20 µM z-FF-FMK in the presence or absence of low molecular weight thiols (5 mM) or 0.5 mM BSO where indicated. BrdU incorporation was assessed after 72 h by measuring absorbance on a plate reader as outlined in the Materials and Methods. Results are the means ± SEM of at least three independent experiments. *, Significantly decreased ($p < 0.05$) from control; #, Significantly increased ($p < 0.05$) from the respective peptidyl-FMK treatment alone.

4.2.4 Mechanisms that underlie the depletion of GSH mediated by z-FA-FMK and z-FF-FMK in primary T cells

So far, the data indicate that z-FA-FMK and z-FF-FMK block T cell proliferation via the depletion of intracellular GSH which is reversed by the presence of GSH, NAC and L-cysteine (Figure 4.3 – 4.5). To examine whether the depletion of intracellular GSH observed after z-FA-FMK and z-FF-FMK treatment is due to direct interaction between GSH and the peptidyl-FMK inhibitors, GSH was incubated with these peptidyl-FMKs in a cell free system (Debiton et al., 2003) and the non-reacted GSH was determined. As shown in Figure 4.6, NEM which reacts directly with GSH reduced MCB-reactive GSH to a very low level. In contrast, the peptidyl-FMK inhibitors had little effect on MCB-reactive GSH which suggest that z-FA-FMK and z-FF-FMK do not react readily with free GSH. The results indicate that the depletion of intracellular GSH by these peptidyl-FMK inhibitors is likely to be due to other mechanisms involving the GSH synthesis pathway. Previous work showed that intracellular deacytelation of NAC provides cysteine for GSH biosynthesis thereby increasing total cellular thiols (Malorni et al., 1993). To further examine the potential role of NAC as a mediator of GSH synthesis, activated T cells were co-treated with z-FA-FMK, or z-FF-FMK and NAC (5 mM) in the presence or absence of BSO (0.5 mM). Since BSO irreversibly blocks the GSH synthesis pathway by inhibiting the enzyme γ-glutamylcysteine synthetase, it was hypothesized that in the presence of BSO, NAC would not be converted into GSH and thus cannot reverse the inhibition of T cell proliferation mediated by the peptidyl-FMK inhibitors. As shown in Figure 4.7, addition of BSO blocked the ability of NAC to restore primary T cells from the immunosuppressive effects of z-FA-FMK and z-FF-FMK as illustrated by the reduction in BrdU incorporation. Taken together, these data strongly suggest that z-FA-FMK and z-FF-FMK block T cell proliferation via GSH depletion.

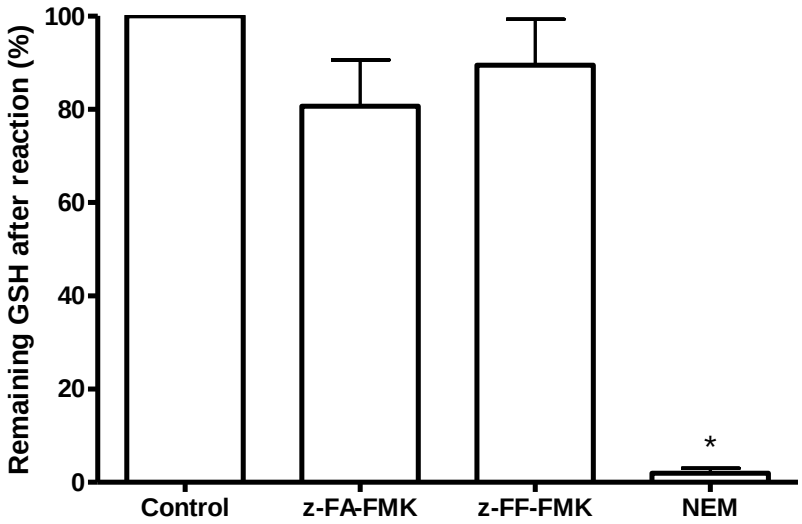

Figure 4.6 Reactivity of peptidyl-FMK inhibitors with GSH in vitro

Peptidyl-FMK inhibitors (100 µM), NEM (100 µM) or PBS (control) were incubated with GSH (100 µM) for 2 h at 37°C. MCB solution (5 mM) was then added and incubated for a further 30 min before the fluorescence was measured at 390/460 nm as described in the Materials and Methods. Results are the means ± SEM of three independent experiments. *, Significantly decreased ($p < 0.05$) from control.

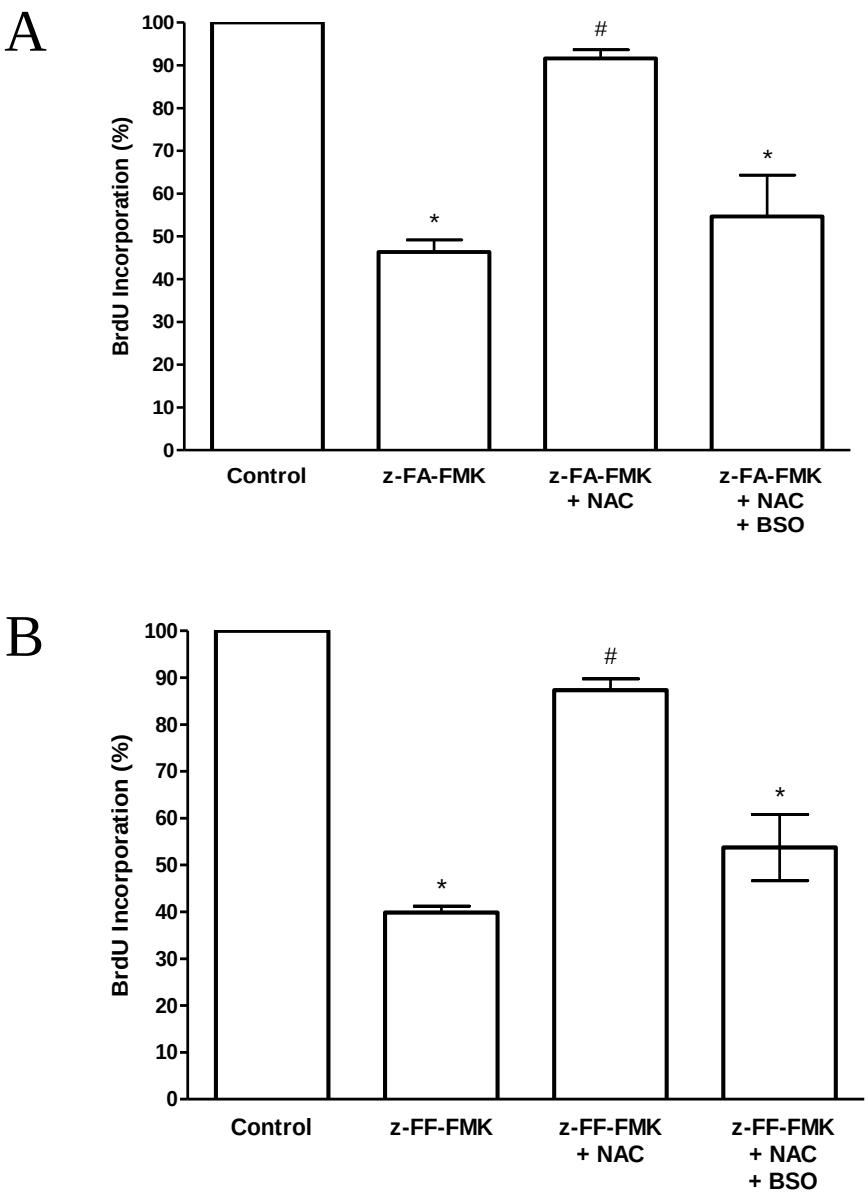

Figure 4.7 Effect of BSO on NAC-induced restoration of the inhibition of T cell proliferation mediated by peptidyl-FMK inhibitors.

PBMCs (1 x 10^6/ml) stimulated with anti-CD3 (5 µg/ml) were treated with (A) 50 µM z-FA-FMK or (B) 20 µM z-FF-FMK with or without 5 mM NAC in the presence or absence of 0.5 mM BSO, as outlined in the Materials and Methods. BrdU incorporation was assessed after 72 h by measuring absorbance on a plate reader. Results are the means ± SEM of at least three independent experiments. *, Significantly decreased ($p < 0.05$) from control; #, Significantly increased ($p < 0.05$) from the respective peptidyl-FMK treatment alone.

4.2.5 Effect of GSH on peptidyl-FMK-induced down-regulation of CD25 and CD69

Cytokine secretion and cell surface receptor up-regulation are some of the early events that occur during T cell activation and proliferation following anti-CD3 stimulation. Since low molecular weight thiols were able to reverse the inhibition of T cell proliferation mediated by z-FA-FMK and z-FF-FMK, the effect of GSH on the expression of IL-2Rα (CD25) and the activated T cell marker, CD69 was examined since resting T cells do not express these markers. As illustrated in Figure 4.8, activation of primary T cells with anti-CD3 markedly enhanced CD25 expression from 0.65 % to 56 % and CD69 expression from 3 % to 51 %. The presence of z-FA-FMK markedly reduced the expression of CD25 to 32.47 % and CD69 to 35.68 %. The addition of GSH to z-FA-FMK-treated activated T cells readily restored the down-regulation of CD25 and CD69 from 32.47 % to 64.62 % and from 35.68 % to 59.2 %, respectively. In contrast, z-FF-FMK was more effective in reducing the expression of CD25 and CD69 expression to 23.78 % and 25.39 %, respectively compared to z-FA-FMK. Similarly, the presence of GSH restored the expression of CD25 in z-FF-FMK-treated T cells to almost two-fold while the level of CD69 expression was restored to control levels in activated T cells. These findings demonstrate that oxidative stress plays an important role in the down-regulation of CD25 and CD69 expression induced by z-FA-FMK and z-FF-FMK in the activated T cells and further confirmed that the immunosuppressive properties of these peptidyl-FMK inhibitors is due to depletion of GSH.

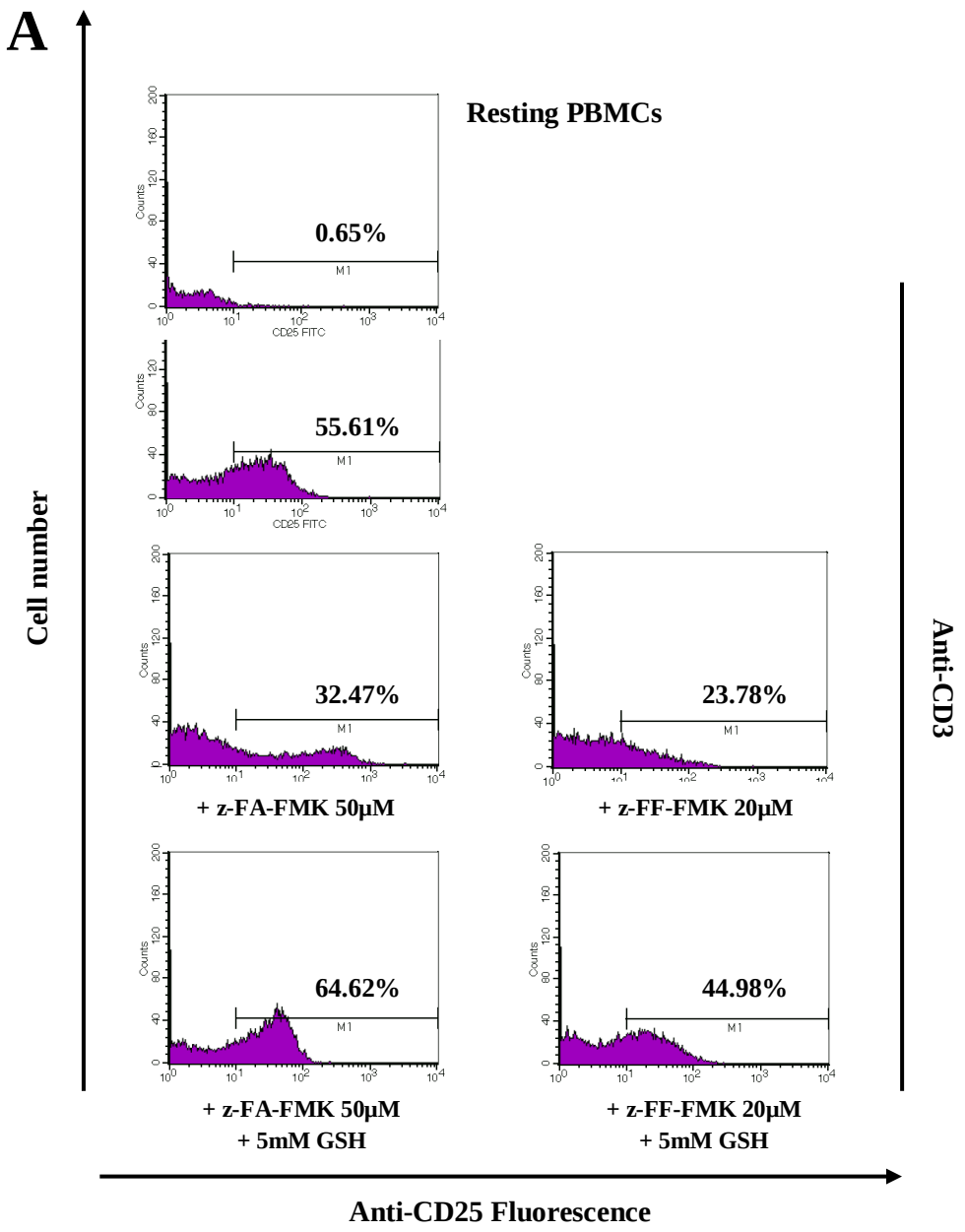
A
Resting PBMCs
0.65%
55.61%
32.47%
23.78%
64.62%
44.98%
+ z-FA-FMK 50μM
+ z-FF-FMK 20μM
+ z-FA-FMK 50μM
+ 5mM GSH
+ z-FF-FMK 20μM
+ 5mM GSH
Cell number
Anti-CD3
Anti-CD25 Fluorescence

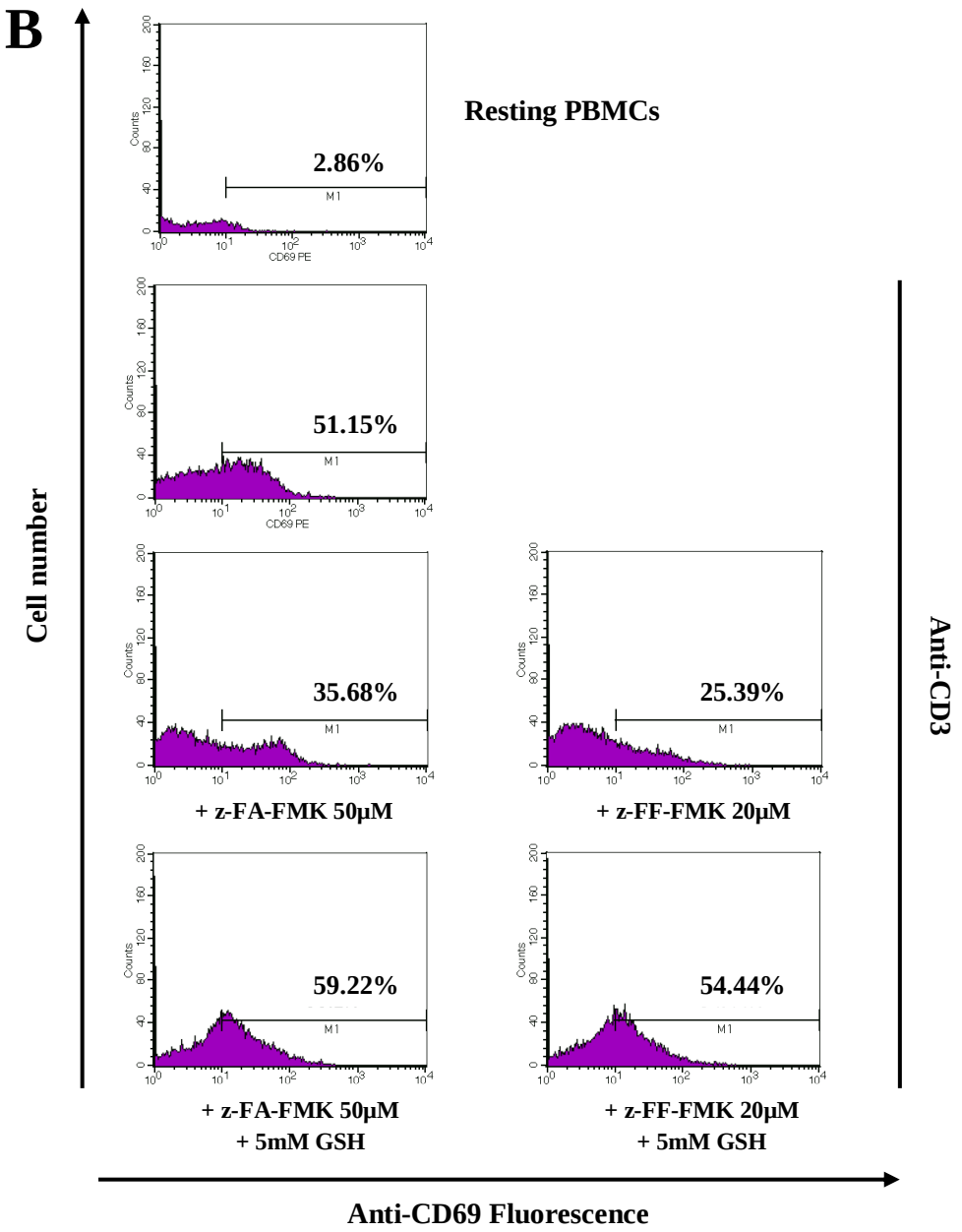

Figure 4.8 Effect of GSH on CD25 and CD69 expression in anti-CD3-treated primary T cells in the presence of z-FA-FMK and z-FF-FMK.

PBMCs ($1x10^6$ cells/ml) were stimulated with anti-CD3 (5 µg/ml) in the presence and absence of z-FA-FMK or z-FF-FMK where indicated. The cells were co-incubated with 5mM GSH immediately following addition of the peptidyl-FMK inhibitors. After 72 h, the cells were incubated with (A) FITC-conjugated anti-CD25 or (B) PE-conjugated anti-CD69 before analysis using flow cytometry. The results are one representative from three independent experiments.

4.2.6 Effect of low molecular weight thiols on the inhibition of caspase-8 and caspase-3 processing in activated primary T cells mediated by z-FA-FMK and z-FF-FMK

Earlier work has showed that z-FA-FMK and z-FF-FMK blocked caspase-8 and caspase-3 processing in activated T cells (Chapter 3, Figure 3.13). The finding that low molecular weight antioxidants could reverse the inhibition of T cell proliferation induced by z-FA-FMK and z-FF-FMK raised the question of whether antioxidants could restore caspase-8 and caspase-3 processing in z-FA-FMK- and z-FF-FMK-treated T cells. To determine this, the effect of these peptidyl-FMK inhibitors on caspase-8 and caspase-3 processing in activated T cells in the presence of various low molecular weight thiols was examined. As illustrated in Figure 4.9, the presence of z-FA-FMK (50 μM) and z-FF-FMK (20 μM) completely blocked the activation and processing of caspase-8 and caspase-3. Addition of GSH, NAC and L-cysteine (5mM each) to the cells was able to reverse the inhibition of caspase-8 and caspase-3 processing in activated T cells mediated by z-FA-FMK and z-FF-FMK. In line with the BrdU incorporation data, addition of D-cysteine had little effect on the inhibition of caspase-8 and caspase-3 processing induced by z-FA-FMK and z-FF-FMK. Taken together, the data strongly suggest that the antioxidants GSH, NAC and L-cysteine readily reverse the inhibition of caspase processing and indicate that z-FA-FMK and z-FF-FMK are not blocking the caspases directly.

A

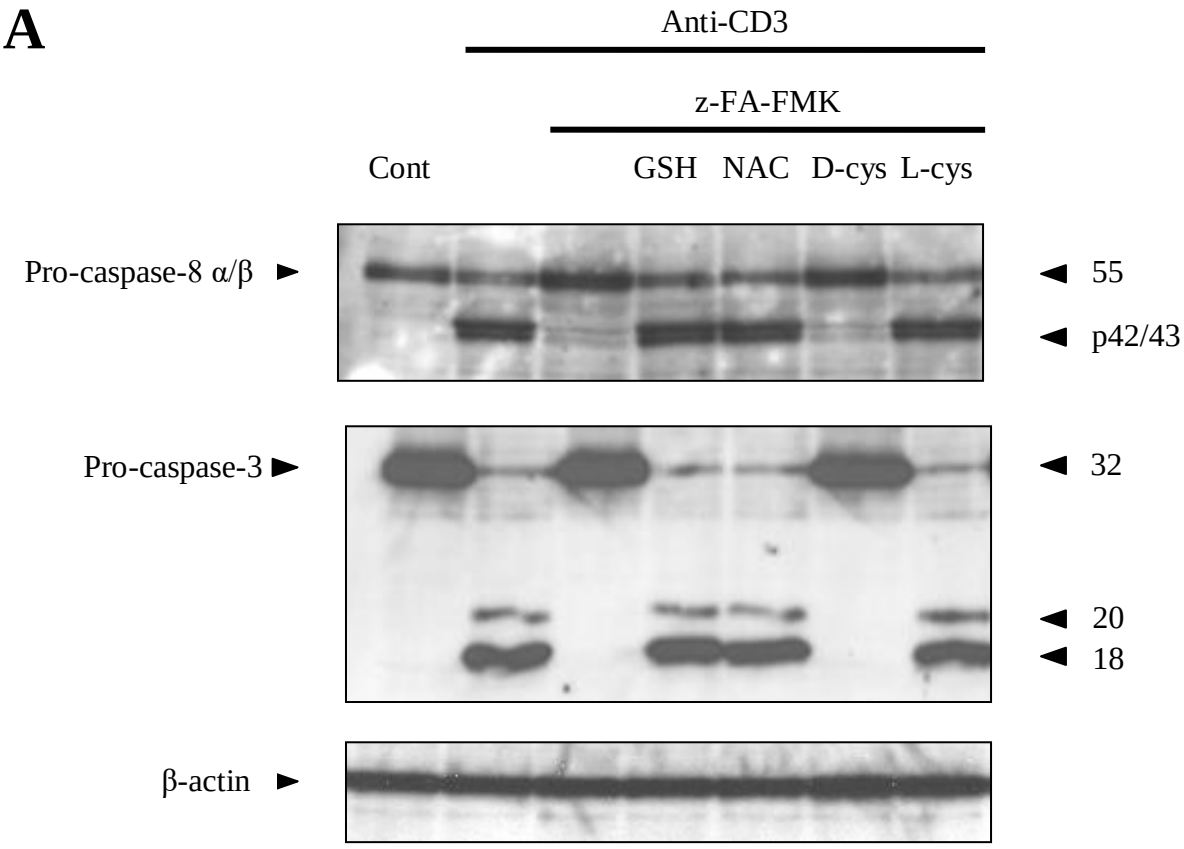
Anti-CD3
z-FA-FMK
Cont
GSH
NAC
D-cys
L-cys
Pro-caspase-8 α/β
55
p42/43
Pro-caspase-3
32
20
18
β-actin

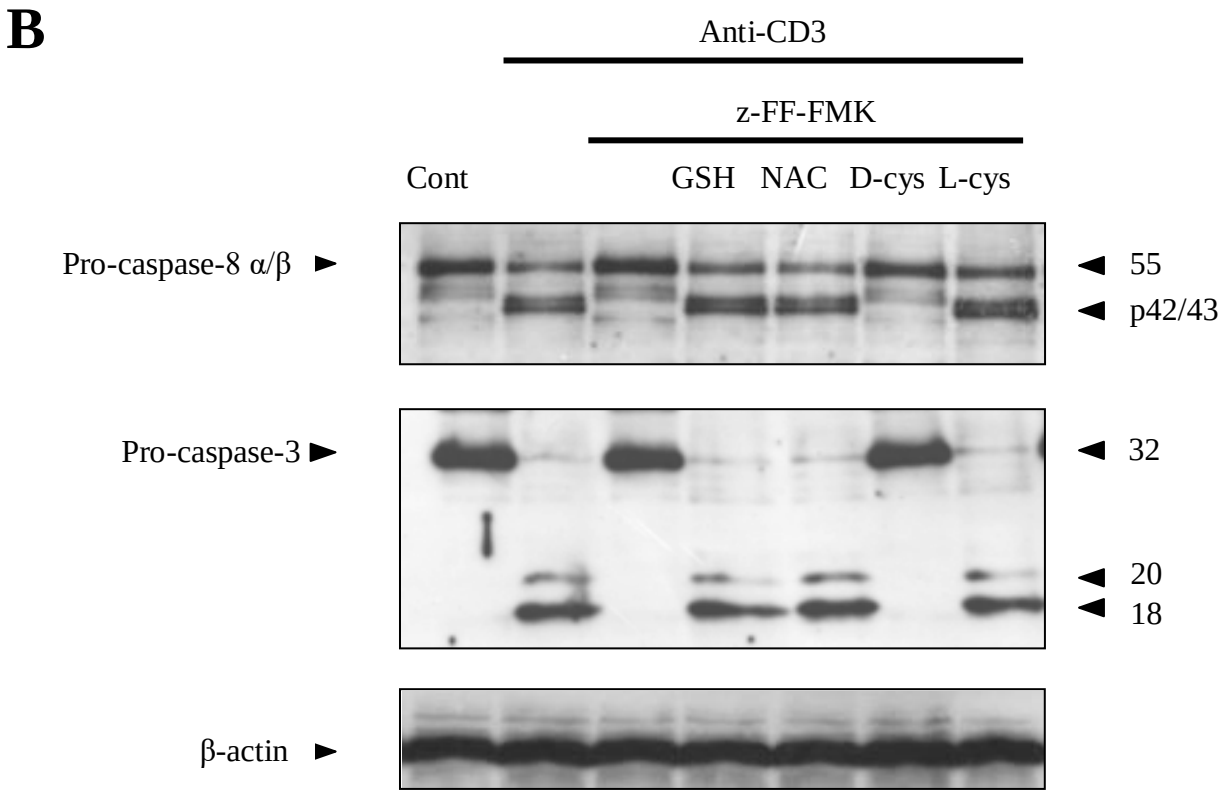

Figure 4.9 Effect of low molecular weight thiols on caspase-8 and caspase-3 processing in peptidyl-FMK-treated activated T cells

PBMCs were treated with anti-CD3 together with (A) 50 µM z-FA-FMK or (B) 20 µM z-FF-FMK in the presence or absence of antioxidants (5mM). After 72 h, the cells were subjected to gradient density centrifugation to obtain pure population of viable activated T cells. Whole cell lysates (20 µg protein) were resolved using 13 % SDS-PAGE, transferred to nitrocellulose membrane and probed for caspase-8, caspase-3 and β-actin. The results are one representative of three independent experiments.

4.3 Discussion

As illustrated in chapter 3, the cathepsin B and L inhibitor, z-FA-FMK and z-FF-FMK respectively, also blocked T cell proliferation as well as caspase processing in activated T cells. However, since both z-FA-FMK and z-FF-FMK are not caspase inhibitors, the data suggests that the inhibition of T cell activation and proliferation may not be through the direct inhibition of caspases.

Thiols such as GSH and cysteine have been implicated to play an important role in T cell proliferation (Zmuda and Friedenson, 1983, Fidelus et al., 1987, Hamilos et al., 1989, Messina and Lawrence, 1989). For example, depletion of intracellular GSH inhibits T cell activation by a mitogen (Hamilos and Wedner, 1985). In addition, low molecular weight thiol compounds such as 2ME are capable of augmenting T cell proliferation in response to mitogen (Zmuda and Friedenson, 1983). Therefore, in the present study, the effect of z-FA-FMK and z-FF-FMK on the cellular redox regulation was examined in proliferating T cells and compared to resting T cells. In activated T cells, z-FA-FMK and z-FF-FMK treatment lead to a depletion of intracellular GSH levels with a concomitant increase in cellular ROS. These findings are in line with a previous study, which demonstrates that peptidyl-FMKs are reactive to GSH (Angliker et al., 1987). This suggests that oxidative stress may be the underlying mechanism of z-FA-FMK and z-FF-FMK immunosuppressive effect.

Indeed, the inhibition of T cell proliferation mediated by z-FA-FMK and z-FF-FMK was readily abolished by exogenous low molecular weight thiols such as GSH, NAC and L-cysteine. NAC is a small molecular weight thiol compound which increases intracellular levels of cysteine through its deacetylation. Cysteine is rate limiting in GSH synthesis and is thus required for T cell growth

and proliferation (Gmunder et al., 1990). T cells require exogenous cysteine, as they are unable to take up and reduce extracellular cysteine (Edinger and Thompson, 2002). Therefore, the data suggests that NAC and L-cysteine restores T cell proliferation in the presence of z-FA-FMK and z-FF-FMK by acting as precursors for GSH biosynthesis. This is further corroborated when D-cysteine, which cannot be enzymatically converted into GSH, was unable to restore T cell proliferation in the presence of these peptidyl-FMK inhibitors. Collectively, these findings suggest that the immunosuppressive effect induced by z-FA-FMK and z-FF-FMK is due to oxidative stress via the depletion of GSH. This is consistent with previous studies showing that GSH plays an important role in T cell proliferation (Zmuda and Friedenson, 1983, Hamilos and Wedner, 1985, Markovic et al., 2007). For instance, human T lymphocytes depleted of intracellular GSH using pharmacological regulators of GSH, such as methionine sulfoximine (Ronzio et al., 1969), diethyl maleate (Hidaka et al., 1990, Weber et al., 1990) and BSO (Griffith et al., 1979, Vaziri et al., 2000, Reliene and Schiestl, 2006) were unable to proliferate and accumulate high levels of ROS (Fidelus et al., 1987, Gmunder et al., 1990, Suthanthiran et al., 1990, Gmunder and Droge, 1991). In contrast, increasing intracellular GSH levels using 2-mercaptoethanol was reported to enhance T cell proliferation mediated by IL-2 and anti-C3-stimulated $CD3^+$ T lymphocytes (Zmuda and Friedenson, 1983, Messina and Lawrence, 1989). These studies implicate GSH as an important regulator of T cell proliferation and suggest a direct relationship between the availability of GSH and the proliferative response of T cells (Chaplin and Wedner, 1978, Fidelus et al., 1987, Suthanthiran et al., 1990). However, the exact mechanism of how z-FA-FMK and z-FF-FMK diminish intracellular GSH levels in activated T cells is still unclear. Although peptidyl-FMKs have been reported to interact with GSH directly in vitro (Angliker et al., 1987), both z-FA-FMK and z-FF-FMK treatment deplete GSH content

in activated T cells only after 24 h, which is a rather long time, thus ruling out direct interaction between these peptidyl-FMK inhibitors and GSH. Furthermore, the chemical reactivity of fluoromethanes as alkylators of GSH is $1/500^{th}$ that of the reactivity of a chloromethane (Angliker et al., 1987). The failure to reverse z-FA-FMK- and z-FF-FMK-mediated block on T cell proliferation by co-treatment with NAC and BSO suggests that these inhibitors block T cell proliferation by interfering with the GSH pathway.

The important role of IL-2 as an autocrine and paracrine T cell growth factor is well established. Following T cell activation, IL-2 is synthesised and secreted, and the α-subunit of the IL-2 receptor (CD25) is up-regulated (Nelson, 2004). The results from the present study have shown that z-FA-FMK and z-FF-FMK inhibit the expression of CD25 and CD69, another early T cell activation marker, when stimulated with anti-CD3 (Kennedy et al., 1999, Falk et al., 2004, Lawrence et al., 2006). The presence of exogenous GSH completely restored the inhibition of anti-CD3-induced CD25 and CD69 expression mediated these peptidyl-FMK inhibitors to control levels. The findings are consistent with previous work which show that the depletion of GSH reduces the expression of CD25 and CD69 surface markers relative to cells with high GSH levels (Roozendaal et al., 2002). Collectively, the data confirms that the depletion of intracellular GSH is the underlying mechanism involved in the down-regulation of these two early T cell activation markers.

Despite z-FA-FMK being a negative control for peptidyl-FMK caspase inhibitors, both caspase-8 and caspase-3 processing was blocked in anti-CD3-activated T cells treated with z-FA-FMK, which is consistent with findings from previous work (Lawrence et al., 2006). Similarly, the

cathepsin L inhibitor, z-FF-FMK, being a more potent immunosuppressant also blocks caspase-8 and caspase-3 processing in activated T cells. Interestingly, the low molecular weight thiols GSH, NAC and L-cysteine were able to fully restore the processing of caspase-8 and caspase-3 into their respective subunits in the presence of both z-FA-FMK and z-FF-FMK. These results strengthen the evidence suggesting that these peptidyl-FMK inhibitors suppress T cell activation proliferation through oxidative stress via GSH depletion.

In summary, the findings in the present study suggest that z-FA-FMK and z-FF-FMK inhibit anti-CD3-induced T cell activation and proliferation through oxidative stress via GSH depletion. The immunosuppressive effect of these peptidyl-FMK inhibitors is readily reversed in the presence of the low molecular weight thiols GSH, NAC and L-cysteine but not D-cysteine, which cannot be metabolised into GSH. Furthermore, because NAC is unable to reverse the immunosuppressive properties of z-FA-FMK and z-FF-FMK in the presence of BSO, it is likely that these inhibitors block T cell proliferation by targeting an enzyme(s) in the GSH synthesis pathway.

CHAPTER FIVE

The effect of z-VAD-FMK and the role of oxidative stress in T cell activation and proliferation

5.1 Introduction

Peptidyl-FMK caspase inhibitors are very useful tools and have been used extensively in cell death research to elucidate the role of caspases during apoptotic cell death (Garcia-Calvo et al., 1998, Ekert et al., 1999, Yagi et al., 2001, Caserta et al., 2003). However, accumulating evidence from a number of studies has suggested that these caspase inhibitors may not be as specific as originally envisaged. For instance the most widely used broad spectrum caspase inhibitor, z-VAD-FMK, has been shown to inhibit other enzymes besides the caspases. These include the lysosomal cysteine protease, cathepsin B (Schotte et al., 1999), peptide:N-glycanase (PNGase) (Misaghi et al., 2006) and picornaviral 2A proteinases (Deszcz et al., 2004).

Some of the non-specific effects of these caspase inhibitors may account for some of the inconsistencies observed in the blocking of T cell activation and proliferation reported in several early studies (Zapata et al., 1998, Kennedy et al., 1999, Boissonnas et al., 2002, Mack and Hacker, 2002). For example, in one study, z-VAD-FMK had no effect on T cell proliferation (Zapata et al., 1998), despite effectively inhibiting T cell proliferation in several other studies (Alam et al., 1999, Kennedy et al., 1999, Boissonnas et al., 2002, Mack and Hacker, 2002, Falk et al., 2004). There are also several discrepancies concerning the effects of z-VAD-FMK on the hallmarks of T cell activation. For example, z-VAD-FMK did not inhibit IL-2 secretion in activated T cells (Mack and Hacker, 2002) or has any effect on the up-regulation of the α-subunit of the IL-2 receptor (CD25) (Alam et al., 1999).

More recently, it was demonstrated that z-VAD-FMK readily inhibits primary T cell proliferation without blocking the activation and processing of caspase-8 and caspase-3

(Lawrence and Chow, 2012). However, z-VAD-FMK is extremely effective in blocking the activation of caspases in these cells during apoptosis. Because caspase-8 plays a pivotal role in T cell activation and proliferation (Chun et al., 2002, Salmena et al., 2003, Falk et al., 2004), the suppression of T cell proliferation mediated by z-VAD-FMK is independent of its caspase-inhibitory properties.

In this chapter, the molecular mechanism that underlies the immunosuppressive properties of the pan-caspase inhibitor, z-VAD-FMK, was examined. Additionally, since caspase-8 and caspase-3 have been shown to be cleaved during T cell activation and proliferation (Lawrence and Chow, 2012), a detailed profiling of the caspases activated and substrates cleaved following T cell activation was carried out.

5.2 Results

5.2.1 Effect of z-VAD-FMK on primary T cell proliferation

In order to characterise the underlying mechanism of z-VAD-FMK-induced immunosuppression, the effect of z-VAD-FMK on OKT3-induced T cell proliferation in PBMCs was determined. As illustrated in Figure 5.1, z-VAD-FMK induced suppression of anti-CD3-mediated T cell proliferation in a concentration-dependent manner as determined by the incorporation of BrdU. Although lower concentration of z-VAD-FMK (25 μM) was less effective in blocking anti-CD3-induced T cell proliferation, significant inhibition was observed with 50 and 100 μM z-VAD-FMK, which is very much in line with previous work (Lawrence and Chow, 2012). From the results in Figure 5.1, an IC_{50} of 70 μM was determined and this concentration of z-VAD-FMK was used in all subsequent experiments, unless stated otherwise.

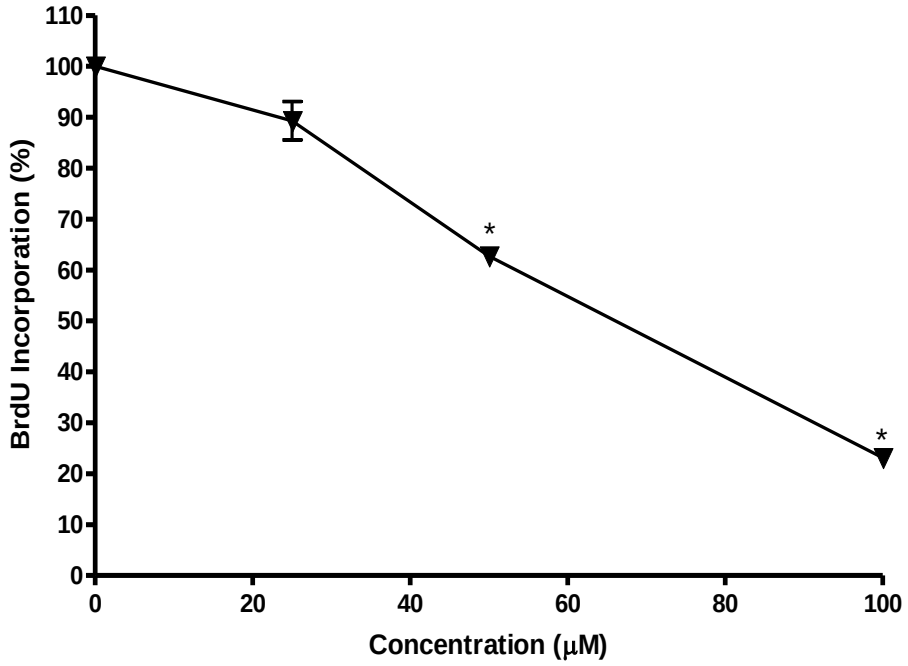

Figure 5.1 Effect of z-VAD-FMK in PBMCs

PBMCs (1 x 10^6/ml) were stimulated with anti-CD3 (5 µg/ml) and seeded in duplicate into 96-well plates in the presence of various concentrations of z-VAD-FMK for 72 h. T cell proliferation was assessed using BrdU incorporation by measuring absorbance on a plate reader as described in the Materials and Methods. Results are the means ± SEM of at least three independent experiments. * Significantly decreased ($p < 0.05$) from control.

5.2.2 Toxicity of z-VAD-FMK in primary T cells

As z-VAD-FMK blocked T cell proliferation in a dose-dependent manner, it was necessary to determine whether the reduction in BrdU incorporation was due to the lack of T cell proliferation or T cell death. As shown in Figure 5.2, there was no significant ($p > 0.05$) increase in PI uptake in resting PBMCs incubated with z-VAD-FMK for 24 h, compared to untreated cells. This suggests that the inhibition of T cell proliferation mediated by z-VAD-FMK is not due to toxicity. To ascertain whether T cells become susceptible to z-VAD-FMK-mediated toxicity following stimulation with anti-CD3, the experiment was repeated using activated T cells. To obtain a pure sample of live proliferating T cells, PBMCs were first activated with anti-CD3 for 24 h before layering onto Lymphoprep^{TM} to remove any dead cells. After centrifugation, the activated T cells were cultured in the presence of rIL-2 (25 U/ml) prior to the treatment with various concentrations of z-VAD-FMK. As shown in Figure 5.2, the increase in PI uptake was not significant ($p > 0.05$) suggesting that the inhibition of T cell proliferation is unlikely to be due to the toxicity of z-VAD-FMK.

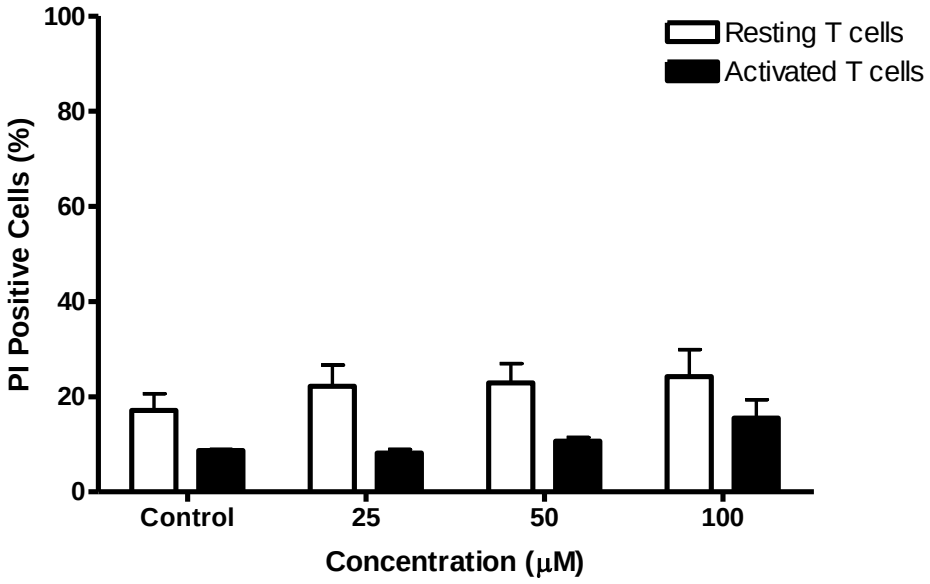

Figure 5.2 Toxicity of z-VAD-FMK in primary T cells

Resting PBMCs (1 x 10^6/ml) were incubated in 24-well plates with various concentrations of z-VAD-FMK for 24 h while activated T cells (1 x 10^6/ml) were seeded in 24-well plates in the presence of rIL-2 (25 U/ml) and treated with z-VAD-FMK for 72 h. At the indicated time points, dead cells were identified as PI positive using flow cytometry as described in Materials and Methods. Results are the means ±SEM of three independent experiments.

5.2.3 Effect of z-VAD-FMK on mitogen-induced primary T cell division using CFSE labeling

In order to confirm the BrdU incorporation data in Figure 5.1, T cell proliferation in the presence of z-VAD-FMK was assessed using the CFSE dye. Prior to stimulation, PBMCs were stained with the CFSE to allow the binding of the dye to intracellular and cell surface proteins. During cell division, the dye is equally distributed between daughter cells (Parish, 1999) allowing for the identification of successive divisions by the halving of cellular fluorescence intensity using flow cytometry (Lyons and Parish, 1994). As shown in Figure 5.3, cellular CFSE fluorescence intensity remained high in resting T cells after 72 h, indicating that the cells were quiescent. In contrast, anti-CD3-activated T cells were actively dividing by 72 h, as shown by a decrease in cellular CFSE fluorescence intensity. In the presence of z-VAD-FMK, the decrease in cellular CFSE fluorescence intensity was reduced compared to control activated T cells, suggesting that cell division was blocked by the pan-caspase inhibitor. This effect was more apparent at 100 µM z-VAD-FMK, where nearly all the cells retained high cellular fluorescence.

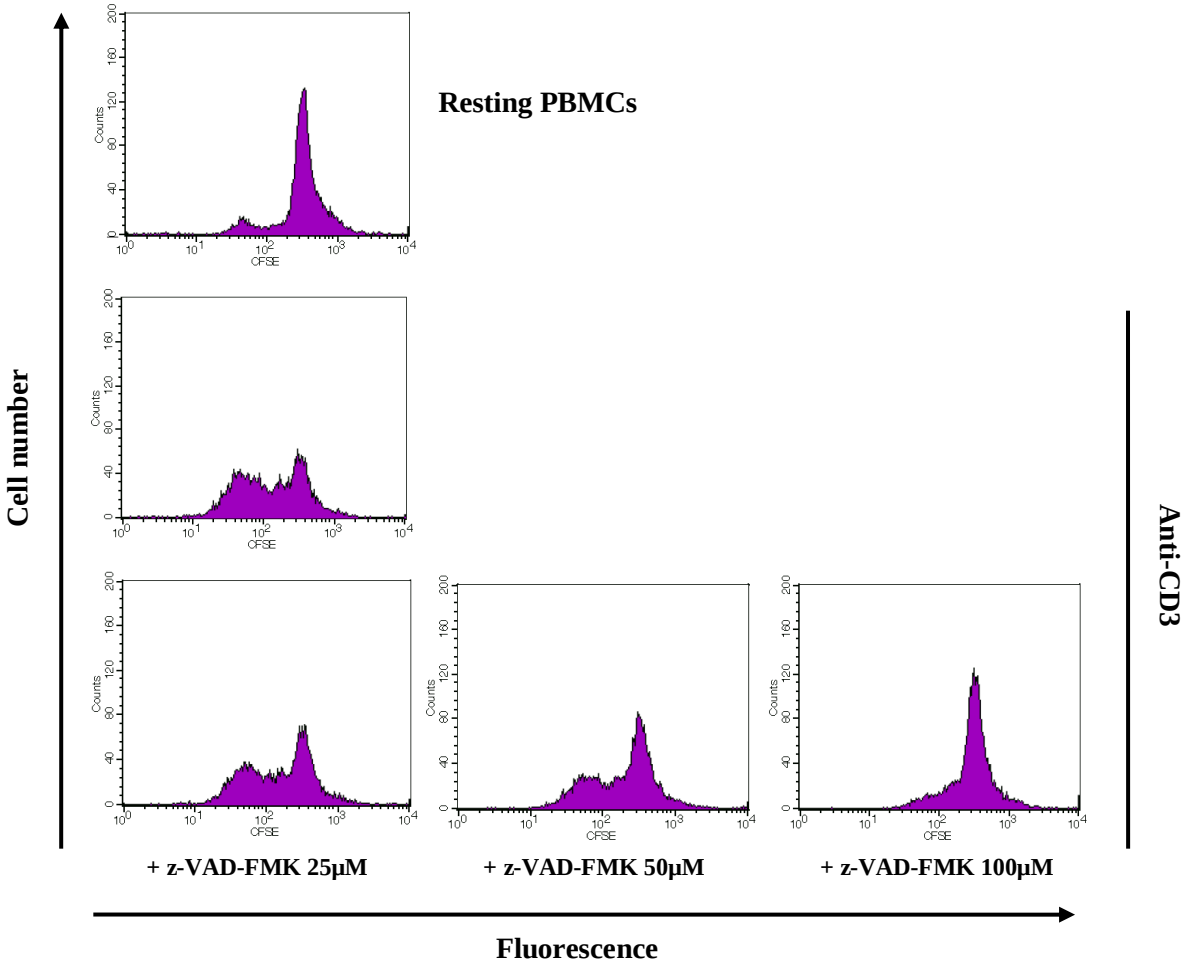

Figure 5.3 Inhibition of anti-CD3-induced cell division by z-VAD-FMK

PBMCs (1 x 10^6/ml) were stained with CFSE (5 µM) prior to stimulation with anti-CD3 (5 µg/ml) in the presence or absence of z-VAD-FMK. After 72 h, cell division was analysed using flow cytometry as described in Materials and Methods. Unstained cells (both resting and stimulated) were consistently $<10^1$ FL-1. The results are one representative from three independent experiments.

5.2.4 Effect of z-VAD-FMK on primary T cell blast formation

Another hallmark of T cell activation is the increase in cell size due to the transformation of resting cells into blasts. Therefore, T cells activated with anti-CD3 antibodies in the presence of z-VAD-FMK were examined after 72 h to determine whether T cell blast formation is blocked by z-VAD-FMK. As illustrated in Figure 5.4, the percentage of blasts in resting control T cells increased from 11.1 % (control) to 58.8 % following T cell activation. In the presence of z-VAD-FMK (25 and 50 μM), there was a slight decrease in the number of blasts formed to 52.3 % and 48.2 %, respectively. However, at 100 μM z-VAD-FMK, the formation of T cell blasts was reduced to 24.7 %. These results indicate that z-VAD-FMK blocks the transformation of resting cells into T cell blasts and are in good agreement with the BrdU incorporation and cell division results with CFSE (Figure 5.1 and Figure 5.3).

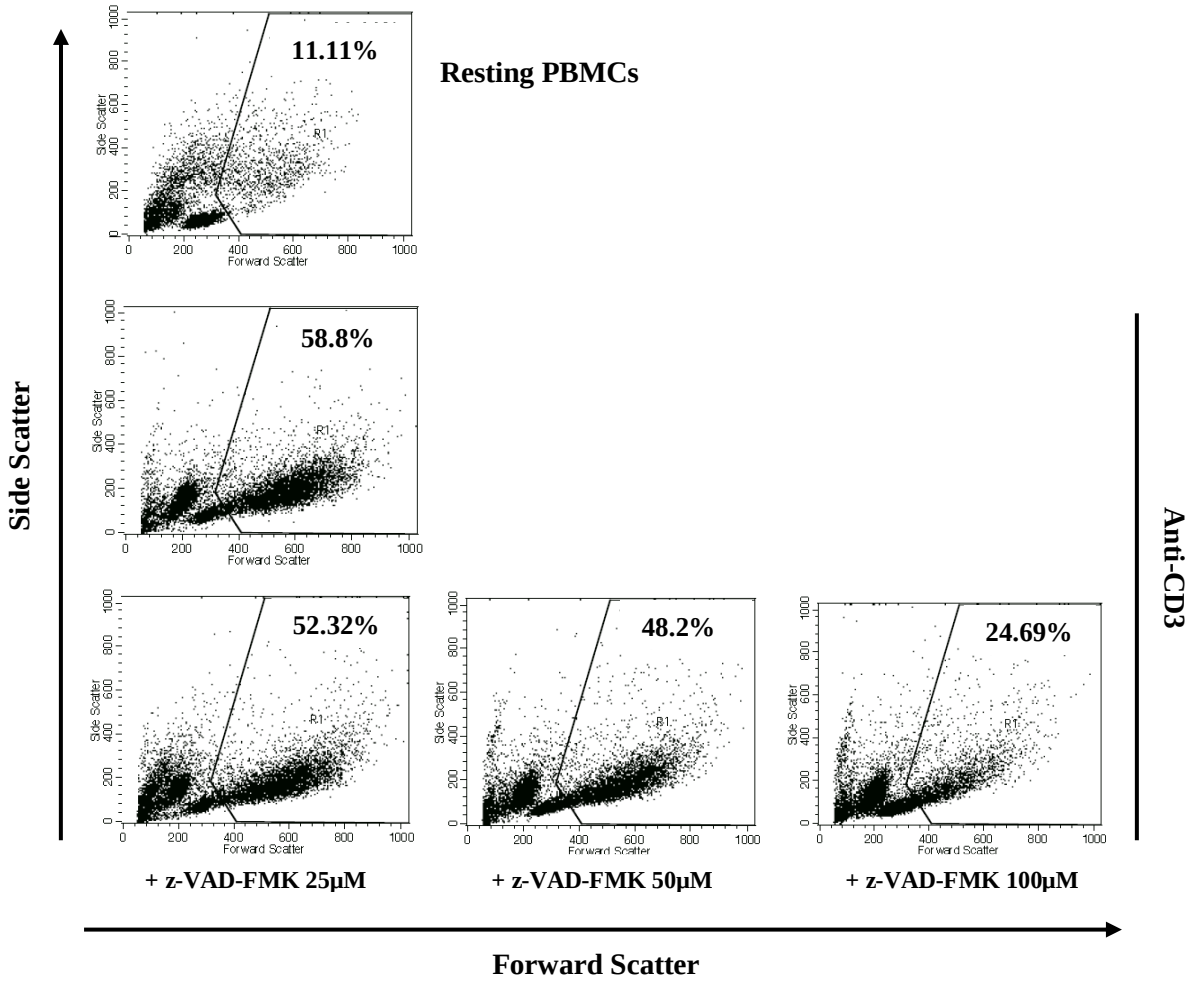

Figure 5.4 Inhibition of T cell blasts formation by z-VAD-FMK

PBMCs (1 x 10^6/ml) were activated with anti-CD3 (5 µg/ml) in the presence or absence of the indicated concentrations of z-VAD-FMK. After 72 h, transformation of resting T cells into lymphoblasts was determined using flow cytometry as described in Materials and Methods. The results are one representative of three independent experiments. Solvent control percentage blasts = 57.5 %.

5.2.5 Effect of z-VAD-FMK on CD25 and CD69 up-regulation

The IL-2 receptor (CD25) and CD69 are both early markers of T cell activation. Therefore, the effect of z-VAD-FMK on these early T cell activation markers was examined to determine if z-VAD-FMK blocks their up-regulation. A shown in Figure 5.5, the percentage of cells which stained positive for CD25 increased from 3.6 % in resting T cells to 60.1 % following anti-CD3 activation for 72 h. In the presence of z-VAD-FMK, the up-regulation of CD25 was reduced to 43.6 % at 25 μM. The inhibition of CD25 up-regulation was more pronounced at 50 and 100 μM, with only 34.5 % and 21.5 % of cells expressing CD25, respectively. As for CD69, the expression of this early T cell activation marker was increased from 2.87 % in resting T cells to 51.2 % in activated T cells after 72 h (Figure 5.6). Although z-VAD-FMK at 25 μM did not have any significant effect ($p > 0.05$) on CD69 expression, the percentage of cells which stained positive for CD69 expression was reduced by z-VAD-FMK, to 39.0 % and 32.0 % at 50 and 100 μM. This trend was similar to that observed with CD25 and suggests that z-VAD-FMK blocks the signaling pathways leading to both CD25 and CD69 up-regulation.

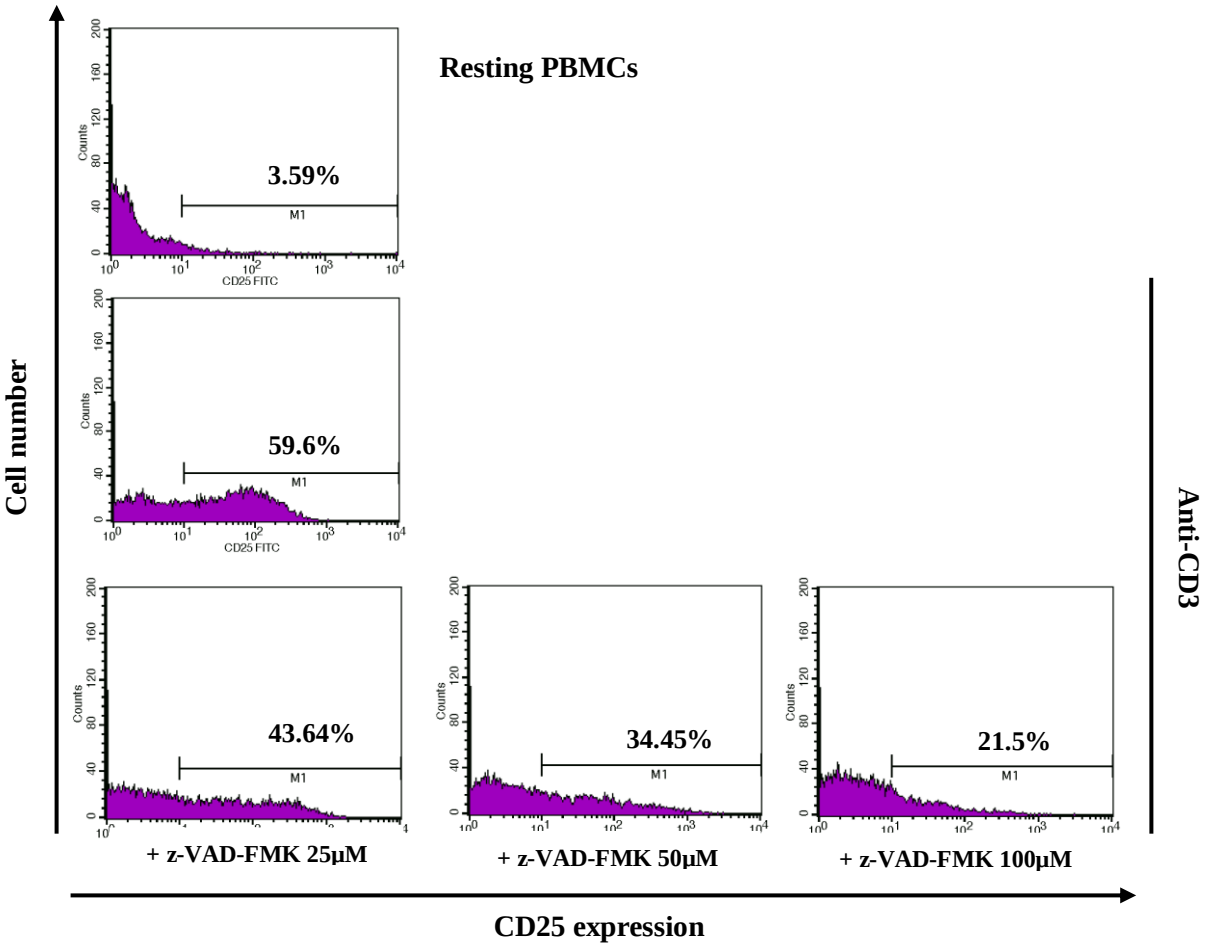

Figure 5.5 Inhibition of CD25 up-regulation by z-VAD-FMK

PBMCs (1 x 10^6/ml) were activated with anti-CD3 (5 µg/ml) in the presence or absence of the indicated concentrations of z-VAD-FMK. After 72 h, the cells were stained with FITC-conjugated anti-CD25 and analysed using flow cytometry as described in Materials and Methods. The percentage of cells which stained positive for CD25 is presented. The results are one representative of three independent experiments.

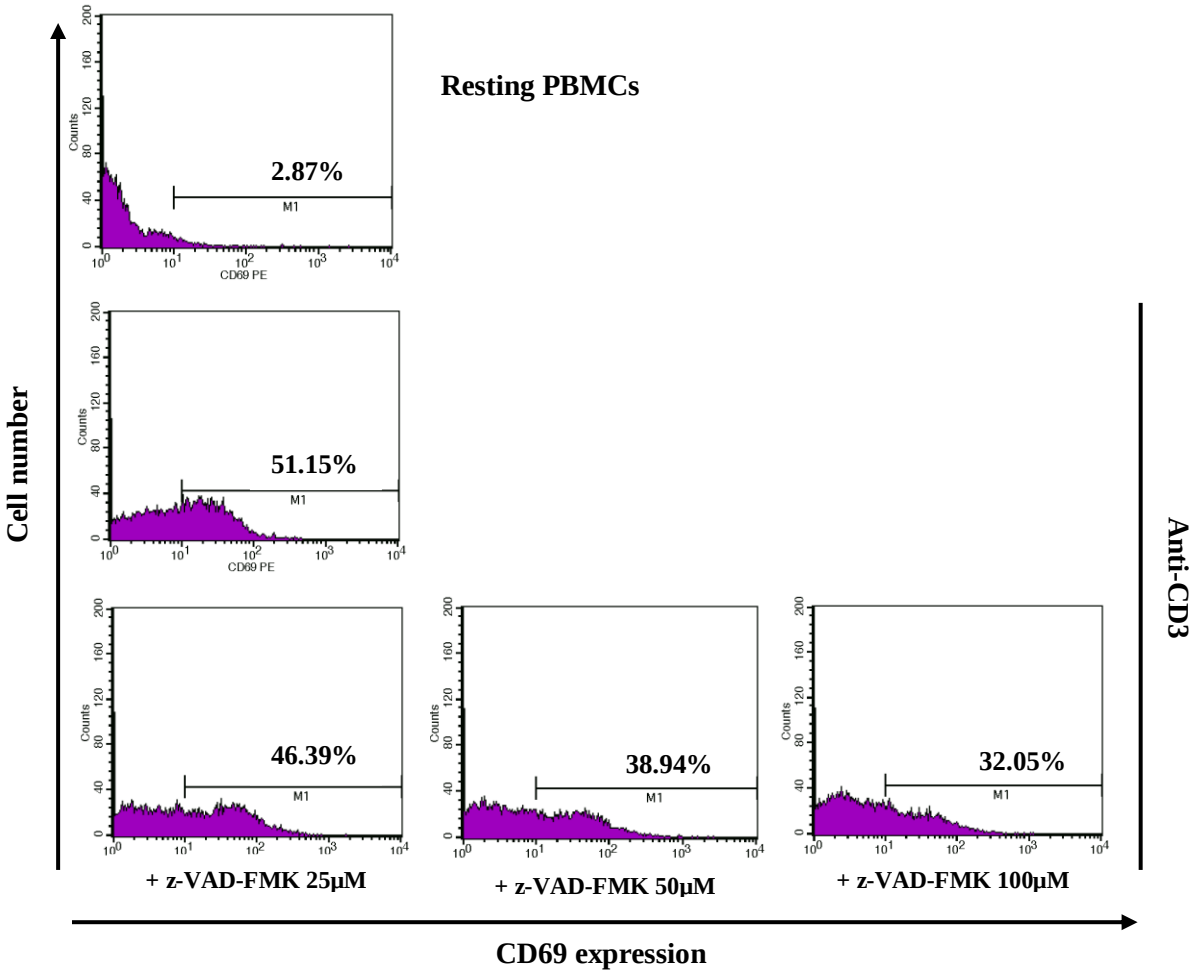

Figure 5.6 Inhibition of CD69 up-regulation by z-VAD-FMK

PBMCs (1 x 10^6/ml) were activated with anti-CD3 (5 µg/ml) in the presence or absence of the indicated concentrations of z-VAD-FMK. After 72 h, the cells were stained with FITC-conjugated anti-CD69 and analysed using flow cytometry as described in Materials and Methods. The percentage of cells which stained positive for CD69 is presented. The results are one representative of three independent experiments.

5.2.6 Effect of z-VAD-FMK on IL-2 driven T cell proliferation

The secretion of, and response to, the cytokine IL-2 are central to T cell activation and proliferation. Following T cell activation, IL-2 is synthesised and secreted, and the α-subunit of the IL-2 receptor (CD25) is up-regulated. According to Figure 5.5, z-VAD-FMK inhibited the up-regulation of CD25. Therefore, the reduction of IL-2 concentration in the extracellular milieu may have resulted in the decrease in T cell proliferation. To examine this possibility, the effect of z-VAD-FMK on IL-2 driven T cell proliferation was examined. PBMCs were activated with anti-CD3 (5 μg/ml) for 24 h and the T cell blasts isolated using density gradient centrifugation to remove the dead cells. The activated T cells were seeded in fresh medium supplemented with 25 U/ml rIL-2 every 3 days. After 7 days, the cells were re-seeded in the presence or absence of z-VAD-FMK. BrdU incorporation into DNA was determined after a further 72 h of cell culture. As shown in Figure 5.7, the addition of 25 U/ml human rIL-2 did not reverse the inhibition of T cell proliferation caused by z-VAD-FMK at all concentrations tested. This suggests that the lack of IL-2 in the cell culture medium is not responsible for the decrease in T cell proliferation.

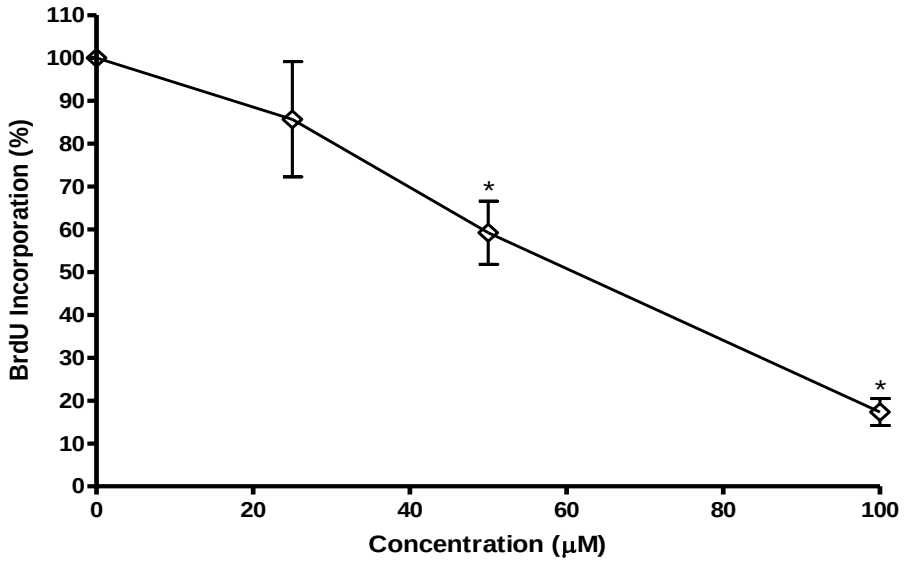

Figure 5.7 Effect of z-VAD-FMK on IL-2 driven cycling T cells

Cycling T cells (1 x 10^6/ml) were generated and seeded in duplicate in 96-well plates in the presence of human rIL-2 (25 U/ml) and the indicated concentrations of z-VAD-FMK. BrdU incorporation was assessed after 72 h by measuring absorbance on a plate reader as described in Materials and Methods. Results are the means ± SEM of three independent experiments. *, Significantly decreased ($p < 0.05$) from control.

5.2.7 Effect of z-VAD-FMK on cell cycle progression in primary T cells

As shown in Figure 5.5, z-VAD-FMK inhibits the up-regulation of CD25 which suggest that the inhibition of proliferation mediated by z-VAD-FMK may be due, in part, by its effect on signaling downstream of the IL-2 receptor. To further characterise this, the inhibitory effect of z-VAD-FMK on primary T cell cycle progression was examined. To this end, PBMCs were activated in the presence of z-VAD-FMK and cell cycle progression was determined after 72 h. As can be seen in Figure 5.8, resting T cells remained in the G_1 phase (91.2 %), whereas upon anti-CD3-stimulation, the cells entered the cell cycle as shown by the reduction in the number of cells in the G_0/G_1 phase (65.3 %) and distribution of the cells in the $S/G_2/M$ phases (31.9 %). Concentrations of 25 and 50 µM z-VAD-FMK had little effect on cell cycle progression whereas 100 µM resulted in cells accumulating in the G_0/G_1 suggesting that the cell cycle is blocked.

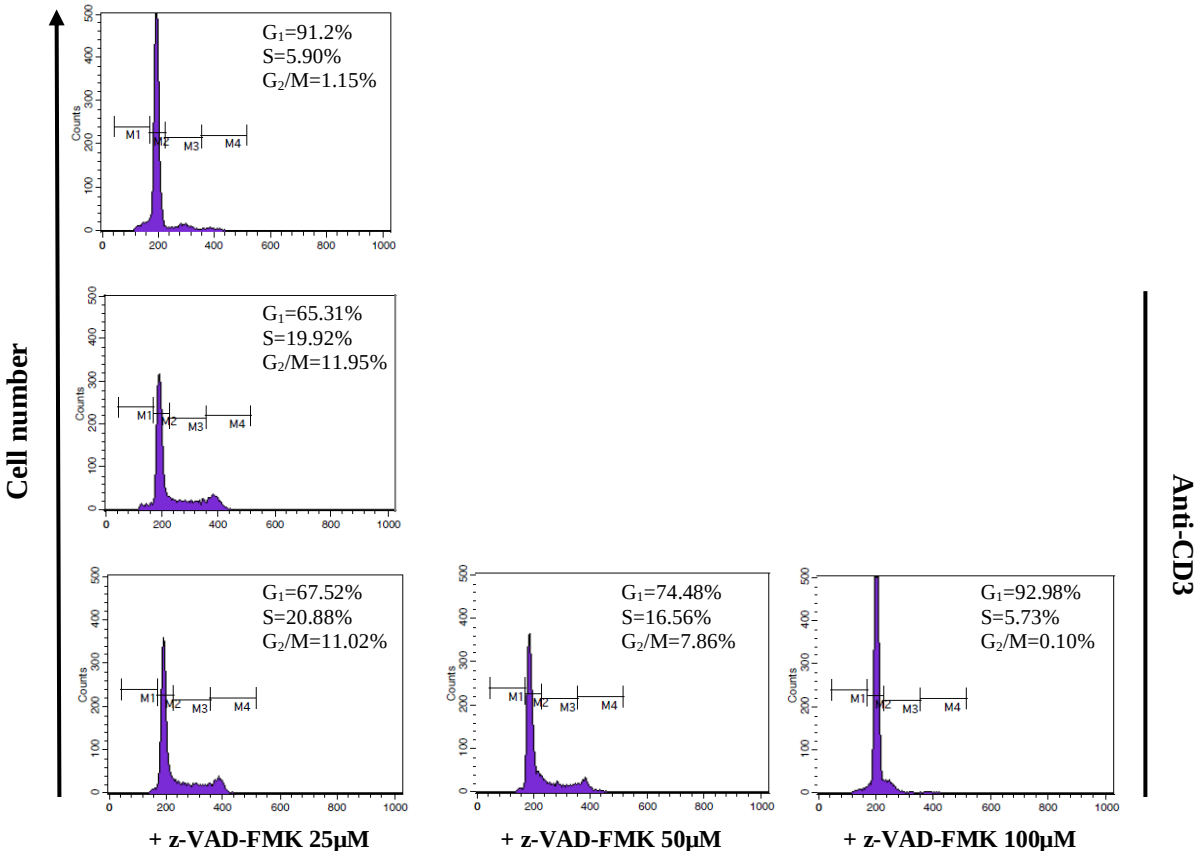

Figure 5.8 Effect of z-VAD-FMK on primary T cell cycle

PBMCs (1 x 10^6/ml) were stimulated with anti-CD3 (5 µg/ml) in the presence or absence of the indicated concentrations of z-VAD-FMK. After 72 h, DNA content was analysed after staining with PI. Solvent control G_1 = 66.37 %, S = 18.21 %, G_2/M = 14.37 %. The results are one representative of three independent experiments.

5.2.8 Effect of z-VAD-FMK on caspase processing in activated primary T cells

The data presented in chapter 3 illustrate that the initiator caspase-8, caspase-2, caspase-9, and the effector caspase-3 and caspase-6 undergo proteolytic processing in activated T cells, in the absence of apoptotic characteristics (Figure 3.11). Since z-VAD-FMK inhibits T cell activation (Figure 5.1), it would be expected to block caspase processing in activated T cells. However, work by Lawrence and Chow (2012) showed that z-VAD-FMK up to 100 µM had no effect on the activation of caspase-8 and caspase-3 following T cell activation. Nevertheless, it was interesting to determine whether z-VAD-FMK blocks other caspases which are also cleaved in proliferating T cells. As shown in Figure 5.9, treatment with the pan-caspase inhibitor, z-VAD-FMK, did not inhibit the processing of pro-caspase-8 and only partially prevented the processing of the p20 subunit of caspase-3 to the smaller subunit, p18 at 100 µM concentration. This is in agreement with previous work by Lawrence and Chow (2012). At 100 µM, z-VAD-FMK partially inhibited the processing of pro-caspase-6 but failed to block the processing of both caspase-2 and caspase-9 into their smaller subunits.

Anti-CD3	–	+	+	+	+
Concentration (μM) of z-VAD-FMK	–	–	25	50	100

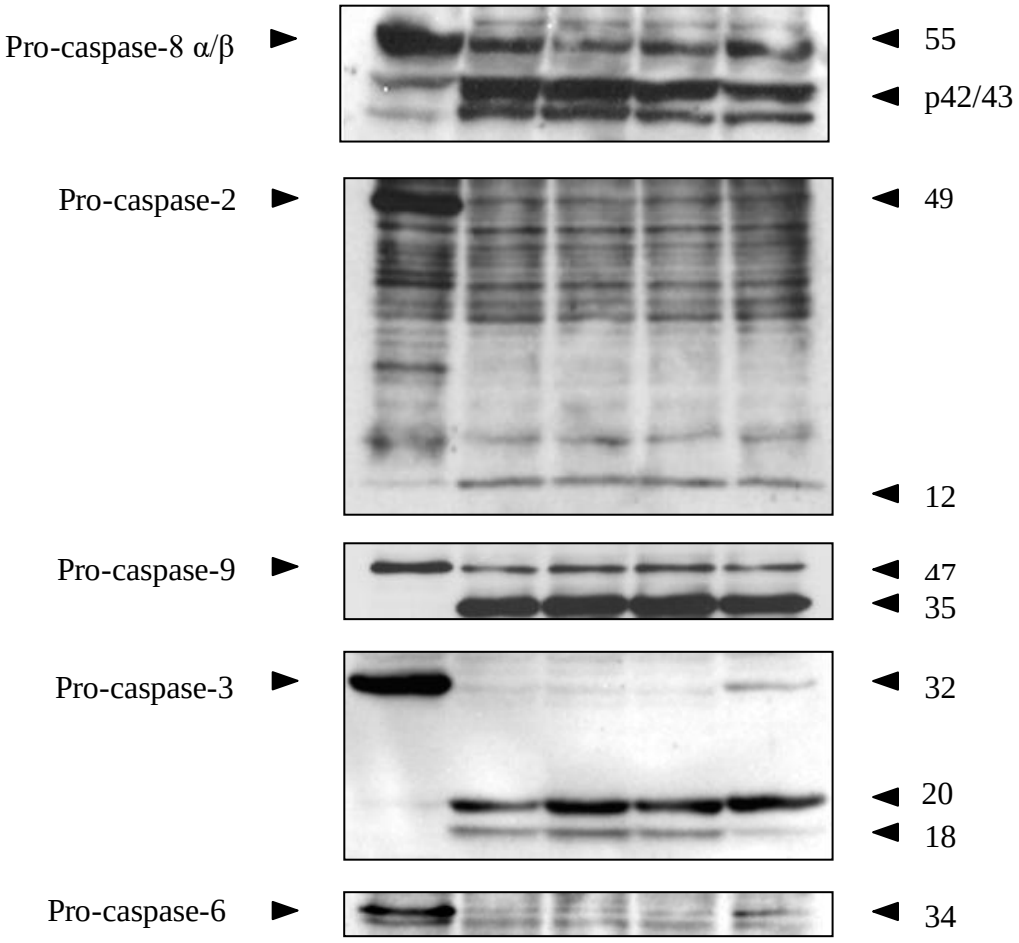

Figure 5.9 Effect of z-VAD-FMK on caspase processing in activated T cells

T cells (1 x 10^6/ml) were activated with anti-CD3 (5 μg/ml) in the absence or presence of z-VAD-FMK. After 72 h, the cells were subjected to gradient density centrifugation to obtain pure, activated T cells. Whole cell lysates (20 μg protein) were resolved using 13 % SDS-PAGE, transferred to nitrocellulose membrane and probed for caspases. The results are one representative of three independent experiments.

5.2.9 Effect of z-VAD-FMK on intracellular GSH and ROS levels in primary T cells

Since GSH depletion has been shown to increase ROS levels and block T cell proliferation (Fidelus et al., 1987, Gmunder et al., 1990, Suthanthiran et al., 1990, Gmunder and Droge, 1991), it was thought that oxidative stress may be responsible for the immunosuppressive effects induced by z-VAD-FMK in T cells. To this end, PBMCs were activated with anti-CD3 in the presence or absence of z-VAD-FMK and the intracellular GSH and ROS levels determined. As illustrated in Figure 5.10, z-VAD-FMK at varying concentrations (25 – 100 μM) has little effect on the GSH level in activated primary T cells after 6 h compared to control cells. However, after 24 h there was a significant reduction of intracellular GSH level in T cells treated with 50 and 100 μM z-VAD-FMK ($p < 0.05$). These results suggest that z-VAD-FMK is capable of depleting GSH in activated T cells.

With the level of intracellular GSH decreasing in the presence of z-VAD-FMK, the level of ROS under similar conditions was also examined. Anti-CD3-activated T cells were incubated with the DHE dye, which selectively detects intracellular superoxide anion ($O_2^{\bullet -}$) production (Bindokas et al., 1996, D'Agostino et al., 2007) prior to flow cytometry analysis. As shown in Figure 5.11, addition of z-VAD-FMK at 25 and 50 μM had little effect on ROS levels in anti-CD3-activated T cells after 6 h. However, at 100 μM z-VAD-FMK the ROS level in activated T cells was significantly increased ($p < 0.05$). The level of ROS in anti-CD3-activated T cells was further increased significantly ($p < 0.05$) by z-VAD-FMK in a concentration-dependent manner (25 – 100 μM) after 24 h. Collectively, these results suggest that z-VAD-FMK induced oxidative stress via GSH depletion in anti-CD3-activated T cells.

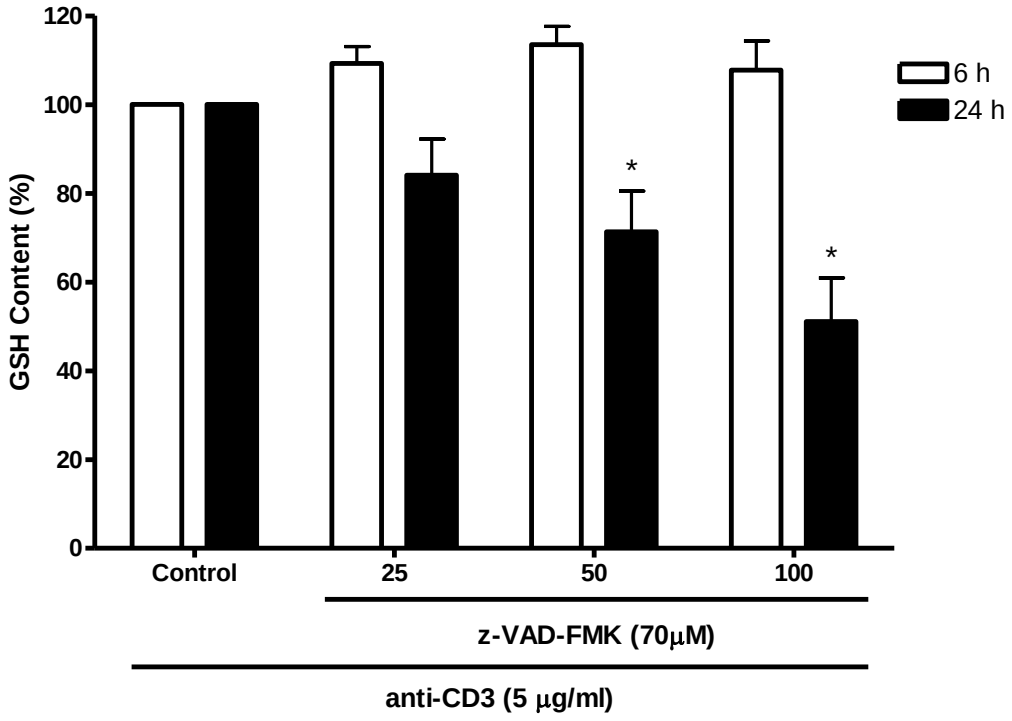

Figure 5.10 Effect of z-VAD-FMK on intracellular GSH levels in activated primary T cells

PBMCs (1 x 10^6/ml) stimulated with anti-CD3 (5 μg/ml) in the presence of the indicated concentrations of z-VAD-FMK. The level of intracellular glutathione was measured after 6 and 24 h using the fluorescent dye MCB and analysed using a spectrophotometer. Results are the mean ± SEM of three independent experiments. *, Significantly decreased ($p < 0.05$) from control.

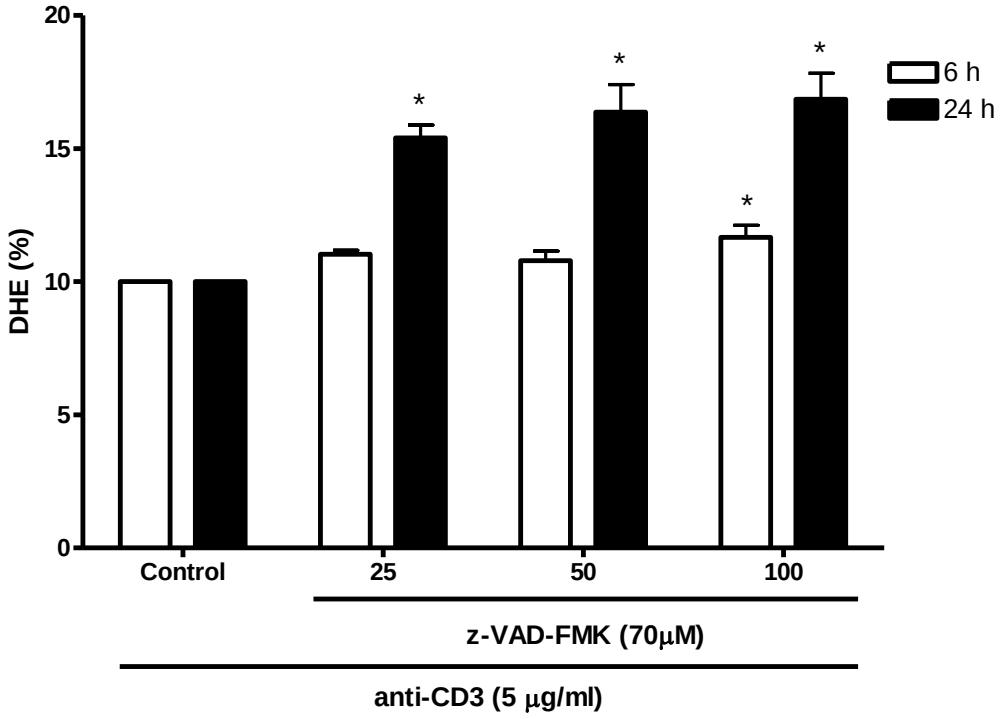

Figure 5.11 Effect of z-VAD-FMK on ROS levels in activated primary T cells

PBMCs (1 x 10^6/ml) stimulated with anti-CD3 (5 μg/ml) in the presence of the indicated concentrations of z-VAD-FMK. ROS levels were measured after 6 and 24 h using the DHE probe and analysed using flow cytometry. Results are the means ± SEM of three independent experiments. *, Significantly increased ($p < 0.05$) from control.

5.2.10 Effect of GSH and NAC on the suppression of primary T cell proliferation mediated by z-VAD-FMK

Since z-VAD-FMK treatment depletes intracellular GSH and increases ROS levels in PBMCs, exogenous GSH was added to PBMCs activated with anti-CD3 in the presence of z-VAD-FMK to determine if this could inhibit its immunosuppressive effect. To this end, anti-CD3-activated T cells were treated with 70 µM z-VAD-FMK in the presence of GSH (1.25 – 5 mM) for 72 h. As shown in Figure 5.12, z-VAD-FMK-induced inhibition of T cell proliferation was restored to control level by GSH in a dose-dependent manner with concentrations of 2.5 and 5 mM GSH significantly increasing ($p < 0.05$) the level of T cell proliferation as compared to z-VAD-FMK-treated T cells on its own.

Next, the thiol NAC, a known precursor of GSH synthesis (Arranz et al., 2008, Lavoie et al., 2008, Berk et al., 2008) and ROS scavenger (Sandstrom et al., 1994) was added to activated primary T cells to determine if NAC could also reverse the immunosuppressive effects of z-VAD-FMK. Intracellular GSH levels were measured in T cells stimulated with anti-CD3 plus z-VAD-FMK at 70 µM, in the presence or absence of NAC (1.25 – 5 mM) for 72 h. As illustrated in Figure 5.13, z-VAD-FMK on its own markedly inhibited anti-CD3-induced T cell proliferation, whereas NAC blocked this effect in a dose-dependent manner (1.25 – 5 mM). At the highest concentration of NAC (5 mM), the suppression of T cell proliferation induced by z-VAD-FMK was nearly abolished.

Collectively, these results suggest that the inhibition of anti-CD3-induced T cell proliferation mediated by z-VAD-FMK is due to oxidative stress via the depletion of GSH. Based on these

results, a concentration of 5 mM low molecular weight thiols was chosen for subsequent experiments.

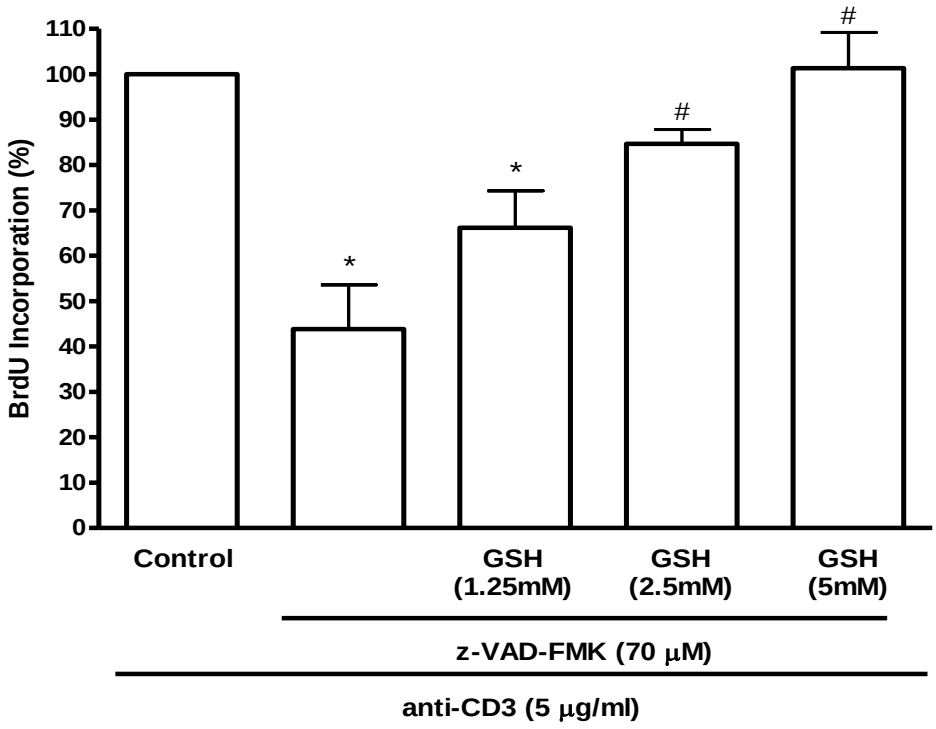

Figure 5.12 Effect of increasing dose of GSH on z-VAD-FMK-induced inhibition of T cell proliferation

PBMCs (1 x 10^6/ml) stimulated with anti-CD3 (5 µg/ml) were treated with 70 µM z-VAD-FMK and increasing concentrations of GSH. BrdU incorporation was assessed after 72 h by measuring absorbance on a plate reader. Results are the means ± SEM of at least three independent experiments. *, Significantly decreased ($p < 0.05$) from control; $^{\#}$, Significantly increased ($p < 0.05$) from z-VAD-FMK treatment alone.

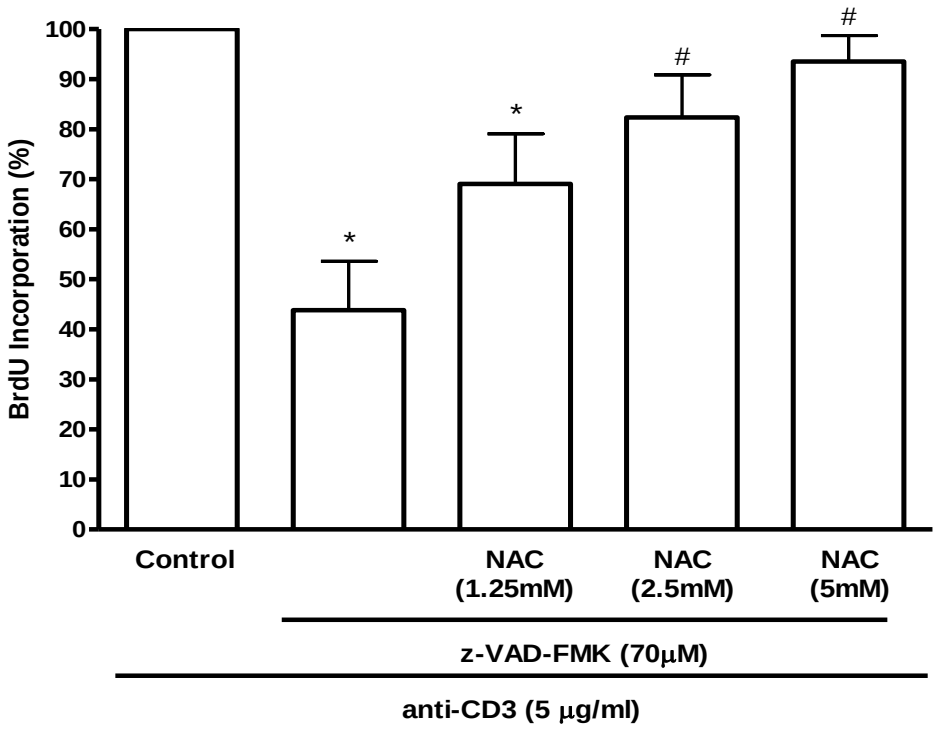

Figure 5.13 Effect of increasing dose of NAC on z-VAD-FMK-induced inhibition of T cell proliferation

PBMCs (1 x 10^6/ml) stimulated with anti-CD3 (5 µg/ml) were treated with 70 µM z-VAD-FMK and increasing concentrations of NAC. BrdU incorporation was assessed after 72 h by measuring absorbance on a plate reader. Results are the means ± SEM of at least three independent experiments. *, Significantly decreased ($p < 0.05$) from control; #, Significantly increased ($p < 0.05$) from z-VAD-FMK treatment alone.

5.2.11 Effect of various low molecular weight thiols on z-VAD-FMK-induced suppression of primary T cell activation and proliferation

The data so far indicate that z-VAD-FMK inhibits T cell proliferation via GSH depletion and subsequent oxidative stress. Furthermore, addition of the low molecular weight thiols GSH and NAC is capable of abolishing z-VAD-FMK-induced inhibition of T cell proliferation. Therefore, the effect of other low molecular weight thiols on anti-CD3-stimulated T cell activation and proliferation in the presence of z-VAD-FMK was examined. The first low molecular weight thiol chosen was L-cysteine which is produced by intracellular deacetylation of NAC and is required for GSH synthesis (Monick et al., 2003, Hadzic et al., 2005). As illustrated in Figure 5.14, the presence of 5 mM L-cysteine attenuated the inhibition of T cell proliferation mediated by z-VAD-FMK. On the other hand, D-cysteine which cannot be metabolized into GSH (Jones et al., 1995) has virtually no effect. These results suggest that only thiols which are able to promote GSH synthesis can abolish the immunosuppressive effect of z-VAD-FMK. As a control, BSO, the selective inhibitor of γ-glutamylcysteine synthetase (Griffith and Meister, 1979), was added to anti-CD3-activated T cells. In agreement with several previous reports (Hamilos et al., 1989, Messina and Lawrence, 1989, Walsh et al., 1995), the addition of 0.5 mM BSO significantly blocked ($p < 0.05$) the proliferation of activated T cells (Figure 5.14). Taken together, the data strongly indicates that z-VAD-FMK-mediated immunosuppression in activated T cells is due to oxidative stress via the depletion of intracellular GSH.

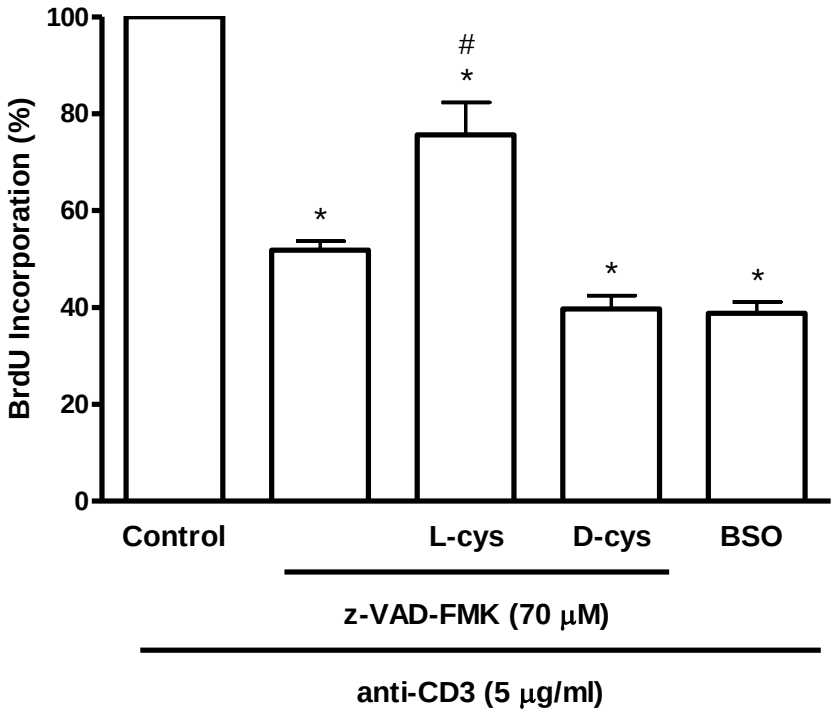

Figure 5.14 Effect of low molecular weight thiols on z-VAD-FMK treatment in PBMCs

PBMCs (1 x 10^6/ml) stimulated with anti-CD3 (5 µg/ml) were treated with 70 µM z-VAD-FMK in the presence or absence of low molecular weight thiols (5 mM) or 0.5 mM BSO, as indicated. BrdU incorporation was assessed after 72 h by measuring absorbance on a plate reader. Results are the means ± SEM of at least three independent experiments. *, Significantly decreased ($p < 0.05$) from control; #, Significantly increased ($p < 0.05$) from z-VAD-FMK treatment alone.

5.2.12 Mechanisms that underlie the depletion of GSH mediated by z-VAD-FMK in primary T cells

As demonstrated earlier (Figures 5.12 – 5.14), z-VAD-FMK blocks T cell proliferation via the depletion of intracellular GSH which is reversed by the presence of GSH, NAC and L-cysteine. However, it was interesting to determine whether z-VAD-FMK initiates GSH depletion via direct chemical interaction. To this end, GSH was incubated with z-VAD-FMK in a cell free system using an adapted MCB assay (Debiton et al., 2003) which permits direct determination of residual GSH. As shown in Figure 5.15, no significant decrease ($p > 0.05$) in free GSH was observed with addition of z-VAD-FMK (100 µM). On the other hand, NEM, which is known to react directly with GSH and was used as positive control, essentially reduced the available GSH to a very low level. Approximately 2 % of the initial GSH content remained after 120 min versus 76 % with z-VAD-FMK. This suggests that the depletion of intracellular GSH by z-VAD-FMK is unlikely to be via direct interaction.

Therefore, it is probable that z-VAD-FMK blocks the GSH synthesis pathway. To examine whether NAC restores T cell proliferation by functioning as a precursor for GSH biosynthesis or as a ROS scavenger, anti-CD3-activated T cells were co-treated with z-VAD-FMK (70 µM) and NAC (5 mM) in the presence or absence of BSO (0.5 mM). As illustrated in Figure 5.16, the proliferation of anti-CD3-activated T cells treated with z-VAD-FMK plus NAC (5 mM) was significantly increased ($p < 0.05$) compared to T cells treated with z-VAD-FMK alone. However, BSO completely blocked the effect of NAC which strongly suggests that by inhibiting the enzyme γ-glutamylcysteine synthetase, BSO has blocked the ability of NAC to be converted to GSH, thereby exhausting the intracellular pool of GSH. Collectively, these data strengthen the

evidence suggesting that z-VAD-FMK mediated immunosuppression in activated T cells is due to oxidative stress via the depletion of intracellular GSH and further suggests that NAC functions as a precursor for GSH biosynthesis.

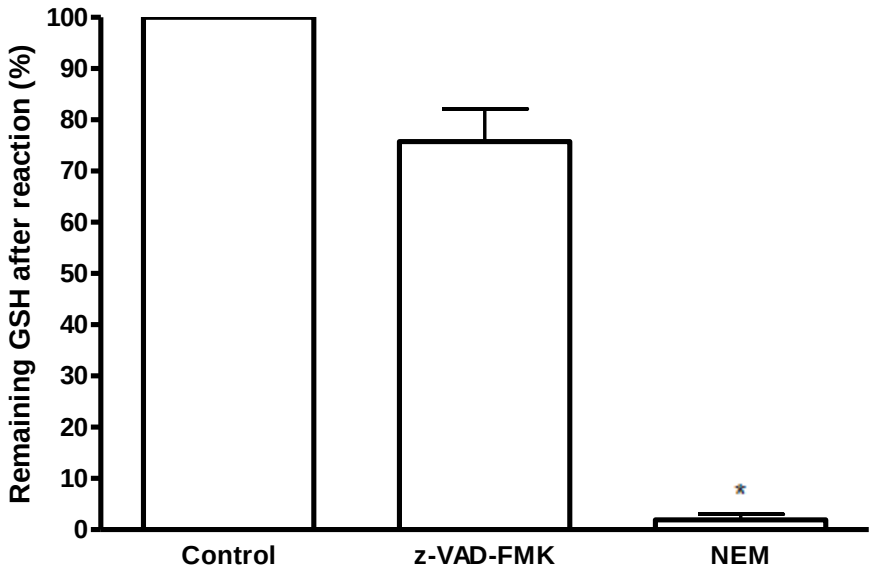

Figure 5.15 Reactivity of z-VAD-FMK with GSH in vitro

z-VAD-FMK (final concentration 100 µM), NEM (final concentration 100 µM) or PBS (control) and GSH (final concentration 100 µM) were added together and incubated for 2 h at 37°C. MCB solution (final concentration 5 mM) was then added and incubated for a further 30 min before measurement of fluorescence at 390/460 nm. Results are the means ± SEM of three independent experiments. *, Significantly decreased ($p < 0.05$) from control.

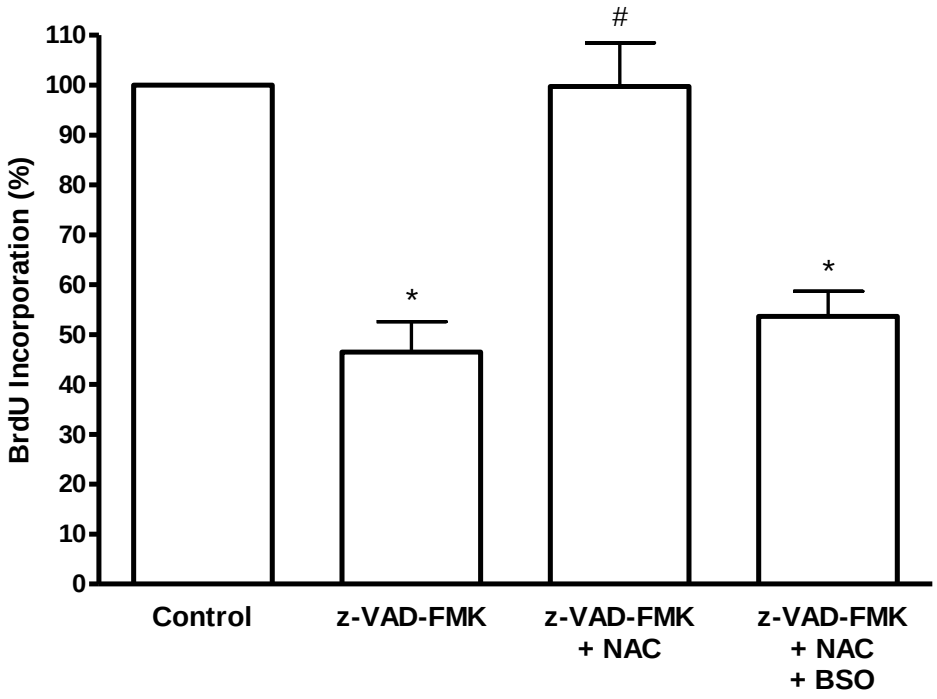

Figure 5.16 NAC is unable to rescue z-VAD-FMK-induced block on T cell proliferation in the presence of BSO

PBMCs (1 x 10^6/ml) stimulated with anti-CD3 (5 µg/ml) were treated with 70 µM z-VAD-FMK with or without 5 mM NAC in the presence or absence of 0.5 mM BSO, as indicated. BrdU incorporation was assessed after 72 h by measuring absorbance on a plate reader. Results are the means ± SEM of at least three independent experiments. *, Significantly decreased ($p < 0.05$) from control; #, Significantly increased ($p < 0.05$) from z-VAD-FMK treatment alone.

5.2.13 Effect of GSH on z-VAD-FMK-induced down-regulation of CD25 and CD69

Up-regulation of the IL-2R α-chain (CD25) and CD69 are some of the earliest cell surface markers to occur after T cell activation following anti-CD3 stimulation. Since low molecular weight thiols are able to reverse the inhibition of T cell proliferation mediated by z-VAD-FMK, the effect of GSH on the expression of CD25 and the activated T cell marker, CD69 was examined. As shown in Figure 5.17, the percentage of cells that stained positive for CD25 and CD69 expression increased from around 0.65 % and 3 % in resting cells to 55.6 % and 51.2 % in activated T cells, respectively. In the presence of z-VAD-FMK (70 μM), the up-regulation of CD25 and CD69 in activated T cells were reduced to 32.3 % and 32.1 %, respectively. The presence of 5 mM GSH completely restored the inhibition of OKT3-induced up-regulation of CD25 and CD69 induced by z-VAD-FMK. These findings demonstrate that oxidative stress plays an important role in the down-regulation of CD25 and CD69 expression induced by z-VAD-FMK in activated T cells.

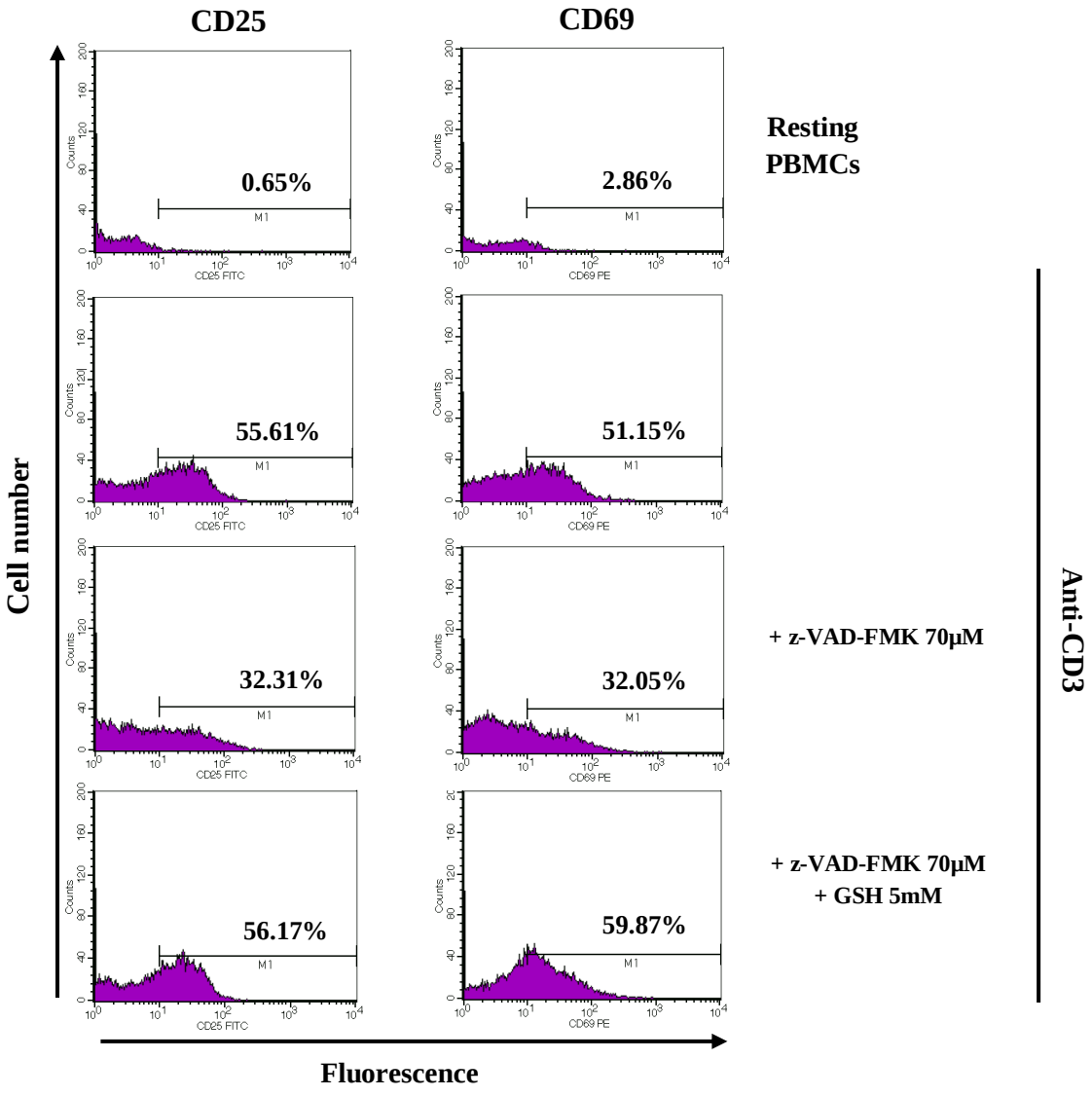

Figure 5.17 Effect of GSH on CD25 and CD69 expression in primary T cells treated with z-VAD-FMK

PBMCs (1 x 10^6/ml) were stimulated with anti-CD3 (5 µg/ml) plus 70 µM z-VAD-FMK in the presence or absence of 5mM GSH. After 72 h, the cells were stained with FITC-conjugated anti-CD25 or PE-conjugated anti-CD69 before analysis using flow cytometry as described in the Materials and Methods. The results are one representative from three independent experiments.

5.2.14 Effect of low molecular weight thiols on caspase-8 and caspase-3 processing in activated primary T cells mediated by z-VAD-FMK

It was shown that z-VAD-FMK had no effect on the activation of caspase-8 and caspase-3 (Figure 5.9), which is in agreement with previous work by Lawrence and Chow (2012). Since the low molecular weight thiols GSH, NAC and L-cysteine could overcome the inhibition of T cell proliferation induced by z-VAD-FMK, the effect of these thiols on caspase processing in z-VAD-FMK-treated activated T cells was examined. In order to exclude cells dying of activation-induced cell death and growth factor deprivation, living activated T cells were purified using Lymphoprep^{TM} prior to western blot analysis. As illustrated in Figure 5.18, neither caspase-8 nor caspase-3 was activated in resting T cells whereas both caspases were activated and processed into their respective subunits following anti-CD3 stimulation. As shown in Figure 5.9 and reported previously (Lawrence and Chow, 2012), z-VAD-FMK had little effect on the activation of caspase-8 and caspase-3 as shown by the presence of the cleaved intermediates. In the presence of GSH, NAC and L-cysteine, the processing of caspase-8 to the p42/43 subunits was partially blocked by z-VAD-FMK. Interestingly, D-cysteine was more effective in blocking the processing of caspase-8 to its p42/43 subunits although it has little effect on z-VAD-FMK-induced suppression of T cell proliferation. However, GSH, NAC and L-cysteine had little effect on the activation and processing of caspase-3 in activated T cells in the presence of z-VAD-FMK. Taken together, the presence of low molecular weight thiols appears to have little effect on z-VAD-FMK caspase-inhibitory properties.

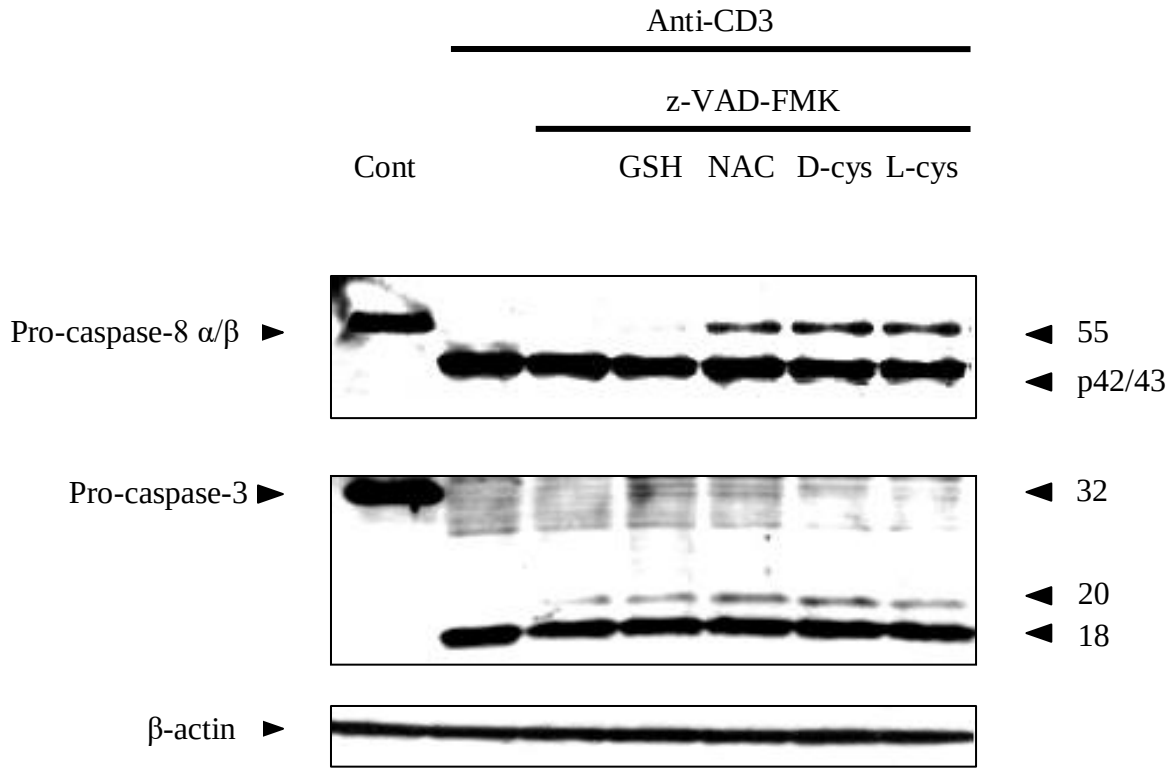

Figure 5.18 Effect of low molecular weight thiols on caspase-8 and caspase-3 processing in z-VAD-FMK-treated activated T cells

PBMCs (1 x 10^6/ml) were stimulated with anti-CD3 (5 μg/ml) plus 70 μM z-VAD-FMK in the presence or absence of antioxidants (5 mM). After 72 h, the cells were taken through a gradient density centrifugation using Lymphoprep™ to obtain living activated T cells. Whole cell lysates (20 μg protein) from activated T cells were resolved using 13 % SDS-PAGE, transferred to nitrocellulose membrane and probed for caspase-8, caspase-3 and β-actin as described in the Materials and Methods. The results are one representative of three independent experiments.

5.3 Discussion

Besides cell death, caspases are also involved in cytokine maturation, cell growth and differentiation (Wang and Lenardo, 2000, Schwerk and Schulze-Osthoff, 2003, Lamkanfi et al., 2007). Among the family of caspases, caspase-8 plays a pivotal role in cell signalling during mitogen-induced T cell activation and proliferation (Chun et al., 2002, Salmena et al., 2003, Falk et al., 2004). It is therefore not surprising that peptidyl-FMK based caspase inhibitors are capable of blocking T cell proliferation as shown in a number of studies (Alam et al., 1999, Kennedy et al., 1999, Boissonnas et al., 2002, Mack and Hacker, 2002, Falk et al., 2004). However, accumulating evidence suggested that peptidyl-FMK caspase inhibitors may not be as specific as originally thought (Schotte et al., 1999, Deszcz et al., 2004, Misaghi et al., 2006). A recent study demonstrated that z-VAD-FMK inhibits T cell proliferation but fails to block the activation of caspase-8 and caspase-3 in proliferating T cells (Lawrence and Chow, 2012). This suggests that the suppression of T cell proliferation mediated by z-VAD-FMK has little to do with caspase inhibition. In the present study, the underlying mechanism involved in the inhibition of T cell proliferation induced by z-VAD-FMK was examined.

In anti-CD3 activated T cells, z-VAD-FMK treatment leads to the depletion of intracellular GSH with a corresponding increase in cellular ROS. This suggests that oxidative stress may be the underlying mechanism of z-VAD-FMK immunosuppressive effect. Indeed, the inhibition of T cell proliferation mediated by z-VAD-FMK was readily abolished by exogenous low molecular weight thiols such as GSH, NAC and L-cysteine. Since both NAC and L-cysteine are precursors for GSH biosynthesis, the results suggest that GSH may be the rate-limiting thiol necessary for T

cell proliferation. This is further corroborated when D-cysteine, which cannot be metabolised to GSH, was unable to restore T cell proliferation in the presence of z-VAD-FMK.

Taken together, the ability of GSH, NAC and L-cysteine to restore T cell proliferation suggests that the immunosuppressive effect induced by z-VAD-FMK is due to oxidative stress via the depletion of GSH. These findings are very much in line with numerous studies showing that GSH plays an important role in T cell proliferation (Zmuda and Friedenson, 1983, Hamilos and Wedner, 1985, Markovic et al., 2007). For instance, human T lymphocytes depleted of intracellular GSH using pharmacological regulators of GSH, such as methionine sulfoximine (Ronzio et al., 1969), diethyl maleate (Hidaka et al., 1990, Weber et al., 1990) and BSO (Griffith and Meister, 1979, Griffith et al., 1979, Vaziri et al., 2000, Reliene and Schiestl, 2006) were unable to proliferate and accumulate high levels of ROS (Fidelus et al., 1987, Gmunder et al., 1990, Suthanthiran et al., 1990, Gmunder and Droge, 1991). In contrast, increasing intracellular GSH levels using 2-mercaptoethanol was reported to enhance T cell proliferation mediated by IL-2 and anti-CD3-stimulated CD3+ T lymphocytes (Zmuda and Friedenson, 1983, Messina and Lawrence, 1989). All these studies implicate GSH as an important regulator for T cell proliferation and suggest a direct relationship between the proliferative response of T cells and the availability of GSH (Chaplin and Wedner, 1978, Fidelus et al., 1987, Suthanthiran et al., 1990). How z-VAD-FMK treatment diminishes the intracellular GSH level in activated T cells is unclear, although peptidyl-FMKs have been reported to interact with GSH directly in vitro (Angliker et al., 1987). However, the time taken for z-VAD-FMK to reduce intracellular GSH level in activated T cells is rather long, thus ruling out a direct interaction between z-VAD-FMK and GSH.

Besides blocking T cell proliferation, z-VAD-FMK also inhibits the expression of CD25 and CD69 in T cells, two early T cell activation markers when stimulated with anti-CD3 (Kennedy et al., 1999, Falk et al., 2004, Lawrence and Chow, 2012). The up-regulation of CD25 and CD69 expression in activated T cells has been reported previously to be dependent on the intracellular GSH levels or redox state of the cells (Roozendaal et al., 2002). This suggests that the depletion of intracellular GSH mediated by z-VAD-FMK could also account for the down-regulation of CD25 and CD69 expression in activated T cells. Indeed, the presence of exogenous GSH completely restored the inhibition of anti-CD3-induced CD25 and CD69 expression mediated by z-VAD-FMK to control levels, confirming that the depletion of intracellular GSH is the underlying mechanism of the down-regulation of these two early T cell activation markers.

Being a pan-caspase inhibitor, z-VAD-FMK has been used extensively in apoptosis research to block the activation of caspases. Therefore, its failure to block the activation and processing of caspase-8 and caspase-3 to their subunits in activated T cells was rather unexpected (Lawrence and Chow, 2012). None of the low molecular weight thiols were able to restore the failure of z-VAD-FMK in blocking caspase-8 and caspase-3, suggesting that the inhibition of T cell proliferation mediated by the caspase inhibitor can be uncoupled from its caspase-inhibitory properties, and that oxidative stress is unlikely to be involved in the latter.

How proliferating T cells are able to cope with the pro-apoptotic activity of caspases remains unclear. It has been suggested that restricted localisation of the active caspases helps to restrain them from cleaving substrates that trigger apoptosis in proliferating T cells (Lamkanfi et al., 2007, Koenig et al., 2008, Paulsen et al., 2008). However, peptidyl-FMK based caspase

inhibitors are designed as substrates and function as competitive inhibitors. Being membrane permeable, z-VAD-FMK should be able to block the active caspases without being affected by their subcellular localisation (Lamkanfi et al., 2007, Paulsen et al., 2008). Alternatively, the activated caspases are restrained by cellular inhibitors of apoptosis proteins, such as XIAP as shown recently in proliferating T cells (Paulsen et al., 2008). This could explain the failure of z-VAD-FMK in blocking the activated caspases and the lack of PARP cleavage in proliferating T cells (Lawrence and Chow, 2012). However, it cannot account for the processing of caspase-8 and caspase-3, which are caspase-dependent.

In summary, our results demonstrate that z-VAD-FMK inhibits T cell activation and proliferation induced by anti-CD3 through oxidative stress via GSH depletion. The immunosuppressive effect of z-VAD-FMK is readily reversed in the presence of low molecular weight thiols such as GSH, NAC and L-cysteine, whereas D-cysteine which cannot be metabolised to GSH has no effect. Furthermore, these thiols were unable to restore the failure of z-VAD-FMK to block the processing of caspase-8 and caspase-3, suggesting that the inhibition of T cell proliferation can be uncoupled from the caspase-inhibitory properties of z-VAD-FMK.

CHAPTER SIX

Structure activity relationship of peptidyl-methyl ketones on Jurkat T cell proliferation and the role of oxidative stress

6.1 Introduction

The findings in the previous chapters indicate that z-FA-FMK, z-FF-FMK and z-VAD-FMK inhibit primary T cell activation through GSH depletion and oxidative stress. The data are in agreement with previous reports which suggest that the immunosuppressive effects of these peptidyl-FMK inhibitors are not mediated through the inhibition of caspase processing (Lawrence et al., 2006, Lawrence and Chow, 2012). So far, the effect of the peptidyl-FMK inhibitors have only been examined in primary T cells which require an activation signal to proliferate. However, it is not clear whether cell lines, which do not require activation signal to drive proliferation, would be susceptible to the immunosuppressive effects of these methyl ketone peptides.

In this chapter, the effect of z-FA-FMK, z-FF-FMK and z-VAD-FMK on cell proliferation was examined using Jurkat T cells, a well established leukemic T cell line. The Jurkat T cells are an immortalized line of human leukemia T cells established from the peripheral blood of a 14 year old boy (Schneider et al., 1977). In contrast to primary T cells, Jurkat T cells proliferate continuously without the need of any activation signal.

6.2 Results

6.2.1 Effect of peptidyl-FMKs and their analogues on Jurkat T cell proliferation

Since previous data show that z-FA-FMK blocked antigen- and IL-2-driven cycling T cells (Figure 3.2 and Figure 3.10), the effect of peptidyl-methyl ketones on Jurkat T cell proliferation was examined. To this end, the effect of z-FA-FMK, z-FA-DMK and z-FA-CMK on Jurkat T cells proliferation was determined by counting the increase in cell density after 24, 48 and 72 h. As illustrated in Figure 6.1A, Jurkat T cells were seeded at a density of 2.5 x 10^5 cells/ml and doubled every 24 h to a final density of between 2 to 2.5 x 10^6 cells/ml after 72 h. In the presence of z-FA-FMK, Jurkat T cell proliferation was reduced in a dose-dependent manner compared to untreated cells. At 100 µM z-FA-FMK, the cell density was reduced to 2 x 10^5 cells/ml compared to 2 x 10^6 cells/ml in the control. As shown in Figure 6.1B, z-FA-DMK, at all concentrations tested, had little effect on Jurkat T cell proliferation over 72 h. In sharp contrast, z-FA-CMK (Figure 6.1C) completely blocked Jurkat T cell proliferation from as early as 24 h at the lowest concentration used (25 µM). It is now clear that this peptide is toxic and induced apoptosis and necrosis in Jurkat T cells (Liow and Chow, 2013).

Since only z-FA-FMK blocked Jurkat T cell proliferation the role of the FMK moiety in blocking T cell proliferation was examined. To this end, the effects of other peptidyl-FMK peptides such as z-VRPR-FMK, z-YVAD-FMK and z-VAD-FMK on Jurkat T cell proliferation were determined. As shown in Figure 5.2, the MALT1 inhibitor, z-VRPR-FMK, and the caspase-1 inhibitor, z-YVAD-FMK, had little effect on Jurkat T cell proliferation after 72 h. Interestingly, the broad spectrum caspase inhibitor, z-VAD-FMK, which blocks antigen-driven primary T cell proliferation, had no effect on Jurkat T cell proliferation. Taken together, the data

indicates that the suppression of Jurkat T cell proliferation mediated by z-FA-FMK is likely to involve the combination of the FMK group and other components of z-FA-FMK, suggesting some degree of specificity in z-FA-FMK-induced suppression of Jurkat T cell proliferation.

Since z-FF-FMK, which has the alanine in the P1 position replaced with phenylalanine, blocks primary T cell proliferation; its effect on Jurkat T cells was examined. Similar to primary T cells (Figure 3.4), z-FF-FMK inhibited Jurkat T cell proliferation in a dose-dependent manner (Figure 6.3). Furthermore, z-FF-FMK was found to be more potent in blocking Jurkat T cell proliferation, with an IC_{50} of 25 µM compared to 50 µM with z-FA-FMK. As shown in chapter 3, the role of the benzyloxycarbonyl group at the N-terminal of z-FA-FMK was examined for its role in blocking proliferation in Jurkat T cells. As shown in Figure 6.4, biotin-FA-FMK at all concentrations examined was unable to block Jurkat T cell proliferation. These results suggest that the benzyloxycarbonyl group at the N-terminal of z-FA-FMK is also necessary for blocking Jurkat T cell proliferation. Taken together, these results suggest that the suppression of Jurkat cell proliferation mediated by z-FA-FMK requires not only the FMK group, but also the presence of the benzyloxycarbonyl group at the N-terminal. To further characterize the inhibition of Jurkat T cell proliferation by peptidyl-FMK inhibitors, z-FA-FMK and z-FF-FMK were examined in all subsequent experiments.

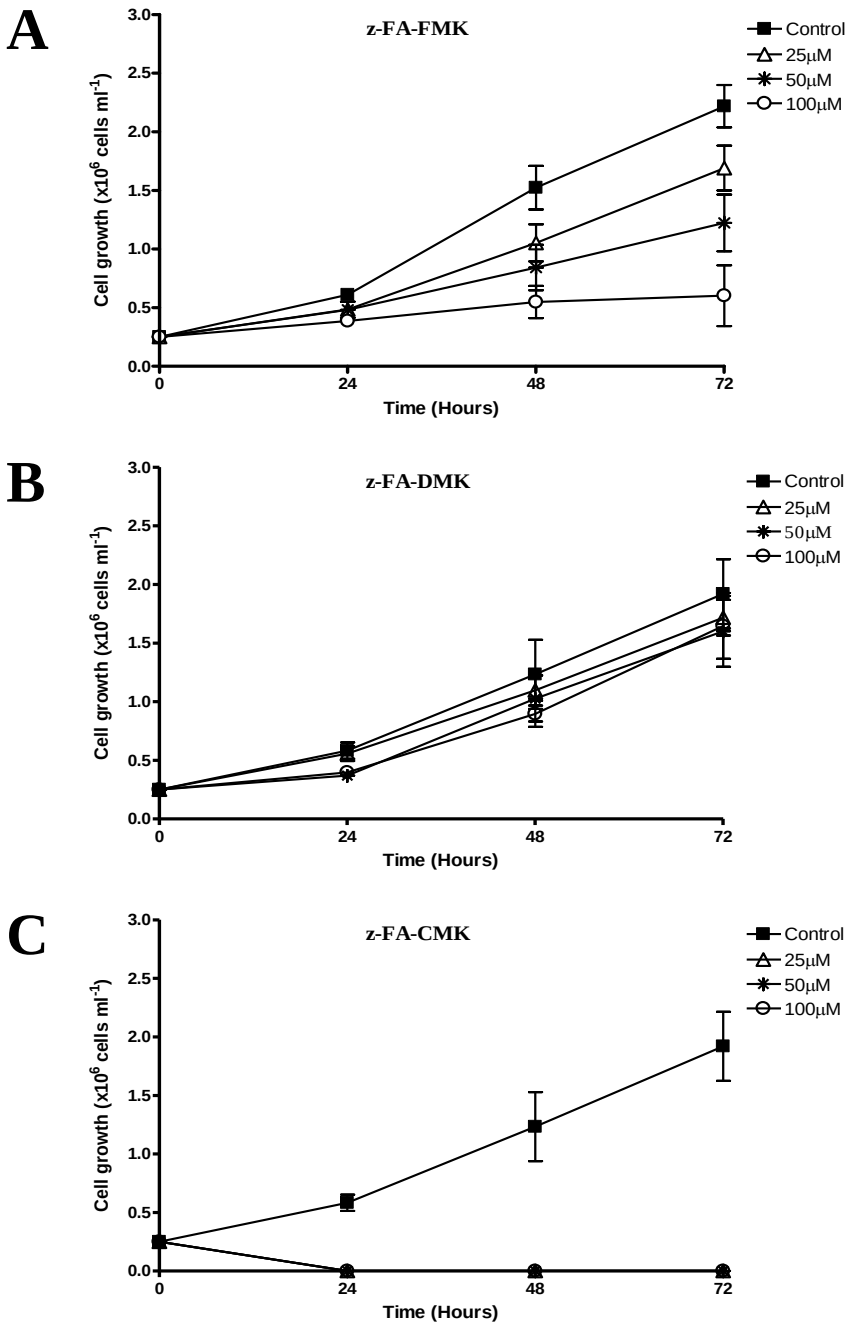

Figure 6.1 Dose-response and time-course studies on the effect of z-FA-FMK analogues on Jurkat T cell proliferation

Jurkat T cells (2.5 x 10^5/ml) were incubated with the indicated concentrations of (A) z-FA-FMK, (B) z-FA-DMK or (C) z-FA-CMK for 24-72 h. Cells were counted at each time point using the trypan blue exclusion assay. Results are the means ± SEM of at least three independent experiments.

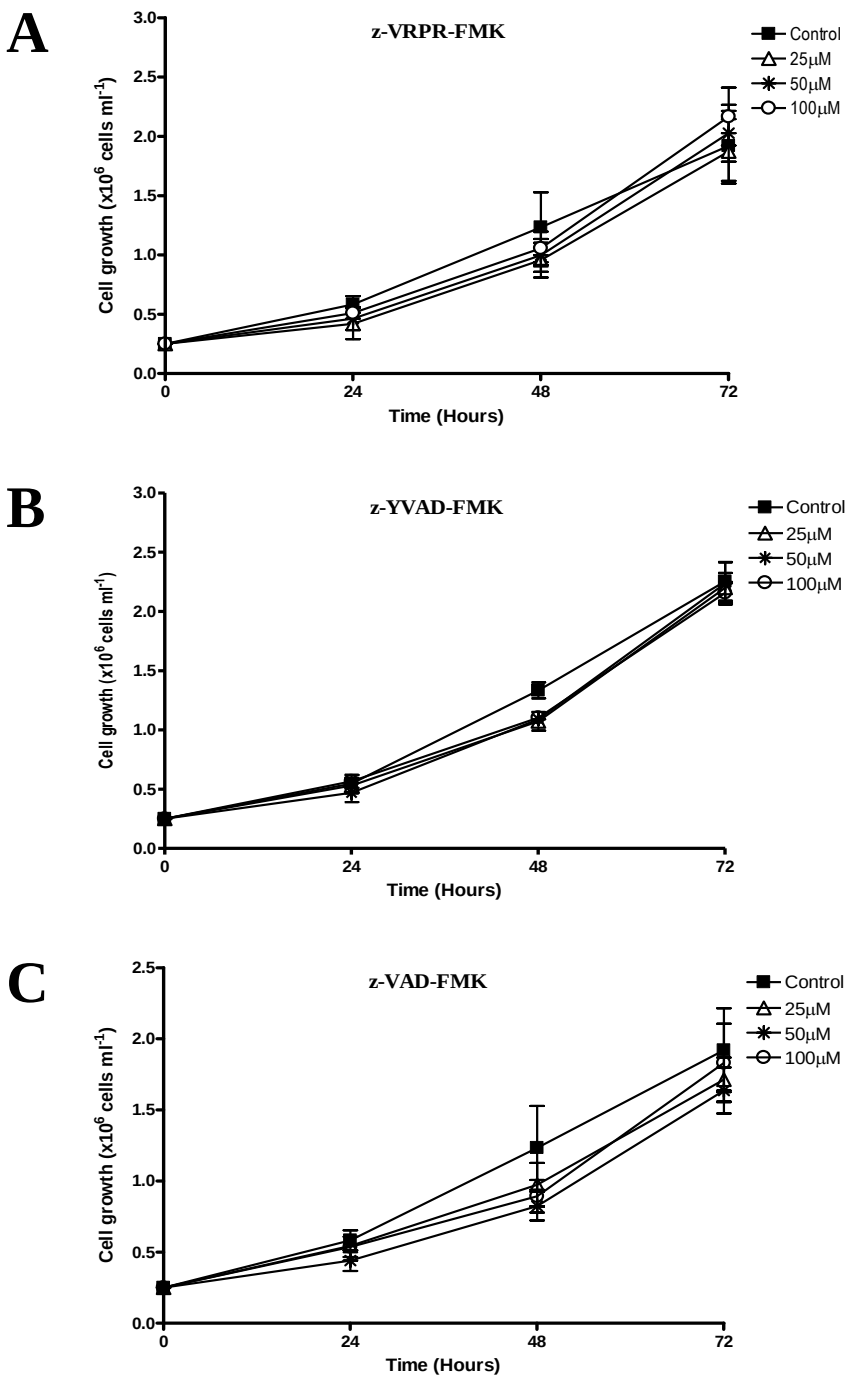

Figure 6.2 Dose-response and time-course studies on the role of the FMK group on Jurkat T cell proliferation

Jurkat T cells (2.5 x 10^5/ml) were incubated with the indicated concentration of (A) z-VRPR-FMK, (B) z-YVAD-FMK and (C) z-VAD-FMK for 24-72 h. Cells were counted at each time point using the trypan blue exclusion assay. Results are the means ± SEM of at least three independent experiments.

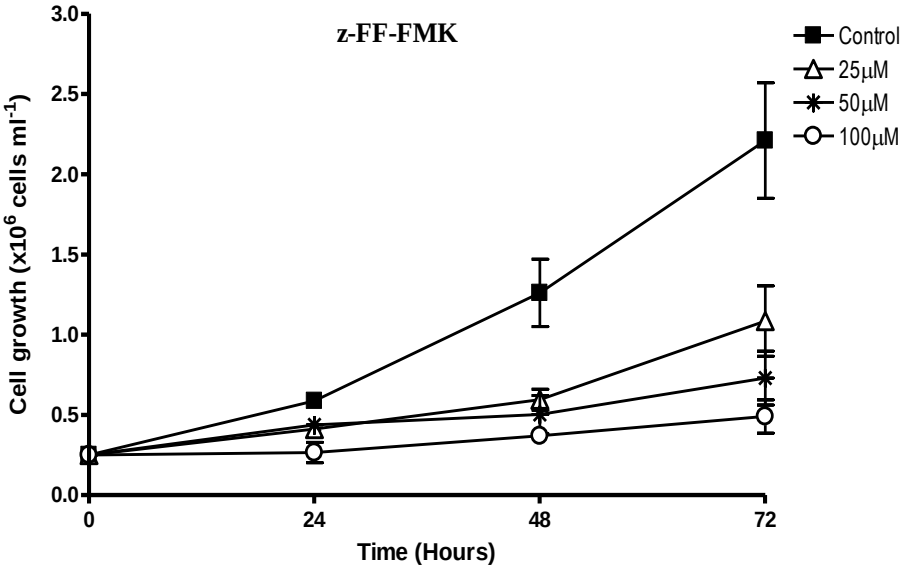

Figure 6.3 Dose-response and time-course studies on the role of amino acids on Jurkat T cell proliferation

Jurkat T cells (2.5 x 10^5/ml) were incubated with the indicated concentrations of z-FF-FMK for 24 - 72 h. Cells were counted at each time point using the trypan blue exclusion assay. Results are the means ± SEM of three independent experiments.

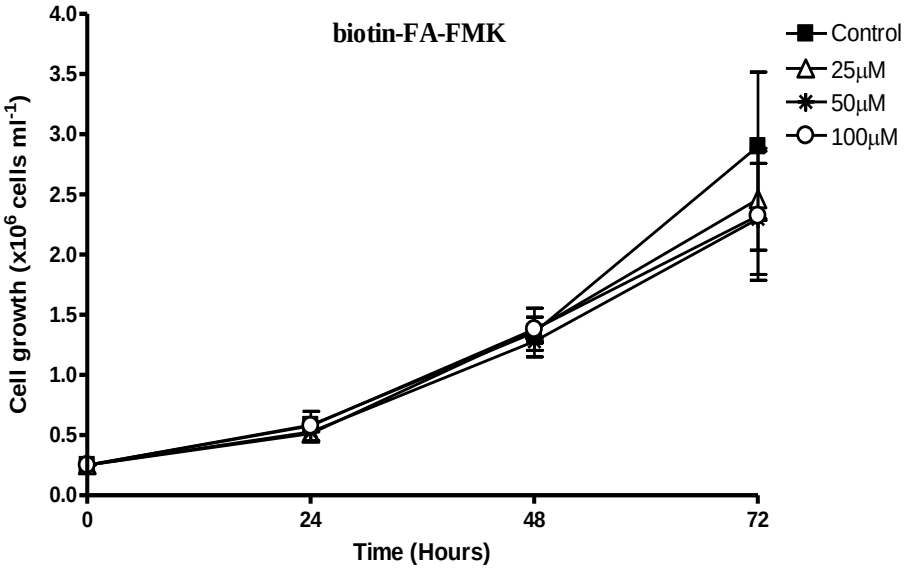

Figure 6.4 Dose-response and time-course studies on the role of the N-terminal blocking group on Jurkat T cell proliferation

Jurkat T cells (2.5 x 10^5/ml) were incubated with the indicated concentrations of biotin-FA-FMK for 24 - 72 h. Cells were counted at each time point using the trypan blue exclusion assay. Results are the means ± SEM of three independent experiments.

6.2.2 Toxicity of the peptidyl-methyl ketones in Jurkat T cells

To examine whether the inhibitory effect of z-FA-FMK, z-FF-FMK and z-FA-CMK on Jurkat T cells was due to toxicity, PI uptake was examined after 72 h of treatments. As illustrated in Figure 6.5, only a small portion of control Jurkat T cells took up PI. The addition of both z-FA-FMK and z-FF-FMK caused a slight increase in PI uptake, compared to control. However, the increase in PI uptake was not significant ($p > 0.05$), suggesting that these peptidyl-FMK inhibitors are not toxic to Jurkat T cells. On the other hand z-FA-CMK treatment resulted in almost all the cells taking up PI which indicates that this peptide is toxic as reported recently (Liow and Chow, 2013).

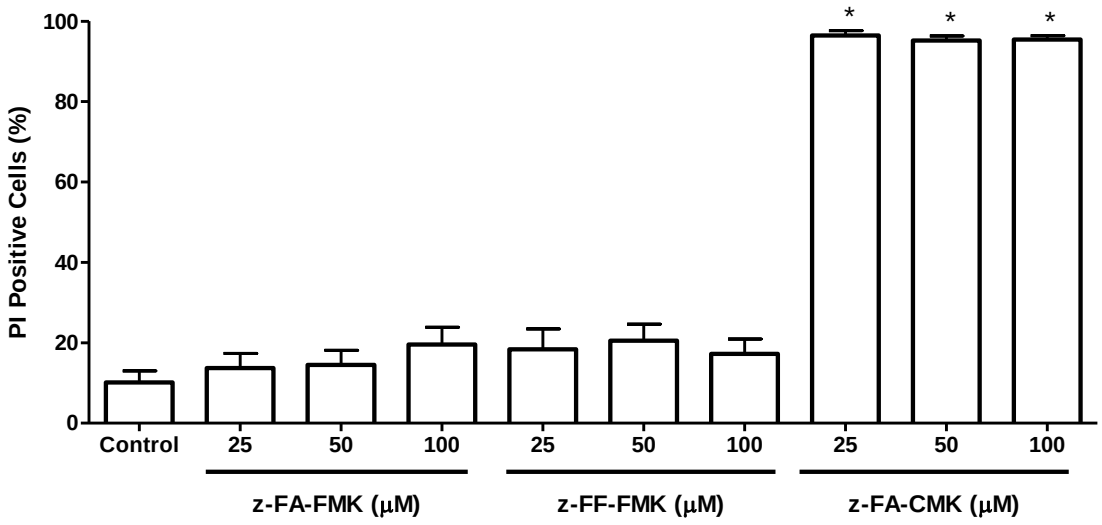

Figure 6.5 Effect of peptidyl-FMK inhibitors on the uptake of PI in Jurkat T cells

Jurkat T cells (2.5 x 10^5/ml) were treated with the indicated concentrations of z-FA-FMK, z-FF-FMK and z-FA-CMK for 72 h. Cells were then stained with PI and analysed by flow cytometry. Results are the means ± SEM of three independent experiments. *, Significantly increased ($p < 0.05$) from control.

6.2.3 Effect of peptidyl-FMK inhibitors on intracellular GSH and ROS generation in Jurkat T cells

Since both z-FA-FMK and z-FF-FMK caused depletion of GSH and a concomitant increased in ROS in primary T cells (Figure 4.1 and Figure 4.2), the effects of these peptidyl-FMKs on Jurkat T cells were examined. As shown in Figure 6.6A, intracellular GSH levels were reduced in a dose-dependent manner following z-FA-FMK treatment for 6 h. Increasing the treatment time to 24 h only further decreased the intracellular GSH levels slightly. Similar to z-FA-FMK, z-FF-FMK also induced a dose-dependent decreased in intracellular GSH levels after 6 h (Figure 6.6B). However, after 24 h there was a further marked decreased in intracellular GSH in z-FF-FMK-treated Jurkat T cells suggesting that z-FF-FMK is more potent in depleting intracellular GSH compared to z-FA-FMK. This finding is in good agreement with earlier findings demonstrating that z-FF-FMK is more effective in blocking Jurkat T cell proliferation compared to z-FA-FMK (Figure 3.4 and Figure 3.10).

Since a decreased in intracellular GSH level is usually associated with an increase in ROS production (Armstrong et al., 2002, Delogu et al., 2004, Han et al., 2010), the generation of ROS in z-FA-FMK- and z-FF-FMK-treated Jurkat T cells were determined using DHE. As illustrated in Figure 6.7A, z-FA-FMK at 25 and 50 μM had little effect on ROS generation in Jurkat T cells after 6 h. However, at 100 μM z-FA-FMK, the increased in ROS z-FA-FMK-treated Jurkat T cells was significantly increased ($p < 0.05$) compared to untreated cells. However, after 24 h treatment there was a dose-dependent increased in ROS production in z-FA-FMK-treated Jurkat T cells ($p < 0.05$). With z-FF-FMK treatment, an increased in ROS in Jurkat T cells was significant ($p < 0.05$) with 50 and 100 μM (Figure 6.7B) after 6 h. The level of ROS was further

increased in a concentration-dependent manner after 24 h treatment with z-FF-FMK. Again, the results suggest that z-FF-FMK was more effective in causing ROS generation compared to z-FA-FMK in Jurkat T cells. Collectively, these results suggest that the inhibition of Jurkat T cell proliferation mediated by z-FA-FMK and z-FF-FMK is likely to be due to the depletion of GSH and concomitant ROS generation.

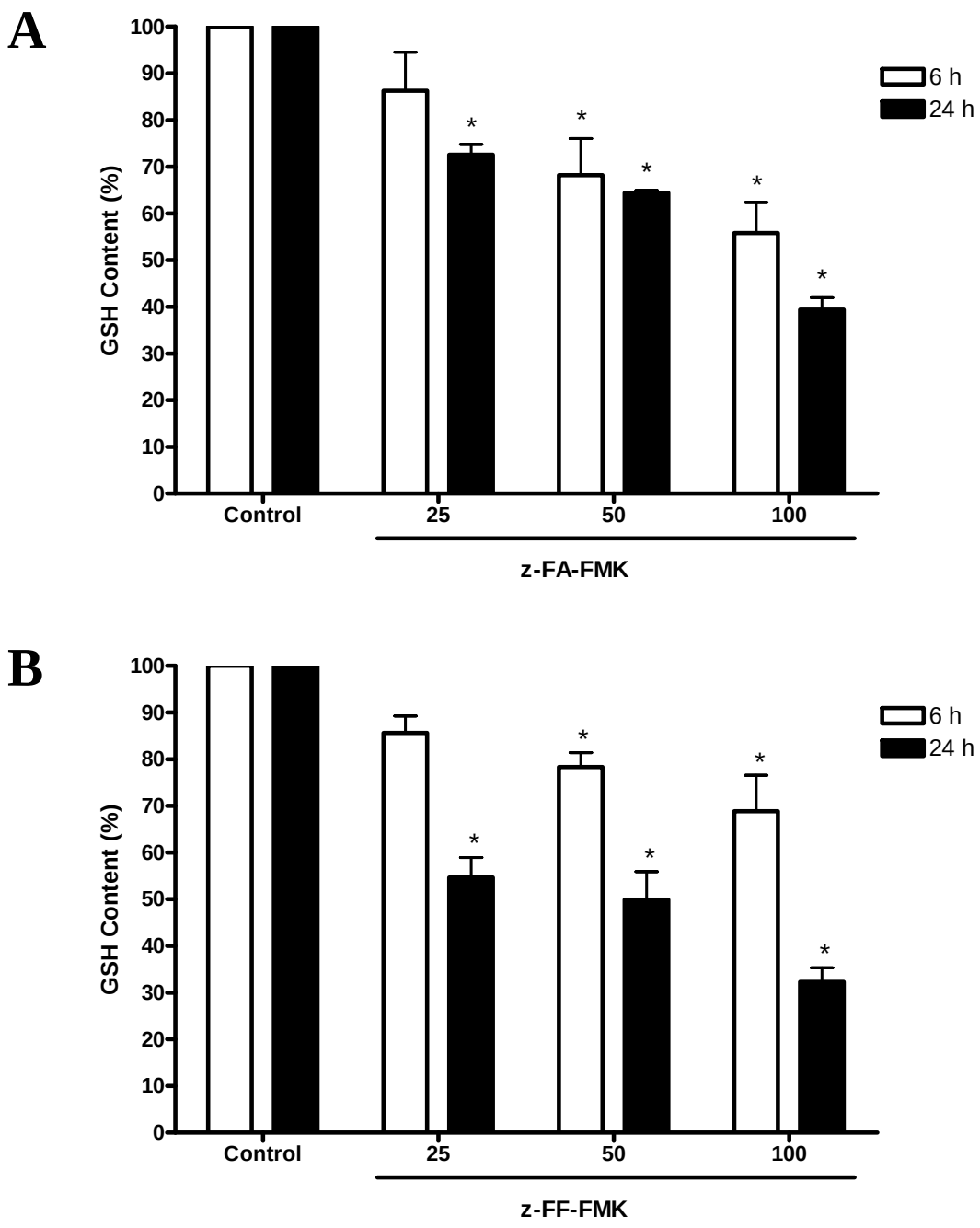

Figure 6.6 Effect of z-FA-FMK and z-FF-FMK on intracellular GSH levels in Jurkat T cells

Jurkat T cells (2.5 x 10^5/ml) were treated with the indicated concentrations of (A) z-FA-FMK or (B) z-FF-FMK. The level of intracellular glutathione was measured after 6 and 24 h using the fluorescent dye MCB and analysed using a spectrophotometer. Results are the means ± SEM of three independent experiments. *, Significantly decreased ($p < 0.05$) from control.

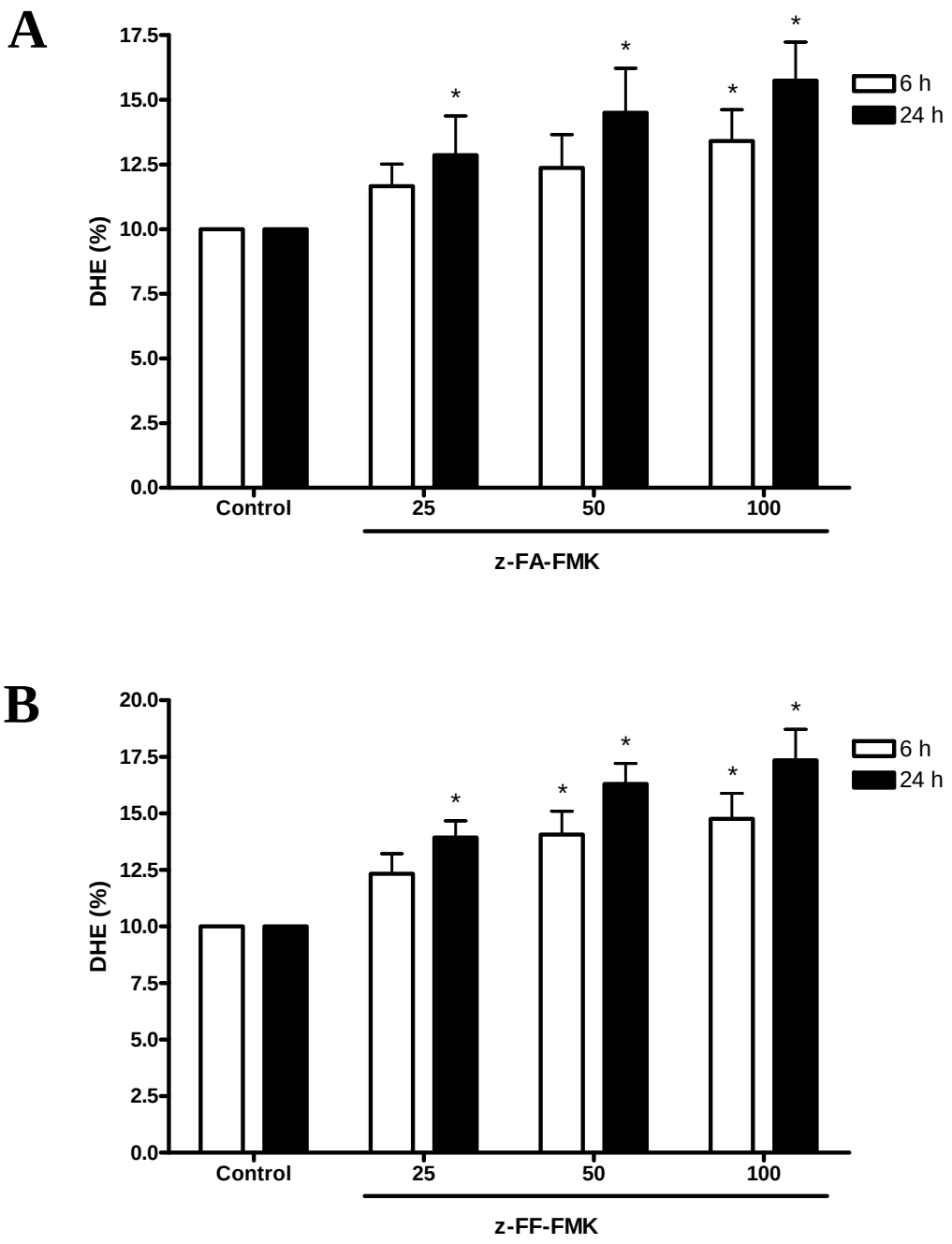

Figure 6.7 Effect of z-FA-FMK and z-FF-FMK on ROS levels in Jurkat T cells

Jurkat T cells (2.5 x 10^5/ml) were treated with the indicated concentrations of (A) z-FA-FMK or (B) z-FF-FMK. ROS levels were measured after 6 and 24 h using the DHE probe and analysed using flow cytometry. Results are the means ± SEM of three independent experiments. *, Significantly increased ($p < 0.05$) from control.

6.2.4 Effect of GSH and NAC on the inhibition of Jurkat cell proliferation mediated by z-FA-FMK and z-FF-FMK

The results so far suggested that z-FA-FMK and z-FF-FMK inhibited Jurkat T cell proliferation through oxidative stress via the depletion of intracellular GSH. Previous data showed that addition of the low molecular weight thiols such GSH and NAC restored the proliferation of peptidyl-FMK-treated primary T cells (Figure 4.3 and Figure 4.4). Therefore, the effect of these thiol antioxidants were examined in Jurkat T cells treated with z-FA-FMK or z-FF-FMK. To this end, Jurkat T cells were treated with z-FA-FMK or z-FF-FMK, at their respective IC_{50}, in the presence or absence of either GSH or NAC (1.25 – 5 mM) for 72 h. As shown in Figure 6.8, the addition of exogenous GSH and NAC dose-dependently reversed the inhibition of Jurkat T cell proliferation mediated by z-FA-FMK. In z-FF-FMK-treated cells, both GSH and NAC also reversed the inhibition of cell proliferation but these effects were only seen with higher concentrations (2.5 and 5 mM) of GSH and NAC whereas lower concentrations (2.5 mM) of these antioxidants had little effect (Figure 6.9). Since GSH and NAC readily reversed the inhibition of Jurkat T cells mediated by both z-FA-FMK and z-FF-FMK, the results suggest that these peptidyl-FMK inhibitors blocked T cell proliferation through the induction of oxidative stress. Based on these results, a concentration of 5 mM low molecular weight thiols was chosen for subsequent experiments.

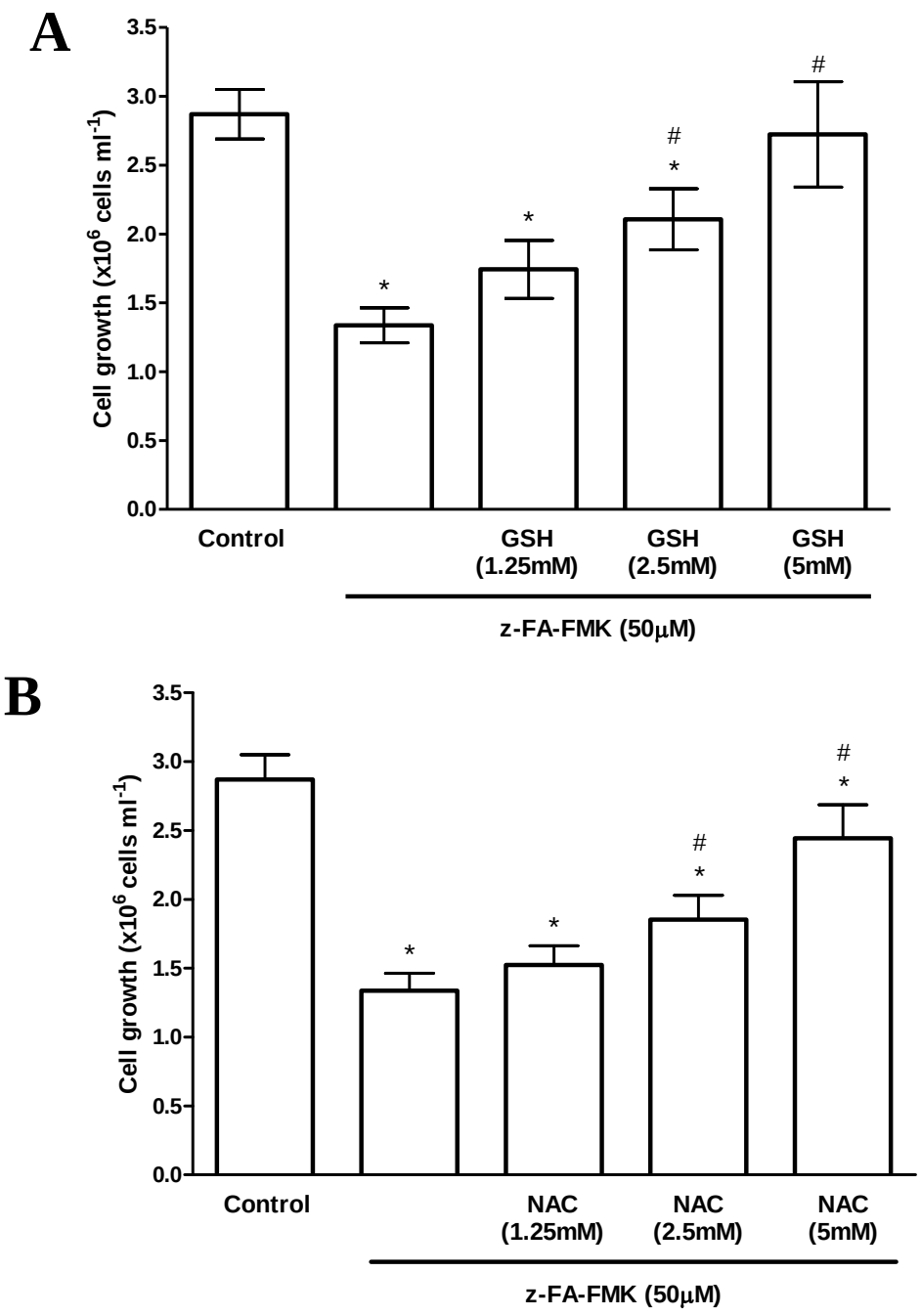

Figure 6.8 Effect of increasing dose of GSH and NAC on z-FA-FMK-induced inhibition of Jurkat T cell proliferation

Jurkat T cells (2.5 x 10^6/ml) were treated with 50 μM z-FA-FMK and various concentrations of (A) GSH or (B) NAC. Cells were counted after 72 h using the trypan blue exclusion assay. Results are the means ± SEM of three independent experiments. *, Significantly decreased ($p < 0.05$) from control; #, Significantly increased ($p < 0.05$) from z-FA-FMK treatment alone.

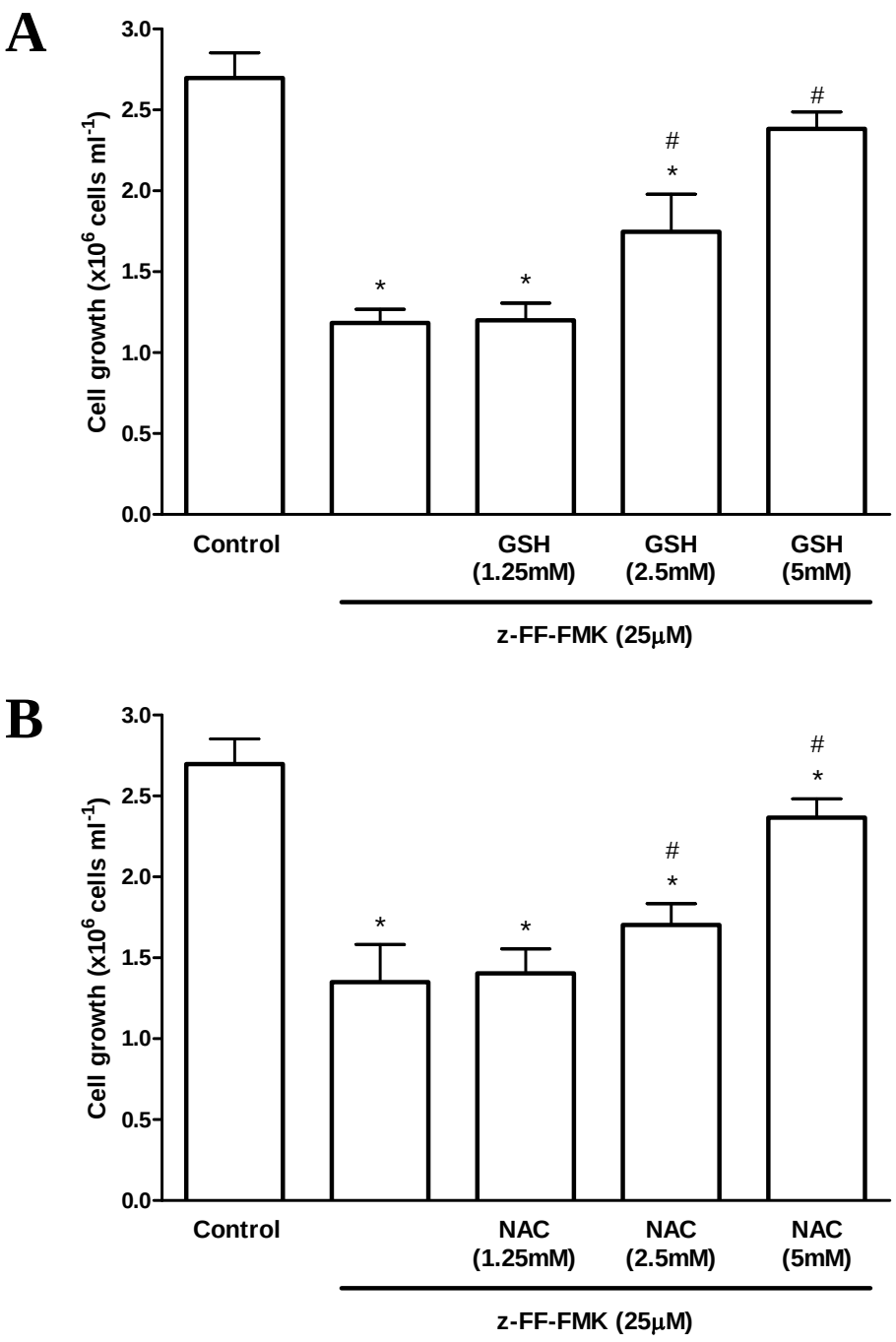

Figure 6.9 Effect of increasing dose of GSH and NAC on z-FF-FMK-induced inhibition of Jurkat T cell proliferation

Jurkat T cells (2.5 x 10^6/ml) were treated with 25 μM z-FF-FMK and various concentrations of (A) GSH or (B) NAC. Cells were counted after 72 h using the trypan blue exclusion assay. Results are the means ± SEM of three independent experiments. *, Significantly decreased ($p < 0.05$) from control; #, Significantly increased ($p < 0.05$) from z-FF-FMK treatment alone.

6.2.5 Effect of various low molecular weight thiols on peptidyl-FMK-induced suppression of Jurkat cell proliferation

Since low molecular weight thiols such as GSH and NAC were able to reverse the inhibition of Jurkat T cell proliferation induced by these peptidyl-FMK inhibitors, various other thiols were also examined. To this end, z-FA-FMK- and z-FF-FMK-treated Jurkat T cells were incubated in the presence of L-cysteine and D-cysteine at 5 mM and cell proliferation examined after 72 h. As shown in Figure 6.10, L-cysteine significantly reversed ($p < 0.05$) the inhibition of Jurkat T cell proliferation compared to treatment with either z-FA-FMK or z-FF-FMK alone. However, D-cysteine, which cannot be metabolised into GSH, had little effect on Jurkat T cell proliferation induced by these peptidyl-FMK inhibitors. Similarly, BSO (0.5 mM) significantly blocked ($p < 0.05$) Jurkat T cell proliferation as compared to control cells. Collectively, the data strongly suggest that GSH depletion may be responsible for the inhibition of Jurkat cell proliferation mediated by z-FA-FMK and z-FF-FMK.

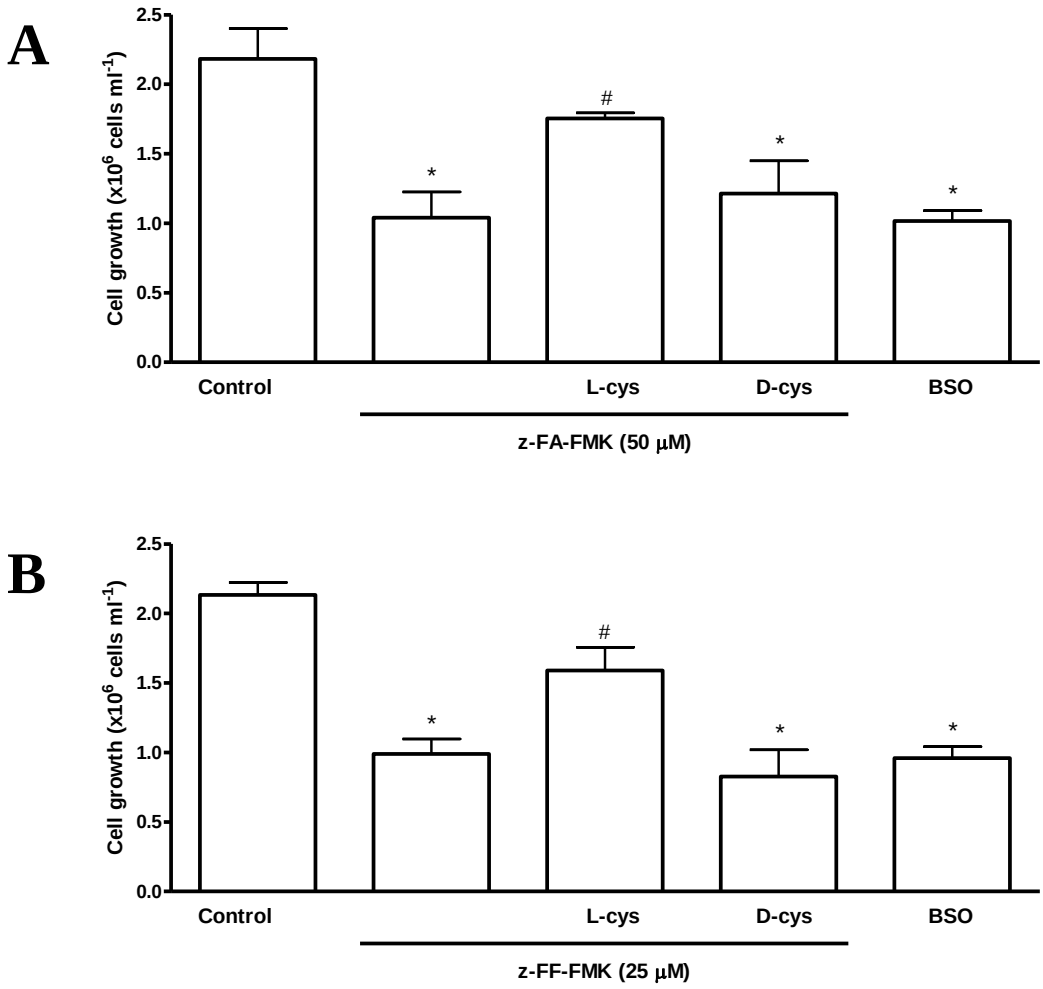

Figure 6.10 Effect of reduced or oxidized low molecular weight thiols on peptidyl-FMK inhibitors treatment in Jurkat T cells

Jurkat T cells (2.5 x 10^6/ml) were treated with (A) 50 μM z-FA-FMK or (B) 25 μM z-FF-FMK in the presence or absence of antioxidants (5 mM) or 0.5 mM BSO, as indicated. After 72 h, cells were counted using the trypan blue exclusion assay. Results are the means ± SEM of three independent experiments. *, Significantly decreased ($p < 0.05$) from control; $^{\#}$, Significantly increased ($p < 0.05$) from the respective peptidyl-FMK treatment alone.

6.2.6 Mechanisms that underlie the depletion of GSH mediated by peptidyl-FMK inhibitors in Jurkat T cells

The data presented so far suggest that z-FA-FMK and z-FF-FMK block Jurkat T cell proliferation by depleting the intracellular pool of GSH thereby shifting the cell towards a more oxidative state. The fact that addition of exogenous GSH, NAC and L-cysteine can reverse the inhibition of Jurkat cell proliferation mediated by these peptidyl-FMK inhibitors suggests that z-FA-FMK and z-FF-FMK may be blocking the GSH synthesis pathway. To investigate this, BSO (0.5 mM) was added to Jurkat T cells cotreated with either z-FA-FMK or z-FF-FMK and NAC (5 mM). Since BSO is known to irreversibly block the GSH synthesis pathway by inhibiting γ-glutamylcysteine synthetase (Griffith and Meister, 1979), it would be expected that in the presence of BSO, NAC would not be converted into GSH and thus be unable to reverse the inhibition of Jurkat T cell proliferation mediated by z-FA-FMK and z-FF-FMK. As illustrated in Figure 6.11, addition of BSO blocked the ability of NAC to reverse the inhibition of Jurkat T cells proliferation mediated by z-FA-FMK and z-FF-FMK. Taken together, these results support the idea that the peptidyl-FMK inhibitors block Jurkat T cell proliferation via GSH depletion and oxidative stress.

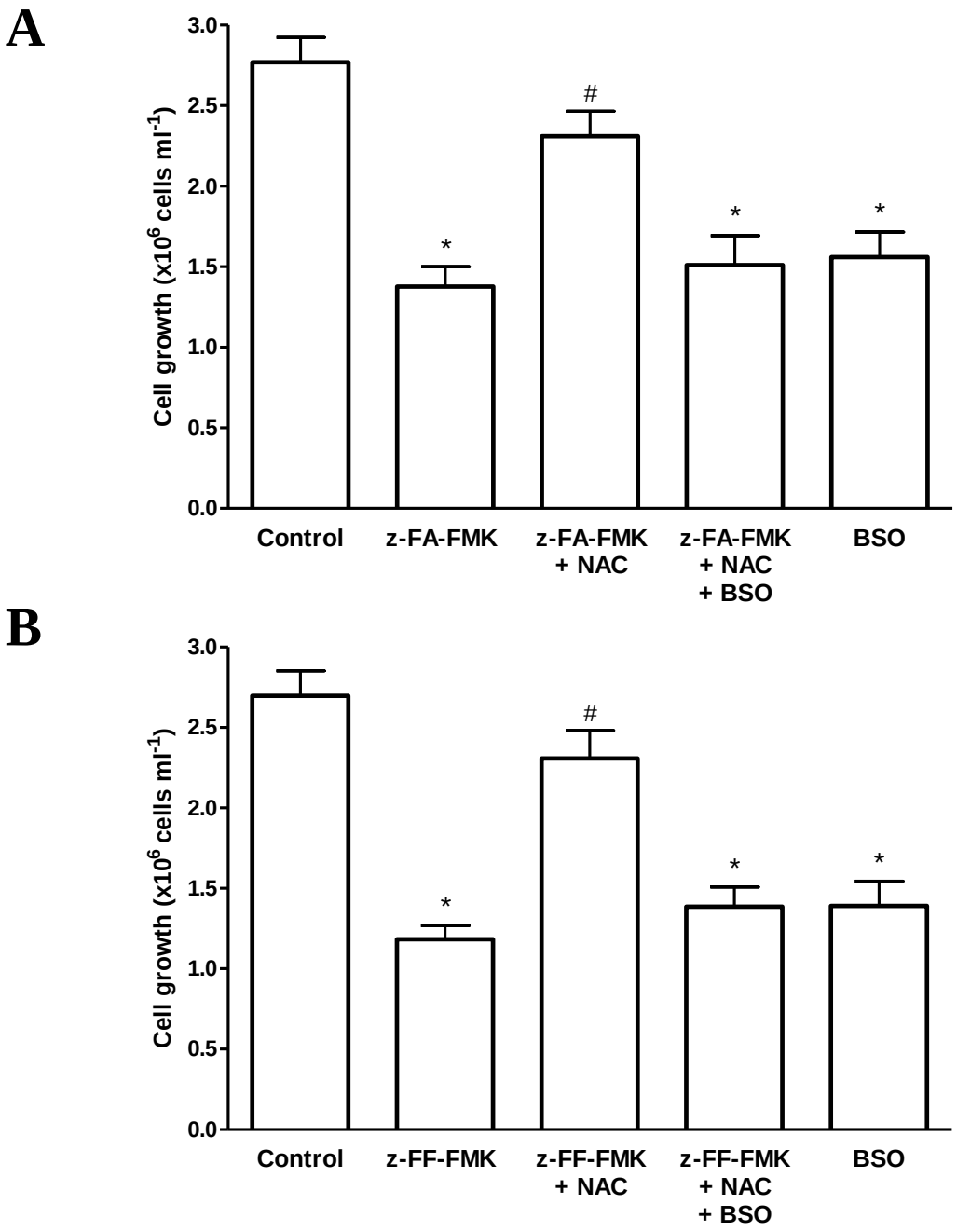

Figure 6.11 NAC is unable to rescue peptidyl-FMK inhibitor induced block on Jurkat T cell proliferation in the presence of BSO

Jurkat T cells were co-treated with (A) 50 µM z-FA-FMK or (B) 25 µM z-FF-FMK and 5 mM NAC in the presence or absence of 0.5 mM BSO, as indicated. After 72 h, cells were counted using the trypan blue exclusion assay. Results are the means ± SEM of two independent experiments. *, Significantly decreased ($p < 0.05$) from control; $^{\#}$, Significantly increased ($p < 0.05$) from the respective peptidyl-FMK treatment alone.

6.3 Discussion

In the previous chapters, several peptidyl-methyl ketones were investigated with regard to their effect on primary T cell proliferation, caspase activation as well as GSH and ROS levels in anti-CD3-stimulated T cells. In contrast to primary T cells, Jurkat T cells proliferate continuously without requiring an activation signal. To further investigate the effect of the peptidyl-methyl ketones on T cell proliferation, their effect on Jurkat T cell proliferation was examined.

As observed in primary T cells cells, z-FA-FMK inhibited Jurkat T cell proliferation in a dose-dependent manner while z-FA-DMK had little effect on proliferation. In agreement with earlier work, z-FA-CMK was toxic as seen by a complete block of Jurkat T cell proliferation at the lowest concentration and time-point tested (Liow and Chow, 2013). Since only z-FA-FMK inhibited Jurkat T cell proliferation, the results suggest that the FMK moiety may be responsible for the block on T cell proliferation. Indeed, the FMK group is known to be highly reactive and has the potential to alkylate non-specifically within the cells, giving rise to non-specific effects (Garcia-Calvo et al., 1998). To rule out this possibility, the effect of three other FMK-containing methyl ketone peptides on Jurkat T cell proliferation was examined. However, neither z-YVAD-FMK, a capase-1 inhibitor, z-VRPR-FMK, a MALT1 inhibitor or z-VAD-FMK, the pan-caspase inhibitor blocked Jurkat T cell proliferation. Interestingly, z-VAD-FMK did not have any effect on Jurkat T cell proliferation while it readily inhibited primary T cell proliferation. These results highlighted the differences in the regulation of proliferation between primary T cell lines and T cell lines. Furthermore, it is possible that z-FA-FMK may inhibit different targets during T cell activation compared to z-VAD-FMK. Since only z-FA-FMK blocked Jurkat T cell proliferation, the data suggest that the FMK group alone is unlikely to be the cause of the immunosuppressive

effect and that other parts of the molecule are also involved. Structure-activity relationship studies revealed that the replacement of the alanine at the P1 position with a phenylalanine readily blocked Jurkat T cell proliferation in a dose-dependent manner. In fact z-FF-FMK was more potent in blocking Jurkat T cell proliferation compared to z-FA-FMK. Being a bigger molecule compared to alanine, phenylalanine at the P1 position seems to increase the effectiveness of z-FF-FMK compared to z-FA-FMK. The N-terminal blocking group, benzyloxycarbonyl also played an important role in the ability of z-FA-FMK to block Jurkat T cell proliferation since replacing it with biotin completely abrogated the ability of biotin-FA-FMK to block Jurkat T cell proliferation. Collectively, the data suggests that the suppression of Jurkat T cell proliferation induced by z-FA-FMK and z-FF-FMK is likely to involve the combination of the FMK moiety, the peptide part of the molecule and the benzyloxycarbonyl group at the N-terminal.

Similar to primary T cells, the addition of z-FA-FMK and z-FF-FMK induced a dose-dependent reduction in intracellular GSH with elevated levels of cellular ROS in Jurkat T cells. Coupled with the finding that the low molecular weight thiols GSH, NAC and L-cysteine were able to abrogate the inhibition of Jurkat T cell proliferation mediated by z-FA-FMK and z-FF-FMK, the results strongly indicate that the inhibitory effect of these peptidyl-FMK inhibitors may be caused by oxidative stress. In addition, D-cysteine, which cannot be enzymatically converted into GSH was unable to restore Jurkat T cell proliferation in the presence of z-FA-FMK and z-FF-FMK which strengthens the evidence suggesting Jurkat T cell inhibition induced by z-FA-FMK and z-FF-FMK is due to oxidative stress via the depletion of GSH. These results are in line with a study that shows Jurkat T cells depleted of GSH by BSO exhibited NFκB transcription

after exposure to H_20_2 that was reduced compared to cells with normal GSH levels (Ginn-Pease and Whisler, 1996). This suggests that optimal NFκB activation requires a functional GSH system that can respond to oxidative stress and maintain intracellular redox homeostasis. Therefore, an intact GSH system was required for optimal NFκB activation. These data are compatible with the current findings which show z-FA-FMK and z-FF-FMK suppress Jurkat T cell proliferation via GSH depletion. Taken together, the data indicate that the suppression of T cell proliferation with depletion of GSH may involve signaling pathways necessary for transcriptional activation of NFκB dependent genes.

It is still currently unclear how z-FA-FMK and z-FF-FMK treatment in Jurkat T cells leads to the depletion of GSH. Although it has been reported that peptidyl-FMKs are able to interact with GSH directly in vitro (Angliker et al., 1987), the time taken for z-FA-FMK and z-FF-FMK to reduce intracellular GSH levels is considerably long thereby ruling out a direct interaction between these peptides and GSH. As a result of this effective recycling reaction, GSSG concentrations are kept low within the cell, i.e. the GSH: GSSG ratio is usually found to be more than 100 times (Asensi et al., 1994). These data were further corroborated by the observed effect that in the presence of BSO, NAC is unable to restore the proliferation of Jurkat T cells treated with either z-FA-FMK or z-FF-FMK.

Collectively, the inhibition of Jurkat T cell proliferation mediated by z-FA-FMK and z-FF-FMK requires not only the FMK group but also the presence of specific amino acids as well as the benzyloxycarbonyl group at the N-terminal. The structure activity studies revealed a degree of specificity in z-FA-FMK and z-FF-FMK-mediated Jurkat T cell suppression. Additionally, the

cathepsin L inhibitor, z-FF-FMK, was identified as a more potent immunosuppressant compared to z-FA-FMK. Furthermore, it is likely that both peptidyl-FMK inhibitors inhibit Jurkat T cell activation through oxidative stress via GSH depletion. This is based on the finding that the low molecular weight thiols GSH, NAC and L-cysteine readily reverse the block on Jurkat T cell proliferation mediated by z-FA-FMK and z-FF-MK while D-cysteine, which cannot be metabolised into GSH. Due to the fact that NAC is unable to reverse the block on Jurkat T cell induce by z-FA-FMK and z-FF-FMK in the presence of BSO, it is likely that NAC functions as a precursor for GSH biosynthesis by providing cysteine through intracellular deacetylation rather than as a ROS scavenger. Taken together, these observations suggest that z-FA-FMK and z-FF-FMK may inhibit Jurkat T cell proliferation by blocking the GSH synthesis pathway.

CHAPTER SEVEN

General discussion & future work

7.1 General Discussion

Peptidyl-FMK caspase inhibitors have long been employed to examine the role of caspases during T cell activation and proliferation (Alam et al., 1999, Kennedy et al., 1999, Boissonnas et al., 2002, Mack and Hacker, 2002, Sturm et al., 2002, Falk et al., 2004, Lawrence et al., 2006). However, z-FA-FMK, the commonly used negative control for FMK-containing peptides, was also found to inhibit T cell activation and proliferation (Lawrence et al., 2006). Furthermore, in contrast to the caspase inhibitors z-VAD-FMK and z-IETD-FMK, z-FA-FMK treatment completely inhibited caspase-8 and caspase-3 processing (Lawrence et al., 2006, Lawrence and Chow, 2012). Thus, these data suggest that the inhibition of T cell activation and proliferation may be due to the non-specific effects of these inhibitors rather than the specific inhibition of caspases. In the present study, the effects of several peptidyl-methyl ketones on T cell activation and proliferation were investigated and compared to z-FA-FMK.

As shown in chapter 3, z-FA-FMK inhibited T cell proliferation, which is in line with previous work (Lawrence et al., 2006). In addition, the cathepsin B and L inhibitor, z-FF-FMK also blocked T cell proliferation and was found to be a more potent inhibitor than z-FA-FMK. Similar to z-FA-FMK, z-FF-FMK inhibited blast formation, CD25 and CD69 expression, IL-2 driven proliferation, cell cycle progression as well as caspase-8 and caspase-3 processing. In addition, the finding that z-FA-FMK and z-FF-FMK readily blocks the processing of caspases in proliferating T cells but do not inhibit caspases per se indicate that the inhibition of caspases is unlikely to be the means by which these peptidyl-FMK inhibitors exert their inhibitory effect on T cell activation.

Several lines of evidence have suggested that GSH is required for T cell activation and proliferation (Zmuda and Friedenson, 1983, Hamilos and Wedner, 1985, Markovic et al., 2007). The depletion of GSH has been shown to block T cell proliferation (Fidelus et al., 1987, Gmunder et al., 1990, Suthanthiran et al., 1990, Gmunder and Droge, 1991, Smyth, 1991) while the re-introduction of exogenous GSH is capable of reversing the inhibition of T cell proliferation (Suthanthiran et al., 1990). Because a number of studies have reported that some peptidyl-methyl ketones are reactive to GSH (Rossman et al., 1974, Angliker et al., 1987, Powers et al., 2002), the effect of the z-FA-FMK and z-FF-FMK on intracellular GSH and ROS levels in activated T cells was examined.

In chapter 4, intracellular GSH levels were depleted in activated T cells treated with z-FA-FMK and z-FF-FMK. This drop in GSH levels was followed by a concomitant increase in ROS which suggests that oxidative stress may be the underlying mechanism of z-FA-FMK and z-FF-FMK immunosuppressive effect. Since low molecular weight thiols like 2ME are capable of augmenting T cell proliferation in response to mitogen (Zmuda and Friedenson, 1983), the effect of several low molecular weight thiols on the suppression of primary T cell activation and proliferation mediated by z-FA-FMK and z-FF-FMK was investigated. The low molecular weight thiols GSH, NAC and L-cysteine readily reversed the inhibition of z-FA-FMK and z-FF-FMK-treated activated T cells. NAC, through intracellular deacetylation, and L-cysteine are a source of cysteine for T cells. Therefore, it is likely that these low molecular thiols restore T cell proliferation in the presence of z-FA-FMK and z-FF-FMK by acting as precursors for GSH biosynthesis. The fact that D-cysteine, which cannot be enzymatically converted into GSH, was unable to restore T cell proliferation in the presence of these peptidyl-FMK inhibitors further

enhances this notion. Furthermore, the failure to reverse z-FA-FMK- and z-FF-FMK-mediated block on T cell proliferation by co-treatment with NAC and BSO suggests that these peptidyl-FMK inhibitors block T cell proliferation by interfering with the GSH pathway. The results from this chapter also demonstrate that exogenous GSH readily restores the inhibition of anti-CD3-induced CD25 and CD69 expression mediated by z-FA-FMK and z-FF-FMK back to control levels. These results are line with the finding that the up-regulation of CD25 and CD69 expression in activated T cells is dependent on the intracellular GSH levels or redox state of the cells (Roozendaal et al., 2002). Therefore, the depletion of intracellular GSH mediated by z-FA-FMK and Z-FF-FMK could also account for the down-regulation of CD25 and CD69 expression in activated T cells. In addition, the low molecular weight thiols GSH, NAC and L-cysteine, but not D-cysteine, are able to fully restore the caspase-8 and caspase-3 processing in anti-CD3-activated T cells treated with z-FA-FMK and z-FF-FMK. Taken together, the results strongly suggest that these peptidyl-FMK inhibitors suppress T cell activation through oxidative stress via GSH depletion.

Recent work demonstrated that z-VAD-FMK readily inhibits anti-CD3-activated primary T cell proliferation without blocking the activation and processing of caspase-8 and caspase-3 (Lawrence and Chow, 2012). This suggests that z-VAD-FMK-mediated immunosuppression may be due to non-specific effects and has little to do with caspase inhibition per se. Since z-FA-FMK and z-FF-FMK treatment lead to a depletion of intracellular GSH and concomitant increase in ROS levels, the effect of z-VAD-FMK on the level of oxidative stress in activated T cells was also examined. Similar to z-FA-FMK and z-FF-FMK, z-VAD-FMK treatment resulted in the depletion of intracellular GSH with a corresponding increase in cellular ROS which suggests that

oxidative stress may be the underlying mechanism of z-VAD-FMK immunosuppression. Addition of exogenous low molecular weight thiols such as GSH, NAC and L-cysteine, but not D-cysteine, also readily abolished the inhibition of T cell proliferation mediated by the pan-caspase inhibitor. Likewise, the presence of exogenous GSH completely restored the inhibition of anti-CD3-induced CD25 and CD69 expression mediated by z-VAD-FMK to control levels. In summary, the results from chapter 4 and 5 demonstrate that the immunosuppressive effects of z-FA-FMK, z-FF-FMK and z-VAD-FMK are likely to inhibit T cell proliferation and activation through oxidative stress via GSH depletion.

As described in chapter 5, z-VAD-FMK effectively blocks the activation and proliferation of T cells without inhibiting the processing of the initiator caspase-8, caspase-2, caspase-9, and the effector caspase-3 and caspase-6. Its failure to block the activation and processing of caspase-8 and caspase-3 to their subunits in activated T cells is in line with previous work (Lawrence and Chow, 2012). One explanation for these effects could be that cellular inhibitors of apoptosis proteins, such as XIAP, interacts with cleaved caspase-3 and -7 thereby blocking their full activation, substrate cleavage and cell death (Paulsen et al., 2008). However, interaction with XIAP still resulted in the incomplete processing of caspase-3 to its p20 subunit, in activated T cells, which is adequate for the cleavage of PARP (Stennicke et al., 1998). A possible mechanism that keeps activated caspases from cleaving substrates that inevitably triggers apoptosis is through limited subcellular compartmentalization of active effector caspases (Lamkanfi et al., 2007). Using subcellular fractionations, the cleavage products of caspase-3 and caspase-7 were shown to be largely confined to the cytoplasm of proliferating T cells, while in apoptotic cells these caspases displayed a rather general distribution (Paulsen et al., 2008).

However, not even cytosolic substrates of these effector caspases were cleaved in proliferating T cells. The reason for this remains unknown. In another study, an aggregation of active caspase-8 within membrane lipid rafts in stimulated T cells was demonstrated (Koenig et al., 2008). In contrast, Fas stimulation of T cells resulted in the activation of caspase-8 that was exclusively cytosolic. The study argued that the localization of active caspase-8 in lipid rafts prevent it from cleaving substrates that promote cell death, and instead target active caspase-8 towards substrates associated with cell activation. In agreement, the traditional cytosolic caspase-8 substrate BID, which promotes mitochondrial permeability, was not cleaved in activated T cells, but was cleaved following Fas stimulation (Koenig et al., 2008).

Next, the effect of peptidyl-FMK inhibitors on normal cell growth in a T cell line that proliferates continuously without the need of any activation signal was investigated. To this end, the T cell leukemia cell line, Jurkat was cultured in the presence of various peptidyl-methyl ketones. As illustrated in chapter 6, z-FA-FMK and z-FF-FMK blocked Jurkat T cell proliferation with z-FF-FMK being the more potent immunosuppressant. However, z-VAD-FMK had no effect on Jurkat T cell proliferation which suggests that the pan-caspase inhibitor may be targeting activation signals leading to cell proliferation. Furthermore, these findings demonstrate that the regulation of proliferation is different between primary T cells and T cell lines. Similar to primary T cells, z-FA-FMK and z-FF-FMK treatment resulted in reduced GSH levels and elevated ROS in Jurkat T cells. Addition of exogenous low molecular weight thiols such a GSH, NAC and L-cysteine reversed the inhibition of Jurkat T cell proliferation mediated by z-FA-FMK and z-FF-FMK. This, coupled with the finding that D-cysteine which cannot be enzymatically converted into GSH was unable to restore Jurkat T cell proliferation in the

presence of z-FA-FMK and z-FF-FMK, strengthens the evidence suggesting that the immunosuppressive effect induced by z-FA-FMK and z-FF-FMK is due to oxidative stress via the depletion of GSH. The data are supported by the finding that Jurkat T cells with deficient GSH levels result in a lower rate of NFκB transcription as compared to cells with normal GSH levels (Ginn-Pease and Whisler, 1996). Further, since NAC is unable to reverse the inhibition of Jurkat T cell proliferation in the presence of BSO, it is likely that NAC functions as a precursor for GSH biosynthesis by providing cysteine through intracellular deacetylation rather than as a ROS scavenger. In summary, the results from chapter 6 suggest that z-FA-FMK and z-FF-FMK inhibit Jurkat T cell proliferation by blocking the GSH synthesis pathway.

In conclusion, the results from the present study suggest that z-FA-FMK, z-FF-FMK and z-VAD-FMK inhibit primary T cell proliferation through the induction of oxidative stress via GSH depletion. Furthermore, it is likely that the low molecular weight thiol NAC functions as a precursor for GSH biosynthesis and not a ROS scavenger as addition of BSO and NAC failed to reverse the block on T cell proliferation mediated by these peptidyl-FMK inhibitors. These results tie in with previous studies which suggest that the immunosuppressive effects of peptidyl-FMK inhibitors on T cell activation and proliferation may not involve the inhibition of caspases (Lawrence et al., 2006, Lawrence and Chow, 2012). z-FA-FMK and z-FF-FMK also blocked Jurkat T cell proliferation and caused a depletion of intracellular GSH with a concomitant increase in ROS levels. Thus, it is likely that these peptidyl-FMK inhibitors block Jurkat T cell proliferation via GSH depletion and oxidative stress.

7.2 Future Work

The data in the present study suggest that z-FA-FMK, z-FF-FMK and z-VAD-FMK block T cell proliferation by depleting intracellular GSH levels and generating ROS, the result of which is oxidative stress. However, how these peptidyl-FMK inhibitors interrupt the GSH synthesis pathway is still unknown. Because biotinylated z-FA-FMK and biotinylated z-VAD-FMK (data not shown) failed to block T cell activation and proliferation, these compounds cannot be used to pull down protein extracts derived from activated T cells for the purpose of proteomic analysis. Thus, cell-free systems can be used to help identify the upstream non-caspase enzyme that activates caspases during T cell activation and proliferation.

Furthermore, it is also important to determine why activated T cells do not undergo apoptosis despite the presence of cleaved caspases. Because the caspase inhibitor XIAP was shown to interact with cleaved caspase-3 and caspase-7 thereby blocking their full activation, substrate cleavage and cell death (Paulsen et al., 2008), it will be interesting to examine the protein levels of XIAP in activated T cells before and after compound treatment to better understand the contribution of XIAP. The possible up-regulation of various other IAP (e.g. cIAP1, cIAP2, Bruce, Survivin) can be examined by analyzing their RNA levels in proliferating T cells. Once the presence of an up-regulated IAP is confirmed, lysates from proliferating T cells could be immunoprecipitated with caspases and tested for a coprecipitating IAP. During T cell proliferation, active caspase-8 is confined to membrane lipid rafts as opposed to the cytoplasm of Fas-stimulated apoptotic T cells (Koenig et al., 2008). Active caspase-3 and -7 have also been shown to be largely confined to the cytoplasm of proliferating T cells using subcellular fractionations (Paulsen et al., 2008). However, this approach lacked the ability to analyze

individual cells. Furthermore, in apoptotic cells, the broader distribution of caspase-3 and caspase-7 fragments observed could be the result of the destruction of cellular structures since the marker protein histone, specific for the nucleus, was also present in the cytoplasmic fraction. Therefore, a high-resolution multicolour confocal laser scanning microscopy (CLSM) could be used to determine if active caspase-3 and caspase-7 are compartmentalized during T cell proliferation. Active caspase-3 and caspase-7 can be detected by CLSM through affinity labelling. Counterstaining the cell nuclei with Hoechst will allow for the detection of apoptosis based on the amount of nuclear condensation and fragmentation.

The results in the present study indicate the peptidyl-FMK inhibitors, at non-toxic doses, have immunosuppresive properties and may provide opportunities for the development of immune-modulating drugs. Identifying the exact targets of these inhibitors may allow for the selective blocking of T cell activation for immunosuppresive therapy.

BIBLIOGRAPHY

ADEREM, A. & UNDERHILL, D. M. 1999. Mechanisms of phagocytosis in macrophages. *Annu Rev Immunol,* 17**,** 593-623.

AHMED, N. K., MARTIN, L. A., WATTS, L. M., PALMER, J., THORNBURG, L., PRIOR, J. & ESSER, R. E. 1992. Peptidyl fluoromethyl ketones as inhibitors of cathepsin B. Implication for treatment of rheumatoid arthritis. *Biochem Pharmacol,* 44**,** 1201-7.

ALAM, A., COHEN, L. Y., AOUAD, S. & SEKALY, R. P. 1999. Early activation of caspases during T lymphocyte stimulation results in selective substrate cleavage in nonapoptotic cells. *J Exp Med,* 190**,** 1879-90.

ALEGRE, M. L., FRAUWIRTH, K. A. & THOMPSON, C. B. 2001. T-cell regulation by CD28 and CTLA-4. *Nat Rev Immunol,* 1**,** 220-8.

ANGELINI, G., GARDELLA, S., ARDY, M., CIRIOLO, M. R., FILOMENI, G., DI TRAPANI, G., CLARKE, F., SITIA, R. & RUBARTELLI, A. 2002. Antigen-presenting dendritic cells provide the reducing extracellular microenvironment required for T lymphocyte activation. *Proc Natl Acad Sci U S A,* 99**,** 1491-6.

ANGLIKER, H., WIKSTROM, P., RAUBER, P. & SHAW, E. 1987. The synthesis of lysylfluoromethanes and their properties as inhibitors of trypsin, plasmin and cathepsin B. *Biochem J,* 241**,** 871-5.

ARENDS, M. J., MORRIS, R. G. & WYLLIE, A. H. 1990. Apoptosis. The role of the endonuclease. *Am J Pathol,* 136**,** 593-608.

ARMSTRONG, J. S., STEINAUER, K. K., HORNUNG, B., IRISH, J. M., LECANE, P., BIRRELL, G. W., PEEHL, D. M. & KNOX, S. J. 2002. Role of glutathione depletion and reactive oxygen species generation in apoptotic signaling in a human B lymphoma cell line. *Cell Death Differ,* 9**,** 252-63.

ARRANZ, L., FERNANDEZ, C., RODRIGUEZ, A., RIBERA, J. M. & DE LA FUENTE, M. 2008. The glutathione precursor N-acetylcysteine improves immune function in postmenopausal women. *Free Radic Biol Med,* 45**,** 1252-62.

ASENSI, M., SASTRE, J., PALLARDO, F. V., GARCIA DE LA ASUNCION, J., ESTRELA, J. M. & VINA, J. 1994. A high-performance liquid chromatography method for measurement of oxidized glutathione in biological samples. *Anal Biochem,* 217**,** 323-8.

BALLATORI, N., KRANCE, S. M., NOTENBOOM, S., SHI, S., TIEU, K. & HAMMOND, C. L. 2009. Glutathione dysregulation and the etiology and progression of human diseases. *Biol Chem,* 390**,** 191-214.

BAUMGARTNER, H. K., GERASIMENKO, J. V., THORNE, C., ASHURST, L. H., BARROW, S. L., CHVANOV, M. A., GILLIES, S., CRIDDLE, D. N., TEPIKIN, A. V., PETERSEN, O. H., SUTTON, R., WATSON, A. J. & GERASIMENKO, O. V. 2007. Caspase-8-mediated apoptosis induced by oxidative stress is independent of the intrinsic pathway and dependent on cathepsins. *Am J Physiol Gastrointest Liver Physiol,* 293**,** G296-307.

BERK, M., COPOLOV, D., DEAN, O., LU, K., JEAVONS, S., SCHAPKAITZ, I., ANDERSON-HUNT, M., JUDD, F., KATZ, F., KATZ, P., ORDING-JESPERSEN, S., LITTLE, J., CONUS, P., CUENOD, M., DO, K. Q. & BUSH, A. I. 2008. N-acetyl cysteine as a glutathione precursor for schizophrenia--a double-blind, randomized, placebo-controlled trial. *Biol Psychiatry,* 64**,** 361-8.

BIDERE, N., BRIET, M., DURRBACH, A., DUMONT, C., FELDMANN, J., CHARPENTIER, B., DE SAINT-BASILE, G. & SENIK, A. 2002. Selective inhibition of dipeptidyl peptidase I, not caspases, prevents the partial processing of procaspase-3 in CD3-activated human CD8(+) T lymphocytes. *J Biol Chem,* 277**,** 32339-47.

BINDOKAS, V. P., JORDAN, J., LEE, C. C. & MILLER, R. J. 1996. Superoxide production in rat hippocampal neurons: selective imaging with hydroethidine. *J Neurosci,* 16**,** 1324-36.

BOATRIGHT, K. M. & SALVESEN, G. S. 2003. Mechanisms of caspase activation. *Curr Opin Cell Biol,* 15**,** 725-31.

BOISSONNAS, A., BONDUELLE, O., LUCAS, B., DEBRE, P., AUTRAN, B. & COMBADIERE, B. 2002. Differential requirement of caspases during naive T cell proliferation. *Eur J Immunol,* 32**,** 3007-15.

BOJES, H. K., DATTA, K., XU, J., CHIN, A., SIMONIAN, P., NUNEZ, G. & KEHRER, J. P. 1997. Bcl-xL overexpression attenuates glutathione depletion in FL5.12 cells following interleukin-3 withdrawal. *Biochem J,* 325 (Pt 2)**,** 315-9.

BOTTA, D., FRANKLIN, C. C., WHITE, C. C., KREJSA, C. M., DABROWSKI, M. J., PIERCE, R. H., FAUSTO, N. & KAVANAGH, T. J. 2004. Glutamate-cysteine ligase attenuates TNF-induced mitochondrial injury and apoptosis. *Free Radic Biol Med,* 37**,** 632-42.

BRECKENRIDGE, D. G. & XUE, D. 2004. Regulation of mitochondrial membrane permeabilization by BCL-2 family proteins and caspases. *Curr Opin Cell Biol,* 16**,** 647-52.

BROWN, G. C. & BORUTAITE, V. 2008. Regulation of apoptosis by the redox state of cytochrome c. *Biochim Biophys Acta,* 1777**,** 877-81.

CALLUS, B. A. & VAUX, D. L. 2007. Caspase inhibitors: viral, cellular and chemical. *Cell Death Differ,* 14**,** 73-8.

CARRINGTON, P. E., SANDU, C., WEI, Y., HILL, J. M., MORISAWA, G., HUANG, T., GAVATHIOTIS, E., WEI, Y. & WERNER, M. H. 2006. The structure of FADD and its mode of interaction with procaspase-8. *Mol Cell,* 22**,** 599-610.

CASERTA, T. M., SMITH, A. N., GULTICE, A. D., REEDY, M. A. & BROWN, T. L. 2003. Q-VD-OPh, a broad spectrum caspase inhibitor with potent antiapoptotic properties. *Apoptosis,* 8**,** 345-52.

CERRETTI, D. P., KOZLOSKY, C. J., MOSLEY, B., NELSON, N., VAN NESS, K., GREENSTREET, T. A., MARCH, C. J., KRONHEIM, S. R., DRUCK, T., CANNIZZARO, L. A. & ET AL. 1992. Molecular cloning of the interleukin-1 beta converting enzyme. *Science,* 256**,** 97-100.

CHAPLIN, D. D. & WEDNER, J. H. 1978. Inhibition of lectin-induced lymphocyte activation by diamide and other sulfhydryl reagents. *Cell Immunol,* 36**,** 303-11.

CHEN, G., WANG, S. H. & CONVERSE, C. A. 1994. Glutathione increases interleukin-2 production in human lymphocytes. *Int J Immunopharmacol,* 16**,** 755-60.

CHEN, L., WILLIS, S. N., WEI, A., SMITH, B. J., FLETCHER, J. I., HINDS, M. G., COLMAN, P. M., DAY, C. L., ADAMS, J. M. & HUANG, D. C. 2005. Differential targeting of prosurvival Bcl-2 proteins by their BH3-only ligands allows complementary apoptotic function. *Mol Cell,* 17**,** 393-403.

CHENG, E. H., WEI, M. C., WEILER, S., FLAVELL, R. A., MAK, T. W., LINDSTEN, T. & KORSMEYER, S. J. 2001. BCL-2, BCL-X(L) sequester BH3 domain-only molecules preventing BAX- and BAK-mediated mitochondrial apoptosis. *Mol Cell,* 8**,** 705-11.

CHUN, H. J., ZHENG, L., AHMAD, M., WANG, J., SPEIRS, C. K., SIEGEL, R. M., DALE, J. K., PUCK, J., DAVIS, J., HALL, C. G., SKODA-SMITH, S., ATKINSON, T. P., STRAUS, S. E. & LENARDO, M. J. 2002. Pleiotropic defects in lymphocyte activation caused by caspase-8 mutations lead to human immunodeficiency. *Nature,* 419**,** 395-9.

CIRCU, M. L. & AW, T. Y. 2008. Glutathione and apoptosis. *Free Radic Res,* 42**,** 689-706.

COLLINS, A. V., BRODIE, D. W., GILBERT, R. J., IABONI, A., MANSO-SANCHO, R., WALSE, B., STUART, D. I., VAN DER MERWE, P. A. & DAVIS, S. J. 2002. The interaction properties of costimulatory molecules revisited. *Immunity,* 17**,** 201-10.

COPPOLA, S. & GHIBELLI, L. 2000. GSH extrusion and and the mitochondrial pathway of apoptotic signalling. *Biochem Soc Trans,* 28**,** 56-61.

CORCOS, D., GRANDIEN, A., VAZQUEZ, A., DUNDA, O., LORES, P. & BUCCHINI, D. 2001. Expression of a V region-less B cell receptor confers a tolerance-like phenotype on transgenic B cells. *J Immunol,* 166**,** 3083-9.

CORY, S. & ADAMS, J. M. 2002. The Bcl2 family: regulators of the cellular life-or-death switch. *Nat Rev Cancer,* 2**,** 647-56.

D'AGOSTINO, D. P., PUTNAM, R. W. & DEAN, J. B. 2007. Superoxide (*O2-) production in CA1 neurons of rat hippocampal slices exposed to graded levels of oxygen. *J Neurophysiol,* 98**,** 1030-41.

DALTON, T. P., CHEN, Y., SCHNEIDER, S. N., NEBERT, D. W. & SHERTZER, H. G. 2004. Genetically altered mice to evaluate glutathione homeostasis in health and disease. *Free Radic Biol Med,* 37**,** 1511-26.

DANIAL, N. N. & KORSMEYER, S. J. 2004. Cell death: critical control points. *Cell,* 116**,** 205-19.

DEBITON, E., MADELMONT, J. C., LEGAULT, J. & BARTHOMEUF, C. 2003. Sanguinarine-induced apoptosis is associated with an early and severe cellular glutathione depletion. *Cancer Chemother Pharmacol,* 51**,** 474-82.

DELOGU, G., ANTONUCCI, A., MORETTI, S., MARANDOLA, M., TELLAN, G., SIGNORE, M. & FAMULARO, G. 2004. Oxidative stress and mitochondrial glutathione in human lymphocytes exposed to clinically relevant anesthetic drug concentrations. *J Clin Anesth,* 16**,** 189-94.

DELVES, P. J. & ROITT, I. M. 2000a. The immune system. First of two parts. *N Engl J Med,* 343**,** 37-49.

DELVES, P. J. & ROITT, I. M. 2000b. The immune system. Second of two parts. *N Engl J Med,* 343**,** 108-17.

DESZCZ, L., SEIPELT, J., VASSILIEVA, E., ROETZER, A. & KUECHLER, E. 2004. Antiviral activity of caspase inhibitors: effect on picornaviral 2A proteinase. *FEBS Lett,* 560**,** 51-5.

DEUSSING, J., ROTH, W., SAFTIG, P., PETERS, C., PLOEGH, H. L. & VILLADANGOS, J. A. 1998. Cathepsins B and D are dispensable for major histocompatibility complex class II-mediated antigen presentation. *Proc Natl Acad Sci U S A,* 95**,** 4516-21.

DIAZ-HERNANDEZ, J. I., ALMEIDA, A., DELGADO-ESTEBAN, M., FERNANDEZ, E. & BOLANOS, J. P. 2005. Knockdown of glutamate-cysteine ligase by small hairpin RNA reveals that both catalytic and modulatory subunits are essential for the survival of primary neurons. *J Biol Chem,* 280**,** 38992-9001.

EDINGER, A. L. & THOMPSON, C. B. 2002. Antigen-presenting cells control T cell proliferation by regulating amino acid availability. *Proc Natl Acad Sci U S A,* 99**,** 1107-9.

EKERT, P. G., SILKE, J. & VAUX, D. L. 1999. Caspase inhibitors. *Cell Death Differ,* 6**,** 1081-6.

ELIAS, P. M. 2007. The skin barrier as an innate immune element. *Semin Immunopathol,* 29**,** 3-14.

ELLERBY, L. M., ELLERBY, H. M., PARK, S. M., HOLLERAN, A. L., MURPHY, A. N., FISKUM, G., KANE, D. J., TESTA, M. P., KAYALAR, C. & BREDESEN, D. E. 1996. Shift of the cellular oxidation-reduction potential in neural cells expressing Bcl-2. *J Neurochem,* 67**,** 1259-67.

FADEEL, B., ORRENIUS, S. & ZHIVOTOVSKY, B. 2000. The most unkindest cut of all: on the multiple roles of mammalian caspases. *Leukemia,* 14**,** 1514-25.

FADOK, V. A., VOELKER, D. R., CAMPBELL, P. A., COHEN, J. J., BRATTON, D. L. & HENSON, P. M. 1992. Exposure of phosphatidylserine on the surface of apoptotic lymphocytes triggers specific recognition and removal by macrophages. *J Immunol,* 148**,** 2207-16.

FALK, M., USSAT, S., REILING, N., WESCH, D., KABELITZ, D. & ADAM-KLAGES, S. 2004. Caspase inhibition blocks human T cell proliferation by suppressing appropriate regulation of IL-2, CD25, and cell cycle-associated proteins. *J Immunol,* 173**,** 5077-85.

FAN, Y., WU, D., JIN, L. & YIN, Z. 2005. Human glutamylcysteine synthetase protects HEK293 cells against UV-induced cell death through inhibition of c-Jun NH2-terminal kinase. *Cell Biol Int,* 29**,** 695-702.

FIDELUS, R. K., GINOUVES, P., LAWRENCE, D. & TSAN, M. F. 1987. Modulation of intracellular glutathione concentrations alters lymphocyte activation and proliferation. *Exp Cell Res,* 170**,** 269-75.

FISCHMAN, C. M., UDEY, M. C., KURTZ, M. & WEDNER, H. J. 1981. Inhibition of lectin-induced lymphocyte activation by 2-cyclohexene-1-one: decreased intracellular glutathione inhibits an early event in the activation sequence. *J Immunol,* 127**,** 2257-62.

FORMAN, H. J., ZHANG, H. & RINNA, A. 2009. Glutathione: overview of its protective roles, measurement, and biosynthesis. *Molecular aspects of medicine,* 30**,** 1-12.

FRANCO, R., SCHONEVELD, O. J., PAPPA, A. & PANAYIOTIDIS, M. I. 2007. The central role of glutathione in the pathophysiology of human diseases. *Arch Physiol Biochem,* 113**,** 234-58.

FRANK, M. M. & FRIES, L. F. 1991. The role of complement in inflammation and phagocytosis. *Immunol Today,* 12**,** 322-6.

FRIESEN, C., KIESS, Y. & DEBATIN, K. M. 2004. A critical role of glutathione in determining apoptosis sensitivity and resistance in leukemia cells. *Cell Death Differ,* 11 Suppl 1**,** S73-85.

GAFFEN, S. L. 2001. Signaling domains of the interleukin 2 receptor. *Cytokine,* 14**,** 63-77.

GALLO, R. L., MURAKAMI, M., OHTAKE, T. & ZAIOU, M. 2002. Biology and clinical relevance of naturally occurring antimicrobial peptides. *J Allergy Clin Immunol,* 110**,** 823-31.

GARCIA-CALVO, M., PETERSON, E. P., LEITING, B., RUEL, R., NICHOLSON, D. W. & THORNBERRY, N. A. 1998. Inhibition of human caspases by peptide-based and macromolecular inhibitors. *J Biol Chem,* 273**,** 32608-13.

GERSCHENSON, L. E. & ROTELLO, R. J. 1992. Apoptosis: a different type of cell death. *FASEB J,* 6**,** 2450-5.

GINN-PEASE, M. E. & WHISLER, R. L. 1996. Optimal NF kappa B mediated transcriptional responses in Jurkat T cells exposed to oxidative stress are dependent on intracellular glutathione and costimulatory signals. *Biochem Biophys Res Commun,* 226**,** 695-702.

GMUNDER, H. & DROGE, W. 1991. Differential effects of glutathione depletion on T cell subsets. *Cell Immunol,* 138**,** 229-37.

GMUNDER, H., ECK, H. P., BENNINGHOFF, B., ROTH, S. & DROGE, W. 1990. Macrophages regulate intracellular glutathione levels of lymphocytes. Evidence for an immunoregulatory role of cysteine. *Cell Immunol,* 129**,** 32-46.

GRIFFITH, O. W., ANDERSON, M. E. & MEISTER, A. 1979. Inhibition of glutathione biosynthesis by prothionine sulfoximine (S-n-propyl homocysteine sulfoximine), a selective inhibitor of gamma-glutamylcysteine synthetase. *J Biol Chem,* 254**,** 1205-10.

GRIFFITH, O. W. & MEISTER, A. 1979. Potent and specific inhibition of glutathione synthesis by buthionine sulfoximine (S-n-butyl homocysteine sulfoximine). *J Biol Chem,* 254**,** 7558-60.

GROMME, M. & NEEFJES, J. 2002. Antigen degradation or presentation by MHC class I molecules via classical and non-classical pathways. *Mol Immunol,* 39**,** 181-202.

HADZIC, T., LI, L., CHENG, N., WALSH, S. A., SPITZ, D. R. & KNUDSON, C. M. 2005. The role of low molecular weight thiols in T lymphocyte proliferation and IL-2 secretion. *J Immunol,* 175**,** 7965-72.

HAMILOS, D. L., MASCALI, J. J. & WEDNER, H. J. 1991. The role of glutathione in lymphocyte activation--II. Effects of buthionine sulfoximine and 2-cyclohexene-1-one on early and late activation events. *Int J Immunopharmacol,* 13**,** 75-90.

HAMILOS, D. L. & WEDNER, H. J. 1985. The role of glutathione in lymphocyte activation. I. Comparison of inhibitory effects of buthionine sulfoximine and 2-cyclohexene-1-one by nuclear size transformation. *J Immunol,* 135**,** 2740-7.

HAMILOS, D. L., ZELARNEY, P. & MASCALI, J. J. 1989. Lymphocyte proliferation in glutathione-depleted lymphocytes: direct relationship between glutathione availability and the proliferative response. *Immunopharmacology,* 18**,** 223-35.

HAN, Y. H., MOON, H. J., YOU, B. R., KIM, S. Z., KIM, S. H. & PARK, W. H. 2010. Effects of arsenic trioxide on cell death, reactive oxygen species and glutathione levels in different cell types. *Int J Mol Med,* 25**,** 121-8.

HAN, Z., HENDRICKSON, E. A., BREMNER, T. A. & WYCHE, J. H. 1997. A sequential two-step mechanism for the production of the mature p17:p12 form of caspase-3 in vitro. *J Biol Chem,* 272**,** 13432-6.

HARTMANN, O., LE CORROLLER, A. G., BLAISE, D., MICHON, J., PHILIP, I., NOROL, F., JANVIER, M., PICO, J. L., BARANZELLI, M. C., RUBIE, H., COZE, C., PINNA, A., MERESSE, V. & BENHAMOU, E. 1997. Peripheral blood stem cell and bone marrow transplantation for solid tumors and lymphomas: hematologic recovery and costs. A randomized, controlled trial. *Ann Intern Med,* 126**,** 600-7.

HELBING, C. C., JI, L., BAILEY, C. M., VELDHOEN, N., ZHANG, F., HOLCOMBE, G. W., KOSIAN, P. A., TIETGE, J., KORTE, J. J. & DEGITZ, S. J. 2007. Identification of gene expression indicators for thyroid axis disruption in a Xenopus laevis metamorphosis screening assay. Part 2. Effects on the tail and hindlimb. *Aquat Toxicol,* 82**,** 215-26.

HENDERSON, S., ROWE, M., GREGORY, C., CROOM-CARTER, D., WANG, F., LONGNECKER, R., KIEFF, E. & RICKINSON, A. 1991. Induction of bcl-2 expression by Epstein-Barr virus latent membrane protein 1 protects infected B cells from programmed cell death. *Cell,* 65**,** 1107-15.

HENGARTNER, M. O. 2000. The biochemistry of apoptosis. *Nature,* 407**,** 770-6.

HENTSCH, B., MOUZAKI, A., PFEUFFER, I., RUNGGER, D. & SERFLING, E. 1992. The weak, fine-tuned binding of ubiquitous transcription factors to the Il-2 enhancer contributes to its T cell-restricted activity. *Nucleic Acids Res,* 20**,** 2657-65.

HIDAKA, T., FURUNO, H., INOKUCHI, T. & OGURA, R. 1990. Effects of diethyl maleate (DEM), a glutathione depletor, on prostaglandin synthesis in the isolated perfused spleen of rabbits. *Arch Toxicol,* 64**,** 103-8.

HUTCHINS, J. B. & BARGER, S. W. 1998. Why neurons die: cell death in the nervous system. *Anat Rec,* 253**,** 79-90.

ISIDRO-LLOBET, A., ÁLVAREZ, M. & ALBERICIO, F. 2009. Amino Acid-Protecting Groups. *Chemical Reviews,* 109**,** 2455-2504.

JAYARAMAN, S. 2005. Flow cytometric determination of mitochondrial membrane potential changes during apoptosis of T lymphocytic and pancreatic beta cell lines: comparison of tetramethylrhodamineethylester (TMRE), chloromethyl-X-rosamine (H2-CMX-Ros) and MitoTracker Red 580 (MTR580). *J Immunol Methods,* 306**,** 68-79.

JONES, D. P., MAELLARO, E., JIANG, S., SLATER, A. F. & ORRENIUS, S. 1995. Effects of N-acetyl-L-cysteine on T-cell apoptosis are not mediated by increased cellular glutathione. *Immunol Lett,* 45**,** 205-9.

KAGAN, V. E., BORISENKO, G. G., SERINKAN, B. F., TYURINA, Y. Y., TYURIN, V. A., JIANG, J., LIU, S. X., SHVEDOVA, A. A., FABISIAK, J. P., UTHAISANG, W. & FADEEL, B. 2003. Appetizing rancidity of apoptotic cells for macrophages: oxidation, externalization, and recognition of phosphatidylserine. *Am J Physiol Lung Cell Mol Physiol,* 285**,** L1-17.

KAPLOWITZ, N., AW, T. Y. & OOKHTENS, M. 1985. The regulation of hepatic glutathione. *Annu Rev Pharmacol Toxicol,* 25**,** 715-44.

KENNEDY, N. J., KATAOKA, T., TSCHOPP, J. & BUDD, R. C. 1999. Caspase activation is required for T cell proliferation. *J Exp Med,* 190**,** 1891-6.

KERR, J. F., WINTERFORD, C. M. & HARMON, B. V. 1994. Apoptosis. Its significance in cancer and cancer therapy. *Cancer,* 73**,** 2013-26.

KERR, J. F., WYLLIE, A. H. & CURRIE, A. R. 1972. Apoptosis: a basic biological phenomenon with wide-ranging implications in tissue kinetics. *Br J Cancer,* 26**,** 239-57.

KOENIG, A., RUSSELL, J. Q., RODGERS, W. A. & BUDD, R. C. 2008. Spatial differences in active caspase-8 defines its role in T-cell activation versus cell death. *Cell Death Differ,* 15**,** 1701-11.

KOOPMAN, G., REUTELINGSPERGER, C. P., KUIJTEN, G. A., KEEHNEN, R. M., PALS, S. T. & VAN OERS, M. H. 1994. Annexin V for flow cytometric detection of phosphatidylserine expression on B cells undergoing apoptosis. *Blood,* 84**,** 1415-20.

LABADIA, M. E., JEANFAVRE, D. D., CAVINESS, G. O. & MORELOCK, M. M. 1998. Molecular regulation of the interaction between leukocyte function-associated antigen-1 and soluble ICAM-1 by divalent metal cations. *J Immunol,* 161**,** 836-42.

LAMKANFI, M., FESTJENS, N., DECLERCQ, W., VANDEN BERGHE, T. & VANDENABEELE, P. 2007. Caspases in cell survival, proliferation and differentiation. *Cell Death Differ,* 14**,** 44-55.

LAROUX, F. S. 2004. Mechanisms of inflammation: the good, the bad and the ugly. *Front Biosci,* 9**,** 3156-62.

LAVOIE, S., MURRAY, M. M., DEPPEN, P., KNYAZEVA, M. G., BERK, M., BOULAT, O., BOVET, P., BUSH, A. I., CONUS, P., COPOLOV, D., FORNARI, E., MEULI, R., SOLIDA, A., VIANIN, P., CUENOD, M., BUCLIN, T. & DO, K. Q. 2008. Glutathione precursor, N-acetyl-cysteine, improves mismatch negativity in schizophrenia patients. *Neuropsychopharmacology,* 33**,** 2187-99.

LAW, S. K. 1988. C3 receptors on macrophages. *J Cell Sci Suppl,* 9**,** 67-97.

LAWRENCE, C. P. & CHOW, S. C. 2012. Suppression of human T cell proliferation by the caspase inhibitors, z-VAD-FMK and z-IETD-FMK is independent of their caspase inhibition properties. *Toxicol Appl Pharmacol,* 265**,** 103-12.

LAWRENCE, C. P., KADIOGLU, A., YANG, A. L., COWARD, W. R. & CHOW, S. C. 2006. The cathepsin B inhibitor, z-FA-FMK, inhibits human T cell proliferation in vitro and modulates host response to pneumococcal infection in vivo. *J Immunol,* 177**,** 3827-36.

LI, P., NIJHAWAN, D., BUDIHARDJO, I., SRINIVASULA, S. M., AHMAD, M., ALNEMRI, E. S. & WANG, X. 1997. Cytochrome c and dATP-dependent formation of Apaf-1/caspase-9 complex initiates an apoptotic protease cascade. *Cell,* 91**,** 479-89.

LIOW, K. Y. & CHOW, S. C. 2013. The cathepsin B inhibitor, z-FA-CMK is toxic and readily induced cell death in human T lymphocytes. *Toxicol Appl Pharmacol,* 272**,** 559-67.

LOCKSHIN, R. A. & WILLIAMS, C. M. 1964. PROGRAMMED CELL DEATH .2. ENDOCRINE POTENTIATION OF THE BREAKDOWN OF THE INTERSEGMENTAL MUSCLES OF SILKMOTHS. *Journal of Insect Physiology,* 10**,** 643-649.

LOCKSHIN, R. A. & ZAKERI, Z. 2001. Programmed cell death and apoptosis: origins of the theory. *Nat Rev Mol Cell Biol,* 2**,** 545-550.

LOLLO, B. A., CHAN, K. W., HANSON, E. M., MOY, V. T. & BRIAN, A. A. 1993. Direct evidence for two affinity states for lymphocyte function-associated antigen 1 on activated T cells. *J Biol Chem,* 268**,** 21693-700.

LU, S. C. 2009. Regulation of glutathione synthesis. *Mol Aspects Med,* 30**,** 42-59.

LU, S. C. 2013. Glutathione synthesis. *Biochim Biophys Acta,* 1830**,** 3143-53.

LYONS, A. B. & PARISH, C. R. 1994. Determination of lymphocyte division by flow cytometry. *J Immunol Methods,* 171**,** 131-7.

MACK, A. & HACKER, G. 2002. Inhibition of caspase or FADD function blocks proliferation but not MAP kinase-activation and interleukin-2-production during primary stimulation of T cells. *Eur J Immunol,* 32**,** 1986-92.

MAJNO, G. & JORIS, I. 1995. Apoptosis, oncosis, and necrosis. An overview of cell death. *Am J Pathol,* 146**,** 3-15.

MALEK, T. R., YU, A., VINCEK, V., SCIBELLI, P. & KONG, L. 2002. CD4 regulatory T cells prevent lethal autoimmunity in IL-2Rbeta-deficient mice. Implications for the nonredundant function of IL-2. *Immunity,* 17**,** 167-78.

MALORNI, W., RIVABENE, R., SANTINI, M. T. & DONELLI, G. 1993. N-acetylcysteine inhibits apoptosis and decreases viral particles in HIV-chronically infected U937 cells. *FEBS Lett,* 327**,** 75-8.

MARGOLIN, N., RAYBUCK, S. A., WILSON, K. P., CHEN, W., FOX, T., GU, Y. & LIVINGSTON, D. J. 1997. Substrate and inhibitor specificity of interleukin-1 beta-converting enzyme and related caspases. *J Biol Chem,* 272**,** 7223-8.

MARKOVIC, J., BORRAS, C., ORTEGA, A., SASTRE, J., VINA, J. & PALLARDO, F. V. 2007. Glutathione is recruited into the nucleus in early phases of cell proliferation. *J Biol Chem,* 282**,** 20416-24.

MATES, J. M., PEREZ-GOMEZ, C. & NUNEZ DE CASTRO, I. 1999. Antioxidant enzymes and human diseases. *Clin Biochem,* 32**,** 595-603.

MCCARTHY, N., SMITH, C. & WILLIAMS, G. 1992. Apoptosis in the development of the immune system: Growth factors, clonal selection and bcl-2. *Cancer and Metastasis Reviews,* 11**,** 157-178.

MCCOLL, K. S., HE, H., ZHONG, H., WHITACRE, C. M., BERGER, N. A. & DISTELHORST, C. W. 1998. Apoptosis induction by the glucocorticoid hormone dexamethasone and the calcium-ATPase inhibitor thapsigargin involves Bc1-2 regulated caspase activation. *Mol Cell Endocrinol,* 139**,** 229-38.

MEDZHITOV, R. & JANEWAY, C. A., JR. 1997. Innate immunity: impact on the adaptive immune response. *Curr Opin Immunol,* 9**,** 4-9.

MEIER, P., FINCH, A. & EVAN, G. 2000. Apoptosis in development. *Nature,* 407**,** 796-801.

MEISTER, A. 1988. Glutathione metabolism and its selective modification. *J Biol Chem,* 263**,** 17205-8.

MEISTER, A. & ANDERSON, M. E. 1983. Glutathione. *Annu Rev Biochem,* 52**,** 711-60.

MESSINA, J. P. & LAWRENCE, D. A. 1989. Cell cycle progression of glutathione-depleted human peripheral blood mononuclear cells is inhibited at S phase. *J Immunol,* 143**,** 1974-81.

MILLER, S. D., TURLEY, D. M. & PODOJIL, J. R. 2007. Antigen-specific tolerance strategies for the prevention and treatment of autoimmune disease. *Nat Rev Immunol,* 7**,** 665-77.

MIOSSEC, C., DUTILLEUL, V., FASSY, F. & DIU-HERCEND, A. 1997. Evidence for CPP32 activation in the absence of apoptosis during T lymphocyte stimulation. *J Biol Chem,* 272**,** 13459-62.

MISAGHI, S., KORBEL, G. A., KESSLER, B., SPOONER, E. & PLOEGH, H. L. 2006. z-VAD-fmk inhibits peptide:N-glycanase and may result in ER stress. *Cell Death Differ,* 13**,** 163-5.

MISRA, R. S., JELLEY-GIBBS, D. M., RUSSELL, J. Q., HUSTON, G., SWAIN, S. L. & BUDD, R. C. 2005. Effector CD4+ T cells generate intermediate caspase activity and cleavage of caspase-8 substrates. *J Immunol,* 174**,** 3999-4009.

MIURA, M., ZHU, H., ROTELLO, R., HARTWIEG, E. A. & YUAN, J. 1993. Induction of apoptosis in fibroblasts by IL-1 beta-converting enzyme, a mammalian homolog of the C. elegans cell death gene ced-3. *Cell,* 75**,** 653-60.

MONICK, M. M., SAMAVATI, L., BUTLER, N. S., MOHNING, M., POWERS, L. S., YAROVINSKY, T., SPITZ, D. R. & HUNNINGHAKE, G. W. 2003. Intracellular thiols contribute to Th2 function via a positive role in IL-4 production. *J Immunol,* 171**,** 5107-15.

NELSON, B. H. 2004. IL-2, regulatory T cells, and tolerance. *J Immunol,* 172**,** 3983-8.

NELSON, B. H. & WILLERFORD, D. M. 1998. Biology of the interleukin-2 receptor. *Adv Immunol,* 70**,** 1-81.

NICHOLSON, D. W. 1996. ICE/CED3-like proteases as therapeutic targets for the control of inappropriate apoptosis. *Nat Biotechnol,* 14**,** 297-301.

NICHOLSON, D. W. & THORNBERRY, N. A. 1997. Caspases: killer proteases. *Trends Biochem Sci,* 22**,** 299-306.

OBERHAMMER, F., FRITSCH, G., SCHMIED, M., PAVELKA, M., PRINTZ, D., PURCHIO, T., LASSMANN, H. & SCHULTE-HERMANN, R. 1993. Condensation of the chromatin at the membrane of an apoptotic nucleus is not associated with activation of an endonuclease. *J Cell Sci,* 104 (Pt 2)**,** 317-26.

OTTO, H. H. & SCHIRMEISTER, T. 1997. Cysteine Proteases and Their Inhibitors. *Chem Rev,* 97**,** 133-172.

OWUSU-ANSAH, E., YAVARI, A. & BANERJEE, U. 2008. A protocol for _in vivo_ detection of reactive oxygen species.

PALLARDÓ, F. V., MARKOVIC, J., GARCÍA, J. L. & VIÑA, J. 2009. Role of nuclear glutathione as a key regulator of cell proliferation. *Molecular aspects of medicine,* 30**,** 77-85.

PARISH, C. R. 1999. Fluorescent dyes for lymphocyte migration and proliferation studies. *Immunol Cell Biol,* 77**,** 499-508.

PARKIN, J. & COHEN, B. 2001. An overview of the immune system. *Lancet,* 357**,** 1777-89.

PARSONS, M. J. & GREEN, D. R. 2010. Mitochondria in cell death. *Essays Biochem,* 47**,** 99-114.

PASTORE, A., FEDERICI, G., BERTINI, E. & PIEMONTE, F. 2003. Analysis of glutathione: implication in redox and detoxification. *Clin Chim Acta,* 333**,** 19-39.

PAULSEN, M., USSAT, S., JAKOB, M., SCHERER, G., LEPENIES, I., SCHUTZE, S., KABELITZ, D. & ADAM-KLAGES, S. 2008. Interaction with XIAP prevents full caspase-3/-7 activation in proliferating human T lymphocytes. *Eur J Immunol,* 38**,** 1979-87.

POWELL, J. D., RAGHEB, J. A., KITAGAWA-SAKAKIDA, S. & SCHWARTZ, R. H. 1998. Molecular regulation of interleukin-2 expression by CD28 co-stimulation and anergy. *Immunol Rev,* 165**,** 287-300.

POWERS, J. C., ASGIAN, J. L., EKICI, O. D. & JAMES, K. E. 2002. Irreversible inhibitors of serine, cysteine, and threonine proteases. *Chem Rev,* 102**,** 4639-750.

RAFF, M. 1998. Cell suicide for beginners. *Nature,* 396**,** 119-22.

RASNICK, D. 1985. Synthesis of Peptide Fluoromethyl Ketones and the Inhibition of Human Cathepsin B. *Analytical Biochemistry,* 149**,** 461-465.

RATHMELL, J. C. & THOMPSON, C. B. 2002. Pathways of apoptosis in lymphocyte development, homeostasis, and disease. *Cell,* 109 Suppl**,** S97-107.

RAUBER, P., ANGLIKER, H., WALKER, B. & SHAW, E. 1986. The synthesis of peptidylfluoromethanes and their properties as inhibitors of serine proteinases and cysteine proteinases. *Biochem J,* 239**,** 633-40.

REALES, E., MORA-LOPEZ, F., RIVAS, V., GARCIA-POLEY, A., BRIEVA, J. A. & CAMPOS-CARO, A. 2005. Identification of soluble N-ethylmaleimide-sensitive factor attachment protein receptor exocytotic machinery in human plasma cells: SNAP-23 is essential for antibody secretion. *J Immunol,* 175**,** 6686-93.

RELIENE, R. & SCHIESTL, R. H. 2006. Glutathione depletion by buthionine sulfoximine induces DNA deletions in mice. *Carcinogenesis,* 27**,** 240-4.

RONZIO, R. A., ROWE, W. B. & MEISTER, A. 1969. Studies on the mechanism of inhibition of glutamine synthetase by methionine sulfoximine. *Biochemistry,* 8**,** 1066-75.

ROOZENDAAL, R., KAUFFMAN, H. F., DIJKHUIS, A. J., OMMEN, E. T., POSTMA, D. S., DE MONCHY, J. G. & VELLENGA, E. 2002. Interaction between nitric oxide and subsets of human T lymphocytes with differences in glutathione metabolism. *Immunology,* 107**,** 334-9.

ROSSMAN, T., NORRIS, C. & TROLL, W. 1974. Inhibition of macromolecular synthesis in Escherichia coli by protease inhibitors. Specific reversal by glutathione of the effects of chloromethyl ketones. *J Biol Chem,* 249**,** 3412-7.

SAKAMOTO, M., FUJISAWA, Y. & NISHIOKA, K. 1998. Physiologic role of the complement system in host defense, disease, and malnutrition. *Nutrition,* 14**,** 391-8.

SALLUSTO, F., LENIG, D., FORSTER, R., LIPP, M. & LANZAVECCHIA, A. 1999. Two subsets of memory T lymphocytes with distinct homing potentials and effector functions. *Nature,* 401**,** 708-12.

SALMENA, L., LEMMERS, B., HAKEM, A., MATYSIAK-ZABLOCKI, E., MURAKAMI, K., AU, P. Y., BERRY, D. M., TAMBLYN, L., SHEHABELDIN, A., MIGON, E., WAKEHAM, A., BOUCHARD, D., YEH, W. C., MCGLADE, J. C., OHASHI, P. S. & HAKEM, R. 2003. Essential role for caspase 8 in T-cell homeostasis and T-cell-mediated immunity. *Genes Dev,* 17**,** 883-95.

SALVESEN, G. S. & DUCKETT, C. S. 2002. IAP proteins: blocking the road to death's door. *Nat Rev Mol Cell Biol,* 3**,** 401-10.

SANDSTROM, P. A., MANNIE, M. D. & BUTTKE, T. M. 1994. Inhibition of activation-induced death in T cell hybridomas by thiol antioxidants: oxidative stress as a mediator of apoptosis. *J Leukoc Biol,* 55**,** 221-6.

SARIN, A., WU, M. L. & HENKART, P. A. 1996. Different interleukin-1 beta converting enzyme (ICE) family protease requirements for the apoptotic death of T lymphocytes triggered by diverse stimuli. *J Exp Med,* 184**,** 2445-50.

SATO, T., MACHIDA, T., TAKAHASHI, S., IYAMA, S., SATO, Y., KURIBAYASHI, K., TAKADA, K., OKU, T., KAWANO, Y., OKAMOTO, T., TAKIMOTO, R., MATSUNAGA, T., TAKAYAMA, T., TAKAHASHI, M., KATO, J. & NIITSU, Y. 2004. Fas-mediated apoptosome formation is dependent on reactive oxygen species derived from mitochondrial permeability transition in Jurkat cells. *J Immunol,* 173**,** 285-96.

SCAFFIDI, C., FULDA, S., SRINIVASAN, A., FRIESEN, C., LI, F., TOMASELLI, K. J., DEBATIN, K. M., KRAMMER, P. H. & PETER, M. E. 1998. Two CD95 (APO-1/Fas) signaling pathways. *EMBO J,* 17**,** 1675-87.

SCHAFER, Z. T. & KORNBLUTH, S. 2006. The apoptosome: physiological, developmental, and pathological modes of regulation. *Dev Cell,* 10**,** 549-61.

SCHNEIDER, U., SCHWENK, H. U. & BORNKAMM, G. 1977. Characterization of EBV-genome negative "null" and "T" cell lines derived from children with acute lymphoblastic leukemia and leukemic transformed non-Hodgkin lymphoma. *Int J Cancer,* 19**,** 621-6.

SCHOTTE, P., DECLERCQ, W., VAN HUFFEL, S., VANDENABEELE, P. & BEYAERT, R. 1999. Non-specific effects of methyl ketone peptide inhibitors of caspases. *FEBS Lett,* 442**,** 117-21.

SCHOTTE, P., SCHAUVLIEGE, R., JANSSENS, S. & BEYAERT, R. 2001. The cathepsin B inhibitor z-FA.fmk inhibits cytokine production in macrophages stimulated by lipopolysaccharide. *J Biol Chem,* 276**,** 21153-7.

SCHWARTZ, R. H. 1990. A cell culture model for T lymphocyte clonal anergy. *Science,* 248**,** 1349-56.

SCHWERK, C. & SCHULZE-OSTHOFF, K. 2003. Non-apoptotic functions of caspases in cellular proliferation and differentiation. *Biochem Pharmacol,* 66**,** 1453-8.

SHI, Y. 2002a. A conserved tetrapeptide motif: potentiating apoptosis through IAP-binding. *Cell Death Differ,* 9**,** 93-5.

SHI, Y. 2002b. Mechanisms of caspase activation and inhibition during apoptosis. *Mol Cell,* 9**,** 459-70.

SIEGEL, R. M. 2006. Caspases at the crossroads of immune-cell life and death. *Nat Rev Immunol,* 6**,** 308-17.

SLEE, E. A., HARTE, M. T., KLUCK, R. M., WOLF, B. B., CASIANO, C. A., NEWMEYER, D. D., WANG, H. G., REED, J. C., NICHOLSON, D. W., ALNEMRI, E. S., GREEN, D. R. & MARTIN, S. J. 1999. Ordering the cytochrome c-initiated caspase cascade: hierarchical activation of caspases-2, -3, -6, -7, -8, and -10 in a caspase-9-dependent manner. *J Cell Biol,* 144**,** 281-92.

SMYTH, M. J. 1991. Glutathione modulates activation-dependent proliferation of human peripheral blood lymphocyte populations without regulating their activated function. *J Immunol,* 146**,** 1921-7.

SONG, R., MAHIDHARA, R. S., ZHOU, Z., HOFFMAN, R. A., SEOL, D. W., FLAVELL, R. A., BILLIAR, T. R., OTTERBEIN, L. E. & CHOI, A. M. 2004. Carbon monoxide inhibits T lymphocyte proliferation via caspase-dependent pathway. *J Immunol,* 172**,** 1220-6.

SPRICK, M. R., RIESER, E., STAHL, H., GROSSE-WILDE, A., WEIGAND, M. A. & WALCZAK, H. 2002. Caspase-10 is recruited to and activated at the native TRAIL and CD95 death-inducing signalling complexes in a FADD-dependent manner but can not functionally substitute caspase-8. *EMBO J,* 21**,** 4520-30.

STENNICKE, H. R., JURGENSMEIER, J. M., SHIN, H., DEVERAUX, Q., WOLF, B. B., YANG, X., ZHOU, Q., ELLERBY, H. M., ELLERBY, L. M., BREDESEN, D., GREEN, D. R., REED, J. C., FROELICH, C. J. & SALVESEN, G. S. 1998. Pro-caspase-3 is a major physiologic target of caspase-8. *J Biol Chem,* 273**,** 27084-90.

STERN, J. B. & SMITH, K. A. 1986. Interleukin-2 induction of T-cell G1 progression and c-myb expression. *Science,* 233**,** 203-6.

STURM, A., MOHR, S. & FIOCCHI, C. 2002. Critical role of caspases in the regulation of apoptosis and proliferation of mucosal T cells. *Gastroenterology,* 122**,** 1334-45.

SUTHANTHIRAN, M., ANDERSON, M. E., SHARMA, V. K. & MEISTER, A. 1990. Glutathione regulates activation-dependent DNA synthesis in highly purified normal human T lymphocytes stimulated via the CD2 and CD3 antigens. *Proc Natl Acad Sci U S A,* 87**,** 3343-7.

THEODORIDIS, G. 2000. Nitrogen Protecting Groups: Recent Developments and New Applications. *Tetrahedron,* 56**,** 2339-2358.

THOMPSON, C. B. 1995. Apoptosis in the pathogenesis and treatment of disease. *Science,* 267**,** 1456-62.

THORNBERRY, N. A., BULL, H. G., CALAYCAY, J. R., CHAPMAN, K. T., HOWARD, A. D., KOSTURA, M. J., MILLER, D. K., MOLINEAUX, S. M., WEIDNER, J. R., AUNINS, J. & ET AL. 1992. A novel heterodimeric cysteine protease is required for interleukin-1 beta processing in monocytes. *Nature,* 356**,** 768-74.

THORNBERRY, N. A. & LAZEBNIK, Y. 1998. Caspases: enemies within. *Science,* 281**,** 1312-6.

THORNBERRY, N. A., RANO, T. A., PETERSON, E. P., RASPER, D. M., TIMKEY, T., GARCIA-CALVO, M., HOUTZAGER, V. M., NORDSTROM, P. A., ROY, S., VAILLANCOURT, J. P., CHAPMAN, K. T. & NICHOLSON, D. W. 1997. A combinatorial approach defines specificities of members of the caspase family and granzyme B. Functional relationships established for key mediators of apoptosis. *J Biol Chem,* 272**,** 17907-11.

URBICH, C., HEESCHEN, C., AICHER, A., SASAKI, K.-I., BRUHL, T., FARHADI, M. R., VAJKOCZY, P., HOFMANN, W. K., PETERS, C., PENNACCHIO, L. A., ABOLMAALI, N. D., CHAVAKIS, E., REINHECKEL, T., ZEIHER, A. M. & DIMMELER, S. 2005. Cathepsin L is required for endothelial progenitor cell-induced neovascularization. *Nat Med,* 11**,** 206-213.

VALKO, M., LEIBFRITZ, D., MONCOL, J., CRONIN, M. T., MAZUR, M. & TELSER, J. 2007. Free radicals and antioxidants in normal physiological functions and human disease. *Int J Biochem Cell Biol,* 39**,** 44-84.

VAN NOORDEN, C. J. 2001. The history of Z-VAD-FMK, a tool for understanding the significance of caspase inhibition. *Acta Histochem,* 103**,** 241-51.

VAZIRI, N. D., WANG, X. Q., OVEISI, F. & RAD, B. 2000. Induction of oxidative stress by glutathione depletion causes severe hypertension in normal rats. *Hypertension,* 36**,** 142-6.

VILLADANGOS, J. A. & PLOEGH, H. L. 2000. Proteolysis in MHC class II antigen presentation: who's in charge? *Immunity,* 12**,** 233-9.

WALSH, A. C., MICHAUD, S. G., MALOSSI, J. A. & LAWRENCE, D. A. 1995. Glutathione depletion in human T lymphocytes: analysis of activation-associated gene expression and the stress response. *Toxicol Appl Pharmacol,* 133**,** 249-61.

WANG, J. & LENARDO, M. J. 2000. Roles of caspases in apoptosis, development, and cytokine maturation revealed by homozygous gene deficiencies. *J Cell Sci,* 113 (Pt 5)**,** 753-7.

WEBER, C. A., DUNCAN, C. A., LYONS, M. J. & JENKINSON, S. G. 1990. Depletion of tissue glutathione with diethyl maleate enhances hyperbaric oxygen toxicity. *Am J Physiol,* 258**,** L308-12.

WYLLIE, A. H., KERR, J. F. & CURRIE, A. R. 1980. Cell death: the significance of apoptosis. *Int Rev Cytol,* 68**,** 251-306.

YAGI, T., HARDIN, J. A., VALENZUELA, Y. M., MIYOSHI, H., GORES, G. J. & NYBERG, S. L. 2001. Caspase inhibition reduces apoptotic death of cryopreserved porcine hepatocytes. *Hepatology,* 33**,** 1432-40.

YAN, N. & SHI, Y. 2005. Mechanisms of apoptosis through structural biology. *Annu Rev Cell Dev Biol,* 21**,** 35-56.

YIM, C. Y., HIBBS, J. B., JR., MCGREGOR, J. R., GALINSKY, R. E. & SAMLOWSKI, W. E. 1994. Use of N-acetyl cysteine to increase intracellular glutathione during the induction of antitumor responses by IL-2. *J Immunol,* 152**,** 5796-805.

YIN, X. M. 2006. Bid, a BH3-only multi-functional molecule, is at the cross road of life and death. *Gene,* 369**,** 7-19.

YUAN, J., SHAHAM, S., LEDOUX, S., ELLIS, H. M. & HORVITZ, H. R. 1993. The C. elegans cell death gene ced-3 encodes a protein similar to mammalian interleukin-1 beta-converting enzyme. *Cell,* 75**,** 641-52.

ZAPATA, J. M., TAKAHASHI, R., SALVESEN, G. S. & REED, J. C. 1998. Granzyme release and caspase activation in activated human T-lymphocytes. *J Biol Chem,* 273**,** 6916-20.

ZEUNER, A., ERAMO, A., PESCHLE, C. & DE MARIA, R. 1999. Caspase activation without death. *Cell Death Differ,* 6**,** 1075-80.

ZHENG, T. S. & FLAVELL, R. A. 2000. Divinations and surprises: genetic analysis of caspase function in mice. *Exp Cell Res,* 256**,** 67-73.

ZIMMERMANN, K. C., BONZON, C. & GREEN, D. R. 2001. The machinery of programmed cell death. *Pharmacol Ther,* 92**,** 57-70.

ZMUDA, J. & FRIEDENSON, B. 1983. Changes in intracellular glutathione levels in stimulated and unstimulated lymphocytes in the presence of 2-mercaptoethanol or cysteine. *J Immunol,* 130**,** 362-4.

ZOU, H., LI, Y., LIU, X. & WANG, X. 1999. An APAF-1.cytochrome c multimeric complex is a functional apoptosome that activates procaspase-9. *J Biol Chem,* 274**,** 11549-56.

APPENDIX ONE

RAJAH, T. & CHOW, S. C. 2014. The inhibition of human T cell proliferation by the caspase inhibitor z-VAD-FMK is mediated through oxidative stress. *Toxicol Appl Pharmacol,* 278(2)**,** 100-6.

Toxicology and Applied Pharmacology 278 (2014) 100–106

Contents lists available at ScienceDirect

Toxicology and Applied Pharmacology

journal homepage: www.elsevier.com/locate/ytaap

The inhibition of human T cell proliferation by the caspase inhibitor z-VAD-FMK is mediated through oxidative stress

T. Rajah, S.C. Chow *

School of Science, Monash University Sunway Campus, Jalan Lagoon Selatan, Bandar Sunway, 46150 Selangor Darul Ehsan, Malaysia

ARTICLE INFO

Article history:
Received 23 January 2014
Revised 7 April 2014
Accepted 15 April 2014
Available online 24 April 2014

Keywords:
T lymphocytes
Caspases
z-VAD-FMK
T cell activation
Oxidative stress
Thiols

ABSTRACT

The caspase inhibitor benzyloxycarbony (Cbz)-L-Val-Ala-Asp (OMe)-fluoromethylketone (z-VAD-FMK) has recently been shown to inhibit T cell proliferation without blocking caspase-8 and caspase-3 activation in primary T cells. We showed in this study that z-VAD-FMK treatment leads to a decrease in intracellular glutathione (GSH) with a concomitant increase in reactive oxygen species (ROS) levels in activated T cells. The inhibition of anti-CD3-mediated T cell proliferation induced by z-VAD-FMK was abolished by the presence of low molecular weight thiols such as GSH, N-acetylcysteine (NAC) and L-cysteine, whereas D-cysteine which cannot be metabolised to GSH has no effect. These results suggest that the depletion of intracellular GSH is the underlying cause of z-VAD-FMK-mediated inhibition of T cell activation and proliferation. The presence of exogenous GSH also attenuated the inhibition of anti-CD3-induced CD25 and CD69 expression mediated by z-VAD-FMK. However, none of the low molecular weight thiols were able to restore the caspase-inhibitory properties of z-VAD-FMK in activated T cells where caspase-8 and caspase-3 remain activated and processed into their respective subunits in the presence of the caspase inhibitor. This suggests that the inhibition of T cell proliferation can be uncoupled from the caspase-inhibitory properties of z-VAD-FMK. Taken together, the immunosuppressive effects in primary T cells mediated by z-VAD-FMK are due to oxidative stress via the depletion of GSH.

Introduction

Peptidyl fluoromethylketone (FMK) caspase inhibitors are very useful tools and have been used extensively in cell death research to elucidate the role of caspases during apoptotic cell death (Caserta et al., 2003; Ekert et al., 1999; Garcia-Calvo et al., 1998; Yagi et al., 2001). All peptidyl-FMK caspase inhibitors contain a peptide sequence based on the target cleavage sequence of the substrate. The family of caspases recognises a sequence of four amino acids in the substrates, designated P4-P3-P2-P1 and cleave substrates after an Asp residue at P1 (Shi, 2002; Yuan et al., 1993). All the peptide based caspase inhibitors used to date consist of a peptide sequence culminating in an Asp residue, whereas the requirements for amino acid residues at the other positions vary with members of the caspase family (Garcia-Calvo et al., 1998). By exploiting the differences in their substrate specificities, more specific inhibitors can be developed for the caspases (Garcia-Calvo et al., 1998; Thornberry et al., 1997). Conjugated to the C-terminal of the peptide sequence in the caspase inhibitor is a halomethylketone, such as FMK or chloromethylketone (CMK), which forms an irreversible covalent bond with the S-H group of the cysteine residue in the caspase active site (Caserta et al., 2003; Garcia-Calvo et al., 1998). Finally, to enhance the permeability of the inhibitor, a benzyloxycarbonyl (z) or an acetyl (Ac) group attached to the amino-terminal of the peptide sequence will increase the hydrophobicity of the compound (Van Noorden, 2001). Together, these caspase inhibitors act as competitive inhibitors by mimicking the substrates and irreversibly blocking the caspase activities.

However, accumulating evidence from a number of studies have suggested that these caspase inhibitors may not be as specific as originally envisaged. For instance the most widely used broad spectrum caspase inhibitor, z-VAD-FMK, has been shown to inhibit other enzymes besides the caspases. These include the lysosomal cysteine protease, cathepsin B (Schotte et al., 1999), peptide:N-glycanase (Misaghi et al., 2006) and picornaviral 2A proteinases (Deszcz et al., 2004). Similarly, the caspase-8 inhibitor, z-IETD-FMK, also inhibited picornaviral 2A proteinases (Deszcz et al., 2004). Some of the non-specific effects of these caspase inhibitors may account for some of the inconsistencies observed in the blocking of T cell activation and proliferation reported in several early studies (Boissonnas et al., 2002; Kennedy et al., 1999; Mack and Hacker, 2002; Zapata et al., 1998). More recently, we showed that z-VAD-FMK readily inhibits primary T cell proliferation without blocking the activation and processing of caspase-8 and caspase-3 (Lawrence and Chow, 2012). However, z-VAD-FMK is extremely effective in blocking the activation of caspases in these cells during apoptosis. Because caspase-8 plays a pivotal role in T cell activation and

* Corresponding author.
E-mail address: [redacted] (S.C. Chow).

http://dx.doi.org/10.1016/j.taap.2014.04.014
0041-008X/

proliferation (Chun et al., 2002; Falk et al., 2004; Salmena et al., 2003), the suppression of T cell proliferation mediated by z-VAD-FMK is independent of its caspase-inhibitory properties.

In the present study we examined the molecular mechanism that underlies the immunosuppressive properties of z-VAD-FMK. Our results showed that z-VAD-FMK treatment induced depletion of intracellular GSH level in cells in a time-dependent manner with a concomitant increase in ROS level. The inhibition of mitogen-induced T cell proliferation mediated by z-VAD-FMK was readily abolished by low molecular weight thiols such as NAC, L-cysteine and GSH but not with D-cysteine. Taken together, these results suggest that the inhibition of T cell proliferation mediated by z-VAD-FMK is due to oxidative stress via the depletion of GSH.

Materials and methods

Reagents. The following chemicals were obtained from Sigma Aldrich (USA): Glutathione (GSH), L-cysteine, D-cysteine, N-acetylcysteine (NAC), L-Buthionine-S, R-sulfoximine (BSO), monochlorobimane (MCB) and dihydroethidium (DHE). Benzyloxycarbonyl-Val-Ala-Asp-(O-methyl)-fluoromethylketone (z-VAD-FMK) was purchased from ICN (USA). Monoclonal antibody (mAb) against CD3 (clone OKT3) was purified from hybridoma (ATCC) culture supernatants as previously described (Lawrence et al., 2006). Lymphoprep was from Axis-Shield PoCAS (Norway) while RPMI 1640 and FCS were from Gibco (UK). FITC-conjugated anti-CD25 and PE-conjugated anti-CD69 were acquired from BD Pharmingen (UK). The 5-bromo-2′-deoxyuridine (BrdU) labelling kit was obtained from Roche (Switzerland). Goat-anti caspase-8 and rabbit anti-caspase-3 was from Santa Cruz Biotechnology (USA) while secondary HRP-conjugated antibodies were from Dako (UK).

Peripheral mononuclear blood cell isolation. Peripheral venous blood was obtained from normal healthy volunteers, with appropriate ethical clearance, and collected into heparinised Vacutainer tubes (Becton Dickinson). Human peripheral blood mononuclear cells (PBMCs) were isolated from the red blood cells using density gradient centrifugation. In brief, the peripheral blood was diluted with RPMI and layered onto lymphoprep (density gradient of 1.077), and centrifuged at 800 ×g for 30 min. The PBMCs at the interface between lymphoprep and plasma were collected, washed and re-suspended in RPMI containing 10% (v/v) foetal calf serum (FCS), 10 mM L-glutamine (Invitrogen, UK), penicillin (100 U/ml) and streptomycin (100 μg/ml) until used. The viability of PBMCs was assessed using trypan blue exclusion assay and routinely determined to be >95%.

Cell proliferation assays. The proliferation of T cells following stimulation with anti-CD3 was determined using a colorimetric immunoassay based on the measurement of incorporated BrdU in the DNA during synthesis (Roche, Switzerland). The BrdU assay was performed according to the manufacturer's instructions. In brief, PBMCs (1×10^6 cells/ml) in RPMI 1640 supplemented with 10% FCS were stimulated with plate bound 5 μg/ml anti-CD3 in the absence or presence of z-VAD-FMK for various time periods in an atmosphere of 5% CO_2 in air at 37 °C. The cells were cultured for 72 h with the last 3 h pulsed with 10 μM BrdU per well. At the end of the culture period, the plates were centrifuged and cells fixed with 200 μl ethanol (70%) in HCl (final concentration 0.5 M) for 30 min at −20 °C. Following fixation, the DNA in the cells was partially digested by nuclease treatment for 30 min at 37 °C before incubating with a horse radish peroxidase-conjugated BrdU antibody. After three rounds of washing, a substrate was added and the coloured product cleaved was measured after 20 min incubation (room temperature) at 405 nm with a reference wavelength of 495 nm using a microplate reader (Tecan 200).

Determination of intracellular GSH in activated T cells. The intracellular GSH level in activated T cells was determined as described previously (Aoshiba et al., 2001; Apostolova et al., 2010; Osseni et al., 1999; Sun et al., 2009). Following treatments, the cells (1×10^4 cells) were centrifuged down at 3500 rpm for 10 min and washed with 100 μl PBS. The supernatants were carefully removed before adding 100 μl of MCB (100 μM) in PBS for 30 min at 37 °C in the dark. Unbound MCB is almost nonfluorescent, whereas the dye fluoresces blue when bound to GSH. The fluorescence in the samples was determined using a Tecan Infinite M200 fluoro-plate reader with excitation and emission wavelengths of 390 and 460 nm, respectively. A control containing media alone plus MCB was used as a blank and subtracted from the sample absorbance.

Detection of ROS in activated T cells. Intracellular ROS in activated T cells was detected by using the redox sensitive fluorescent dye, DHE. Once inside the cells DHE will be oxidised by the ROS to form ethidium, which binds the nuclear DNA and emits a red fluorescence that can be detected with a flow cytometer. Following treatments, cells (1×10^6) were washed and the cell pellet re-suspended in 1 ml of pre-warmed serum-free RPMI. DHE was added to a final concentration of 5 mM and the cells were incubated in the dark for 30 min at 37 °C, washed with ice-cold PBS before re-suspending in 1 ml of PBS prior to analysis by flow cytometry. The samples were gated to include 1×10^4 small resting T cells and large activated T cells, excluding cell debris, based on the forward- and side-scatter profiles. For the fluorescent 2-hydroxyethidium, an excitation wavelength of 532 nm (FL-2 channel) was used and the machine was calibrated using unstained cells prior to each experiment.

Western blotting. Following treatments, the PBMCs were layered over lymphoprep and centrifuged to remove the dead cells. The viable cells were washed in PBS and cell lysates prepared by three consecutive freeze–thaw cycles in an appropriate volume (10 μl per 1×10^6 cells) of lysis buffer (0.1 M NaCl, 1 mM Tris HCl at pH7.6, 1 mM EDTA, 1% Triton-X, 1 mM PMSF). The protein concentration was determined using the Bradford assay (Biorad, Germany). Protein equivalent to 20 μg whole-cell lysates was diluted in loading buffer (2% SDS, 10% Glycerol, 50 mM Tris-HCl pH 6.8, 0.2% Bromophenol Blue and 100 mM DTT) and resolved using 13% SDS-polyacrylamide gel electrophoresis. The separated proteins were transfered onto Hybond C membrane (Amersham, UK) and probed with antibodies to caspase-8 and caspase-3. Detection was carried out using chemiluminescence (Amersham). Following caspase detection, the membrane was incubated with stripping buffer before reprobing with antibodies to β-actin.

Statistical analysis of the data. The experimental data were analysed using Student's *t* test or one-way analysis of variance followed by Dunnet's test.

Results

z-VAD-FMK inhibits anti-CD3-induced T cell proliferation in PBMCs

In order to characterise the underlying mechanism of z-VAD-FMK-induced immunosuppression, the effect of z-VAD-FMK on T cell proliferation induced by anti-CD3 in PBMCs was determined. As illustrated in Fig. 1, z-VAD-FMK induced suppression of anti-CD3-mediated T cell proliferation in a concentration-dependent manner as determined by the incorporation of BrdU. Although lower concentration of z-VAD-FMK (25 μM) was less effective in blocking T cell proliferation induced by anti-CD3, significant inhibition was observed with 50 and 100 μM, which is very much in line with our previous report (Lawrence and Chow, 2012). From the results in Fig. 1, an IC_{50} of 70 μM was determined and this concentration of z-VAD-FMK was used in all subsequent experiments.

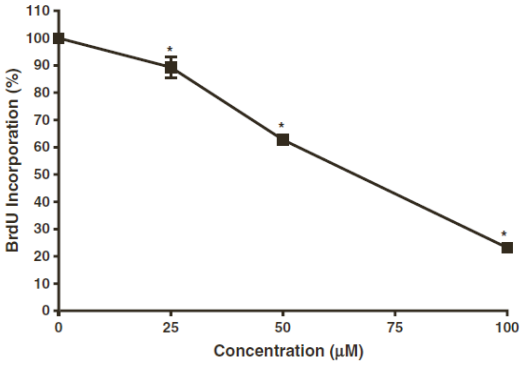

Fig. 1. Dose-dependent inhibition of T cell proliferation by z-VAD-FMK. PBMCs (1×10^6/ml) were stimulated with anti-CD3 (5 μg/ml) in the presence of various concentrations of z-VAD-FMK for 72 h. T cell proliferation was determined using BrdU incorporation as outlined in Materials and methods. The results are the means ± SEM from three separate donors. *Significantly decreased ($p < 0.05$) from control with anti-CD3 alone.

Effect of z-VAD-FMK on intracellular GSH and ROS levels in primary T cells

Since GSH depletion has been shown to increase ROS levels and block T cell proliferation (Fidelus et al., 1987; Gmunder and Droge, 1991; Gmunder et al., 1990; Suthanthiran et al., 1990), we examined whether oxidative stress may be responsible for the immunosuppressive effects induced by z-VAD-FMK in T cells. To this end, PBMCs were activated with anti-CD3 in the presence or absence of z-VAD-FMK and the intracellular GSH and ROS levels determined. As illustrated in Fig. 2, z-VAD-FMK at varying concentrations (25–100 μM) has little effect on the GSH level in activated primary T cells after 6 h compared to control cells. However, after 24 h there was a significant reduction of intracellular GSH level in cells treated with 50 and 100 μM z-VAD-FMK ($p < 0.05$). These results suggest that z-VAD-FMK is capable of depleting GSH in T cells activated with anti-CD3. With the level of intracellular GSH decreasing in the presence of z-VAD-FMK, we examined whether ROS is generated under similar conditions. T cells activated with anti-CD3 were incubated with the DHE dye, which selectively detects intracellular superoxide anion ($\bullet O_{2-}$) production (Bindokas et al., 1996; D'Agostino et al., 2007) prior to flow cytometry analysis. As shown in Fig. 3, addition of z-VAD-FMK at 25 or 50 μM had little effect on the ROS levels in T cells activated with anti-CD3 for 6 h. However, at 100 μM z-VAD-FMK the ROS level in the activated T cells was significantly increased ($p < 0.05$). The level of ROS in anti-CD3- activated T cells was further increased significantly by z-VAD-FMK in a concentration-dependent manner (25–100 μM) after 24 h. The carrier solvent DMSO (>0.1%) has no effect on the intracellular GSH and ROS levels (results not shown). Collectively, these results suggest that z-VAD-FMK induced oxidative stress in anti-CD3-activated T cells.

Effect of antioxidants on the suppression of primary T cell proliferation mediated by z-VAD-FMK

Since z-VAD-FMK treatment depletes intracellular GSH and increases ROS levels in PBMCs, we examined whether the antioxidant, NAC, could reverse the inhibition of T cell proliferation mediated by the caspase inhibitor. As shown in Fig. 4, z-VAD-FMK (70 μM) on its own markedly inhibited T cell proliferation induced by anti-CD3, whereas NAC abolished this effect in a concentration-dependent manner (1.25–5 mM). At the highest concentration of NAC (5 mM), the suppression of T cell proliferation induced by z-VAD-FMK was nearly completely abolished. Although NAC is frequently use as a source of sulfhydryl groups for GSH biosynthesis (Arranz et al., 2008; Berk et al., 2008; Lavoie et al., 2008) it can act as oxygen free radical scavenger and directly interact with ROS (Sandstrom et al., 1994). To determine whether NAC is acting as a precursor for GSH biosynthesis or ROS scavenging, BSO, which irreversibly blocks the GSH synthesis pathway by inhibiting the enzyme γ-glutamylcysteine synthetase (Griffith and Meister, 1979), was added to anti-CD3-activated T cells co-treated with z-VAD-FMK and NAC for 72 h. As illustrated in Fig. 5, NAC effectively abolished the inhibition of T cell proliferation mediated by z-VAD-FMK and BSO completely blocked the effect of NAC. Similar to NAC, GSH (1.25–5 mM) added exogenously blocked the inhibition of T cell proliferation induced by z-VAD-FMK in a concentration-dependent manner (Fig. 6). Complete abolishment was achieved with the highest concentration of GSH (5 mM). Taken together, these results suggest that z-VAD-FMK mediated immunosuppression in activated T cells is due to oxidative stress via the depletion of intracellular GSH. Since the

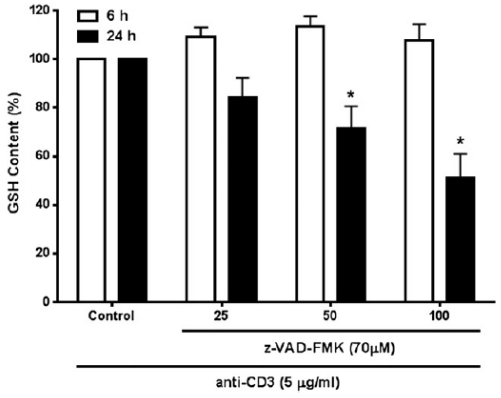

Fig. 2. Effect of z-VAD-FMK on intracellular GSH levels in activated primary T cells. PBMCs (1×10^6/ml) were stimulated with anti-CD3 (5 μg/ml) in the presence of various concentrations of z-VAD-FMK. The level of GSH was measured after 6 and 24 h using the fluorescent dye MCB as described in Materials and methods. Results are based on 1×10^4 cells per sample and are means ± SEM from three separate donors. *Significantly different ($p < 0.05$) from control with anti-CD3 alone.

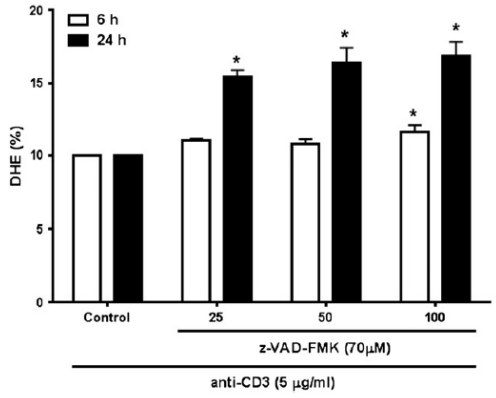

Fig. 3. Effect of z-VAD-FMK on ROS levels in activated primary T cells. PBMCs (1×10^6/ml) stimulated with anti-CD3 (5 μg/ml) in the presence of various concentrations of z-VAD-FMK. ROS levels were measured after 6 and 24 h using the DHE probe and analysed using flow cytometry as described in Materials and methods. Results are the mean ± SEM of three independent experiments. *Significantly different ($p < 0.05$) from control with anti-CD3 alone.

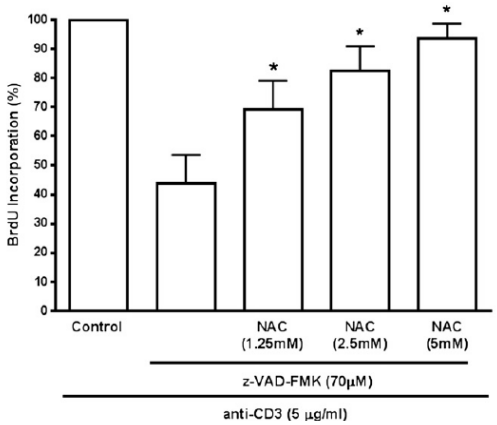

Fig. 4. Effect of NAC on the inhibition of T cell proliferation mediated by z-VAD-FMK. PBMCs (1×10^6/ml) were stimulated with anti-CD3 (5 μg/ml) in the presence of 70 μM z-VAD-FMK and varying concentrations of NAC. BrdU incorporation was determined after 72 h as described in Materials and methods. Results are the mean ± SEM of at least three independent experiments. *Significantly increased ($p < 0.05$) compared to z-VAD-FMK + anti-CD3.

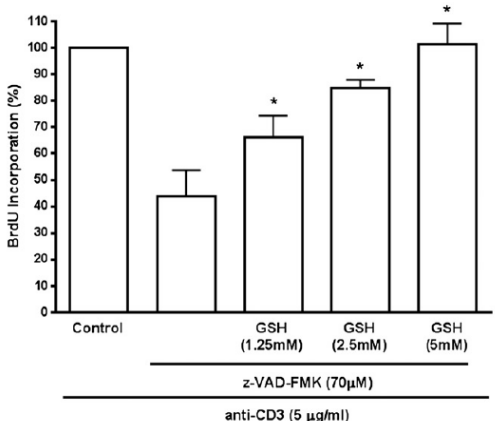

Fig. 6. Effect of GSH on the inhibition of T cell proliferation mediated by z-VAD-FMK. PBMCs (1×10^6/ml) were stimulated with anti-CD3 (5 μg/ml) in the presence of 70 μM z-VAD-FMK in the presence of varying concentrations of GSH. BrdU incorporation was determined after 72 h as described in Materials and methods. Results are the mean ± SEM of at least three independent experiments. *Significantly increased ($p < 0.05$) compared to z-VAD-FMK + anti-CD3.

inhibition of T cell proliferation mediated by z-VAD-FMK was abolished by NAC and GSH, we examined whether other low molecular weight thiols, such as L-cysteine and D-cysteine would have a similar effect. As illustrated in Fig. 7, the presence of 5 mM L-cysteine, which is another precursor for GSH biosynthesis attenuated the inhibition of T cell proliferation mediated by z-VAD-FMK, whereas D-cysteine which cannot be metabolised into GSH had virtually no effect. Taken together, our results suggest that only thiols which are able to promote GSH biosynthesis can abolish the immunosuppressive effect of z-VAD-FMK.

GSH inhibits z-VAD-FMK-induced down-regulation of CD25 and CD69 in activated T cells

Up-regulation of the IL-2R α-chain (CD25) and CD69 is one of the earliest cell surface markers that occur after T cell activation following anti-CD3 stimulation. Since low molecular weight thiols were able to reverse the inhibition of T cell proliferation mediated by z-VAD-FMK, the effect of GSH on the expression of CD25 and the activated T cell marker, CD69 was examined. As shown in Fig. 8, the percentage of cells that stained positive for CD25 and CD69 expression increased from around 0.65% and 3% in resting cells to 55.6% and 51.2% in activated T cells, respectively. In the presence of z-VAD-FMK (70 μM), the up-regulation of CD25 and CD69 in activated T cells was reduced to 32.3% and 32.1%, respectively. The presence of 5 mM GSH completely restored the inhibition of anti-CD3-induced up-regulation of CD25 and CD69 induced by z-VAD-FMK. These findings demonstrated that oxidative stress plays an important role in the down-regulation of CD25 and CD69 expression induced by z-VAD-FMK in activated T cells.

Effect of low molecular weight thiols on caspase-8 and caspase-3 processing in activated primary T cells

We have recently shown that z-VAD-FMK up to 100 μM had no effect on the activation of caspase-8 and caspase-3 in activated T cells (Lawrence and Chow, 2012). Since the low molecular weight thiols

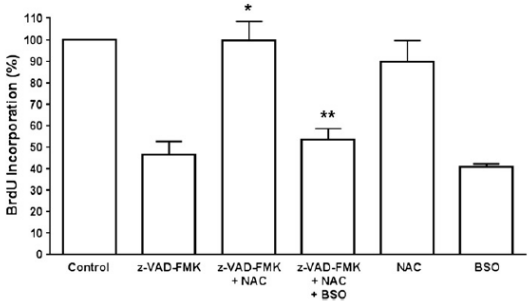

Fig. 5. The effect of NAC on the inhibition of T cell proliferation mediated by z-VAD-FMK is abolished by BSO. PBMCs (1×10^6/ml) were stimulated with anti-CD3 (5 μg/ml) plus 70 μM z-VAD-FMK in the presence or absence of NAC (5 mM) and BSO (0.5 mM) where indicated. BrdU incorporation was determined after 72 h as described in Materials and methods. Results are the mean ± SEM of at least three independent experiments. *Significantly increased ($p < 0.01$) compared to z-VAD-FMK; **Significantly decreased ($p < 0.05$) from z-VAD-FMK + NAC.

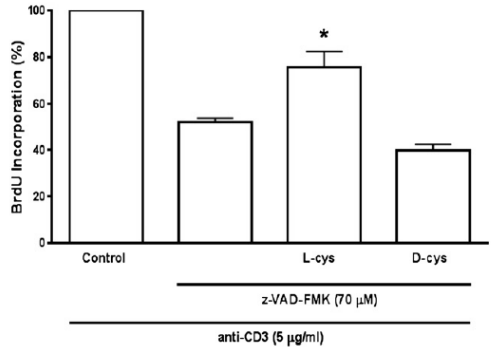

Fig. 7. Effect of low molecular weight thiols on the inhibition of T cell proliferation mediated by z-VAD-FMK. PBMCs (1×10^6/ml) were stimulated with anti-CD3 (5 μg/ml) plus 70 μM z-VAD-FMK in the presence or absence of L-cysteine (5 mM) and D-cysteine (5 mM) where indicated. BrdU incorporation was determined after 72 h as described in Materials and methods. Results are the mean ± SEM of at least three independent experiments. *Significantly increased ($p < 0.01$) compared to z-VAD-FMK + anti-CD3.

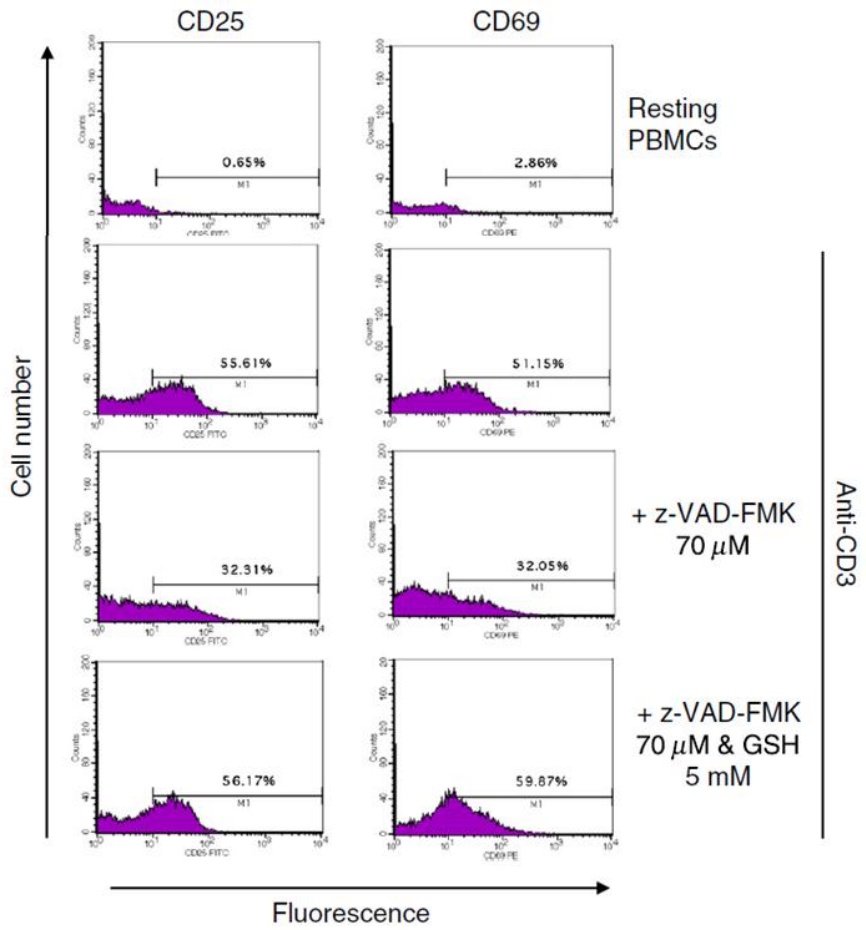

GSH, NAC and L-cysteine could overcome the inhibition of T cell proliferation induced by z-VAD-FMK, we examined whether they have any effect on caspase processing in z-VAD-FMK-treated activated T cells. In order to exclude cells dying of activation-induced cell death and growth factor deprivation, living activated T cells were purified using lymphoprep prior to Western blot analysis. As illustrated in Fig. 9, neither caspase-8 nor caspase-3 was activated in resting T cells whereas both caspases were activated and processed into their respective subunits following anti-CD3 stimulation. As reported previously, z-VAD-FMK had little effect on the activation of caspase-8 and caspase-3 as shown by the presence of the cleaved intermediates (Lawrence and Chow, 2012). In the presence of NAC, D-cysteine and L-cysteine, the processing of caspase-8 to the p42/43 subunits was partially blocked by z-VAD-FMK. Interestingly, D-cysteine was more effective in blocking the processing of caspase-8 to its p42/43 subunits although it has little effect on z-VAD-FMK-induced suppression of T cell proliferation. However, GSH, NAC and L-cysteine had little effect on the activation and processing of caspase-3 in activated T cells in the presence of z-VAD-FMK. Taken together, the presence of low molecular weight thiols appears to have little effect on z-VAD-FMK caspase-inhibitory properties.

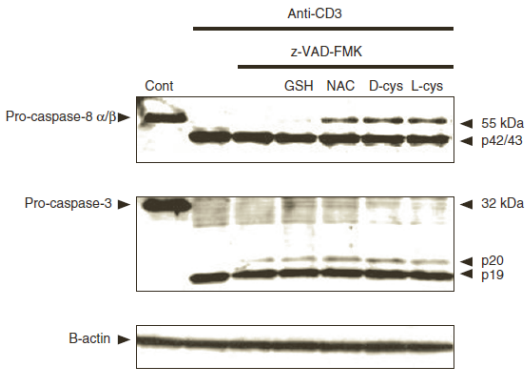

Fig. 9. Effect of low molecular weight thiols on caspase-8 and caspase-3 processing in z-VAD-FMK-treated activated T cells. PBMCs (1×10^6/ml) were stimulated with anti-CD3 (5 μg/ml) plus 70 μM z-VAD-FMK in the presence or absence of antioxidants (5 mM). After 72 h, the cells were taken through a gradient density centrifugation using lymphoprep to obtain activated T cells. Whole cell lysates (20 μg protein) from activated T cells were resolved using 13% SDS-PAGE, transferred to nitrocellulose membrane and probed for caspase-8, caspase-3 and β-actin as described in Materials and methods. The results are one representative of three independent experiments.

Discussion

Besides cell death, caspases are also involved in cytokine maturation, cell growth and differentiation (Lamkanfi et al., 2007; Schwerk and

Schulze-Osthoff, 2003; Wang and Lenardo, 2000). Among the family of caspases, caspase-8 plays a pivotal role in cell signalling during mitogen-induced T cell activation and proliferation (Chun et al., 2002; Falk et al., 2004; Salmena et al., 2003). It is therefore not surprising that peptidyl-FMK based caspase inhibitors are capable of blocking T cell proliferation as shown in a number of studies (Alam et al., 1999; Boissonnas et al., 2002; Falk et al., 2004; Kennedy et al., 1999; Mack and Hacker, 2002). However, accumulating evidence suggested that peptidyl-FMK caspase inhibitors may not be as specific as originally thought (Deszcz et al., 2004; Misaghi et al., 2006; Schotte et al., 1999). Recently, we showed that z-VAD-FMK inhibits T cell proliferation but fails to block the activation of caspase-8 and caspase-3 in proliferating T cells (Lawrence and Chow, 2012). This suggests that the suppression of T cell proliferation mediated by z-VAD-FMK has little to do with caspase inhibition. In the present study, we examined the underlying mechanism involved in the inhibition of T cell proliferation induced by z-VAD-FMK.

Our results demonstrated that z-VAD-FMK treatment leads to depletion of intracellular GSH level in activated T cells and a corresponding increase in cellular ROS. This suggests that oxidative stress may be the underlying mechanism of z-VAD-FMK immunosuppressive effect. Indeed, the inhibition of T cell proliferation mediated by z-VAD-FMK was readily abolished by exogenous low molecular weight thiols such as GSH, NAC and L-cysteine. Since both NAC and L-cysteine are precursors for GSH biosynthesis the results suggest that GSH may be the rate-limiting thiol necessary for T cell proliferation. This is further corroborated when D-cysteine, which cannot be metabolised to GSH was unable to restore T cell proliferation in the presence of z-VAD-FMK. Taken together, the ability of GSH, NAC and L-cysteine to restore the inhibition of T cell proliferation suggests that the immunosuppressive effect induced by z-VAD-FMK is due to oxidative stress via the depletion of GSH. These findings are very much in line with numerous studies showing that GSH plays an important role in T cell proliferation (Hamilos and Wedner, 1985; Markovic et al., 2007; Zmuda and Friedenson, 1983). For instance, human T lymphocytes depleted of intracellular GSH using pharmacological regulators of GSH, such as methionine sulfoximine (Ronzio et al., 1969), diethyl maleate (Hidaka et al., 1990; Weber et al., 1990) and BSO (Griffith et al., 1979; Reliene and Schiestl, 2006; Vaziri et al., 2000) were unable to proliferate and accumulate high levels of ROS (Fidelus et al., 1987; Gmunder and Droge, 1991; Gmunder et al., 1990; Suthanthiran et al., 1990). In contrast, increasing intracellular GSH levels using 2-mercaptoethanol was reported to enhance T cell proliferation mediated by IL-2 and anti-CD3-stimulated $CD3^+$ T lymphocytes (Messina and Lawrence, 1989; Zmuda and Friedenson, 1983). All these studies implicate GSH as an important regulator for T cell proliferation and suggest a direct relationship between the proliferative response of T cells and the availability of GSH (Chaplin and Wedner, 1978; Fidelus et al., 1987; Suthanthiran et al., 1990). How z-VAD-FMK-treatment diminishes the intracellular GSH level in activated T cells is unclear, although peptidyl-FMKs have been reported to interact with GSH directly in vitro (Angliker et al., 1987). However, the time taken for z-VAD-FMK to reduce intracellular GSH level in activated T cells is rather long, thus ruling out a direct interaction between z-VAD-FMK and GSH. Previous studies have suggested that peptidyl methylketones can inhibit GSH reductase (Angliker et al., 1987; Powers et al., 2002), which is a critical enzyme in the homeostasis of thiol redox state in cells. The enzyme catalyses the reduction of oxidised GSH (GSSH) to GSH to maintain a high GSH:GSSG ratio, therefore blocking it will deplete intracellular GSH.

Besides blocking T cell proliferation, z-VAD-FMK also inhibits the expression of CD25 and CD69 in T cells, two early T cell activation markers when stimulated with anti-CD3 (Falk et al., 2004; Kennedy et al., 1999; Lawrence and Chow, 2012). The up-regulation of CD25 and CD69 expression in activated T cells has been reported previously to be dependent on the intracellular GSH levels or redox state of the cells (Roozendaal et al., 2002). This suggests that the depletion of intracellular GSH mediated by z-VAD-FMK could also account for the down-regulation of CD25 and CD69 expression in activated T cells. Indeed, the presence of exogenous GSH completely restored the inhibition of anti-CD3-induced CD25 and CD69 expression mediated by z-VAD-FMK to control levels, confirming that the depletion of intracellular GSH is the underlying mechanism of the down-regulation of these two early T cell activation markers.

Being a pan-caspase inhibitor, z-VAD-FMK has been used extensively in apoptosis research to block the activation of caspases. Therefore, its failure to block the activation and processing of caspase-8 and caspase-3 to their subunits in activated T cells was rather unexpected (Lawrence and Chow, 2012). We found that none of the low molecular weight thiols were able to restore the failure of z-VAD-FMK in blocking caspase-8 and caspase-3, suggesting that the inhibition of T cell proliferation mediated by the caspase inhibitor can be uncoupled from its caspase-inhibitory properties, and that oxidative stress is unlikely to be involved in the latter. How proliferating T cells are able to cope with the pro-apoptotic activity of caspases remains unclear. It has been suggested that restricted localisation of the active caspases helps to restrain them from cleaving substrates that trigger apoptosis in proliferating T cells (Koenig et al., 2008; Lamkanfi et al., 2007; Paulsen et al., 2008). However, peptidyl-FMK based caspase inhibitors are designed as substrates and function as competitive inhibitors. Being membrane permeable, z-VAD-FMK should be able to block the active caspases without being affected by their subcellular localisation (Lamkanfi et al., 2007; Paulsen et al., 2008). Alternatively, the activated caspases are restrained by cellular inhibitors of apoptosis proteins, such as XIAP as shown recently in proliferating T cells (Paulsen et al., 2008). This could explain the failure of z-VAD-FMK in blocking the activated caspases and the lack of PARP cleavage in proliferating T cells (Lawrence and Chow, 2012). However, it cannot account for the processing of caspase-8 and caspase-3, which are caspase-dependent.

In summary, our results demonstrate that z-VAD-FMK inhibits T cell activation and proliferation induced by anti-CD3 through oxidative stress via GSH depletion. The immunosuppressive effect of z-VAD-FMK is readily reversed in the presence of low molecular weight thiols such as GSH, NAC and L-cysteine, whereas D-cysteine which cannot be metabolised to GSH has no effect. Furthermore, these thiols were unable to restore the failure of z-VAD-FMK to block the processing of caspase-8 and caspase-3, suggesting that the inhibition of T cell proliferation can be uncoupled from the caspase-inhibitory properties of z-VAD-FMK.

Conflict of interest

The authors declare that there are no conflicts of interest.

Funding

This work was supported by funding provided by Monash University Malaysia Campus, Malaysia.

References

Alam, A., Cohen, L.Y., Aouad, S., Sekaly, R.P., 1999. Early activation of caspases during T lymphocyte stimulation results in selective substrate cleavage in nonapoptotic cells. J. Exp. Med. 190, 1879–1890.

Angliker, H., Wikstrom, P., Rauber, P., Shaw, E., 1987. The synthesis of lysylfluoromethanes and their properties as inhibitors of trypsin, plasmin and cathepsin B. Biochem. J. 241, 871–875.

Aoshiba, K., Tamaoki, J., Nagai, A., 2001. Acute cigarette smoke exposure induces apoptosis of alveolar macrophages. Am. J. Physiol. Lung Cell. Mol. Physiol. 281, 1392–1401.

Apostolova, N., Gomez-Sucerquia, L.J., Moran, A., Alvarez, A., Blas-Garcia, A., Esplugues, A., 2010. Enhanced oxidative stress and increased mitochondrial mass during Efavirenz-induced apoptosis in human hepatic cells. Br. J. Pharmacol. 160, 2069–2084.

Arranz, L., Fernandez, C., Rodriguez, A., Ribera, J.M., De La Fuente, M., 2008. The glutathione precursor N-acetylcysteine improves immune function in postmenopausal women. Free Radic. Biol. Med. 45, 1252–1262.

Berk, M., Copolov, D., Dean, O., Lu, K., Jeavons, S., Schapkaitz, I., Anderson-Hunt, M., Judd, F., Katz, F., Katz, P., Ording-Jespersen, S., Little, J., Conus, P., Cuenod, M., Do, K.Q., Bush, A.I.,

2008. N-acetyl cysteine as a glutathione precursor for schizophrenia—a double-blind, randomized, placebo-controlled trial. Biol. Psychiatry 64, 361–368.
Bindokas, V.P., Jordan, J., Lee, C.C., Miller, R.J., 1996. Superoxide production in rat hippocampal neurons: selective imaging with hydroethidine. J. Neurosci. 16, 1324–1336.
Boissonnas, A., Bonduelle, O., Lucas, B., Debre, P., Autran, B., Combadiere, B., 2002. Differential requirement of caspases during naive T cell proliferation. Eur. J. Immunol. 32, 3007–3015.
Caserta, T.M., Smith, A.N., Gultice, A.D., Reedy, M.A., Brown, T.L., 2003. Q-VD-OPh, a broad spectrum caspase inhibitor with potent antiapoptotic properties. Apoptosis 8, 345–352.
Chaplin, D.D., Wedner, J.H., 1978. Inhibition of lectin-induced lymphocyte activation by diamide and other sulfhydryl reagents. Cell. Immunol. 36, 303–311.
Chun, H.J., Zheng, L., Ahmad, M., Wang, J., Speirs, C.K., Siegel, R.M., Dale, J.K., Puck, J., Davis, J., Hall, C.G., Skoda-Smith, S., Atkinson, T.P., Straus, S.E., Lenardo, M.J., 2002. Pleiotropic defects in lymphocyte activation caused by caspase-8 mutations lead to human immunodeficiency. Nature 419, 395–399.
D'Agostino, D.P., Putnam, R.W., Dean, J.B., 2007. Superoxide ($^{\bullet}O_2^-$) production in CA1 neurons of rat hippocampal slices exposed to graded levels of oxygen. J. Neurophysiol. 98, 1030–1041.
Deszcz, L., Seipelt, J., Vassilieva, E., Roetzer, A., Kuechler, E., 2004. Antiviral activity of caspase inhibitors: effect on picornaviral 2A proteinase. FEBS Lett. 560, 51–55.
Ekert, P.G., Silke, J., Vaux, D.L., 1999. Caspase inhibitors. Cell Death Differ. 6, 1081–1086.
Falk, M., Ussat, S., Reiling, N., Wesch, D., Kabelitz, D., Adam-Klages, S., 2004. Caspase inhibition blocks human T cell proliferation by suppressing appropriate regulation of IL-2, CD25, and cell cycle-associated proteins. J. Immunol. 173, 5077–5085.
Fidelus, R.K., Ginouves, P., Lawrence, D., Tsan, M.F., 1987. Modulation of intracellular glutathione concentrations alters lymphocyte activation and proliferation. Exp. Cell Res. 170, 269–275.
Garcia-Calvo, M., Peterson, E.P., Leiting, B., Ruel, R., Nicholson, D.W., Thornberry, N.A., 1998. Inhibition of human caspases by peptide-based and macromolecular inhibitors. J. Biol. Chem. 273, 32608–32613.
Gmunder, H., Droge, W., 1991. Differential effects of glutathione depletion on T cell subsets. Cell. Immunol. 138, 229–237.
Gmunder, H., Eck, H.P., Benninghoff, B., Roth, S., Droge, W., 1990. Macrophages regulate intracellular glutathione levels of lymphocytes. Evidence for an immunoregulatory role of cysteine. Cell. Immunol. 129, 32–46.
Griffith, O.W., Meister, A., 1979. Potent and specific inhibition of glutathione synthesis by buthionine sulfoximine (S-n-butyl homocysteine sulfoximine). J. Biol. Chem. 254, 7558–7560.
Griffith, O.W., Anderson, M.E., Meister, A., 1979. Inhibition of glutathione biosynthesis by prothionine sulfoximine (S-n-propyl homocysteine sulfoximine), a selective inhibitor of gamma-glutamylcysteine synthetase. J. Biol. Chem. 254, 1205–1210.
Hamilos, D.L., Wedner, H.J., 1985. The role of glutathione in lymphocyte activation. I. Comparison of inhibitory effects of buthionine sulfoximine and 2-cyclohexene-1-one by nuclear size transformation. J. Immunol. 135, 2740–2747.
Hidaka, T., Furuno, H., Inokuchi, T., Ogura, R., 1990. Effects of diethyl maleate (DEM), a glutathione depletor, on prostaglandin synthesis in the isolated perfused spleen of rabbits. Arch. Toxicol. 64, 103–108.
Kennedy, N.J., Kataoka, T., Tschopp, J., Budd, R.C., 1999. Caspase activation is required for T cell proliferation. J. Exp. Med. 190, 1891–1896.
Koenig, A., Russell, J.Q., Rodgers, W.A., Budd, R.C., 2008. Spatial differences in active caspase-8 defines its role in T-cell activation versus cell death. Cell Death Differ. 15, 1701–1711.
Lamkanfi, M., Festjens, N., Declercq, W., Vanden Berghe, T., Vandenabeele, P., 2007. Caspases in cell survival, proliferation and differentiation. Cell Death Differ. 14, 44–55.
Lavoie, S., Murray, M.M., Deppen, P., Knyazeva, M.G., Berk, M., Boulat, O., Bovet, P., Bush, A. I., Conus, P., Copolov, D., Fornari, E., Meuli, R., Solida, A., Vianin, P., Cuenod, M., Buclin, T., Do, K.Q., 2008. Glutathione precursor, N-acetyl-cysteine, improves mismatch negativity in schizophrenia patients. Neuropsychopharmacology 33, 2187–2199.
Lawrence, C.P., Kadioglu, A., Yang, A.-L., Coward, W.R., Chow, S.C., 2006. The cathepsin B inhibitor, z-FA-FMK, inhibits human T cell proliferation in vitro and modulates host response to Pneumococcal infection in vivo. J. Immunol. 177, 3827–3836.
Lawrence, C.P., Chow, S.C., 2012. Suppression of human T cell proliferation by the caspase inhibitors, z-VAD-FMK and z-IETD-FMK is independent of their caspase inhibition properties. Toxicol. Appl. Pharmacol. 265, 103–112.
Mack, A., Hacker, G., 2002. Inhibition of caspase or FADD function blocks proliferation but not MAP kinase-activation and interleukin-2-production during primary stimulation of T cells. Eur. J. Immunol. 32, 1986–1992.
Markovic, J., Borras, C., Ortega, A., Sastre, J., Vina, J., Pallardo, F.V., 2007. Glutathione is recruited into the nucleus in early phases of cell proliferation. J. Biol. Chem. 282, 20416–20424.
Messina, J.P., Lawrence, D.A., 1989. Cell cycle progression of glutathione-depleted human peripheral blood mononuclear cells is inhibited at S phase. J. Immunol. 143, 1974–1981.
Misaghi, S., Korbel, G.A., Kessler, B., Spooner, E., Ploegh, H.L., 2006. z-VAD-fmk inhibits peptide:N-glycanase and may result in ER stress. Cell Death Differ. 13, 163–165.
Osseni, R.A., Debbasch, C., Christen, M.O., Rat, P., Warnet, J.M., 1999. Tacrine-induced reactive oxygen species in a human liver cell line: the role of anethole dithiolethione as a scavenger. Toxicol. In Vitro 13, 683–688.
Paulsen, M., Ussat, S., Jakob, M., Scherer, G., Lepenies, I., Schutze, S., Kabelitz, D., Adam-Klages, S., 2008. Interaction with XIAP prevents full caspase-3/-7 activation in proliferating human T lymphocytes. Eur. J. Immunol. 38, 1979–1987.
Powers, J.C., Asgian, J.L., Ekici, O.D., James, K.E., 2002. Irreversible inhibitors of serine, cysteine, and threonine proteases. Chem. Rev. 102, 4639–4750.
Reliene, R., Schiestl, R.H., 2006. Glutathione depletion by buthionine sulfoximine induces DNA deletions in mice. Carcinogenesis 27, 240–244.
Ronzio, R.A., Rowe, W.B., Meister, A., 1969. Studies on the mechanism of inhibition of glutamine synthetase by methionine sulfoximine. Biochemistry 8, 1066–1075.
Roozendaal, R., Kauffman, H.F., Dijkhuis, A.J., Ommen, E.T., Postma, D.S., De Monchy, J.G., Vellenga, E., 2002. Interaction between nitric oxide and subsets of human T lymphocytes with differences in glutathione metabolism. Immunology 107, 334–339.
Salmena, L., Lemmers, B., Hakem, A., Matysiak-Zablocki, E., Murakami, K., Au, P.Y., Berry, D.M., Tamblyn, L., Shehabeldin, A., Migon, E., Wakeham, A., Bouchard, D., Yeh, W.C., Mcglade, J.C., Ohashi, P.S., Hakem, R., 2003. Essential role for caspase 8 in T-cell homeostasis and T-cell-mediated immunity. Genes Dev. 17, 883–895.
Sandstrom, P.A., Mannie, M.D., Buttke, T.M., 1994. Inhibition of activation-induced death in T cell hybridomas by thiol antioxidants: oxidative stress as a mediator of apoptosis. J. Leukoc. Biol. 55, 221–226.
Schotte, P., Declercq, W., Van Huffel, S., Vandenabeele, P., Beyaert, R., 1999. Non-specific effects of methyl ketone peptide inhibitors of caspases. FEBS Lett. 442, 117–121.
Schwerk, C., Schulze-Osthoff, K., 2003. Non-apoptotic functions of caspases in cellular proliferation and differentiation. Biochem. Pharmacol. 66, 1453–1458.
Shi, Y., 2002. A conserved tetrapeptide motif: potentiating apoptosis through IAP-binding. Cell Death Differ. 9, 93–95.
Sun, H.L., Tsai, A.C., Pan, S.L., Ding, Q.Q., Yamaguchi, H., Lin, C.N., Hung, M.C., Teng, C.M., 2009. EPOX inhibits angiogenesis by degradation of Mcl-1 through ERK inactivation. Clin. Cancer Res. 15, 4904–4914.
Suthanthiran, M., Anderson, M.E., Sharma, V.K., Meister, A., 1990. Glutathione regulates activation-dependent DNA synthesis in highly purified normal human T lymphocytes stimulated via the CD2 and CD3 antigens. Proc. Natl. Acad. Sci. U. S. A. 87, 3343–3347.
Thornberry, N.A., Rano, T.A., Peterson, E.P., Rasper, D.M., Timkey, T., Garcia-Calvo, M., Houtzager, V.M., Nordstrom, P.A., Roy, S., Vaillancourt, J.P., Chapman, K.T., Nicholson, D.W., 1997. A combinatorial approach defines specificities of members of the caspase family and granzyme B. Functional relationships established for key mediators of apoptosis. J. Biol. Chem. 272, 17907–17911.
Van Noorden, C.J., 2001. The history of Z-VAD-FMK, a tool for understanding the significance of caspase inhibition. Acta Histochem. 103, 241–251.
Vaziri, N.D., Wang, X.Q., Oveisi, F., Rad, B., 2000. Induction of oxidative stress by glutathione depletion causes severe hypertension in normal rats. Hypertension 36, 142–146.
Wang, J., Lenardo, M.J., 2000. Roles of caspases in apoptosis, development, and cytokine maturation revealed by homozygous gene deficiencies. J. Cell Sci. 113 (Pt 5), 753–757.
Weber, C.A., Duncan, C.A., Lyons, M.J., Jenkinson, S.G., 1990. Depletion of tissue glutathione with diethyl maleate enhances hyperbaric oxygen toxicity. Am. J. Physiol. 258, L308–L312.
Yagi, T., Hardin, J.A., Valenzuela, Y.M., Miyoshi, H., Gores, G.J., Nyberg, S.L., 2001. Caspase inhibition reduces apoptotic death of cryopreserved porcine hepatocytes. Hepatology 33, 1432–1440.
Yuan, J., Shaham, S., Ledoux, S., Ellis, H.M., Horvitz, H.R., 1993. The *C. elegans* cell death gene ced-3 encodes a protein similar to mammalian interleukin-1 beta-converting enzyme. Cell 75, 641–652.
Zapata, J.M., Takahashi, R., Salvesen, G.S., Reed, J.C., 1998. Granzyme release and caspase activation in activated human T-lymphocytes. J. Biol. Chem. 273, 6916–6920.
Zmuda, J., Friedenson, B., 1983. Changes in intracellular glutathione levels in stimulated and unstimulated lymphocytes in the presence of 2-mercaptoethanol or cysteine. J. Immunol. 130, 362–364.

APPENDIX TWO

RAJAH, T. & CHOW, S. C. 2015. Suppression of human T cell proliferation mediated by the cathepsin B inhibitor, z-FA-FMK is due to oxidative stress. *PLoS ONE*, 10(4).

PLOS | ONE

RESEARCH ARTICLE

Suppression of Human T Cell Proliferation Mediated by the Cathepsin B Inhibitor, z-FA-FMK Is Due to Oxidative Stress

Tanuja Rajah, Sek Chuen Chow*

School of Science, Monash University Sunway Campus, Jalan Lagoon Selatan, Bandar Sunway, 46150, Selangor Darul Ehsan, Malaysia

* [redacted]

Abstract

The cathepsin B inhibitor, benzyloxycarbonyl-phenylalanine-alanine-fluoromethyl ketone (z-FA-FMK) readily inhibits anti-CD3-induced human T cell proliferation, whereas the analogue benzyloxycarbonyl-phenylalanine-alanine-diazomethyl ketone (z-FA-DMK) had no effect. In contrast, benzyloxycarbonyl-phenylalanine-alanine-chloromethyl ketone (z-FA-CMK) was toxic. The inhibition of T cell proliferation mediated by z-FA-FMK requires not only the FMK moiety, but also the benzyloxycarbonyl group at the N-terminal, suggesting some degree of specificity in z-FA-FMK-induced inhibition of primary T cell proliferation. We showed that z-FA-FMK treatment leads to a decrease in intracellular glutathione (GSH) with a concomitant increase in reactive oxygen species (ROS) levels in activated T cells. The inhibition of anti-CD3-induced T cell proliferation mediated by z-FA-FMK was abolished by the presence of low molecular weight thiols such as GSH, N-acetylcysteine (NAC) and L-cysteine, whereas D-cysteine which cannot be metabolised to GSH has no effect. The inhibition of anti-CD3-induced up-regulation of CD25 and CD69 expression mediated by z-FA-FMK was also attenuated in the presence of exogenous GSH. Similar to cell proliferation, GSH, NAC and L-cysteine but not D-cysteine, completely restored the processing of caspase-8 and caspase-3 to their respective subunits in z-FA-FMK-treated activated T cells. Our collective results demonstrated that the inhibition of T cell activation and proliferation mediated by z-FA-FMK is due to oxidative stress via the depletion of GSH.

Citation: Rajah T, Chow SC (2015) Suppression of Human T Cell Proliferation Mediated by the Cathepsin B Inhibitor, z-FA-FMK Is Due to Oxidative Stress. PLoS ONE 10(4): e0123711. doi:10.1371/journal.pone.0123711

Academic Editor: Georg Häcker, University Freiburg, GERMANY

Received: December 2, 2014

Accepted: March 5, 2015

Published: April 27, 2015

Data Availability Statement: All relevant data are within the paper.

Funding: The project was funded by Monash University Malaysia student grant.

Competing Interests: The authors have declared that no competing interests exist.

Introduction

Halomethylketone peptides such as peptidyl chloromethylketones were the first active site directed irreversible enzyme inhibitors synthesised and were originally designed as potential drugs for the treatment of certain diseases [1,2]. However, the highly electrophilic chloromethylketone moiety was too reactive and results in the alkylation of non-target molecules indiscriminately [3,4]. Efforts to replace the reactive chlorine atom led to the eventual synthesis of peptidyl fluoromethylketones [3]. Because of the much stronger carbon-fluorine bonds

relative to carbon-chlorine bonds, fluoromethylketones were expected to be poorer alkylating agents and should reduce the non-specific alkylation significantly compared to chloromethylketones. However, once synthesised, peptidyl fluoromethylketones were found to be highly reactive and are selective irreversible inhibitors for cysteine proteases [4].

Benzyloxycarbonyl-phenylalanine-alanine-fluoromethylketone (z-FA-FMK) was originally designed as an affinity label to irreversibly block cathepsin B, a cysteine protease [3,4]. It was found to bind tightly to the enzyme active site and became a very potent inhibitor of cathepsin B. The enzyme is normally found in the lysosomes of cells, but in rheumatoid arthritis (RA) patients the enzyme activity of cathepsin B was found to be increased in the synovial fluid and synovial lining [5,6]. This suggests that cathepsin B may be a good target for therapeutic intervention for the treatment of RA using z-FA-FMK. Indeed, in vivo studies demonstrate that z-FA-FMK was extremely efficient in preventing the destruction of articular cartilage and bone in chronic inflammatory arthritis induced by adjuvant in mice [7–9]. However, accumulating evidences suggest that the remarkable therapeutic action of z-FA-FMK in the treatment of RA observed in mice may not be due to the inhibition of cathepsin B alone. Previous study has shown that z-FA-FMK inhibits LPS-induced cytokine secretion in macrophages by blocking the transactivation potential of NF-κB [10]. We have shown that besides blocking cathepsin B activity, z-FA-FMK effectively blocked human T cell activation and proliferation in vitro, and modulates host response to pneumococcal infection in vivo [11]. The inhibition of human T cell activation and proliferation mediated by z-FA-FMK was accompanied by the blocking of the activation of caspase-8 and caspase-3 [11]. Although caspases play a pivotal role in apoptosis, it is now established that caspases such as caspase-8 play an important role in T cell activation and proliferation and that blocking the activation of this enzyme will ultimately block T cell activation and proliferation [12,13]. Taken together, these studies suggest that the pleiotropic immunosuppressive effects of z-FA-FMK may account for the remarkable therapeutic effect in suppressing articular cartilage and bone destruction in chronic inflammatory arthritis in mice [7–9].

In the present study, we examined the effects of other z-FA-FMK analogues such as z-FA-DMK and z-FA-CMK on T cell activation and proliferation. Our results showed that z-FA-DMK has no effect on T cell proliferation whereas z-FA-CMK was toxic to primary T cells. The immunosuppression mediated by z-FA-FMK is dependent on the FMK group and the benzyloxycarbonyl group at the N-terminal. We observed that z-FA-FMK treatment leads to depletion of intracellular GSH level in anti-CD3-stimulated primary T cells with a concomitant increase in reactive oxygen species (ROS) level. The inhibition of anti-CD3-induced T cell proliferation mediated by z-FA-FMK was abolished by low molecular weight thiols such as NAC, GSH and L-cysteine but not with D-cysteine. Taken together, these results suggest that z-FA-FMK-mediated inhibition of T cell proliferation is due to oxidative stress via the depletion of intracellular GSH.

Materials and Methods

Reagents

The following chemicals were obtained from Sigma Aldrich (USA): Glutathione (GSH), L-cysteine, D-cysteine, N-acetylcysteine (NAC), L-Buthionine-(S,R)-sulfoximine (BSO), monochlorobimane (MCB) and dihydroethidium (DHE). Monoclonal antibody (mAb) against CD3 (clone OKT3) was purified from hybridoma (ATCC) culture supernatants. Lymphoprep was from Axis-Shield PoCAS (Norway) while RPMI 1640 and FCS were from Gibco (UK). FITC-conjugated anti-CD25 and PE-conjugated anti-CD69 were acquired from BD Pharmingen (UK). The 5-bromo-2'-deoxyuridine (BrdU) labelling kit was obtained from Roche (Switzerland). Rabbit antibodies to caspase-3, mouse antibodies to β–actin and goat

antibodies to caspase-8 were all from Santa Cruz Biotechnology (USA). All secondary HRP-conjugated antibodies were purchased from Dako (UK). Benzyloxycarbonyl-phenylalanine-alanine-fluoromethylketone (z-FA-FMK), benzyloxycarbonyl-tyrosine-valine-alanine-aspartic acid- fluoromethylketone (z-YVAD-FMK), benzyloxycarbonyl-valine-arginine-proline-DL-arginine-fluoromethylketone (z-VRPR-FMK) and benzyloxycarbonyl-phenylalanine-alanine-diazomethylketone (z-FA-DMK) were purchased from Bachem (Switzerland). Benzyloxycarbonyl-phenylalanine-alanine-chloromethylketone (z-FA-CMK) and biotinylated-phenylalanine-alanine-fluoromethylketone (b-FA-FMK) were from MP Biomedicals (USA).

Peripheral mononuclear blood isolation

Peripheral venous blood was obtained from normal healthy volunteers. Each blood donor was individually informed and gave his/her consent for using the collected blood samples in a scientific study. Collection and use of blood samples in this study was approved by Monash University Human Research Ethics Committee (Reference Number: CF09/1065-2009000486). Human peripheral blood mononuclear cells (PBMCs) were separated from the red blood cells using density gradient centrifugation. In brief, the peripheral blood was diluted with RPMI and layered onto lymphoprep (density gradient of 1.077) and centrifuged at 800 x g for 30 min. The PBMCs were then removed from the interface between the lymphoprep and the plasma, washed and re-suspended in RPMI containing 10% (v/v) foetal calf serum (FCS), 10 mM L-glutamine (Invitrogen, UK), penicillin (100 U/ml) and streptomycin (100 μg/ml) until used. The viability of PBMCs was assessed using trypan blue exclusion assay and routinely determined to be >95%.

Cell proliferation assays

The proliferation of T cells following anti-CD3 stimulation was determined using a colorimetric immunoassay based on the measurement of BrdU during DNA synthesis (Roche, Switzerland). The BrdU assay was performed according to the manufacturer's instructions. In brief, PBMCs were seeded at 1 x 10^6 cells/ml in RPMI 1640 supplemented with 10% FCS and stimulated with plate-bound 5 μg/ml anti-CD3 in the absence or presence of various peptidyl halomethylketones in an atmosphere of 5% CO_2 in air at 37°C. The cells were cultured for various time periods with the last 3 h pulsed with 10 μM BrdU per well. At the end of the culture period, the plates were centrifuged and cells fixed with 200 μl ethanol (70%) in HCl (final concentration 0.5 M) for 30 min at -20°C. Following fixation, the DNA in the cells was partially digested by nuclease treatment for 30 min at 37°C before incubating with a horse radish peroxidase-conjugated BrdU antibody. After three rounds of washing, a substrate was added and the coloured product was measured after 20 min incubation (room temperature) at 405 nm with a reference wavelength of 495 nm using a microplate reader (Tecan 200).

Determination of intracellular GSH in activated T cells

The intracellular GSH level in activated T cells was determined as described previously [14–17]. Following treatments, the cells (1 x 10^4 cells) were centrifuged down at 3500 rpm for 10 min and washed with 100 μl PBS. The supernatant was carefully removed before adding 100 μl of 100 μM MCB (in PBS) for 30 min at 37°C in the dark. Unbound MCB is almost nonfluorescent, whereas the dye fluoresces blue when bound to GSH. The fluorescence in the samples was determined using a Tecan Infinite M200 fluoro-plate reader with excitation and emission wavelengths of 390 and 460 nm, respectively. A control containing media alone plus MCB was used as a blank and subtracted from the sample absorbance.

Detection of ROS in activated T cells

Intracellular ROS in activated T cells was detected by using the redox sensitive fluorescent dye, DHE. Once inside the cells DHE will be oxidised by the ROS to form ethidium which binds to the nuclear DNA and emits a red fluorescence that can be detected with a flow cytometer. Following treatments, cells (1 x 10^6) were washed and the cell pellet re-suspended in 1 ml of pre-warmed serum-free RPMI. DHE was added to a final concentration of 5 mM and the cells were incubated in the dark for 30 min at 37°C, washed with ice-cold PBS before re-suspending in 1 ml of PBS prior to analysis by flow cytometry. The samples were gated to include 1 x 10^4 small resting T cells and large activated T cells, excluding cell debris, based on the forward- and side-scatter profiles. For the fluorescent 2-hydroxyethidium, an excitation wavelength of 532 nm (FL- 2 channel) was used and the machine was calibrated using unstained cells prior to each experiment.

Determination of cell surface CD25 and CD69 expression using flow cytometry

Following treatments, PBMCs (1 x 10^6) were centrifuged down and the supernatants discarded. The cell pellets were washed in ice-cold PBS and re-suspended in staining buffer (50 μl PBS containing 2% BSA). Fluorochrome-conjugated antibody (anti-CD25-FITC or anti-CD69-PE) in a final dilution of 1:50 was added to the cells and incubated on ice for 30 min in the dark. The cells were then washed twice in staining buffer before analysis using flow cytometry. Excitation wavelengths of 488 nm (FL-1 channel) (anti-CD25-FITC) and 532 nm (FL-2 channel) (anti-CD69-PE) were used. The machine was calibrated using unstained cells prior to each experiment.

Western Blotting

Following treatments, the PBMCs were layered over lymphoprep and centrifuged to remove the dead cells. The viable cells were washed in PBS and re-suspended in an appropriate volume (10 μl per 1 x 10^6 cells) of lysis buffer (0.1 M NaCl, 1 mM Tris HCl at pH7.6, 1 mM EDTA, 1% Triton-X, 1 mM PMSF). The cells in lysis buffer were taken through 3x freeze/thaw cycles using liquid nitrogen. Protein concentration was measured using the Bradford assay (Biorad, Germany). Protein equivalent to 20 μg whole-cell lysates was diluted in loading buffer (2% SDS, 10% Glycerol, 50 mM Tris-HCl pH 6.8, 0.2% Bromophenol Blue and 100 mM DTT) and resolved using 13% SDS-polyacrylamide gel electrophoresis. The separated proteins were transfer onto Hybond C membrane (Amersham, UK) and probed with antibodies to caspase-8 and caspase-3. Detection was carried out using chemiluminescence (Amersham). Following caspase detection, the membrane was incubated with stripping buffer before re-probing with antibodies to β-actin.

Statistical analysis of the data

The experimental data were analysed using Student's t test or One-way analysis of variance followed by Dunnet's test.

Results

The role of the FMK moiety in z-FA-FMK-induced inhibition of anti-CD3-mediated T cell proliferation

We have previously shown that the cathepsin B inhibitor, z-FA-FMK was immunosuppressive in vitro and in vivo [11]. To further understand the mechanism that underlies the immunosuppression mediated by z-FA-FMK, we first examined whether the FMK group plays a role in

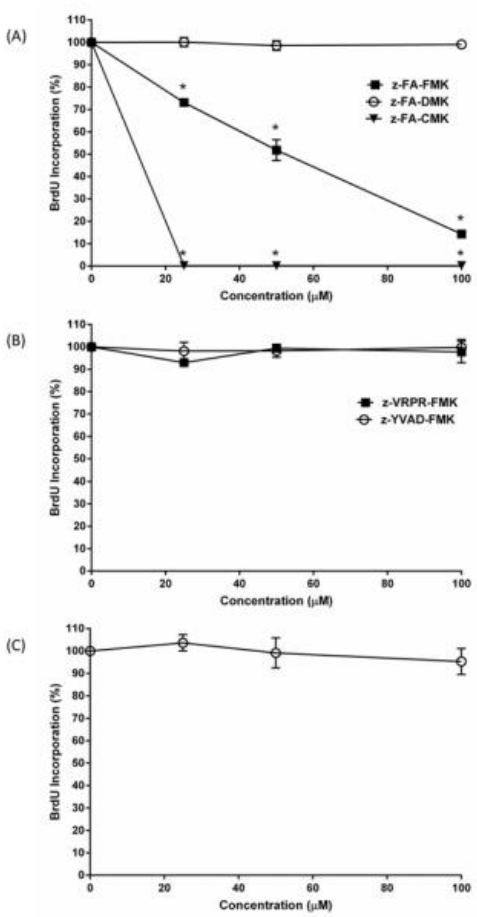

Fig 1. Effect of z-FA-FMK and other peptidyl methylketones on primary T cell proliferation. PBMCs (1 x 10^5/ml) were stimulated with anti-CD3 (5 μg/ml) in the presence of various concentrations of z-FA-FMK analogues (A), different peptidyl FMKs (B), or different N-terminal groups (C) for 72 h. T cell proliferation was determined using BrdU incorporation as outlined in Materials and Methods. The relative incorporation of BrdU into control proliferation T cells (with anti-CD3 only) were normalised to 100%. The results are the means ± SEM from three separate donors. *,Significantly decreased ($p < 0.01$) from control.

doi:10.1371/journal.pone.0123711.g001

suppressing T cell proliferation by comparing it with two of its analogues, z-FA-DMK and z-FA-CMK. As illustrated in Fig 1A, T cell proliferation induced by anti-CD3 was inhibited in a concentration-dependent manner by z-FA-FMK (IC_{50} ~50 μM), which is very much in line with our previous report [11]. However, when the FMK group was replaced with the DMK group, z-FA-DMK up to 100 μM had no inhibitory effect on anti-CD3-induced T cell proliferation. In sharp contrast, when the FMK group was replaced with the CMK group, z-FA-CMK completely abolished T cell proliferation induced by anti-CD3. Complete inhibition of T cell

proliferation was apparent in the presence of 25 μM z-FA-CMK, suggesting that this methylketone peptide may be toxic as reported by us recently in Jurkat T cells, a leukemic T cell line [18]. Indeed, z-FA-CMK-treated cells were dead after 24 h as determined by PI uptake (data not shown). Since only z-FA-FMK blocked T cell activation and proliferation, the results suggest that the FMK moiety plays an important role in the immunosuppressive properties of this peptidyl halomethylketone. However, two other FMK containing methylketone peptides, z-YVAD-FMK, a caspase-1 inhibitor, and z-VRPR-FMK, a MALT1 inhibitor, were found to have no effect on anti-CD3-induced T cell proliferation (Fig 1B). This suggests that the FMK group per se is not causing the immunosuppression and that the inhibition of T cell proliferation mediated by z-FA-FMK involves the combination of the FMK moiety and other parts of the molecule. We next examined whether the benzyloxycarbonyl (z) group at the N-terminal of z-FA-FMK play any role in blocking T cell activation and proliferation. To this end, biotin-FA-FMK, which has a biotin molecule at the N-terminal instead of the benzyloxycarbonyl group, was examined. As illustrated in Fig 1C, biotin-FA-FMK up to 100 μM was unable to block T cell proliferation after 72 h. This lack of inhibition is unlikely to be due to biotin-FA-FMK not getting into the cells since avidin-FITC readily labelled the biotin-FA-FMK inside the cells indicating that the peptide is permeable and readily enters the cells (results not shown). Taken together, these results suggest that the benzyloxycarbonyl group at the N-terminal of the peptidyl methylketone also plays a role in the immunosuppressive effects of z-FA-FMK.

Effect of z-FA-FMK on intracellular GSH and ROS levels in primary T cells

It is well established that reduced levels of intracellular GSH is linked to the increase in ROS levels and diminished T cell proliferation [19–22]. Furthermore, we recently showed that z-VAD-FMK inhibits anti-CD3-induced T cell proliferation via oxidative stress trough the depletion of GSH [23]. We therefore examined whether oxidative stress may be responsible for the immunosuppressive effects induced by z-FA-FMK in primary T cells. To this end, the intracellular GSH and ROS levels were determined in anti-CD3-activated T cells in the presence or absence of z-FA-FMK. As illustrated in Fig 2A, z-FA-FMK at varying concentrations (25–100 μM) had little effect on the intracellular GSH levels in activated primary T cells after 6 h compared to control cells. However, after 24 h, there was a significant dose-dependent decrease in the intracellular GSH in anti-CD3-activated T cells ($p < 0.05$). These results suggest that z-FA-FMK is capable of depleting intracellular GSH in anti-CD3-activated T cells. Since reduced intracellular GSH is associated with an increased in ROS [19–22], the effect of z-FA-FMK on ROS generation was assessed using DHE dye which selectively detects intracellular superoxide anion (• O2–) production [24–26]. As shown in Fig 2B, z-FA-FMK at 25 μM has little effect on ROS levels in anti-CD3-activated T cells after 6 h. However, at higher concentrations (50 and 100 μM) the ROS generated in activated T cells were significantly increased compared to control ($p < 0.05$). After 24 h, the level of ROS in anti-CD3-activated T cells was further increased by z-FA-FMK in a dose-dependent manner. The carrier solvent DMSO (> 0.1%) has no effect on the intracellular GSH and ROS levels (data not shown). Collectively, these results suggest that z-FA-FMK induced oxidative stress in anti-CD3-activated T cells through the depletion of GSH and ROS production.

Effect of antioxidants on the suppression of primary T cell proliferation mediated by z-FA-FMK

GSH is a major low molecular weight thiol in cells and is known to play an important role in T cell proliferation [27–29]. Its depletion suggests that the loss of intracellular GSH may be

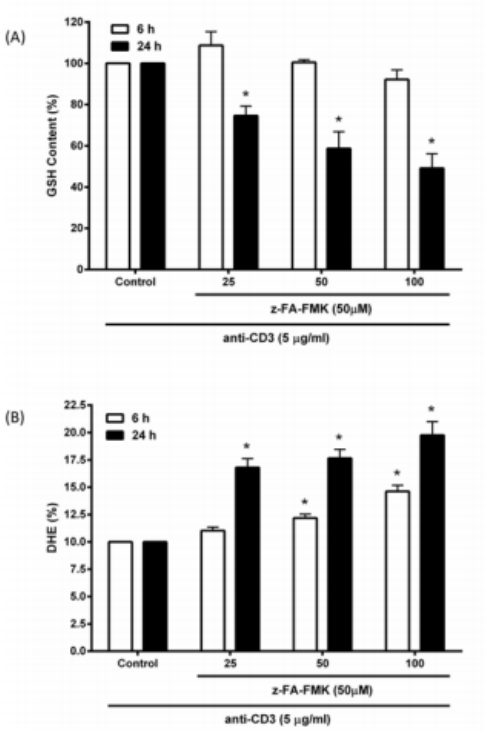

Fig 2. Effect of z-FA-FMK on intracellular GSH and ROS levels in activated primary T cells. PBMCs (1 x 10^5/ml) were stimulated with anti-CD3 (5 μg/ml) in the presence of various concentrations of z-FA-FMK. The level of GSH (A) and ROS (B) was measured after 6 and 24 h using the fluorescent dye MCB and the DHE probe, respectively as described in Materials and Methods. The results for GSH are based on 1 x 10^4 cells per sample and all results are means ± SEM from three separate donors. *,Significantly different ($p < 0.01$) from control with anti-CD3 alone.

doi:10.1371/journal.pone.0123711.g002

responsible for the inhibition of anti-CD3-induced T cell proliferation mediated by z-FA-FMK. We therefore examined whether the antioxidant, NAC could reverse the inhibition of T cell proliferation mediated by z-FA-FMK. As shown in Fig 3A, z-FA-FMK (50 μM) on its own inhibited anti-CD3-induced T cell proliferation and the presence of NAC readily abolished this inhibitory effect in a concentration-dependent manner (1.25–5 mM). Since NAC is a precursor of GSH biosynthesis we examined the effect of extracellular GSH on z-FA-FMK induced suppression of anti-CD3-mediated T cell proliferation. As illustrated in Fig 3B, GSH added exogenously fully restored the inhibition of T cell proliferation mediated by z-FA-FMK in a concentration-dependent manner (1.25–5 mM) suggesting that the depletion of intracellular GSH is the underlying mechanism of z-FA-FMK-induced immunosuppression. To further corroborate this, BSO, which irreversibly blocks the GSH synthesis pathway by inhibiting the enzyme γ-glutamylcysteine synthetase was added to anti-CD3-activated T cells co-treated with z-FA-FMK and NAC for 72 h [30]. As shown in Fig 4, NAC (5 mM) abolished the inhibition of T cell proliferation mediated by z-FA-FMK while the presence of BSO (0.5 mM) effectively

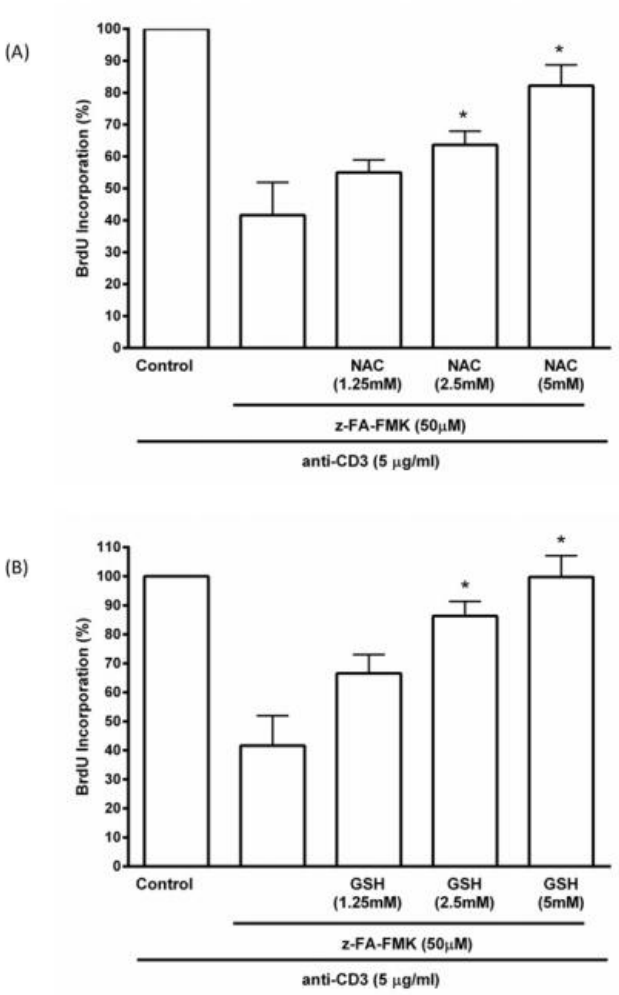

Fig 3. Effect of NAC and GSH on the inhibition of T cell proliferation mediated by z-FA-FMK. PBMCs (1 x 10^5/ml) were stimulated with anti-CD3 (5 μg/ml) in the presence of 50 μM z-FA-FMK and varying concentrations of NAC (A) or GSH (B). BrdU incorporation was determined after 72 h as described in Materials and Methods. The relative incorporation of BrdU into control proliferation T cells (with anti-CD3 only) were normalised to 100%. Results are the mean ± SEM of at least three independent experiments. *, Significantly increased ($p < 0.01$) compared to z-FA-FMK + anti-CD3.

doi:10.1371/journal.pone.0123711.g003

blocked the ability of NAC to restore T cell proliferation. This clearly indicates that the ability of NAC to restore the inhibition of anti-CD3-induced T cell proliferation mediated by z-FA-FMK is via replenishing the intracellular pool of GSH. Since the inhibition of T cell proliferation mediated by z-FA-FMK was abolished by NAC and GSH, we further examined whether

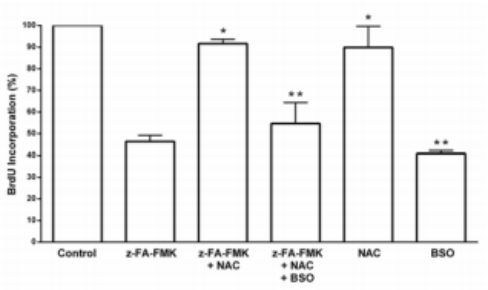

Fig 4. The effect of NAC on the inhibition of T cell proliferation mediated by z-FA-FMK is abolished by BSO. PBMCs (1 x 10^6/ml) were stimulated with anti-CD3 (5 μg/ml) plus 50 μM z-FA-FMK in the presence or absence of NAC (5 mM) and BSO (0.5 mM) where indicated. BrdU incorporation was determined after 72 h as described in Materials and Methods. The relative incorporation of BrdU into control proliferation T cells (with anti-CD3 only) were normalised to 100%. Results are the mean ± SEM of at least three independent experiments. *,Significantly increased ($p < 0.01$) compared to z-FA-FMK; **Significantly decreased ($p < 0.05$) from z-FA-FMK + NAC.

doi:10.1371/journal.pone.0123711.g004

other low molecular weight thiols, such as L-cysteine and D-cysteine, would have the same effect. As illustrated in Fig 5, L-cysteine (5 mM), which is another precursor for GSH biosynthesis significantly restored ($p < 0.05$) the inhibition of T cell proliferation induced by z-FA-FMK, whereas D-cysteine which cannot be metabolised to GSH had little effect. Taken together, these results suggest that the immunosuppressive effects of z-FA-FMK are due to oxidative stress through the depletion of intracellular GSH.

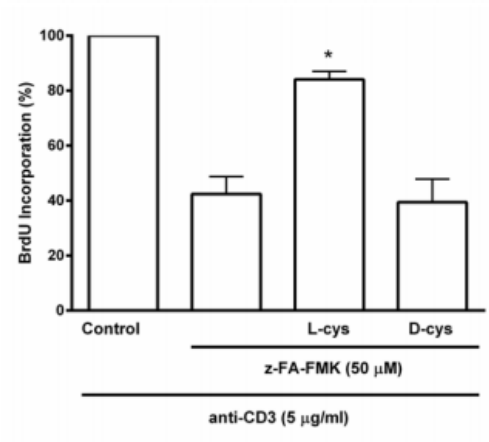

Fig 5. Effect of low molecular weight thiols on the inhibition of T cell proliferation mediated by z-FA-FMK. PBMCs (1 x 10^6/ml) were stimulated with anti-CD3 (5 μg/ml) plus 50 μM z-FA-FMK in the presence or absence of low molecular weight thiols (5 mM) or BSO (0.5 mM) where indicated. BrdU incorporation was determined after 72 h as described in Materials and Methods. The relative incorporation of BrdU into control proliferation T cells (with anti-CD3 only) were normalised to 100%. Results are the mean ± SEM of at least three independent experiments. *,Significantly increased ($p < 0.01$) compared to z-FA-FMK + anti-CD3.

doi:10.1371/journal.pone.0123711.g005

GSH restored z-FA-FMK-induced down-regulation of CD25 and CD69 in anti-CD3-activated T cells

Some of the earliest events that occur after T cell activation such as cytokine secretion and cell surface receptor up-regulation are inhibited by z-FA-FMK [11]. Since low molecular weight thiols were able to reverse the inhibition of T cell proliferation mediated by z-FA-FMK, we examined the effect of extracellular GSH on the expression of IL-2Rα (CD25) and the activated T cell marker, CD69. As shown in Fig 6, the percentage of cells that stained positive for CD25 and CD69 expression increased from around 0.65% and 3% in resting cells to 55.6% and 51.2% in activated T cells, respectively. Following treatment with z-FA-FMK (50 μM) the up-regulation of CD25 and CD69 in anti-CD3 activated T cells was reduced to 32.5% and 35.7%, respectively. In the presence of 5 mM GSH the down-regulation of CD25 and CD69 mediated by z-FA-FMK was completely restored to control levels. These results suggest that oxidative stress plays an important role in the down-regulation of CD25 and CD69 expression induced by z-FA-FMK in activated T cells.

Effect of low molecular weight thiols on the inhibition of caspase-8 and caspase-3 processing mediated by z-FA-FMK in activated primary T cells

We have shown previously that z-FA-FMK completely blocks the processing of caspase-8 and caspase-3 to their subunits in activated T cells [11]. The finding that the low molecular weight thiols such as GSH, NAC and L-cysteine could reverse the inhibition of T cell proliferation as well as the expression of early T cell markers induced by z-FA-FMK raised the question whether these thiols could restore caspase-8 and caspase-3 processing in activated T cells in the

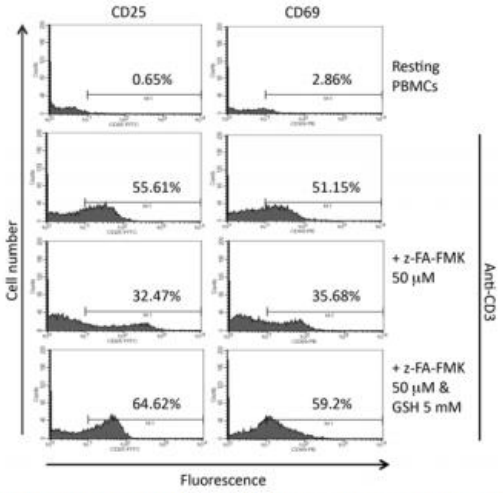

Fig 6. Effect of GSH on the inhibition of CD25 and CD69 expression in activated T cells mediated by z-FA-FMK. PBMCs (1 x 10^6/ml) were stimulated with anti-CD3 (5 μg/ml) plus 50 μM z-FA-FMK in the presence or absence of 5mM GSH. After 72 h, the cells were stained with FITC-conjugated anti-CD25 or PE-conjugated anti-CD69 before analysis using flow cytometry as described in Materials and Methods. The results are one representative from three independent experiments.

doi:10.1371/journal.pone.0123711.g006

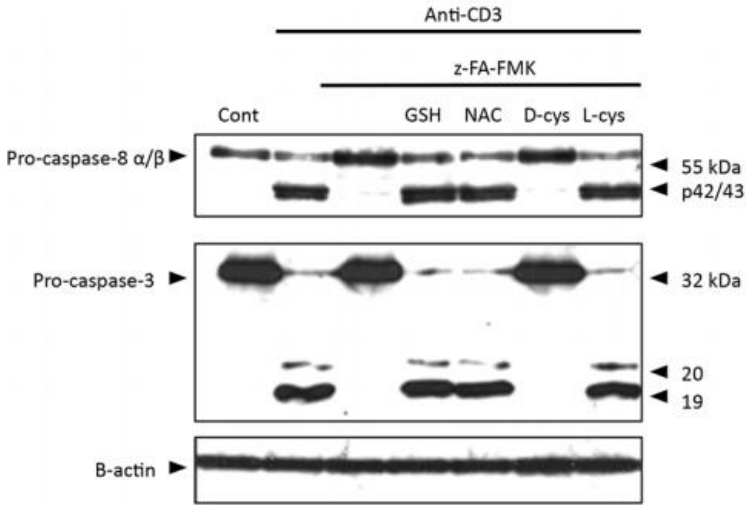

Fig 7. Effect of low molecular weight thiols on caspase-8 and -3 processing in z-FA-FMK-treated activated T cells. PBMCs (1 x 10^6/ml) were stimulated with anti-CD3 (5 μg/ml) plus 50 μM z-FA-FMK in the presence or absence of antioxidants (5 mM). After 72 h, the cells were taken through a gradient density centrifugation using lymphoprep to obtain activated T cells. Whole cell lysates (20 μg protein) from activated T cells were resolved using 13% SDS-PAGE, transferred to nitrocellulose membrane and probed for caspase-8, caspase-3 and β-actin as described in Materials and Methods. The results are one representative of three independent experiments.

doi:10.1371/journal.pone.0123711.g007

presence of z-FA-FMK. In order to exclude the dying cells due to activation-induced cell death and growth factor deprivation, live activated T cells were purified using density gradient centrifugation (lymphoprep) prior to western blot analysis. As illustrated in Fig 7, the presence of z-FA-FMK (50 μM) completely blocked the activation and processing of caspase-8 and caspase-3, which is in good agreement with our previous studies [11]. The presence of 5 mM each of GSH, NAC and L-cysteine completely restored the inhibition of caspase-8 and caspase-3 processing mediated by z-FA-FMK in anti-CD3-activated T cells. The procaspase-8α and β were processed to the p42/43 fragments, respectively. Similar to control anti-CD3-activated T cells, caspase-3 was processed to the p20 and p17 fragments. As expected, D-cysteine which does not have any effect on the inhibition of T cell proliferation mediated by z-FA-FMK had little effect on the inhibition of caspase-8 and caspase-3 processing.

Discussion

Accumulating evidence from a number of studies have now shown that z-FA-FMK is immunosuppressive and blocks LPS-induced cytokine secretion in macrophages [10], inhibits T cell activation and proliferation induced by mitogen as well as IL-2 in vitro [11]. These pleiotropic immunosuppressive effects may account for its remarkable therapeutic effect in suppressing the destruction of articular cartilage and bone in chronic inflammatory arthritis induced by adjuvant in mice [7–9]. In the present study we have examined the underlying mechanism involved in the inhibition of anti-CD3-induced T cell activation and proliferation mediated by z-FA-FMK.

In agreement with our earlier study [11], z-FA-FMK readily inhibited anti-CD3-induced T cell proliferation whereas z-FA-DMK which has a dimethyl group in the methylketone moiety

was found to have little effect. In sharp contrast another analogue, z-FA-CMK, having a chlorine atom instead of a fluorine atom in the methylketone moiety was toxic and induced cell death in primary T cells. The toxicity of z-FA-CMK in primary T cells confirms our recent study where z-FA-CMK was found to induce both apoptosis and necrosis in Jurkat T cells [18]. It is well known that halomethylketone peptides having a chlorine atom instead of a fluorine atom are more reactive and can result in non-specific alkylation of proteins which may lead to their toxicity [3,31–33]. Since all three compounds blocked cathepsin B, it is unlikely that the inhibition of this enzyme play a role in the inhibition of proliferation and toxicity in primary T cells induced by z-FA-FMK and z-FA-CMK, respectively. It is also unlikely that the immunosuppression mediated by z-FA-FMK is caused by the FMK group alone, as other FMK-containing methylketone peptides such as z-YVAD-FMK and z-VRPR-FMK have little effect on anti-CD3-induced T cell proliferation. Interestingly, the N-terminal blocking group, benzyloxycarbonyl appears to play an important role in the immunosuppressive effects of z-FA-FMK since replacing it with biotin (biotin-FA-FMK) completely abrogated its ability to inhibit anti-CD3-induced T cell proliferation. Taken together, these results suggest that the immunosuppression mediated by z-FA-FMK is specific and requires a fluorine atom in the methylketone moiety and the benzyloxycarbonyl group at the N-terminal.

Although fluorometylketone peptides are not very reactive, they are capable of reacting with GSH directly as reported previously [31]. Furthermore, evidence from numerous studies have shown that human T lymphocytes depleted of intracellular GSH using pharmacological regulators [30,34–39] were unable to proliferate and accumulate high levels of ROS [19–21,40] We found that z-FA-FMK treatment leads to depletion of intracellular GSH levels in activated T cells with a concomitant increase in cellular ROS, suggesting that oxidative stress may be the underlying mechanism of z-FA-FMK immunosuppressive effect. Indeed, the inhibition of anti-CD3-induced T cell proliferation mediated by z-FA-FMK was abrogated by low molecular weight thiols such as GSH, NAC and L-cysteine. Both NAC and L-cysteine are precursors for GSH biosynthesis and is readily taken up by the cells. Once inside the cells, deacetylation of NAC will increase the intracellular cysteine levels, which is rate limiting in GSH biosynthesis [40]. Therefore, our results suggest that NAC and L-cysteine restores T cell proliferation in the presence of z-FA-FMK by acting as precursors for GSH biosynthesis. This is further corroborated when D-cysteine, which cannot be enzymatically converted to GSH, was unable to restore anti-CD3-induced T cell proliferation inhibited by z- FA-FMK. We observed that when cells were treated with BSO in addition to NAC and z-FA-FMK, NAC was ineffective and unable to restore T cell proliferation to control levels. Because BSO blocks γ-glutamylcysteine synthetase, the rate limiting step in GSH biosynthesis, low molecular weight thiols such as NAC and L-cysteine will not contribute much to GSH biosynthesis [30]. Our results also indicate that the depletion of intracellular GSH mediated by z-FA-FMK is not due to the inhibition of γ-glutamylcysteine synthetase otherwise both NAC and L-cysteine would not be able to restore the inhibition of anti-CD3-induced T cell proliferation. How z-FA-FMK diminishes intracellular GSH levels in activated T cells remains unclear. Although, peptidyl-FMKs have been reported to be capable of alkylating GSH directly in vitro [31], they are not very reactive toward GSH in vitro compared to CMKs. At physiological pH the rate of alkylation of GSH mediated by peptidyl FMKs is only 0.2% of the rate with peptidyl CMKs [31]. It remains to be determined whether this slow rate of GSH alkylation mediated by FMKs could result in the depletion of GSH in primary activated T cells over time. Collectively, our results and those published previously strongly implicate GSH as an important regulator of T cell proliferation and suggest a direct relationship between the availability of GSH and the proliferative response of T cells [19,21,41].

We and others have shown previously that z-FA-FMK also blocks NFκB signalling induced by antigen receptor stimulation, which in turn leads to the inhibition of IL-2 and IFN-γ

production as well as the expression of CD25 [10,11]. We observed that the expression of CD25 and another early T cell activation marker, CD69 were inhibited by z-FA-FMK following primary T cell activation with anti-CD3. The expression of these two early T cell activation markers has been shown to be down-regulated following the depletion of GSH [28], suggesting that the depletion of intracellular GSH by z-FA-FMK may be responsible for the low expression of CD25 and CD69 in anti-CD3-stimulated T cells. Indeed, when endogenous GSH present, the inhibition of CD25 and CD69 expression mediated by z-FA-FMK following anti-CD3-induced T cell activation was completely restored. Taken together, our results suggest that intracellular GSH play a pivotal role in T cell activation and proliferation following antigen receptor stimulation.

Many studies in apoptosis research have used z-FA-FMK as a negative control for peptidyl-FMK caspase inhibitors because of its inertness towards caspases [42,43]. However, z-FA-FMK treatment effectively blocked both caspase-8 and caspase-3 processing in anti-CD3-activated T cells as shown in this study and previously [11]. Interestingly, GSH, NAC and L-cysteine were all able to fully restore the processing of caspase-8 and caspase-3 into their respective enzyme subunits. This suggests that oxidative stress through the depletion of intracellular GSH mediated by z-FA-FMK inhibits the activation and processing of caspases in activated T cells. However, it is well known that many toxicants induced apoptosis in various cell types including T cell lines via oxidative stress and the activation of caspases plays a central role [44,45]. An explanation that reconciles these seemingly contradictory observations is that the role played by caspases and its regulation in primary T cell activation and proliferation is different from apoptotic cell death. In primary T cells caspases are needed for cell proliferation following activation whereas caspases are needed for the execution of apoptosis leading to cleavage of cellular components and cell death. However, it was suggested previously that the activation of caspases in activated T cells, particularly caspase-3 was an artefact during cell lysis due to the use of detergents such as NP-40, deoxycholate and low concentration of SDS [46]. These detergents cause the release of granzyme B, which in turn activates caspase-3 and cleaved PARP, a caspase-3 substrate. It is unlikely that the activation of caspase-3 in our activated T cell model is due to extraction artefact for a number of reasons. Firstly, we used only Triton-X in our lysis buffer and not Nonidet P-40, deoxycholate or SDS which appears to be the cause of the artefact. Secondly, the activated T cells have no apoptotic characteristics or PARP cleavage even though caspase-3 was activated [47]. Finally, a number of studies have since been published demonstrating the activation of caspase-3 in activated T cells [48–50]. Collectively these evidences argue against the processing of caspase-3 in activated T cells as an extraction artefact. The lack of processing of caspase substrates, including PARP [11,49] in proliferating T cells suggest that the activity of the effector caspases may have been blocked by endogenous inhibitors like the inhibitor-of-apoptosis proteins (IAP) [51,52]. Indeed, previous study demonstrated that the caspase inhibitor X-linked inhibitor-of-apoptosis proteins (XIAP) interacts with cleaved caspase-3 and caspase-7 during human T cell proliferation, thereby blocking their full activation, substrate cleavage and cell death [52]. Another possibility is that the activated caspases are prevented from cleaving substrates that inevitably triggers apoptosis through limited subcellular compartmentalisation [52–54].

In summary, we have shown that the inhibition of anti-CD3-induced T cell activation and proliferation mediated by z-FA-FMK requires a fluorine atom in the methylketone moiety and the benzyloxycarbonyl group at the N-terminal. The immunosuppressive effect of z-FA-FMK is mediated through oxidative stress via the depletion of intracellular GSH, which is reversed by low molecular weight thiols such as GSH, NAC and L-cysteine but not D-cysteine, which cannot be metabolised into GSH. Furthermore, these thiols were able to restore the processing of caspase-8 and caspase-3 in z-FA-FMK treated T cells during activation and proliferation.

Author Contributions

Conceived and designed the experiments: TR SCC. Performed the experiments: TR. Analyzed the data: TR SCC. Wrote the paper: TR SCC.

References

1. Powers JC (1977) Haloketone inhibitors of proteolytic enzymes. In: Chemistry and Biochemistry of amino acids, peptides and proteins., Marcel Dekker: New York. Vol. 4, 65–178.
2. Kwttnwer C, Shaw E (1981) Inactivation of trypsin-like enzymes with peptides of arginine chloromethyl ketone. Methods Enzymol, 80 Pt C, 826–42. PMID: 6210829
3. Rasnick D (1985) Synthesis of Peptide Fluoromethyl Ketones and the Inhibition of Human Cathepsin B. Anal Biochem, 149, 461–465. PMID: 4073501
4. Powers JC, Asgian JL, Ekici OD, James KE (2002) Irreversible inhibitors of serine, cysteine, and threonine proteases. Chem Rev, 102, 4639–750. PMID: 12475205
5. Lenarcic B, Gabrijelcic D, Rozman B, Drobnic-Kosorok M, Turk V (1988) Human cathepsin B and cysteine proteinase inhibitors (CPIs) in inflammatory and metabolic joint diseases. Biol Chem Hoppe Seyler, 369 Suppl, 257–61. PMID: 3264507
6. Gabrijelcic D, Annan-Prah A, Rodic B, Rozman B, Cotic V, Turk V (1990) Determination of cathepsins B and H in sera and synovial fluids of patients with different joint diseases. J Clin Chem Clin Biochem, 28, 149–53. PMID: 2329322
7. Van Noorden CJ, Smith RE, Rasnick D (1988) Cysteine proteinase activity in arthritic rat knee joints and the effects of a selective systemic inhibitor, Z-Phe-AlaCH2F. J Rheumatol, 15, 1525–35. PMID: 3204599
8. Ahmed NK, Martin LA, Wattes LM, Palmer J, Thornburg L, Prior J, et al. (1992) Peptidyl fluoromethyl ketones as inhibitors of cathepsin B. Implication for treatment of rheumatoid arthritis. Biochem Pharmacol, 44, 1201–7. PMID: 1417942
9. Esser RE, Angelo RA, Murphey MD, Watts LM, Thornburg LP, Palmer JT, et al. (1994) Cysteine proteinase inhibitors decrease articular cartilage and bone destruction in chronic inflammatory arthritis. Arthritis Rheum, 37, 236–47. PMID: 8129779
10. Schotte P, Schauvliege R, Janssens S, Beyaert R (2001) The cathepsin B inhibitor z-FA.fmk inhibits cytokine production in macrophages stimulated by lipopolysaccharide. J Biol Chem, 276, 21153–7. PMID: 11290751
11. Lawrence CP, Kadioglu A, Yang AL, Coward WR, Chow SC (2006) The cathepsin B inhibitor, z-FA-FMK, inhibits human T cell proliferation in vitro and modulates host response to pneumococcal infection in vivo. J Immunol, 177, 3827–36. PMID: 16951345
12. Chun HJ, Zheng L, Ahmad M, Wang J, Speirs CK, Siegel RM, et al. (2002) Pleiotropic defects in lymphocyte activation caused by caspase-8 mutations lead to human immunodeficiency. Nature, 419, 395–9. PMID: 12353035
13. Salmena L, Lemmers B, Hakem A, Matysiak-Zablocki E, Murakami K, Au PY, et al. (2003) Essential role for caspase 8 in T-cell homeostasis and T-cell-mediated immunity. Genes Dev, 17, 883–95. PMID: 12654726
14. Osseni RA, Debbasch C, Christen MO, Rat P, Warnet JM (1999) Tacrine-induced Reactive Oxygen Species in a Human Liver Cell Line: The Role of Anethole Dithiolethione as a Scavenger. Toxicol In Vitro, 13, 683–8. PMID: 20654534
15. Aoshiba K, Tamaoki J, Nagai A (2001) Acute cigarette smoke exposure induces apoptosis of alveolar macrophages. Am J Physiol Lung Cell Mol Physiol, 281, L1392–401. PMID: 11704535
16. Apostolova N, Gomez-Sucerauia L, Moran A, Alvarez A, Blas-Garcia A, Esplugues JV (2010) Enhanced oxidative stress and increased mitochondrial mass during efavirenz-induced apoptosis in human hepatic cells. Br J Pharmacol, 160, 2069–84. doi: 10.1111/j.1476-5381.2010.00866.x PMID: 20649602
17. Sun HL, Tsai AC, Pan SL, Ding Q, Yamaguchi H, Lin CN, et al. (2009) EPOX inhibits angiogenesis by degradation of Mcl-1 through ERK inactivation. Clin Cancer Res, 15, 4904–14. doi: 10.1158/1078-0432.CCR-09-0269 PMID: 19622586
18. Liow KY, Chow SC (2013) The cathepsin B inhibitor, z-FA-CMK is toxic and readily induced cell death in human T lymphocytes. Toxicol Appl Pharmacol, 272, 559–67. doi: 10.1016/j.taap.2013.07.022 PMID: 23933532
19. Fidelus RK, Ginouves P, Lawrence D, Tsan MF (1987) Modulation of intracellular glutathione concentrations alters lymphocyte activation and proliferation. *Exp Cell Res*, 170, 269–75. PMID: 3595735

20. Gmunder H, Droge W (1991) Differential effects of glutathione depletion on T cell subsets. Cell Immunol, 138, 229–37. PMID: 1913838

21. Suthanthiran M, Anderson ME, Sharma VK, Meister A (1990) Glutathione regulates activation-dependent DNA synthesis in highly purified normal human T lymphocytes stimulated via the CD2 and CD3 antigens. Proc Natl Acad Sci U S A, 87, 3343–7. PMID: 1970635

22. Walsh AC, Michaud SG, Malossi JA, Lawrence DA (1995) Glutathione depletion in human T lymphocytes: analysis of activation-associated gene expression and the stress response. Toxicol Appl Pharmacol, 133, 249–61. PMID: 7645021

23. Rajah T, Chow SC (2014) The inhibition of human T cell proliferation by the caspase inhibitor z-VAD-FMK is mediated through oxidative stress. Toxicol Appl Pharmacol, 278, 100–6. doi: 10.1016/j.taap.2014.04.014 PMID: 24768707

24. Bindokas VP, Jordan J, Lee CC, Miller RJ (1996). Superoxide production in rat hippocampal neurons: selective imaging with hydroethidine. J Neurosci, 16, 1324–36. PMID: 8778284

25. D'Agostino DP, Putnam RW, Dean JB (2007) Superoxide (*O2-) production in CA1 neurons of rat hippocampal slices exposed to graded levels of oxygen. J Neurophysiol, 98, 1030–41. PMID: 17553943

26. Cai H, Dikalov S, Griendling KK, Harrison DG (2007). Detection of reactive oxygen species and nitric oxide in vascular cells and tissues: comparison of sensitivity and specificity. Methods Mol Med, 139, 293–311. PMID: 18287681

27. Messina JP, Lawrence DA (1989) Cell cycle progression of glutathione-depleted human peripheral blood mononuclear cells is inhibited at S phase. J Immunol, 143, 1974–81. PMID: 2789253

28. Roozendaal R, Kauffman HF, Dijkhuis AJ, Ommen ET, Postma DS, De Monchy JG, et al. (2002) Interaction between nitric oxide and subsets of human T lymphocytes with differences in glutathione metabolism. Immunology, 107, 334–9. PMID: 12423309

29. Yim CY, Hibbs JB Jr, McGregor JR, Galinsky RE, Samlowsk WE (1994) Use of N-acetyl cysteine to increase intracellular glutathione during the induction of antitumor responses by IL-2. J Immunol, 152, 5796–805. PMID: 8207209

30. Griffith OW, Meister A (1979) Potent and specific inhibition of glutathione synthesis by buthionine sulfoximine (S-n-butyl homocysteine sulfoximine). J Biol Chem, 254, 7558–60. PMID: 38242

31. Angliker H, Wikstrom P, Rauber P, Shaw E (1987) The synthesis of lysylfluoromethanes and their properties as inhibitors of trypsin, plasmin and cathepsin B. Biochem J, 241, 871–5. PMID: 2954536

32. Otto HH, Schirmeister T (1997) Cysteine Proteases and Their Inhibitors. Chem Rev, 97, 133–172. PMID: 11848867

33. Rauber P, Angliker H, Walker B, Shaw E (1986) The synthesis of peptidylfluoromethanes and their properties as inhibitors of serine proteinases and cysteine proteinases. Biochem J, 239, 633–40. PMID: 3827817

34. Ronzio RA, Rowe WB, Meister A (1969) Studies on the mechanism of inhibition of glutamine synthetase by methionine sulfoximine. Biochemistry, 8, 1066–75. PMID: 4305484

35. Hidaka T, Furuno H, Inokuchi T, Ogura R (1990) Effects of diethyl maleate (DEM), a glutathione depletor, on prostaglandin synthesis in the isolated perfused spleen of rabbits. Arch Toxicol, 64, 103–8. PMID: 2112376

36. Weber CA, Duncan CA, Lyons MJ, Jenkinson SG (1990) Depletion of tissue glutathione with diethyl maleate enhances hyperbaric oxygen toxicity. Am J Physiol, 258, L308–12. PMID: 2360643

37. Griffith OW, Anderson ME, Meister A (1979). Inhibition of glutathione biosynthesis by prothionine sulfoximine (S-n-propyl homocysteine sulfoximine), a selective inhibitor of gamma-glutamylcysteine synthetase. J Biol Chem, 254, 1205–10. PMID: 33187

38. Vaziri ND, Wang XQ, Oveisi F, Rad B (2000) Induction of oxidative stress by glutathione depletion causes severe hypertension in normal rats. Hypertension, 36, 142–6. PMID: 10904027

39. Reliene R, Schiestl RH (2006) Glutathione depletion by buthionine sulfoximine induces DNA deletions in mice. Carcinogenesis, 27, 240–4. PMID: 16162646

40. Gmunder H, Eck HP, Benninghoff B, Roth S, Droge W (1990) Macrophages regulate intracellular glutathione levels of lymphocytes. Evidence for an immunoregulatory role of cysteine. Cell Immunol, 129, 32–46. PMID: 2364441

41. Chaplin DD, Wedner JH (1978). Inhibition of lectin-induced lymphocyte activation by diamide and other sulfhydryl reagents. Cell Immunol, 36, 303–11. PMID: 630610

42. Sarin A, Wu ML, Henkart PA (1996) Different interleukin-1 beta converting enzyme (ICE) family protease requirements for the apoptotic death of T lymphocytes triggered by diverse stimuli. J Exp Med, 184, 2445–50. PMID: 8976202

43. McColl KS, He H, Zhong H, Whitacre CM, Berger NA, Distelhorst CW (1998) Apoptosis induction by the glucocorticoid hormone dexamethasone and the calcium-ATPase inhibitor thapsigargin involves Bc1-2 regulated caspase activation. Mol Cell Endocrinol, 139, 229–38. PMID: 9705090

44. Stridh H, Kimland M, Jones DP, Orrenius S, Hampton BM (1998) Cytochrome c release and caspase activation in hydrogen peroxide- and tributyltin-induced apoptosis. FEBS Lett, 429, 351–5. PMID: 9662447

45. Hung LF, Huang KY, Yang DH, Chang DM, Lai JH, Ho LJ (2010) Advanced glycation end products induce T cell apoptosis: Involvement of oxidative stress, caspase and the mitochondrial pathway. Mech Ageing Dev, 131, 682–91. doi: 10.1016/j.mad.2010.09.005 PMID: 20888855

46. Zapata JM, Takahashi R, Salvesen GS, Reed JC (1998) Granzyme release and caspase activation in activated human T-lymphocytes. J Biol Chem, 273, 6916–20. PMID: 9506996

47. Lawrence CP, Chow SC (2012). Suppression of human T cell proliferation by caspase inhibitors, z-VAD-FMK and z-IETD-FMK is independent of their caspase inhibition properties. Toxicol Appl Pharmacol, 265,103–12. doi: 10.1016/j.taap.2012.09.002 PMID: 22982538

48. Deas O, Dumont C, MacFarlane M, Rouleau M, Hebib C, Harper F, et al. (1998) Caspase-independent cell death induced by anti-CD2 or staurosporine in activated human peripheral T lymphocytes. J Immunol, 161, 3375–83. PMID: 9759854

49. Alam A, Cohen LY, Aouad S, Sekaly RP (1999) Early activation of caspases during T lymphocyte stimulation results in selective substrate cleavage in nonapoptotic cells. J Exp Med, 190, 1879–90. PMID: 10601362

50. Bidere N, Briet M, Durrbach A, Dumont C, Feldmann J, Charpentier B, et al. (2002) Selective inhibition of dipeptidyl peptidase I, not caspases, prevents the partial processing of procaspase-3 in CD3-activated human CD8(+) T lymphocytes. J. Biol. Chem. 277, 32339–47. PMID: 12080079

51. Callus BA, Vauz DL (2007) Caspase inhibitors: viral, cellular and chemical. Cell Death Differ, 14, 73–8. PMID: 16946729

52. Paulsen M, Ussat S, Jakob M, Scherer G, Lepenies I, Schutze S, et al. (2008). Interaction with XIAP prevents full caspase-3/-7 activation in proliferating human T lymphocytes. Eur J Immunol, 38, 1979–87. doi: 10.1002/eji.200838211 PMID: 18521960

53. Lamkanfi M, Festjens N, Declercq W, Vanden Berghe T, Vandenabeele P (2007) Caspases in cell survival, proliferation and differentiation. Cell Death Differ, 14, 44–55. PMID: 17053807

54. Koenig A, Russell JQ, Rodgers WA, Budd RC (2008) Spatial differences in active caspase-8 defines its role in T-cell activation versus cell death. Cell Death Differ, 15, 1701–11. doi: 10.1038/cdd.2008.100 PMID: 18617900